The Direct Effects of Ionizing Radiation on DNA and its Higher Ordered Structures

A Thesis submitted

for the degree of

Doctor of Philosophy

in the

Faculty of Science

at the

University of Leicester

by

George Donal Dransfield Jones

B.Sc.(Leics), M.Sc.(B'ham)

Department of Chemistry,
The University,
LEICESTER. LE1 7RH

OCTOBER 1987

Original
Contains
Pullouts

Dedicated to my Parents
and Grandparents

STATEMENT

The experimental work described in this thesis has been carried out by the author in the Department of Chemistry of the University of Leicester between July 1984 and July 1987. The work has not been submitted, and is not currently being submitted, for any other degree at this or any other University.

Signed:  Date: 21/10/87

ACKNOWLEDGEMENTS

I am deeply grateful to both Professor Martyn C. R. Symons and Dr. Paul M. Cullis of the Chemistry Department, Leicester for their invaluable help and guidance over the past three years. I would also like to thank members of the Physical Chemistry Laboratory, Leicester in particular John McClymont, Rob Janes, Ian Podmore, Marion Sweeney, Jeremy Lea, Chris Rhodes, Dave Keeble, Philip Jackson and Tony Cooney for many helpful discussions and fruitful collaborations.

The experimental expertise provided by Mr. J. A. Brivati and the assistance provided by the technical personnel of the Chemistry Department is gratefully acknowledged. Sincere thanks are also offered to Vicky Orson-Wright and Ann Crane for their patience and expertise in preparing this thesis.

Finally I would like to thank a certain Jill Dowsett for attempting to come to terms with it all.

Financial support for this work was from the Cancer Research Campaign.

THE DIRECT EFFECTS OF IONIZING RADIATION ON DNA AND ITS HIGHER ORDERED STRUCTURES

George D. D. Jones

ABSTRACT

This thesis investigates the effects of ionizing radiation on frozen aqueous solutions of DNA using e.s.r. spectroscopy and a plasmid (pBR322) strand break assay. To elucidate the mechanisms subsequent to primary ionic radical formation ($G^{\cdot+}$ and $T^{\cdot-}$), additives that influence the radiolytic processes were included prior to irradiation.

The presence of hydrogen peroxide (Chapter Three) switched the mechanism from direct damage to a pathway in part mediated through oxygen centred radicals ($^{\cdot}OH$, $HO_2^{\cdot}$) and resulted in a modest increase in the number of strand breaks (i.e. radiosensitization). E.s.r. observations showed the appearance of sugar radicals (strand break precursors) which were lost at temperatures well below those of base radicals.

The inclusion of a variety of thiols (Chapter Four) resulted in no change to either $G^{\cdot+}$ or $T^{\cdot-}$. However, on warming, the normal pattern of radical reactions was dramatically modified, the DNA radical centres being abruptly reduced in concentration. In anoxia this was concomitant with the appearance of $RS\dot{S}R^{-}$, and strand breaks were noted to decrease (i.e. radioprotection). Under oxic conditions the degree of repair was a function of the relative concentration of oxygen and thiol. E.s.r. indicated repair of DNA centred peroxyl radicals and also $RSO_2^{\cdot}$ formation. The latter may react with DNA and account for attenuation, by oxygen, of protection afforded by thiols at low concentrations.

The effects of ionizing radiation on higher ordered DNA structures (nucleohistone, chromatin and cell nuclei) has been investigated (Chapter Five). Relative to DNA, all systems gave equivalent yields of $G^{\cdot+}$, together with protein electron-loss centres $(Hist)^{\cdot+}$. However, $T^{\cdot-}$ yields were enhanced, the increase being greatest for nuclei. For the protein component it was suggested that $(Hist)^{\cdot+}$ are amide cations, readily trapped by loss of N-H protons, but that the electrons are mobile and able to transfer to DNA.

Mechanisms leading to strand breaks, involving intramolecular hydrogen atom abstraction by directly induced base radicals from neighbouring sugar residues, are proposed (Appendix B) and compared with those obtained for hydroxyl radical damage.

LIST OF CONTENTS

CHAPTER ONE

Introduction

INTRODUCTION

Ionizing radiation constitutes a source of naturally occurring physical damage that living organisms have had to contend with since the beginning of biological evolution. Identification of the critical site or macromolecular target whose damage is primarily responsible for radiation induced cell injury has been the goal of extensive investigations. It is now generally agreed that the target is in the cell nucleus (Zirkle, 1957) and that the principle target molecule, in mammalian cells, is deoxyribonucleic acid (DNA) (Kaplan and Moses, 1964; Hutchinson, 1966; Okada, 1969; Alper, 1979; Grosch and Hopwood, 1979; Biaglow, 1981). Of the various DNA radiation induced alterations so far characterised (Hüttermann *et al.*, 1978), the most lethal lesion has been proposed by many to be the double strand break (d.s.b.) (Hutchinson, 1978; Radford, 1985 and 1986). Biological effects such as gene malfunction, chromosome aberation and even ageing have also been related to DNA radiation induced damage (Dewey *et al.*, 1967; Held, 1986; Auerbach, 1976).

The high energy photons of ordinary X- or γ-radiation act on the absorbing material almost exclusively through the fast electrons (secondary radiation) to which they give rise (photoelectric effect, Compton effect, electron-positron pair production). These in turn act by causing secondary ionizations and excitations which overall results in abrupt changes to the electronic structure of the molecules of the target material, and leads to the dislocation of electrons from their regular state of orbital occupancy in pairs. The resulting molecular species with unpaired electrons are generally referred to as free radicals (Spinks and Wood, 1976). An evaluation of their relevance in radiation damage processes, in principle, involves relating both their chemical structure and concentration at various stages in the chain of reactions, to the nature of the stable chemical and biological alterations detected at later stages of damage (see below). For various reasons this problem is difficult to solve. However, two particular points dictate the importance of radicals. Firstly the concentrations of radiation induced radicals, as measured by various physical techniques, are found to lie within the range of concentrations observed for stable chemically altered products. Secondly, the observed stable chemical alterations can, in general, be successfully explained on the

basis of free radicals as precursors. Both observations leave little doubt about the rôle of free radicals being of primary importance as detectable intermediates in the pathway of reactions leading to chemical, and finally biological radiation induced damage.

The time scale for the effects of ionizing radiation on living systems extends over a considerable period, spanning from the first atomic/sub-atomic physical events (~10^{-16}s) to the later tissue level genetic and carcinogenic effects (years) (Adams and Jameson, 1980; Chapman and Gillespie, 1981). It is convenient to divide the events following exposure into three broad time scales, namely the physical, chemical and biological stages of radiation action. The physical stage (10^{-16}-10^{-12} seconds) commences with the transit of a fast electron or high energy photon and the deposition of energy to atoms in the absorbing medium, resulting in the formation of radicals. The chemical stage (10^{-12}-100 seconds) is the transformation of the radicals into stable products, and finally the biological stage (hours-years) comprises the effects caused by incorporation of the altered products into active living systems.

In the present study electron spin resonance (e.s.r.) spectroscopy was used to identify and quantify the initial ionic damage caused by the direct effects of ionizing radiation (see below) on DNA. After a succession of fast reactions, involving the formation of secondary neutral radicals, these gave rise to stable diamagnetic chemical products. It was at this juncture that a chemical method, using single strand breaks (s.s.b's) and d.s.b's as indices of chemical damage, was employed to complement the physical data. A specific topological form of DNA, plasmid supercoiled DNA, selected for this purpose provided a simple and accurate method for analysis of the disruption of the DNA macromolecule.

In the third stage, the purely biological processes of the radiation effects can be studied using a variety of techniques. An important part of the biological phase is the effect that radiation has on the enzymic repair processes of the cell. These include direct inactivation of the repair enzymes or an inability for the enzyme to function due to irreversible damage of the DNA molecules. Such studies on the biological consequences of radiation are beyond the scope of this

present work and have been reviewed elsewhere (Hüttermann *et al.*, 1978; Simic *et al.*, 1986; Revell, 1974; Hanawalt *et al.*, 1979).

The Structure of DNA

To comprehend fully the behaviour of DNA under the action of ionizing radiation it is important not only to understand the structure of DNA but also the physico-chemical properties which govern the structure and chemical reactivity. The latter points of nucleic acid structure have been discussed in great detail elsewhere (Bloomfield *et al.*, 1974) and only a short summary follows.

The ensuing discussion is restricted to double stranded DNA which takes the form of an unbranched polymer and may have a molecular weight of many millions. The repeating unit is the nucleotide (~320 m.wt.) which consists of a 2'-deoxyribose sugar bonded to a phosphate group and a purine or pyrimidine base. There are four commonly occurring base molecules in DNA, two purines, adenine (A) and guanine (G), and two pyrimidines, thymine (T) and cytosine (C). The repeating units are joined by phosphodiester bonding between the 3'-hydroxyl group of the sugar of one unit to the 5'-hydroxyl group of the next. The architecture proposed by Watson and Crick (1953), was for two polynucleotide chains, running in opposite directions (anti-parallel), to be wound helically about the same axis constrained by hydrogen bonding between the bases. A sugar and phosphate attached at one side of a base-pair is related by a two-fold rotation axis in the plane of the base, the helical symmetry generates a further set of axes bisecting the base-pair planes. Base-pairing occurs between a purine and pyrimidine as shown in Figure 1.1. The allowed combinations are A-T and G-C, hence the ratio of (G,A) to (C,T) remains constant while the amount of G-C to A-T may vary, dependent on the origin of the DNA.

The molecular structure may be described in terms of a set of conformational or torsion angles. These are the projected angles between two adjacent bonds when viewed along the central bond. The convention used here is presented in Figure 1.2. The angle χ defines a rotation about the glycosidic bond and relates the sugar O_1' to the purine C8 or pyrimidine C6. It has been observed to take values from slightly less than zero to more than 90° and again around 270°. The low

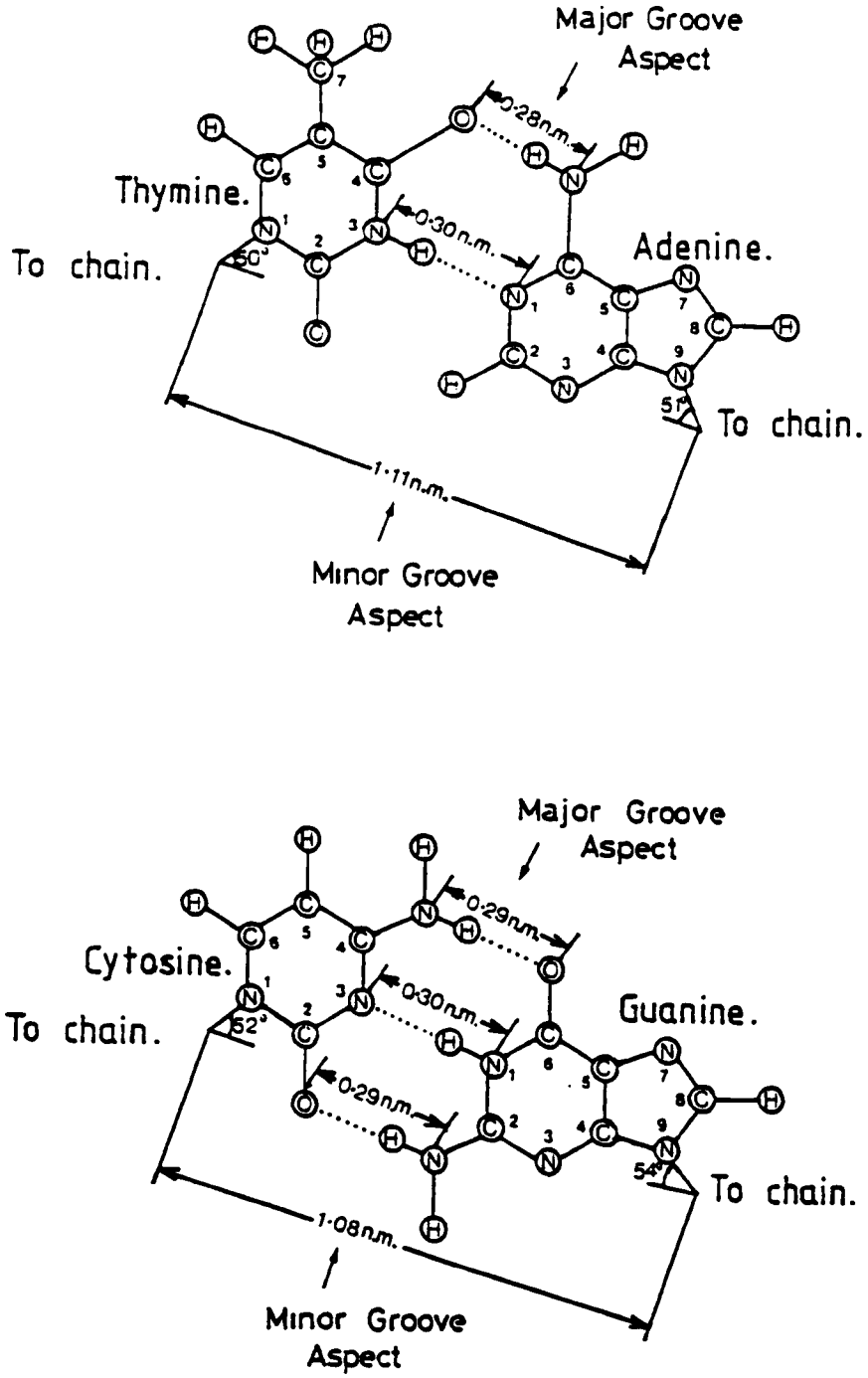

FIGURE 1.1

Watson-Crick base-pairing geometry.

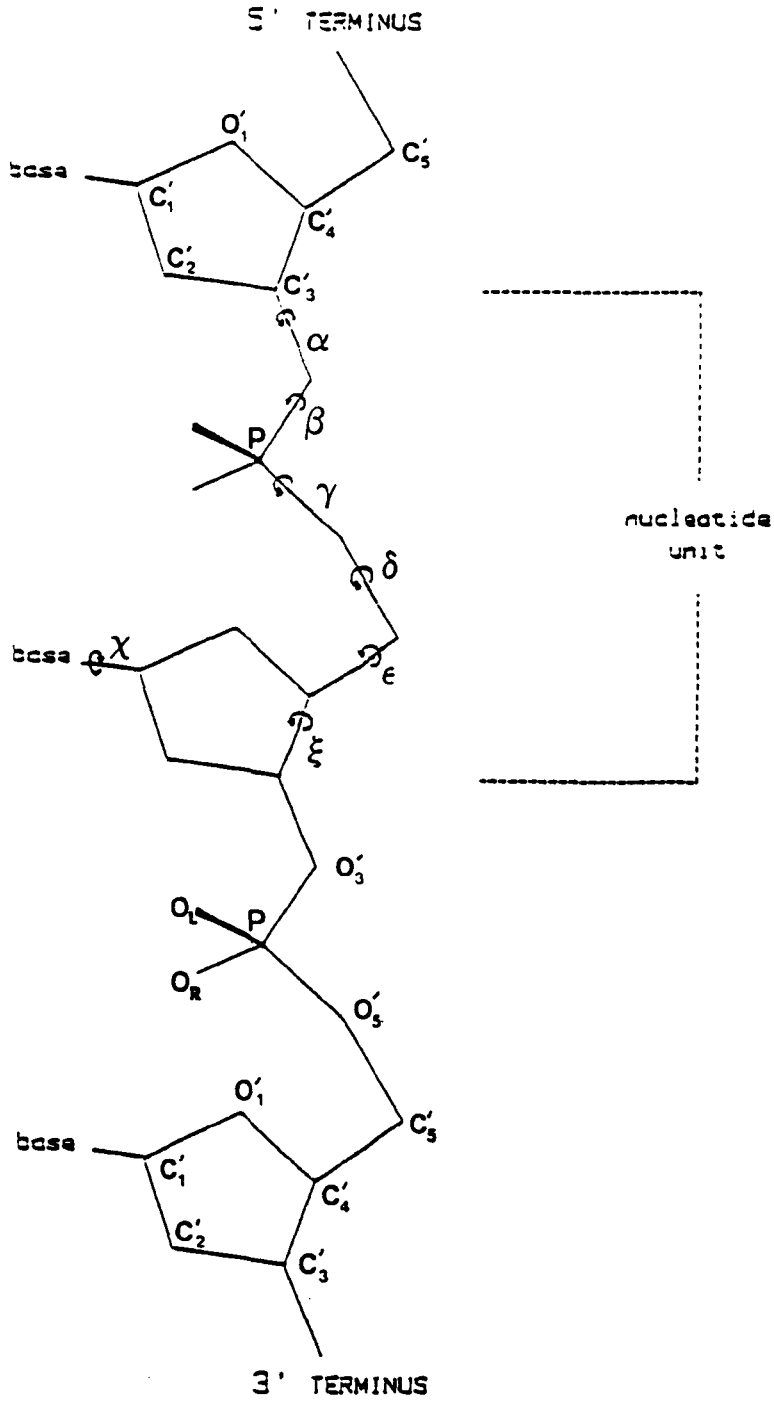

FIGURE 1.2

A schematic section of nucleotide backbone defining nomenclature.

value angles are termed *anti*, those in the 90° range as *high anti* while those around 270° are *syn*. The backbone torsion angles are divided into three regions, given below:-

a) gauche$^+$ (g^+) 0° - 120°
b) gauche$^-$ (g^-) -120° - 0°
c) trans (t) 120° - 240°

The molecular conformation is also influenced by the sugar pucker. This describes the deviation of the sugar ring atoms from co-planar. The C_2' or C_3' atom may be displaced giving four possible puckers (Fig. 1.3).

To define the position and orientation of the base-pairs with respect to the helix axis the following parameters are commonly defined; twist, tilt, roll, displacement and slide (Dickerson and Drew, 1981; Neidle and Berman, 1983; Keeble, 1986). The twist is the rotation of a rigid base-pair around the helix axis; the tilt is the rotation of a rigid base-pair around the pseudo two-fold axis; roll is a rotation about a line connecting the purine C8 and pyrimidine C6 (or about the N3-N1 hydrogen bond); displacement (D) is the distance from the helix axis to the base-pair and slide is defined as the translation of the base-pairs relative to one another down their long axis. The base-pairs themselves are also flexible and are rarely perfectly co-planar. They can either be propeller-twisted or bent. The former is a rotation of the two bases with respect to each other about the C8-C6 (or N3-N1) link, whilst the latter is the rotation of the individual bases in a pair around the pseudo two-fold axis in the plane of the bases (Fig. 1.4).

Running the length of the DNA structure are two grooves (Fig. 1.5). These are the (i) major and (ii) minor grooves which may vary in depth and width dependent on molecular conformation. They are important as potential sites for interactions.

It should be noted that the stability of the helix cannot be accounted for by base-pair hydrogen bonding alone, since the bond energy is too small. However an additional source of stabilization is base stacking. The stacking mechanism arises from interactions between the π-electrons of the aromatic bases and accounts for the stability of single strand polynucleotides. Indeed bases free in solution show a preference for

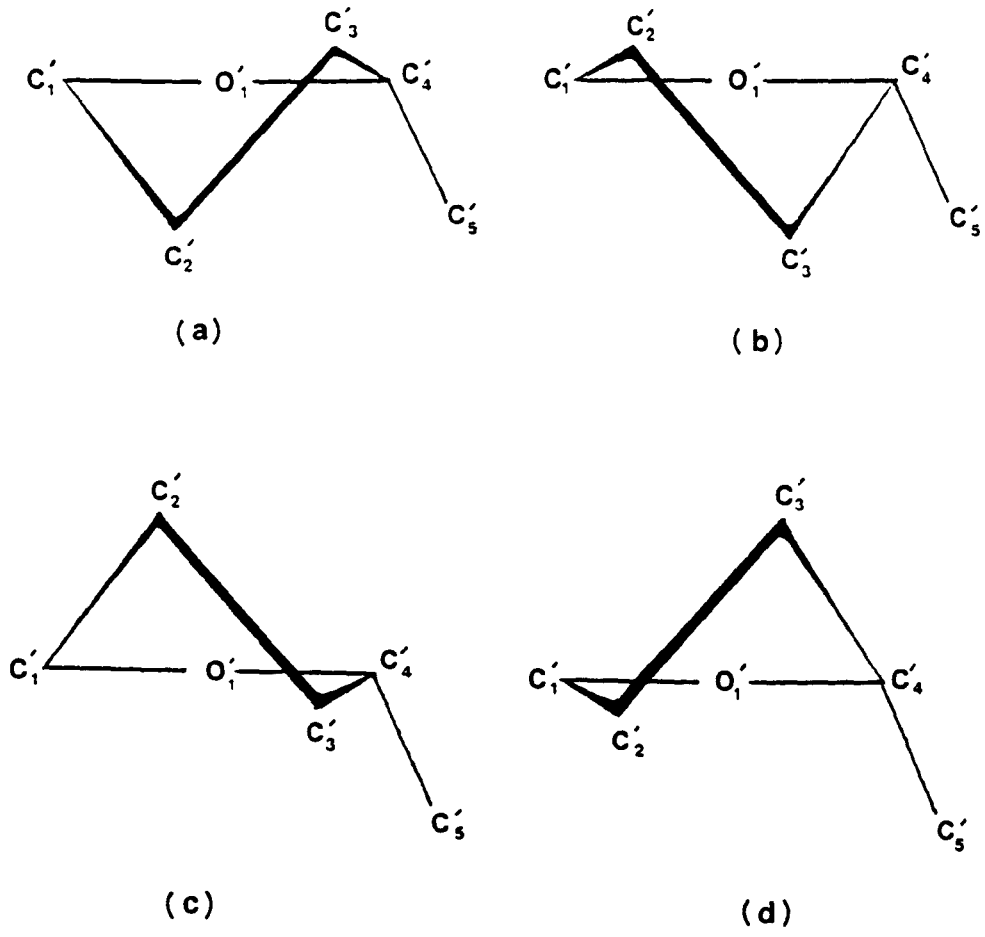

FIGURE 1.3

The four possible sugar puckers, (a) C_2'-endo, (b) C_3'-endo, (c) C_2'-exo and (d) C_3'-exo.

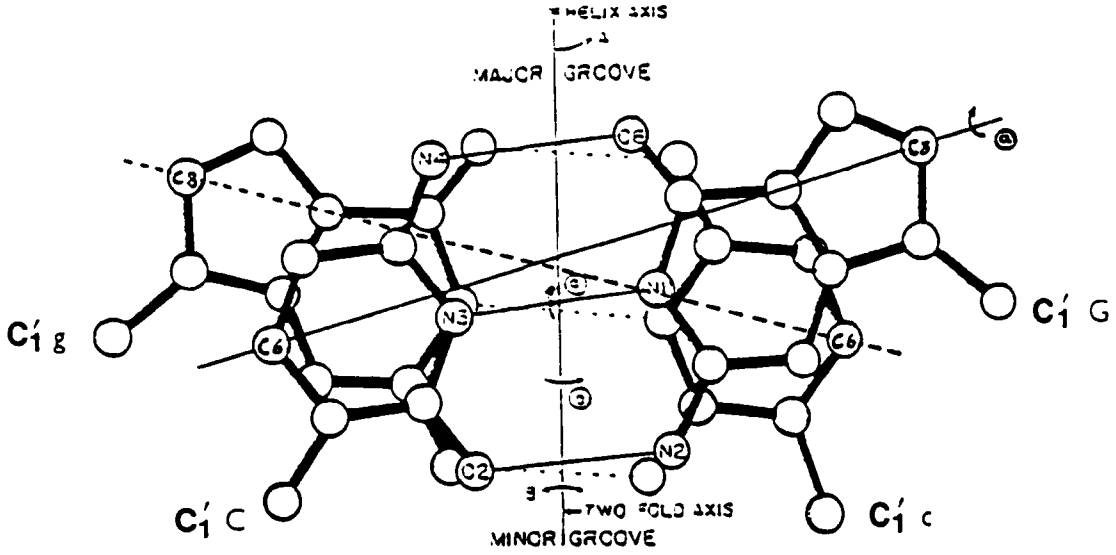

FIGURE 1.4

Two hydrogen bonded base-pairs with the helix axis (*) perpendicular to the plane of the page. The propellor twist (a) is defined as the rotation of the bases relative to each other around the line connecting C6 of a pyrimidine and C8 of a purine (or around the N3-N1 hydrogen bond). The base-pair bend (b) is the rotation of the individual bases in a pair around the pseudo twofold axis in the plane of the bases. The twist (A) is the rotation of a rigid base-pair around the helix axis. The base turn angle is the projection of the vector C_1' C → C_1' G on C_1' c → C_1' g. The tilt (B) is the rotation of a rigid base-pair around the pseudo twofold axis. The roll is the rotation of a rigid base-pair about the C6-C9 pyrimidine-purine line or about the N3-N1 hydrogen bond.

stacking. This results in some hydration water being removed, however the hydrogen bonding sites are taken up by water. Base-pair stacking within the confines of the DNA superstructure results in the further exclusion of water and, under these conditions, hydrogen bonding between the base-pairs is a favourable interaction. The repulsive influence between the negative phosphate groups of the backbone is counterbalanced by interactions with small, positively charged salt ions, such as Na^+ and K^+.

So far the main features of the Watson-Crick model have been examined and the terminology necessary for an accurate description of molecular structure given. DNA, however, does not exhibit a unique arrangement and the molecule may be induced into making transitions between several distinct forms.

From the first X-ray studies on DNA fibres, conducted by Franklin and Gosling (1953) over 30 years ago, it was discovered that the molecule was able to switch between two double-helical forms, A and B, on changing the state of hydration. Subsequent studies varying concentration and type of counter-ion under a range of hydration conditions have yielded further forms. Naturally occurring DNA in the fibre state is found to exhibit A (Fuller *et al.*, 1965), B (Arnott and Hukins, 1973) and C (Marvin *et al.*, 1961) forms (Fig. 1.5a,b,c) while synthetic polymers such as polydeoxyadenylic acid-polythymidylic acid [poly(dA).poly(dT)] and polydeoxyguanylic-deoxycytidylic acid [poly(dG-dC)] have been found in the D and S forms (Mahendrasingam, 1983). Single crystal DNA oligonucleotide segments have so far been observed in A, B and Z forms (Wang *et al.*, 1979). Only the three forms for natural fibre state DNA, A, B and C, shall be discussed.

The B-form is observed under conditions of high humidity and/or high salt. It is thought to be the predominant form in solution and hence in biological systems. The glycosidic bond takes on *high anti* conformation while the backbone angles from α to ζ, of Figure 1.2, are t, $g^{(-)}$, $g^{(-)}$, t, $g^{(+)}$, t respectively (Arnott and Hukins, 1973). The molecule has a 10 base per turn, right handed, helical structure with almost horizontal base-pairs packed in the centre core. It has two equally deep grooves, a wide major one and a narrower minor one.

FIGURE 1.5

Side and end views of (a) A-DNA, (b) B-DNA and (c) C-DNA, with the three side views showing the (i) major and (ii) minor grooves.

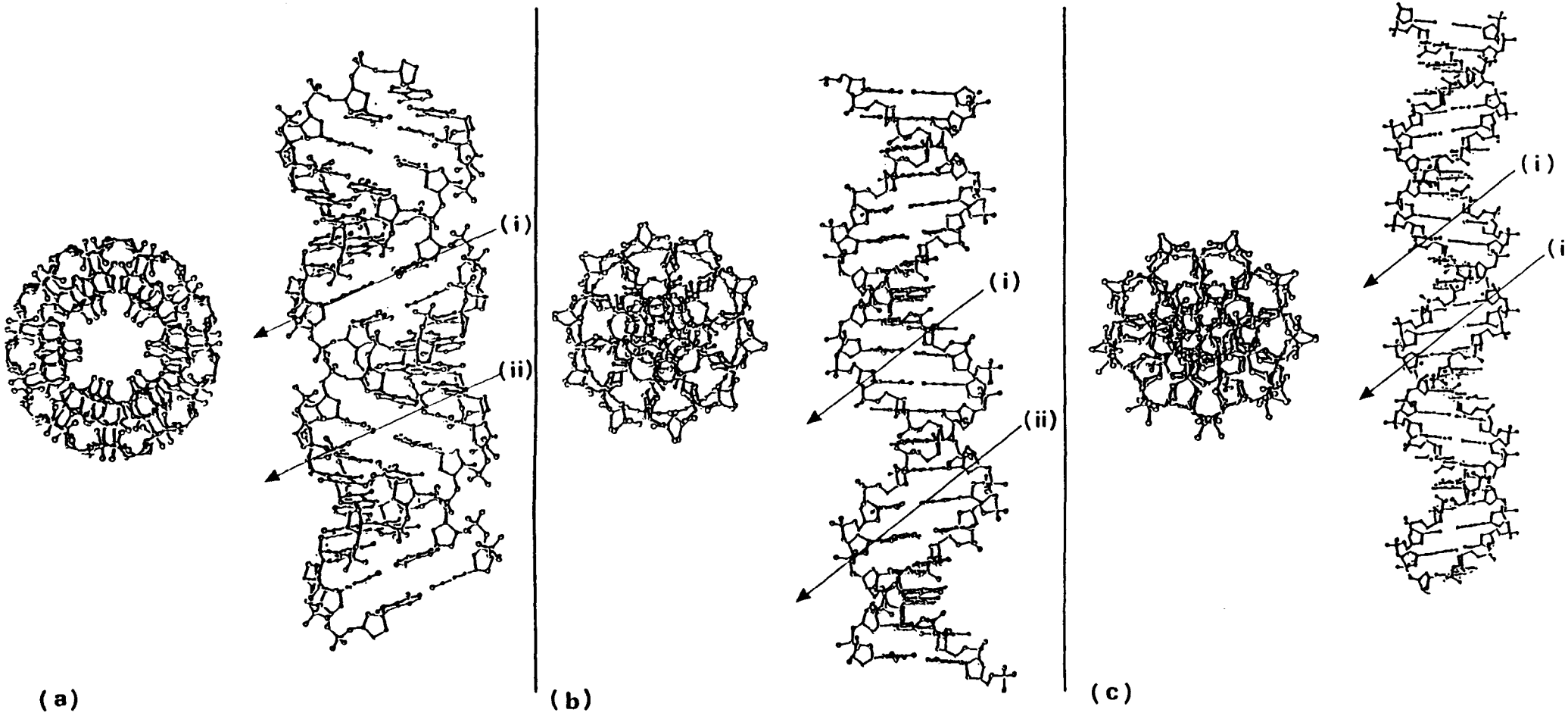

The C-form is similar but with 9.3 bases per turn and the bases are displaced slightly further from the helical axis. In this case the glycosidic angle is *high anti* and the torsion angles are t, t, $g^{(-)}$, t, $g^{(+)}$ and t (Marvin *et al.*, 1961). The C-form, however, exists under opposing conditions compared to B, that is, low salt concentrations and low humidities. The B-form observed from fibres has been found to comprise a family of structures exhibiting small variations dependent on the counter-ion present and type of DNA used (Mahendrasingam, 1983). Since B and C forms show many similarities, the C-form may be considered a member of the B family.

The A-form of DNA is stouter with a very deep, narrow major groove and a shallow, wide minor groove. The base-pairs are more tightly packed with a rise of 2.56 Å and are displaced well away from the helix axis leaving a hollow core. They are also tilted at an angle of 19°. The glycosidic angle is *anti* and the α to ζ torsion angles are t, $g^{(-)}$, $g^{(-)}$, t, $g^{(+)}$ and $g^{(+)}$ (Arnott *et al.*, 1969). Side and end views of the A, B and C forms are shown in Figure 1.5 and their helical parameters are listed in Table 1.I.

The descriptions above refer to the averaged structures obtained from fibre diffraction studies. However, the possibility of small local sequence dependent variations (Klug *et al.*, 1979) must not be excluded. From diffraction work involving a B-DNA dodecamer, the observation of 72 ordered water molecules gave valuable information concerning hydration (Drew *et al.*, 1981; Dickerson and Drew, 1981). A general preference for association with polar nitrogen and oxygen atoms at the exposed edges of the base-pairs was observed. Hydration within the minor groove was ordered, regular and apparently co-operative. A geometric spine was seen filling the groove, often bridging to phosphate oxygens. The presence of purine N2 amino groups had a disruptive influence on the structure. In the case of the major groove order was restricted to a first hydration shell around the polar N and O atoms, other water molecules in the groove were disordered. Structural disorder was also found on the phosphate backbone except in the region of C7 methyl groups on thymine residues.

Work involving studies on natural DNA fibres has shown that under

TABLE 1.I

The Parameters Defining the Three Conformations of Native DNA in Fibres

	CONFORMATION		
	A	B	C
Sugar Pucker	C_3'-endo	C_2'-endo	C_2'-endo
Pitch (Å)	28.2	33.8	31
Bases per Turn	11	10	9.3
Rise per Base-Pair (Å)	2.56	3.4	3.3
Base Tilt Angle	19°	-6°	-8°
Turn per Residue	32.7°	36°	38.6°
Groove Width (Å)			
Minor	11	5.7	4.8
Major	2.7	11.7	10.5
Groove Depth (Å)			
Minor	2.8	7.5	7.9
Major	13.5	8.5	7.5
Displacement D (Å)	4.72	-0.16	-2.13

conditions of low salt, the DNA molecules may be induced to follow the transition pathway C→A→B with increasing humidity (33%→98%) (Mahendrasingam, 1983). The A conformation exists generally over the 66% to 75% range. At intermediate humidities X-ray patterns exhibiting conformation mixtures, (C/A) or (A/B) have been observed. Mahendrasingam has given an explanation of these patterns in terms of the temporal effect of water migration and the possibility of ion concentration gradients within the fibre, so that at intermediate humidities the fibre may be divided into zones of differing environmental conditions and hence structure. The point of transition has been found to be dependent on both base sequence and water activity. Fibre studies have shown that polydeoxyadenylic-thymidylic acid [poly(dA-dT)] remains in the B-form regardless of water content whilst poly(dG-dC) readily switches from B to A on drying. The polymer polydeoxyguanylic acid-polydeoxycytidylic acid [poly(dG).poly(dC)] was found to favour the A-form even at high humidities.

So far DNA molecules have only been considered as static. However, evidence for dynamic fluctuations has come from nuclear magnetic resonance (n.m.r.) studies (Hogan and Jardetzky, 1980) and more recently from the application of translation, libration, screw rigid (TLS) group model to high resolution X-ray data (Holbrook and Kim, 1984). However, due to the additional higher ordered structures found for DNA in the nucleus, any such motion must be considered less likely *in vivo*. Chapter Five investigates the effects of ionizing radiation on such higher ordered structures of DNA, and an account of their structure is given therein.

Indirect Effects of Radiation

In discussions of radiation effects at the molecular level one distinguishes between so-called *direct effects* and *indirect effects*. Somewhat different interpretations of these concepts are found in the literature. However, one definition is that a direct effect is one which is produced in the same molecule in which the primary process took place. In fluid aqueous solutions, indirect effects are caused by diffusable radical products of the radiolysis of water (Dertinger and Jung, 1969).

Since water constitutes about 70-80% of the mass of a cell, it can be

stated that approximately three quarters of cellular ionization events occur in water molecules. The mobile water radicals produced may attack cellular constituents including DNA. Such reasoning has led to a great deal of research being centred on studies of the indirect action of radiation, with ideal conditions for such work being dilute aqueous solutions. Hence, quite obviously, a knowledge of the radiation chemistry of water is indispensable to the understanding of the indirect effects of ionizing radiation.

The radiation induced decomposition of water is now fairly well understood (Schwarz, 1981) and some details are shown in Table 1.II. The absorption of radiation leads to the formation of three short-lived reactive species, the hydrated electron (e^-_{aq}), the hydrogen atom ($H^\cdot$) and the hydroxyl radical ($^\cdot OH$). These radical products are formed by the processes of ionization and excitation. The microscopic distribution of these primary species is not uniform, despite a homogeneous macroscopic appearance of their action, with most ionization events being distinct and separated from each other by about 500 nm. A proportion of the total ionization events appear in clusters. Two sorts of clusters have been identified "spurs" (Mozumder and Magee, 1966) and "blobs" (Chatterjee and Magee, 1985), with the former being the product of lower energy depositions (<100 eV) and the latter of higher depositions (100-500 eV). For γ-rays and high energy electrons the energy is essentially all deposited in spurs (80%) and blobs (20%). Due to the non-homogeneity of energy loss, recombination between the reactive species can occur resulting in molecular products, i.e. hydrogen and hydrogen peroxide, see Table 1.II. For γ-radiation the sum of the yields of the various molecular products (given in G-values, molecules or radical species or events per 100 eV) are lower than that of the radical products and the $H^\cdot$ atom yields are lower than that of e^-_{aq} or $^\cdot OH$.

Some of the reactions of $^\cdot OH$, $H^\cdot$ and e^-_{aq} are given in Table 1.III. Abstraction is usually from a C-H bond and addition occurs at olefinic or aromatic centres. Both result in organic free radical formation. The hydrated electron, a reactive nucleophile, may react with a carbonyl moiety or a conjugated system to yield radical anions which can then protonate. These organic free radicals are themselves short-lived for

TABLE 1.II

Action of Ionizing Radiations on Water

$$H_2O \xrightarrow{\gamma} e^-_{aq},\ H^{\cdot},\ {}^{\cdot}OH,\ H_3O^+,\ H_2,\ H_2O_2$$

Radical products

$$H_2O \xrightarrow{\gamma} H_2O^{\cdot +} + e^-$$

$$e^- + nH_2O \rightarrow e^-_{aq}$$

$$H_2O^{\cdot +} + H_2O \rightarrow {}^{\cdot}OH + H_3O^+$$

$$H_2O \rightarrow H_2O^* \rightarrow H^{\cdot} + {}^{\cdot}OH$$

$$e^-_{aq} + H_3O^+ \rightarrow H^{\cdot} + H_2O$$

Molecular products

$$H^{\cdot} + H^{\cdot} \rightarrow H_2$$

$$e^-_{aq} + e^-_{aq} \xrightarrow{2H_2O} H_2 + 2OH^-$$

$$e^-_{aq} + H^{\cdot} \xrightarrow{H_2O} H_2 + OH^-$$

$${}^{\cdot}OH + {}^{\cdot}OH \rightarrow H_2O_2$$

Yields

Species:	e^-_{aq}	$H^{\cdot}$	${}^{\cdot}OH$	H_3O^+	H_2	H_2O_2
G :	2.7	0.55	2.7	2.7	0.45	0.7

[G = molecules per 100 eV]

TABLE 1.III

Formation and Reactions of Organic Free Radicals

Abstraction

$$RH + {}^{\cdot}OH(H^{\cdot}) \rightarrow R^{\cdot} + H_2O(H_2)$$

Addition

$$R + {}^{\cdot}OH(H^{\cdot}) \rightarrow \dot{R}OH(\dot{R}H)$$

Nucleophilic attack by e^-_{aq}

$$R + e^-_{aq} \rightarrow R^{\cdot -} \overset{H^+}{\leftrightharpoons} \dot{R}H$$

Dimerisation

$$2R^{\cdot} \rightarrow R_2$$
$$2\dot{R}OH \rightarrow (ROH)_2$$

Dismutation

$$2R^{\cdot} \rightarrow RH + \text{product}$$
$$2\dot{R}OH \rightarrow R\text{-}OH + \text{product}$$
(H)

Oxidation

$$R^{\cdot}(\dot{R}OH) + Ox \rightarrow R^+(ROH^+) + Ox^-$$

[Ox = oxidant]

$$R^{\cdot}(\dot{R}OH) + O_2 \rightarrow RO_2^{\cdot}(ROHO_2^{\cdot})$$

Reduction

$$R^{\cdot}(\dot{R}OH) + R'SH \rightarrow RH(R\text{-}OH) + R'S^{\cdot}$$
(H)

they contain an unpaired electron and subsequently react to satisfy their own valence requirements (Table 1.III). Interception of the organic radicals, for instance, by an oxidant or molecular O_2 can result in carbocation and peroxy radical formation respectively. Such action may prevent restitution processes and is one of the factors involved in radiobiological sensitization. Alternatively, reduction of the organic radical can result in restitution and will, of course, be relevant to radioprotection.

With three reactive water species being present on radiolysis, it is clear that the radiation chemistry of aqueous systems can become quite complex, particularly in cases where the solute reacts with all three species. However, through the use of selective scavengers the system can be greatly simplified (Table 1.IV) and it is possible to study each component in isolation.

A method commonly employed in the monitoring of indirect action towards DNA is chemical analysis of the various products, both released and bound, to determine their structural nature and yield. With a complicated biomolecule like DNA this can present formidable problems. Hence, quite often, simple model compounds have been used, i.e. sugars (Bothe *et al.*, 1978; Schuchmann and von Sonntag, 1977; von Sonntag and Dizdaroglu, 1977), phosphoric acid esters (Behrens *et al.*, 1978; Steenken *et al.*, 1974), sugar phosphates (Stelter *et al.*, 1975a,b), nucleosides (Dizdaroglu *et al.*, 1976), nucleotides (Cadet *et al.*, 1974; Ducolomb *et al.*, 1974; for reviews, see von Sonntag, 1980 and von Sonntag and Schulte-Frohlinde, 1978) and homologous polynucleotides (Schulte-Frohlinde *et al.*, 1985a; Akaboshi *et al.*, 1985), in the hope of explaining the transformation undertaken by DNA on irradiation in aqueous solution. The analysing techniques employed include, amongst others, high performance liquid chromatography (HPLC) (Belfi *et al.*, 1986; Fuciarelli *et al.*, 1986), thin layer chromatography (TLC) (Cadet *et al.*, 1983b), gas liquid chromatography-mass spectroscopy (GLC-MS) (Dizdaroglu *et al.*, 1975b), and ^{13}C and ^{1}H n.m.r. spectroscopy (Berger *et al.*, 1985; Hruska *et al.*, 1985). The majority of these techniques require the synthesis of the altered molecules for use as standards in absolute assignment. A biochemical technique that has proved to be most informative is enzymatic end group analysis. This determines the

TABLE 1.IV

Radiolysis of Aqueous Solutions: Use of Selective Scavengers

	Additive	Reaction	Active Species
a.	Acid	$e^-_{aq} + H^+ \rightarrow H^\cdot$	$H^\cdot, {}^\cdot OH$
b.	Oxygen	$e^-_{aq} + O_2 \rightarrow O_2^{\cdot -}$	
		$\Downarrow H^+$	${}^\cdot OH, HO_2^\cdot, O_2^{\cdot -}$
		$H^\cdot + O_2 \rightarrow HO_2^\cdot$	
c.	Nitrous oxide	$e^-_{aq} + N_2O \xrightarrow{+H_2O} {}^\cdot OH + OH^- + N_2$	${}^\cdot OH(H^\cdot)$
d.	Nitrous oxide + oxygen	*c* + *b*	${}^\cdot OH(HO_2^\cdot, O_2^{\cdot -})$
e.	${}^\cdot OH$ scavenger	$RH + {}^\cdot OH \rightarrow R^\cdot + H_2O$	$e^-_{aq}(H^\cdot)$
f.	${}^\cdot OH$ scavenger + acid	*e* + *a*	$H^\cdot$

biochemical reactivity of the end groups on the 3′ and 5′ termini of the strand breaks (Lennartz *et al.*, 1975; Bopp and Hagen, 1970; Henner *et al.*, 1983a,b). Enzymatic methods are considered more sensitive than chemical analysis, but both approaches have proved useful in determining the mechanisms of indirect damage towards DNA (von Sonntag *et al.*, 1981).

A physical technique commonly used to study the indirect action of radiation is pulse radiolysis which was pioneered in this country by Boag (1963) and Keene (1964). A pulse of high energy electrons (nanosecond duration) is delivered to the system and by suitable detection techniques, i.e. optical (Fujita and Steenken, 1981), conductimetric (Bothe and Schulte-Frohlinde, 1982), or laser light scattering (Washino and Schnabel, 1982), the formation and/or decay or radical transients (or products) can be followed over very short periods of time, i.e. over pico- or nanosecond timescales.

As mentioned earlier the radiation induced lethal lesion is considered by many to be the DNA d.s.b., and it has been the aim of a number of research groups, using the techniques outlined above, to establish the mechanism of DNA strand breakage under conditions of indirect damage.

Several released base and phosphate free sugars have been identified upon γ-irradiation of N_2O saturated aqueous solutions of DNA (Fig. 1.6a) (Dizdaroglu *et al.*, 1975b). Not only were these sugars found in the free form but also bound to DNA strands *via* phosphate ester linkages, as end groups of broken DNA chains (Fig. 1.6b) (Beesk *et al.*, 1979). All the sugars share the property of being oxidized at the C_4' position. Hydrogen atom abstraction was therefore assumed to be the primary reaction leading to these sugars, with the DNA C_4' radical (7) being the all important precursor (see Fig. 1.7). From studies involving model reactions for the degradation of DNA C_4' radicals (Behrens *et al.*, 1982), reaction schemes professing the mechanisms of C_4' radical decay, resulting in the observed structures (1→6) (and hence strand breakage), have been put forward (Fig. 1.7). The initial step is considered to be the hydrolysis of the α-alkoxyalkyl C_4' radical (7) *via* either the 4′-3′ radical cation or 4′-5′ radical cation, formed *via* the elimination of the 3′ or 5′ phosphate moiety respectively. With the ensuing entry of

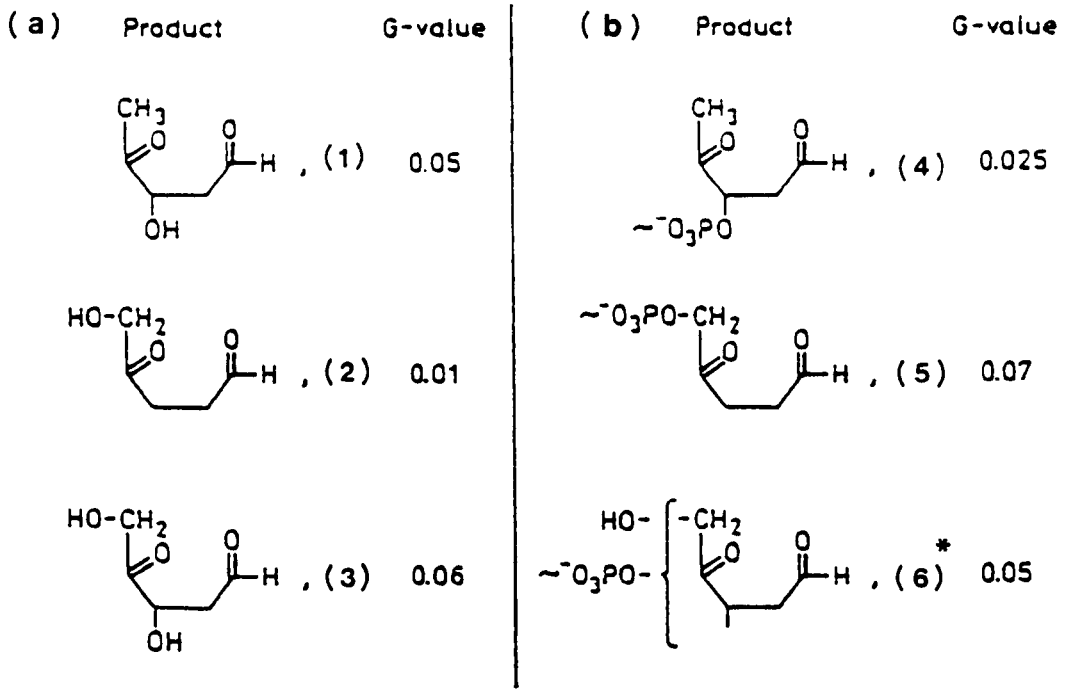

FIGURE 1.6

Products, both (a) released and (b) bound, identified upon γ-irradiation of N_2O saturated aqueous solutions of DNA and their G-values (number of molecules or end groups formed per 100 eV of energy absorbed by the solution). [* Site of OH and remaining strand, $-OPO_3^-$~ is not exactly known.]

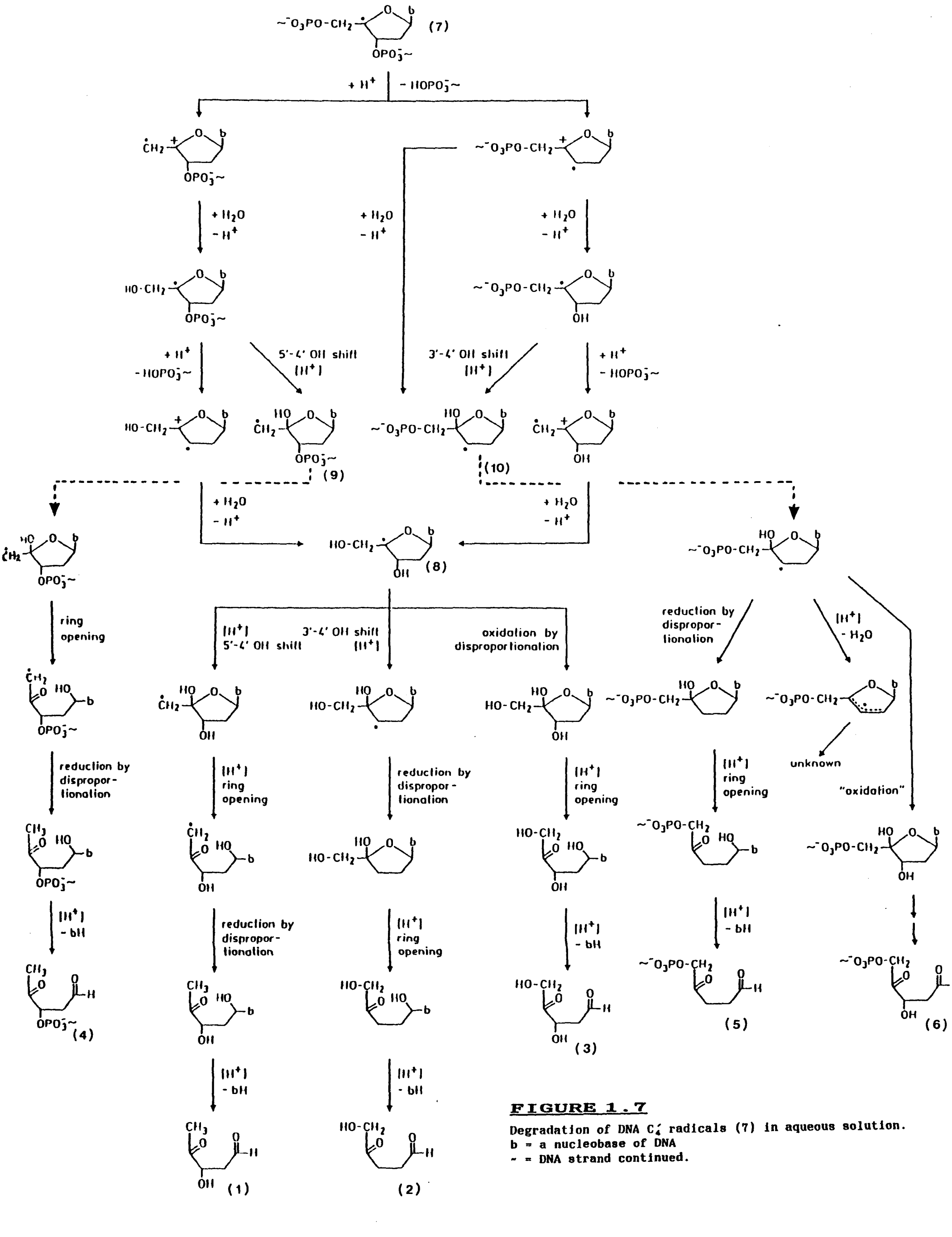

FIGURE 1.7

Degradation of DNA C_4' radicals (7) in aqueous solution.
b = a nucleobase of DNA
~ = DNA strand continued.

OH^- being regiospecific, a second round of hydrolysis may occur resulting in the common radical (8), the proposed precursor of the base and phosphate free sugars (1), (2) and (3) (Fig. 1.7). Alternatively, particular OH shifts may occur resulting in radicals (9) and (10), precursors of the end group base free sugars (4) and (5), (6) respectively (Fig. 1.7). These latter OH shifts are dependent on there being a sufficient proton concentration at the DNA. However, with there being protons released upon hydrolysis of the carbocations, and knowing that the proton density in the vicinity of a strand of nucleic acid is higher than that of the bulk solution (Manning, 1979), these rearrangements are considered viable.

From model studies (Behrens *et al.*, 1978) the β-elimination of the phosphate moiety from C_3' of (7) should be faster than the corresponding elimination from C_5'. This was at first supported by quantitative data from the enzymatic analysis of the end groups, see Figure 1.6 (von Sonntag *et al.*, 1981). However, with the possibility of rearrangement reactions [OH shifts or even phosphate shifts (Behrens *et al.*, 1978)] altering the proportions of products once thought indicative of 3' or 5' phosphate elimination (von Sonntag *et al.*, 1981), such conclusions can no longer be taken as totally valid.

Under oxygenated conditions the principle primary species of water radiolysis are $^{\cdot}OH$, the hydroperoxide radical ($HOO^{\cdot}$) and its anion ($O_2^{\cdot -}$) (Table 1.IV), the latter two being in equilibrium. The $O_2^{\cdot -}$ radical is not very reactive and is not reported to produce DNA strand breaks (Blok and Loman, 1973). However it may contribute in redox reactions. $^{\cdot}OH$ mediated abstraction reactions from sugars are followed by diffusion controlled addition of oxygen. The C_4' radical may eliminate at least the C_3' phosphate prior to oxygen addition, so the C_4' peroxyl radical, as such, is not expected to form in appreciable yield. In oxygenated environments the formation of the phosphate and base free sugars (1) and (2) were suppressed. However in addition to (3) a further altered sugar, 2'-deoxy-tetrodialdose, (11) was observed both free and as a 5'-end group derivative (12) (Dizdaroglu *et al.*, 1975a). The proposed mechanism for their formation is shown in Figure 1.8 and the individual single steps are supported by reactions found in model systems (Stelter *et al.*, 1975a; Howard, 1973). An interesting aspect of the mechanism

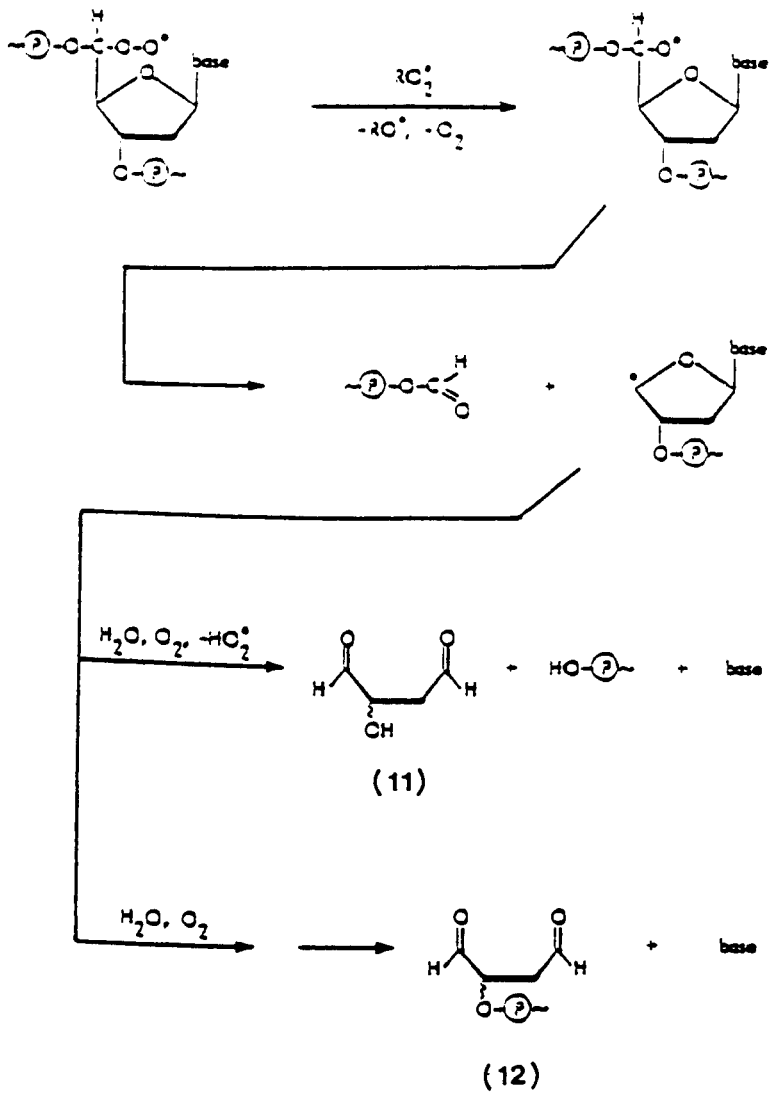

FIGURE 1.8

Mechanisms to account for free 2-deoxy-tetrodialdose (11) and the 5' end group (12), noted on γ-irradiation of DNA under oxic aqueous conditions.

shown is that chain breakage is *via* a C-C scission. No mechanism for the formation of the other products has as yet been offered.

The above reactions can also account for base release noted on irradiation of DNA in solution (Ullrich and Hagen, 1971; Ward and Kuo, 1976). A consequence of base release is the generation of altered sugars which do not immediately lead to strand breaks but which do so on alkali treatment (alkali labile sites). Two such sites are the 2'-deoxy-D-erythropentonolactone subunit (13) and the D-erythrose site (14) (Table 1.V) (Dizdaroglu *et al.*, 1977a,b). They are believed to be the products of H$^{\cdot}$ abstraction from C_1' and C_2' respectively (see below).

Despite the importance attributed to the C_4' radical mechanism, abstraction from the sugar moiety is random (cf. Schuchmann and von Sonntag, 1977) and other radicals generated at the other carbon atoms must be considered. Table 1.V lists both the bound and free altered sugars so far recognized on γ-radiolysis of oxygenated and deoxygenated DNA solutions, and denotes the precursor carbon centred sugar radical. From this it can be generally stated that at neutral pH strand breaks are formed from C_4' radicals under both oxic and anoxic conditions. However under oxic conditions an additional route to strand breakage *via* the C_5' peroxyl radical is available.

An important factor concerning indirectly produced DNA strand breaks arises from the fact that ~80% of the $^{\cdot}$OH radicals react with the bases (Scholes *et al.*, 1960; Jung *et al.*, 1969; Hoard *et al.*, 1974) as probably do almost all of the H$^{\cdot}$ atoms (Dizdaroglu *et al.*, 1975b; cf. Deeble and von Sonntag, 1984). From work involving measurement of radiation induced main chain scission of polyuridylic acid [poly(U)] in aqueous solution (Lemaire *et al.*, 1984), it was found that ~41% of the $^{\cdot}$OH radicals and 19% of the H$^{\cdot}$ atoms reacting with the polymer resulted in strand break formation. On the basis that only ~20% of $^{\cdot}$OH and less than 5% of H$^{\cdot}$ attack the ribose moiety, the large G(s.s.b.)-value of 2.3 could not be explained as solely resulting from radicals produced by the reaction of $^{\cdot}$OH or H$^{\cdot}$ with the sugar moiety. It was therefore proposed that base radicals, produced by the reaction of $^{\cdot}$OH radicals or H$^{\cdot}$ atoms with the uracil moiety, could also lead to chain breakage *via* radical transfer from the base to the sugar moiety. Similar mechanisms

TABLE 1.V

Alterations at the sugar moiety on γ-radiolysis of DNA in deoxygenated and oxygenated solutions and site of precursor radicals

Anoxic	Oxic	Precursor radical at
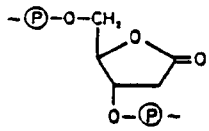 (13)		C'_1
	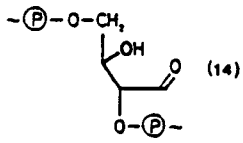 (14)	C'_2
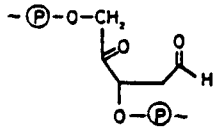 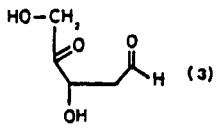 (3) 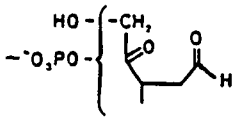 (6) 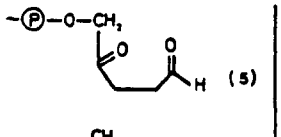 (5) 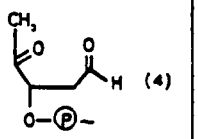 (4) 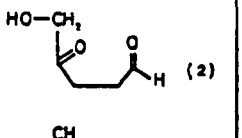 (2) 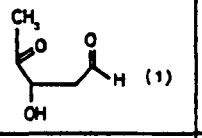 (1)	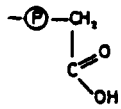	C'_4
	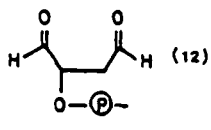 (12) 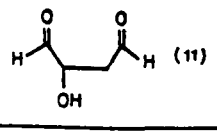 (11)	C'_5

involving base radical adducts have been proposed to explain the high yield of base release noted (G = 2.9) for poly(U) (Deeble and von Sonntag, 1984). Further studies concerning sites of ·OH radical attack and kinetics of strand breakage and base release have been conducted for poly(U) under both deoxygenated and oxygenated conditions (Deeble *et al.*, 1986; Deeble and von Sonntag, 1986; Bothe *et al.*, 1986). Under anoxic conditions it was proposed that it was, to a greater extent, the C_5OH (6-yl radical) base adducts that transfer spin to the sugar by abstracting a hydrogen atom from C_4' or C_2' of the ribose moiety, whilst under oxic conditions it was a base peroxyl radical that abstracts the ribosyl hydrogen.

Mechanisms discussed so far result, in isolation, in single strand breaks. However, as already mentioned, the lethal lesion is considered to be the DNA d.s.b. So how do double strand breaks arise *via* the indirect mechanism? One possibility is that they are the products of multiple radical attack in regions of high local radical density, i.e. spurs (Ward, 1981). In such instances hydrogen atom abstraction, either ·OH or base mediated, occurs from two deoxyribose moieties in close proximity on opposing strands and both deoxyribose radicals react to form strand breaks. D.s.b. formation in this instance would rise linearly with dose. However in dilute aqueous solutions the possibility of a spur overlapping with DNA is considered slight. A second possibility is that d.s.b's occur by two ·OH radicals, independently produced, migrating to the DNA and reacting within 12 base-pairs (b.p.) of each other.† In such cases, a dose-squared dependence for d.s.b. formation would be found. However it has been calculated (Chaterjee and Magee, 1985) that the probability of two ·OH radicals from two tracks (or even the same track) reaching sugars on different strands within 12 b.p. is almost non-existent ($<10^{-6}$). Also the d.s.b's formed (in a companion experimental programme) were found to be linearly dependent on dose. This evokes a mechanism where d.s.b. formation is from single ·OH attack, however, no mechanism was given.

---

† It is presumed that two breaks on opposite strands within 10-12 base pairs will behave as a double strand break, while two breaks further apart than about 10-12 base-pairs will behave as two independent single strand breaks. Clearly this also depends on G-C content.

Direct Effects of Radiation

The second mode through which radiation can act is *via* direct action. In contrast with indirect action, the direct mechanism results in the formation of electron-gain and electron-loss centres in the DNA itself. The probability of having a distinct ionization of DNA in dilute aqueous solution is low (ionization fraction ≈ mass fraction) (Inokuti, 1983). Nevertheless attempts have been made to measure the direct effects of radiation in aqueous solutions using high concentrations of scavenger to screen out a significant proportion of the indirect effects (Freifelder, 1965). However such conditions, referred to as fully protective in terms of indirect damage, were found to be far from satisfactory (Ward, 1975). More recently, a second method of studying direct damage in aqueous solution has been reported. This involved laser photoionization of poly(U) (Schulte-Frohlinde *et al.*, 1985b) in anoxic solutions. A biphotonic process results in the specific ionization of the uracil moiety, which is then followed by single strand break formation. It was proposed that the ionized uracil moiety lead eventually to the same chemical pathway for s.s.b. formation as that induced by ·OH radicals.

The systems most commonly used to study direct damage to DNA comprise of either "dry" DNA† or frozen aqueous solutions, and a physical method prominent in monitoring the direct damage mechanism in these systems is e.s.r. spectroscopy. In the frozen aqueous system the majority of water molecules are present in ice crystallites and the concentration of water remaining with the DNA is low, probably only enough to solvate the anions and cations and residual non-hydrogen bonded groups (Mathur de Vré and Bertinchamps, 1977; Mathur de Vré *et al.*, 1976; Mathur de Vré, 1979). When additives are included the growing ice crystallites tend to exclude the molecules or ions such that they tend to become part of the solvated DNA phase, even when the additive shows little tendency to bind to the DNA. Radiation will, of course, damage the ice crystals, but the radical species produced are contained therein and do not effect the DNA (Gregoli *et al.*, 1982). At 77 K the only remaining magnetic centres of water damage detected by e.s.r. are ·OH radicals. However by 130 K they

† 15-20% bound water

have become mobile and react amongst themselves to yield H_2O_2 molecules.†

Direct radiation damage to the DNA phase in frozen aqueous solutions must initially result from an indiscriminate ionization of all the components of the DNA phase, the solvating water, phosphate [$(RO)_2PO_2^-$] units, the deoxyribose moieties and the bases; and the likely sites to trap the ejected electron are the $(RO)_2PO_2^-$ units and the stacked pyrimidine bases. However the DNA damage formed in frozen aqueous solutions at 77 K is remarkably simple, the products being only the guanine radical cation ($G^{\cdot+}$) and the thymine radical anion ($T^{\cdot-}$) (Figure 1.9) (Sevilla, 1977; Gregoli *et al.*, 1982). No radicals indicative of sugar or phosphate species were detected despite the fact that sugar radicals have been reported as electron-loss species in mononucleotides (Box and Budzinski, 1975; Bernhard *et al.*, 1976). Also it is surprising that $T^{\cdot-}$ should be formed exclusively since in studies involving co-stacking mononucleotides it was noted that the end point of electronic migration was the cytosine base (Gregoli *et al.*, 1979). It was proposed that conjugation of the π-orbitals of complementary bases within the DNA superstructure modifies the relative energy of the lowest unoccupied molecular orbital (LUMO) of T and C, thus modifying their relative electron affinities. Loss of electrons from solvating water gives $H_2O^{\cdot+}$, but under these conditions, instead of deprotonation to yield $^{\cdot}OH$ radicals, such "structured water" behaves by producing positive holes and electrons that migrate to the DNA (Gregoli *et al.*, 1982; Bakale and Gregg, 1978). Such a transfer is termed "dry charge" transfer†† and has been shown to enhance DNA primary damage (Gregoli *et al.*, 1982). The e.s.r. evidence for $G^{\cdot+}$ and $T^{\cdot-}$ being present in γ-irradiated frozen aqueous solutions of DNA, is based on careful computer techniques which involved the precise reconstruction of experimental spectra using the authentic e.s.r. patterns of these radicals (Gregoli *et al.*, 1982). Studies yielding similar results have been conducted using spun DNA

---

† In forthcoming chapters "130 K spectra" will be referred to. These are e.s.r. spectra of γ-irradiated frozen aqueous samples, recorded at 77 K, after warming to 130 K to remove bulk water $^{\cdot}OH$ e.s.r. features.

†† Though dry charge transfer may constitute indirect damage (*via* the involvement of surrounding water), since it results in products typical of direct energy deposition (i.e. $G^{\cdot+}$ and $T^{\cdot-}$) it is considered a direct effect.

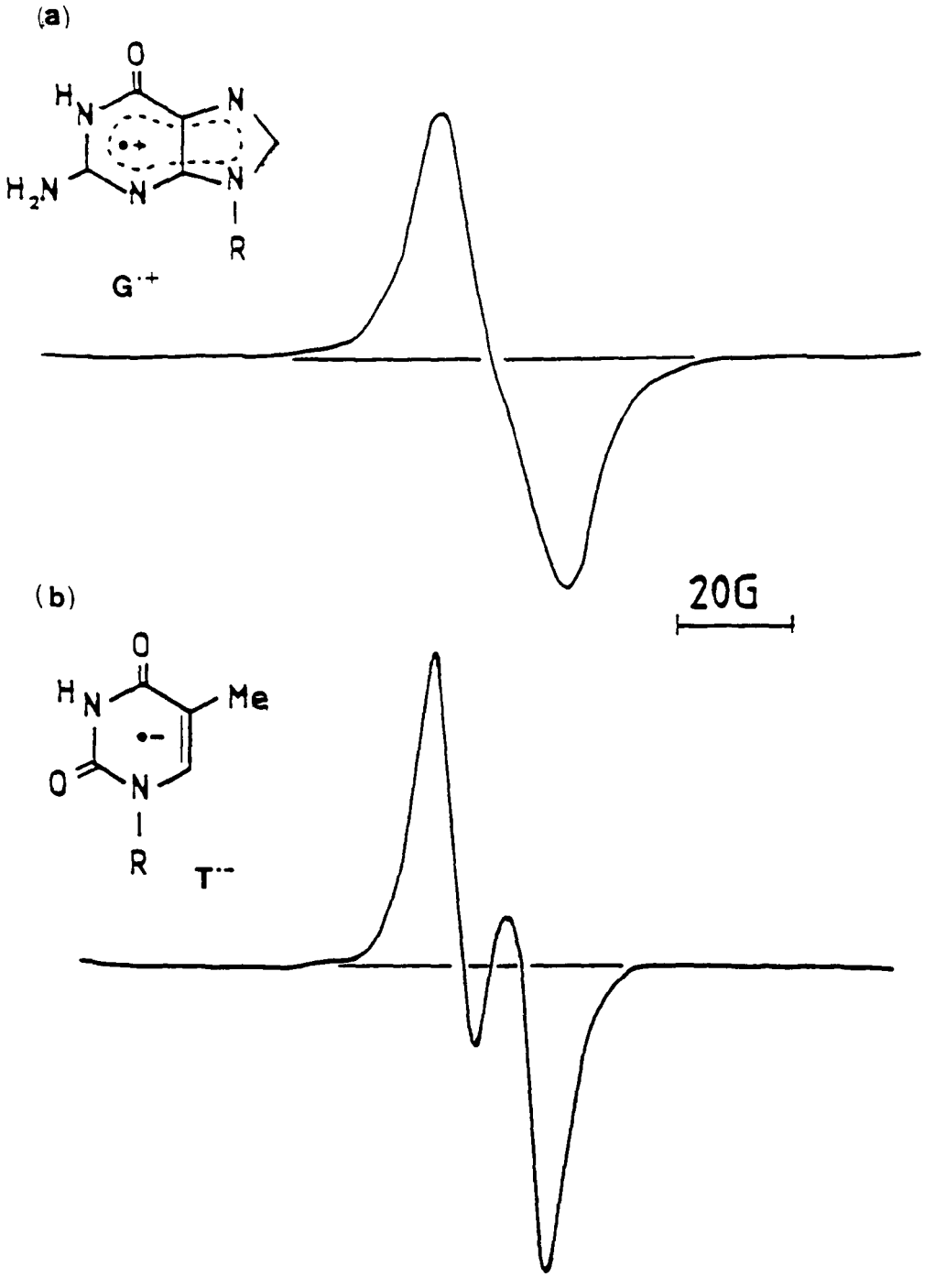

FIGURE 1.9

Chemical structure and e.s.r. profile of (a) the guanine radical cation, $G^{\cdot+}$, and (b) the thymine radical anion, $T^{\cdot-}$.

ribbons which were strongly orientated along the major axis (Gräslund *et al.*, 1971; Hüttermann *et al.*, 1984).

The homogeneity of the DNA signals as determined by e.s.r. studies indicates that, in all cases, the primary sites of electron-loss must undergo electron transfer, possibly by a tunnelling mechanism, thus allowing the 'hole' to migrate to the guanine base. Similarly the ejected electron migrates to thymine. Two proposals for the mode of charge migration have been put forward. The first is that the electron transfer, which effectively constitutes both migrations (positive 'hole' and electron), occurs *via* the stacked bases. As already mentioned, during freezing the growing ice of frozen aqueous solutions tends to eject solute molecules which consequently form aggregates of very high concentration in the interstices of the crystal. The DNA aggregates have a well ordered structure, with the "planar" aromatic DNA bases, the vertical stacking and horizontal hydrogen bonding contributing to their formation (Montenay-Garester *et al.*, 1976). The configuration of these aggregates provides a good overlap of π-orbitals and permits intramolecular energy and charge migration phenomena to occur (Gregoli *et al.*, 1977a, 1979 and 1982; Sevilla, 1977).

However no electron migration from adenine to 5-bromouracil was reported by Bernhard (1981) or Kar and Bernhard (1983) in X-irradiated co-crystals of the two components, even though the geometry of the two moieties in the crystal was similar to those of DNA and should have favoured charge migration. Furthermore, transient electrical conductivity after the application of an electron pulse of a few MeV was found only in samples of DNA at low temperatures when the DNA contained at least 20% water (Verberne *et al.*, 1978; Warman *et al.*, 1980; van Lith *et al.*, 1983). The authors concluded that it was the dry electrons which causes the conductivity, and that these travel through the thin layer of ice-like water that surrounds the DNA. The hydrating water may have a rôle in charge transfer in fully hydrated DNA and it certainly does influence radiolytic action in DNA. However it should be pointed out that reducing the extent of hydration of DNA to below 20% breaks up the double helix. Such action could disrupt the base π-orbital overlap so preventing base mediated charge transfer and account for the lack of conduction observed at low hydration. Additional support for the base

mediated conduction of charges comes from dry studies that investigated spin transfer in irradiated nucleotide co-complexes (Gregoli *et al.*, 1970a,b). In these studies e.s.r. spectroscopy showed that the spins (electronic), induced by the γ-irradiation of equimolar complexes between purine and pyrimidine nucleotides, localize preferentially on the pyrimidine moiety. Considering the way the molecules are associated in these complexes, it was suggested that spin migration occurs vertically *via* the stacked bases with transfer of the electron towards the nucleotide having the empty molecular orbital of lowest energy.

The radical ions $T^{\cdot -}$ and $G^{\cdot +}$ are stable at 77 K and constitute the primary damage to DNA. Normally in hydrated DNA these ionic species are present in almost equal yields. This is also true of dry DNA and DNA ribbons, except that for the latter case careful double integration studies suggest that the yields are not exactly equal and that the ratios of $G^{\cdot +}$ and $T^{\cdot -}$ vary somewhat with different types of DNA (Hüttermann *et al.*, 1984). These inequalities were never explained and would require the presence of other cations and anions which were not detected. However the differences are not large, so for most purposes the yields of $G^{\cdot +}$ and $T^{\cdot -}$ are considered equal.

When the temperature of an irradiated frozen aqueous solution of DNA is increased, the respective yields of the initial DNA ionic radicals decreases, as both radicals enter conversion reactions. In the absence of oxygen protonation of $T^{\cdot -}$ at C6 generally proceeds on annealing to give the well established eight-line e.s.r. spectrum of 5,6-dihydro-5-thymyl radicals ($\dot{T}H$) (Fig. 1.10) (Lenherr and Ormerod, 1968; Gregoli *et al.*, 1982). In an e.s.r. based kinetics study (Gräslund *et al.*, 1975) this conversion was described by a model in terms of a fractional first (or pseudo-first) order reaction between spatially correlated pairs of $T^{\cdot -}$ and XH^{+} with a distribution of activation energies.

Whilst $T^{\cdot -}$ enters an e.s.r. observable conversion reaction, $G^{\cdot +}$ decays, in frozen aqueous solution, without accumulation of any secondary neutral radical that can be readily distinguished from the original singlet by e.s.r. spectroscopy (Gregoli *et al.*, 1982). However a recent study using oriented fibres suggests that $G^{\cdot +}$ converts at ~220 K, *via* loss of a proton from nitrogen, to a neutral radical, symbolised as $G\dot{N}$,

FIGURE 1.10

Chemical structure and e.s.r. profile of the 5 -thymyl radical $\dot{T}H$.

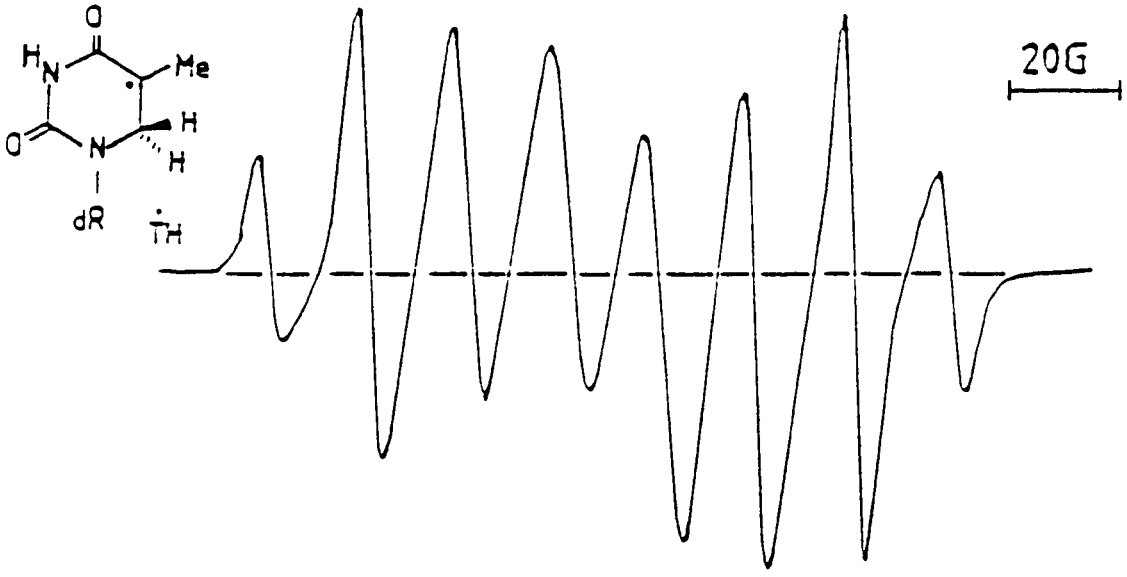

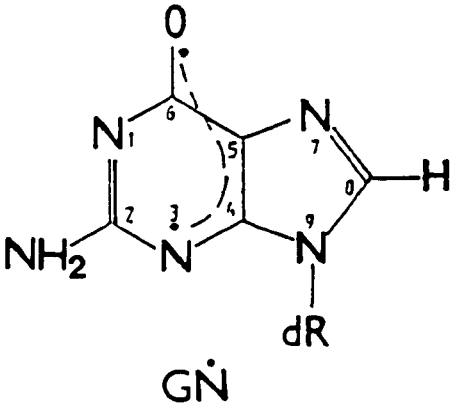

FIGURE 1.11

The radical GṄ.

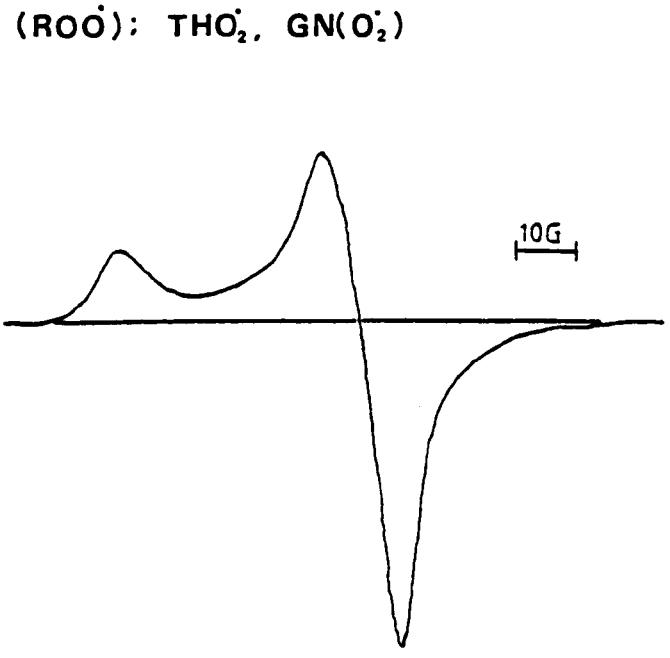

FIGURE 1.12

The e.s.r. profile for peroxyl radicals.

with a high spin-density localized on nitrogen (N3) (Fig. 1.11) (HÜttermann and Voit, 1986). The fact that no successor radical to $G^{\cdot+}$ has been reported in frozen aqueous systems is probably due to the extreme spectral similarity of $G^{\cdot+}$ and $\dot{G}N$ in these "powder"-type systems. Under oxic conditions $\dot{T}H$ radicals rapidly convert to peroxyl radicals ($RO_2^{\cdot}$) (Fig. 1.12) whilst $G^{\cdot+}$ (*via* $\dot{G}N$) probably also give $RO_2^{\cdot}$ radicals (Gregoli *et al.*, 1982; Boon *et al.*, 1984, 1985).

It has been shown under conditions where only $G^{\cdot+}$ and $T^{\cdot-}$ are detected by e.s.r. spectroscopy, that single and double strand breaks occur to significant levels on raising the temperature (Boon *et al.*, 1984). It was also concluded that since the radicals in the ice phase were lost at 130 K, well below the melting point, the strand breaks detected under these conditions must have arisen from the decay of the primary ionic DNA radicals. Furthermore these studies indicated that both $G^{\cdot+}$ and $T^{\cdot-}$ were potential precursors of strand breaks and that some 35-40% of these base radicals acted to give main chain scission. Unfortunately e.s.r. studies have failed to detect the subsequent radical intermediates that must be involved in strand break formation. As mentioned above $T^{\cdot-}$ converts to $\dot{T}H$ on warming and these decay over 208-250 K with no clear e.s.r. evidence for the generation of other trapped radical species. Similarly $G^{\cdot+}/\dot{G}N$ decays without any further detectable species being formed. In particular there was no evidence of sugar centred radicals, suspected intermediates in reactions leading to strand breaks. An explanation for this was that any sugar radicals formed on warming were rapidly lost. This was because they were stable only at low temperatures and decayed at temperatures well below those at which the normal DNA signals were lost (Cullis *et al.*, 1985a).

Under conditions of direct irradiation it has been proposed that strand breaks arise from base radicals *via* base radical mediated intramolecular hydrogen atom abstraction from the adjacent deoxyribose units (Cullis *et al.*, 1985a; Cullis and Symons, 1986; Schulte-Frohlinde *et al.*, 1985a,b). For poly(U) one of the sites of abstraction, as for indirect damage, was suggested as being the C_4' hydrogen atom (Schulte-Frohlinde *et al.*, 1985a,b). Though it has been postulated that this is also the site of base mediated abstraction for DNA, the topological constraints imposed by the double helix dictates that this is unlikely and that

other sites, at least for an initial abstraction, must be considered. Interestingly the chirality of DNA isolated 5,6-dihydrothymidine (TH_2), the expected product of $\dot{T}H$ mediated hydrogen atom abstraction, has been found to be R about the C5 atom (Fig. 1.13) (Furlong *et al.*, 1986). This is in accordance with the constraints imposed by the DNA super-structure, where the closest available sugar hydrogen atoms are in positions, such that, on abstraction they would yield the R-conformer of TH_2 (P. M. Cullis, G. D. D. Jones and M. C. R. Symons, unpublished results). From the sugar radicals thus formed, strand breaks could occur by reactions analogous to those proposed for indirect action.

As stated above the proposed lethal cellular lesion, the DNA d.s.b., was observed on irradiation of frozen aqueous systems. The extent of formation was noted to be several orders of magnitude greater than could be accounted for by the coincidence of two independent s.s.b's (Boon *et al.*, 1984). To account for this it was proposed that both $G^{\cdot+}$ and $T^{\cdot-}$ were precursors for strand breaks and that it was a frequent event for two of these centres to be trapped and react, to yield strand breaks on opposite strands within twelve base-pairs of each other. It is envisaged that this may occur by spur formation both in the DNA and hydration water resulting in a relatively high local density of DNA base radicals, a proportion of which would be situated close enough to each other, on opposite strands, to result in d.s.b. formation.

In γ-irradiated frozen aqueous solutions of DNA, oxygen (Boon *et al.*, 1984), nitroimidazol drugs (Boon *et al.*, 1985) and iodoacetamide (Cullis *et al.*, 1985a) have been shown to capture electrons in competition with the thymine base resulting in a reduction in the yield of $T^{\cdot-}$. The radical anions of the additives were formed in place of $T^{\cdot-}$, leaving the yield of $G^{\cdot+}$ essentially unchanged. For oxygen, $O_2^{\cdot-}$ was partially formed and a detectable conversion to $HO_2^{\cdot}$ noted. These molecules may react with the DNA on warming and an efficient conversion of most radicals to $RO_2^{\cdot}$ species was noted. A small increase in both d.s.b. and s.s.b. formation under oxic conditions was accounted for by the more efficient generation of strand breaks from $RO_2^{\cdot}$. However it was not enough to account for the large radiobiological sensitizing effect of oxygen *in vivo* (Alper, 1955). The nitroimidazoles, metronidazol and misonidazol, important as radiosensitizers (Foster and Willson, 1973;

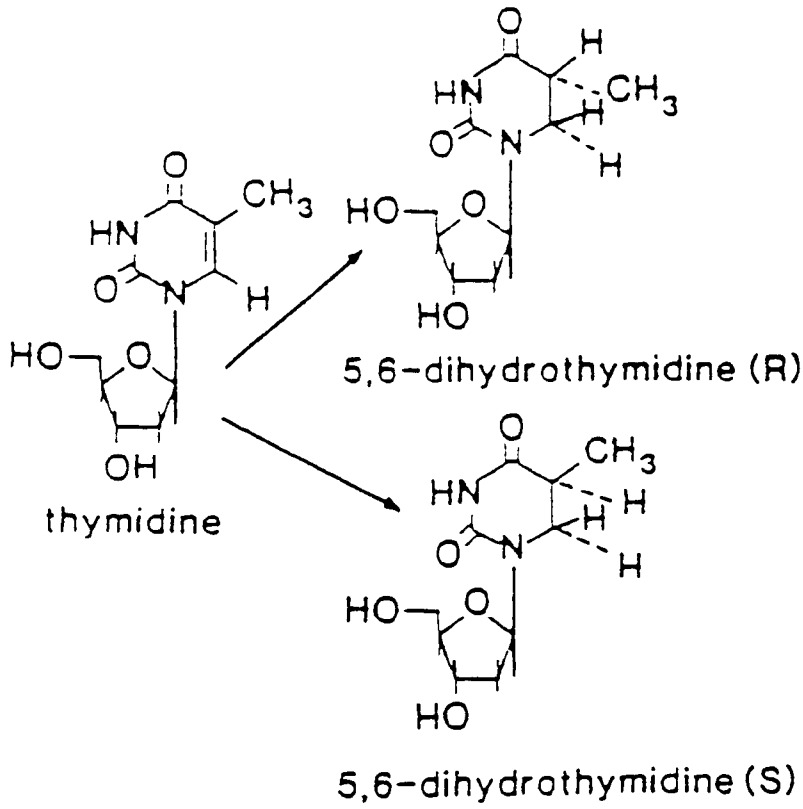

FIGURE 1.13

Structures of thymidine and the two stereoisomers of 5,6-dihydrothymidine.

Dische and Saunders, 1978) captured electrons with a high efficiency. Since their anions were unreactive a decrease in both s.s.b's and d.s.b's was observed. Hence at the molecular level these drugs acted as radioprotectors despite being efficient radiosensitizers at the cellular level. This, along with the observation that $G^{\cdot +}$ was not noted to significantly increase [contrary to Gräslund *et al.* (1977)] indicated that charge recombination [the interruption of which is thought to constitute a fundamental mechanism concerning radiosensitization of direct systems (Adams and Cooke, 1969)] was not important in the frozen aqueous environment. Iodoacetamide also reacted efficiently with electrons in competition with thymine, but suffered dissociative electron capture resulting in the acetamide ($\dot{C}H_2CONH_2$) radicals observed. By 190 K, however, these were lost and replaced by features thought to be largely due to sugar centred radicals. The sugar radicals were also lost at relatively low temperatures and strand break analysis showed the net effect as a small enhancement in breaks.

Overall the conclusion of these studies was that when electron affinic agents were used which gave relatively inert anions, the formation of $T^{\cdot -}$ was suppressed and there was a reduction in the yield of strand breaks. However if the additive anion formed was reactive towards DNA then strand breaks may increase (Cullis *et al.*, 1985b),

Direct versus Indirect Effects of Radiation

The question of the contribution of the direct and indirect effects to DNA deactivation *in vivo* has often been examined in the literature. From scavenger experiments no unequivocal answer concerning the contribution of the two effects can be obtained. For example alcohols, commonly used as hydroxyl radical scavengers (Roots and Okada, 1972) have also been implicated in the reduction of the direct damage component (Schulte-Frohlinde, 1986). Similarly thiols in oxic systems can influence repair systems (Hulsewede, 1985) whilst under anoxic conditions they can interact with the DNA free radicals (Adams, 1972). Other experiments in which cells were irradiated under differing N_2O and CO_2 gassing conditions, conclude that $^{\cdot}OH$ radicals do not participate in cell killing and that it is the direct component which prevails (Pohlit and Drenkard, 1985). However it has been shown that irradiation of a solution containing N_2O, NaCl, O_2 and phosphate produced compounds which

are toxic to cells (Brustad and Wold, 1976).

Michaels and Hunt (1978) made an attempt to calculate a possible contribution of the indirect effect using known rate constants of ·OH radical reactions with the cell compounds assuming a homogeneous distribution of the organic material in the cell. The result was that an indirect effect of ~55% due to ·OH radicals was expected. However the presence of thiols was not taken into account (which could reduce the calculated percentage by ~10%) and the distribution of organic material is not exactly known.

Occasionally an overwhelming contribution of the direct effect is proposed based on the first order dependence of the logarithm of survival on dose if repair is absent. This is based on the assumption that a single hit must be responsible for damage on opposite strands and that this can only occur *via* direct energy absorption in the DNA. However since the energy absorption of ^{60}Co γ-rays occurs in spurs, which contain 1-4 pairs (2-8 radicals), the first order dependency only allows the conclusion that there is no overlapping spurs, i.e. no radical of one spur from one track can contribute to the DNA damage produced by radicals from the spurs of a second track. The damage at the two strands is therefore produced by excitations and ionizations from one spur which will include direct and indirect effects. Even knowing the size of the spurs versus the size of DNA, it is difficult to estimate the contribution of direct to indirect damage (i.e. *via* H·, ·OH and e^-_{aq}, etc.), for it has been suggested that the "structural water" (that is the 15% of total associated water that is required to maintain the double helical structure of DNA) and some water attached to DNA in a secondary hydration layer may behave in a manner in which fewer ·OH radicals are formed but with positive holes and electrons being produced which diffuse to the DNA and cause damage (Bakale and Gregg, 1978). The above discussion indicates that the relative contributions of the direct and indirect effects to radiation damage *in vivo* is still a complicated problem awaiting resolution.

Even though the absolute contributions of these two effects are unknown the circumstances of DNA *in vivo* dictate that the direct mechanism should be significant. Factors that contribute to this are as follows.

Due to the high concentration and tightly folded configuration of nucleohistone fibres in chromatin the local hydration degree of DNA *in vivo* is very low (Bram *et al.*, 1978). Moreover the water molecules closely interacting with the DNA possess a highly ordered ice-like structure and are strongly immobilized by electrostatic interaction with the polar groups of DNA (Bloomfield *et al.*, 1974). As already mentioned the radiation chemistry of such DNA-H_2O sytems, far from being that of dilute aqueous systems, is dominated by the direct effects of radiation.

A model system particularly suitable for the study of radiolytic pathways taking place in hydrated systems, under conditions of direct damage, is the frozen state (see above). The DNA concentrations in cell nuclei (15-50 mg ml^{-1}) (Altman and Katz, 1976) are well modelled by the samples used in frozen aqueous studies and unlike the dry system the DNA radicals formed can readily enter conversion reactions with hydration water molecules.

A possible disadvantage of frozen aqueous systems is that, in the reactions noted on irradiation at such low temperatures (and on annealing), one may be more likely to be monitoring kinetically controlled pathways, whilst for direct damage induced at room temperature thermodynamic pathways could make the greater contribution. However it has been reported that irradiation at various temperatures between 77 K and room temperature, of frozen aqueous solutions and dry films of DNA, does not result in any difference in the nature of the end groups of strand breaks nor in the overall extent of strand break formation (Sweeney, 1986). This tends to negate any disparity existing for the extent to which the various direct radiolytic reactions occur, over the above temperature range.

In this study the direct damage mechanism operative towards DNA in frozen aqueous systems has been investigated using both e.s.r. spectroscopy and a plasmid DNA based strand break assay (see Chapter Two). The use of e.s.r. has enabled determination, both qualitatively and quantitatively, of the initial stages of direct damage and to some extent allowed the subsequent reactions of the radicals to be monitored. The plasmid assay permitted the measurement of chemical

damage in terms of single and double strand break induction. In attempts to further elucidate the radiation induced radical pathways, additives have been incorporated that were potential radiation modifiers. As a consequence of this both radioprotection and radiosensitization have been noted and the results from these studies contribute to the major long-term objectives of this work which are (i) the design of specific compounds that will protect DNA from radiation damage and (ii) to find drugs that sensitize DNA to radiation damage which, hopefully, prove useful in cancer therapy.

Finally, studies have been conducted to determine the effects of direct damage on the various higher ordered structures of DNA, more representative of the nucleic acid *in vivo* and, in particular, the rôle of the high proportion of associated protein.

CHAPTER TWO

Materials and Methods

INTRODUCTION

The purpose of this Chapter is to detail the distinct experimental procedures, employed in this study, for analysing DNA radiation damage. These include, the monitoring of the primary effects of γ-radiation by e.s.r. spectroscopy and the quantifying of chemical damage in terms of single and double strand breaks using a plasmid DNA based assay. The growth, isolation and purification of the plasmid was conducted principally by others, and so will not be described below.

MATERIALS

Plasmid DNA (pBR322), for strand break studies, was isolated according to a modified procedure of Birnboim and Doly (1979) as outlined by Wren (1985) and Sweeney (1986). Typically, pBR322 DNA preparations contained *ca.* 85% of the superhelical Form (I) DNA.

DNA [calf thymus; Type 1: sodium salt "highly polymerized" <3% protein (Lowry)], nucleohistone [calf thymus; ~63% protein (Biuret)], histones (calf thymus; Type II-AS) and the nucleotides 2'-deoxyguanosine 5'-monophosphate (dGMP) and thymidine 5'-monophosphate (TMP), used for the e.s.r. studies, were obtained from the Sigma Chemical Company as were the tris(hydroxymethyl)aminomethane (Tris) buffers, the (ethylenedinitrilo)tetraacetic acid (EDTA) and the 2,7-diamino-10-ethyl-9-phenylphenanthridinium bromide (ethidium bromide) used in the strand break studies. Agarose-ME was obtained from the Miles Laboratory Ltd.

Of the additives, the hydrogen peroxide was purchased from British Drug Houses (Poole) whilst the thiol and thiol derivatives, γ-L-glutamyl-L-cysteinylglycine (Glutathione, GSH), 2-mercaptoethylamine hydrochloride (cysteamine, MEA), L-cysteine, DL-2,3-dihydroxy-1,4-dithiolbutane (dithiothreitol, DTT), 2,2'-dithio-bis(ethylamine) dihydrochloride (cystamine), DL-cystine dihydrochloride and S-methyl-L-cysteine, were purchased from the Sigma Chemical Company and were of the highest quality. The d_3-methyl alcohol (99.5%) and deuterium oxide (99.8%) were obtained from the Aldrich Chemical Company, whilst the iodoacetamide and 3,6-diaminoacridine (proflavine) monohydrochloride were purchased from the Sigma Chemical Company. The sodium perchlorate, the magnesium(II) chloride and both potassium ferro- and ferricyanide were obtained from British Drug Houses (Poole).

All water used was doubly distilled using a Fisons Fi stream cartridge deionizer in series with a Millipore system.

METHODS

E.s.r. Spectroscopy

Sample Preparation and Irradiation

Typically, 50 mg samples of calf thymus DNA were incubated in 1 ml of water (48 hr, 4°C), containing appropriate concentrations of additive. Those samples requiring oxygenation or deoxygenation were gas purged for 30 minutes with oxygen or thoroughly deoxygenated nitrogen respectively. Removal of residual contaminating oxygen from the commercial nitrogen gas was achieved by scrubbing with alkaline pyrogallol solutions.† Frozen samples of DNA for e.s.r. investigation were prepared by cooling in liquid nitrogen a Pyrex tube containing the solution of DNA. Extrusion from the tube yielded identical uniform cylindrical pellets, 2.3 cm in length and 3 mm in diameter. Samples for gamma-ray irradiation†† were exposed in a Vickers Vickrad ^{60}Co γ-ray source under liquid nitrogen for 2-10 hr, depending on the dosage required (dose rate ~0.4 Mrad hr^{-1}).

An alternative method to the deoxygenation procedure mentioned above, was employed in instances where the additive reacted with the ambient 'atmospheric' oxygen present on incubation. In such circumstances it was necessary that the additive solution be prepared in nitrogen flushed apparatus using thoroughly deoxygenated water (60 minutes boiling, with $N_2(-O_2)$ bubbling through on cooling) and that the incubation with DNA be conducted under nitrogen. Where required radical anions of additives were prepared by their irradiation, as outlined above, in glass beads (4:1 $^{v}/_{v}$ CD_3OD/D_2O).

---

† 2 x {KOH (50 g) + benzene-1,2,3-triol (pyrogallol) crystals (15 g) + 130 ml H_2O}.

†† All irradiations, unless otherwise stated, were by gamma(γ)-ray irradiation at 77 K.

E.s.r. Measurements

The DNA e.s.r. spectra† recorded at X-band frequencies were obtained from a Varian E-109 spectrometer of 100 KHz field modulation working at low microwave power levels to avoid saturation. All spectra were recorded at 77 K with the sample placed in a quartz vacuum finger Dewar that was inserted directly into the spectrometer cavity. Care was taken to ensure that the filling factor of the e.s.r. cavity was the same for all samples. A relative *g*-factor reference was supplied by a Varian field frequency lock marker that was matched to a 2,2-di(4-*tert*-octylphenyl)-1-picrylhydrazyl (DPPH) free radical signal prior to each experiment. The samples were annealed by two distinct methods. The first was achieved by decanting the liquid nitrogen from the finger Dewar and then, by rapid scanning, the spectrum was continuously monitored until a significant change was observed. At this point the sample was immediately recooled with liquid nitrogen to 77 K and the spectrum recorded. The approximate temperature that the sample had warmed to could be judged from the time spent annealing, using a time versus temperature profile determined for oxic and anoxic DNA samples (Fig. 2.1). Alternatively through the use of a second spectrometer (Varian E-3, X-band) equipped with a variable temperature accessory designed and built in this laboratory, samples were annealed to a particular temperature for a period of 2 minutes. The samples were then recooled (77 K) prior to their e.s.r. spectra being recorded using the E-109 spectrometer.

To judge the decay of the e.s.r. spectral features of the DNA-additive samples with increasing temperature, the spectra at $g = 4.3$ of a bead containing tris(acetylacetonato)di-iron(III) was recorded in tandem with the DNA samples under identical e.s.r. parameters, and the result employed as an internal intensity standard. In conjunction with the Fe(III) bead, samples of DNA not containing additive, co-irradiated with the DNA-additive samples, were used to further normalize the DNA-additive spectra.

In studies involving DNA samples containing high proportions of

---

† Unless otherwise stated, all spectra referred to in subsequent chapters were obtained by e.s.r. spectroscopy at a microwave power of 0.02 mW and modulation 4 Gauss.

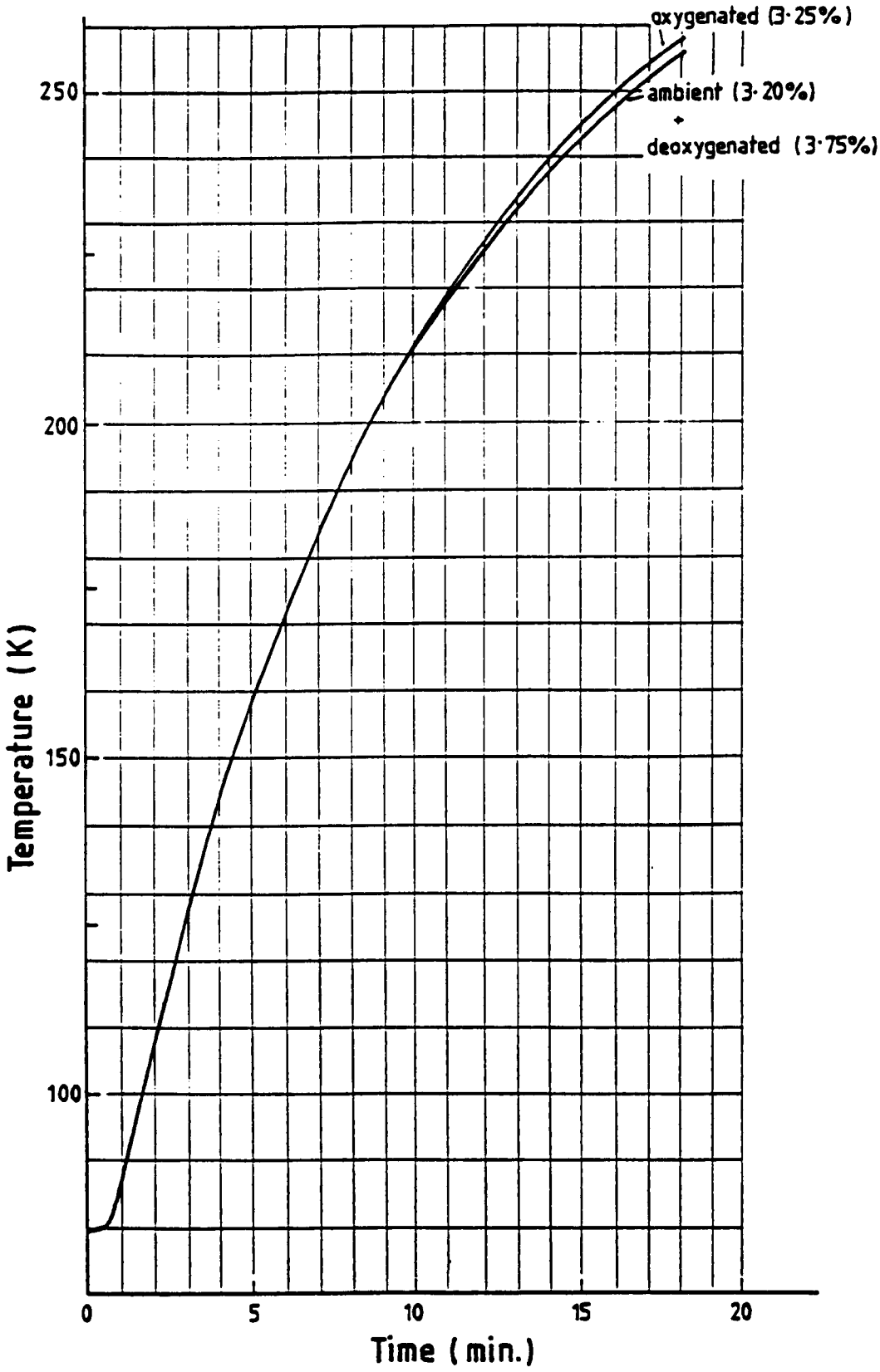

FIGURE 2.1

The time versus temperature annealing profiles determined for oxygenated, ambient and deoxygenated samples of DNA (50 mg + 1 ml H_2O), on warming from 77 K to just below room temperature, when in a particular quartz vacuum finger Dewar within the E-109 spectrometer cavity operating at 0.02 mW. The values in parentheses denote the percentage error for the profiles.

protein, i.e. nucleohistone or chromatin, care was taken to ensure that the DNA concentration of the co-irradiated standard matched that of the protein-DNA sample. In the first instance this was achieved by altering the amount of material used in either standard or protein-DNA sample preparation, so that the respective DNA concentrations would be approximately equal. Then, by weighing the samples and determining the absolute amount of DNA present ($^{w}/_{w}$) in each pellet, the computer accumulated/stored spectra (or spectral data) were adjusted by a small factor so as to be representative of samples equal in their DNA concentration.†

Storage, manipulations and double integrations of spectra were performed with a Hewlett-Packard 9835B computer, which was interfaced with the E-109 spectrometer and a Hewlett-Packard 9845A external flexible disc memory. All spectra were digitized at 1024 equidistant points and stored on disc. G-values, numbers of radicals (or events) per 100 eV, were estimated by comparison with the double integral value taken from a spectrum of di-butylaminoxyl of known spin concentration.

An alternative method of monitoring the spectral decay on warming, sometimes employed, was a modified procedure of that outlined by Gräslund *et al.* (1975). In this instance the spectrometer's magnetic field was set corresponding to a particular point in the DNA spectrum, and with the liquid nitrogen decanted, the decay of the spectral features with time (hence temperature, see Fig. 2.1) was recorded. However, there were several problems inherent to this procedure which deemed that it was seldom employed (see Appendix C).

E.s.r. data at Q-band frequencies were recorded using a Bruker e.s.r. E.R. 200D-SRC spectrometer with a Bruker E.R.05 Q-band microwave bridge. Accurate *in situ* temperature control was achieved by an attached Bruker E.R. 4111 VT Variable Temperature unit.

---

† This latter procedure of weighing the sample was necessary due to the fact that the DNA in these highly concentrated solutions had itself a significant and contributing volume, i.e. 50 mg DNA + 1 ml H_2O ≡ 41.6 mg ml^{-1}.

Generation of the Pure E.s.r. Elementary Signals of γ-Irradiated DNA and Histone

In order to assess DNA radiation damage quantitatively, in terms of the extent to which the various radicals were formed, it was necessary to generate the pure e.s.r. elementary patterns that together compose the DNA e.s.r. spectra, i.e. $\dot{T}H$, $ROO^{\cdot}$, $T^{\cdot -}$ and $G^{\cdot +}$ (Gregoli *et al.*, 1982). These were used, *via* the computer, in either subtraction from experimental spectra or in spectral reconstruction. Both procedures yielded information concerning the individual radical species relative abundance and hence the nature of the radiolytic pathways. The methods by which the pure e.s.r signals were generated were as follows.

The pure octet (T_8) associated with 5,6-dihydro-5-thymyl radicals ($\dot{T}H$) was obtained by one of two methods. Firstly, from a wet DNA sample (100% relative humidity) irradiated at 77 K and successively annealed up to *ca.* 285 K (Fig. 2.2a) (Gregoli *et al.*, 1982), and secondly by photosensitization of TMP by proflavine (van de Vorst and Lion, 1971) where proflavine (2.5×10^{-4} M) and TMP (1 M) were dissolved in aqueous $MgCl_2$ (3 M) and illuminated with white light (λ>320 nm) at 77 K for 10-12 hr (Fig. 2.2b).

The asymmetric doublet associated with peroxyl radicals ($ROO^{\cdot}$) was obtained in isolation by irradiating at 77 K and annealing to 215 K, a sample containing DNA (10 mg + 1 ml H_2O) in O_2 saturated water (Gregoli *et al.*, 1982) (Fig. 2.3).

Tentative isolation of the elementary patterns from which the low temperature DNA spectra are composed, the doublet associated with the thymine radical anion ($T^{\cdot -}$) and the singlet associated with the guanine radical cation ($G^{\cdot +}$), was initially achieved according to a modified procedure of Gregoli *et al.* (1982). Two spectra were recorded at different power levels (0.02 mW and 0.1 mW) for the same irradiated DNA sample (50 mg + 1 ml H_2O, $-O_2$) after annealing to 135 K. With the spectra normalized with respect to each other, increasing amounts of the higher power spectrum were subtracted from the lower power spectrum and *vice versa*. In the former case, the resultant spectra delineates to a doublet (*ca.* 23-25 G p/p width) and in the latter case to a singlet (*ca.* 17-19 G width) (Fig. 2.4). However, due to the difficulty of assessing the purity of these spectra, alternative methods were

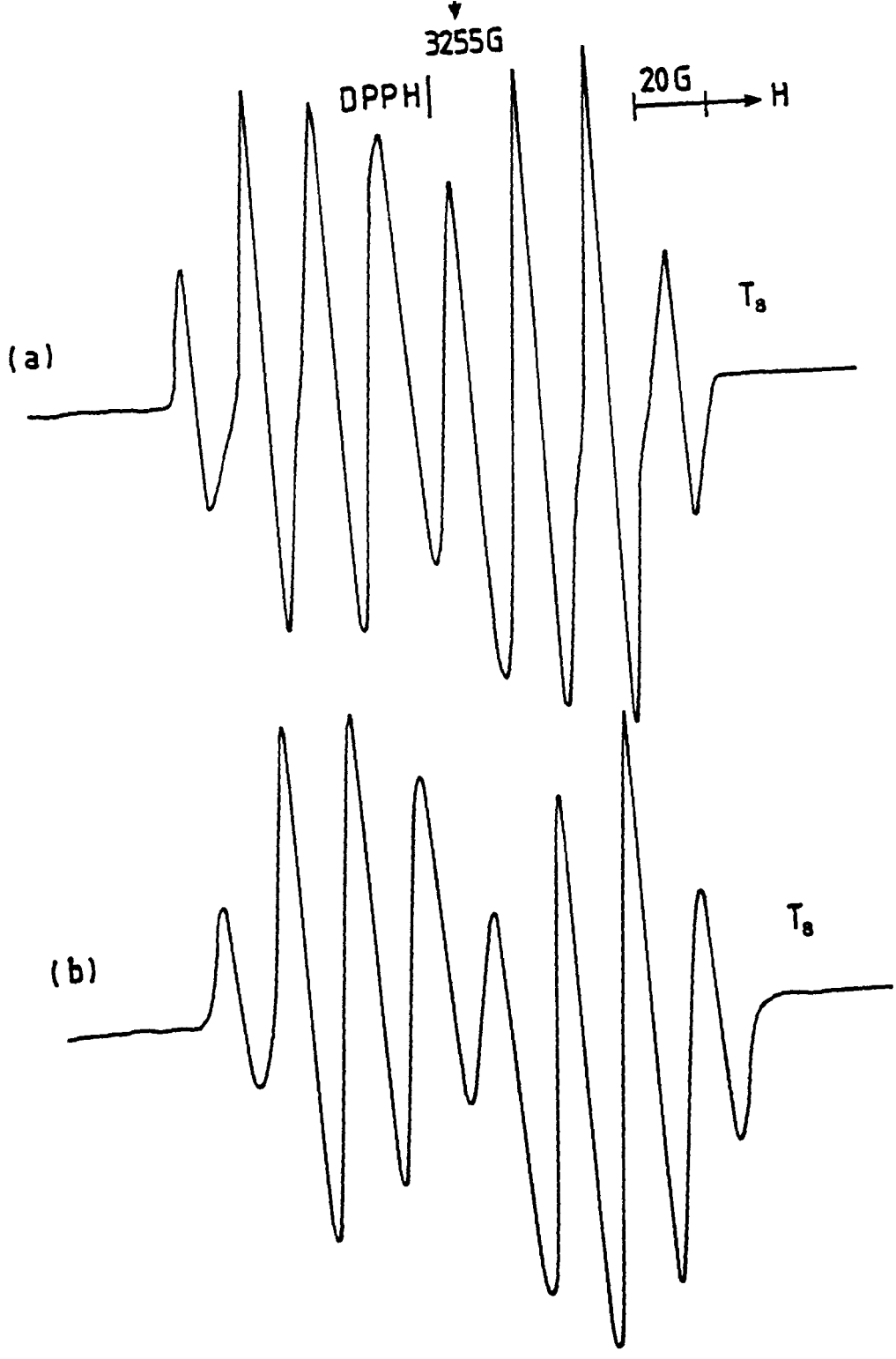

FIGURE 2.2

The e.s.r. octets (T_8) due to 5,6-dihydro-5-thymyl radicals (ṪH) on the thymine residue, obtained from: (a) a wet DNA sample (100% relative humidity), irradiated at 77 K, and successively annealed up to 285 K; (b) the photosensitization (λ>320 nm) of TMP (1 M) by proflavine (2.5×10^{-4} M) at 77 K in aqueous $MgCl_2$ (3 M).

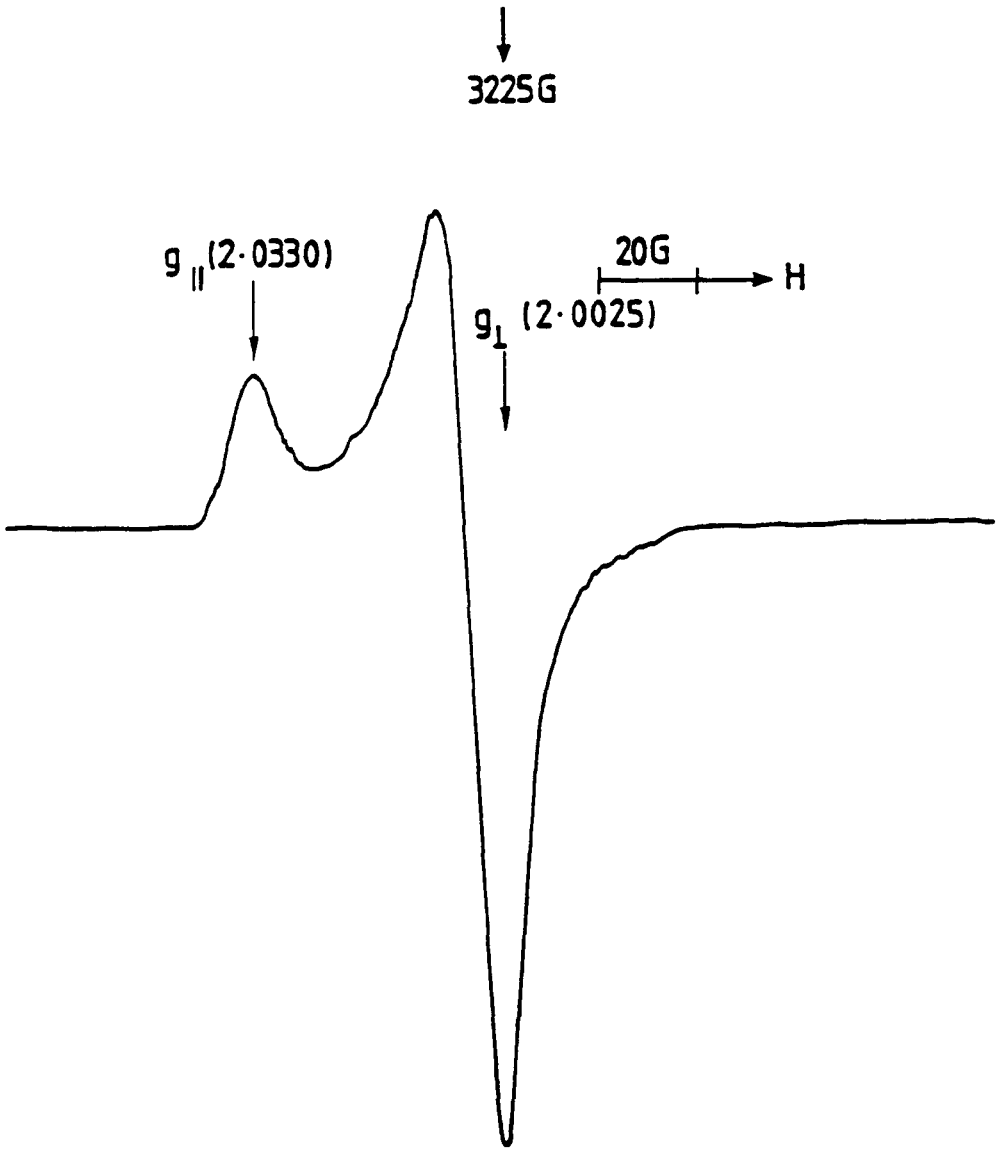

FIGURE 2.3

The typical e.s.r. pattern associated with peroxyl radicals ($ROO^{\cdot}$), obtained from an O_2 saturated DNA solution (10 mg + 1 ml H_2O), irradiated at 77 K and annealed to 215 K.

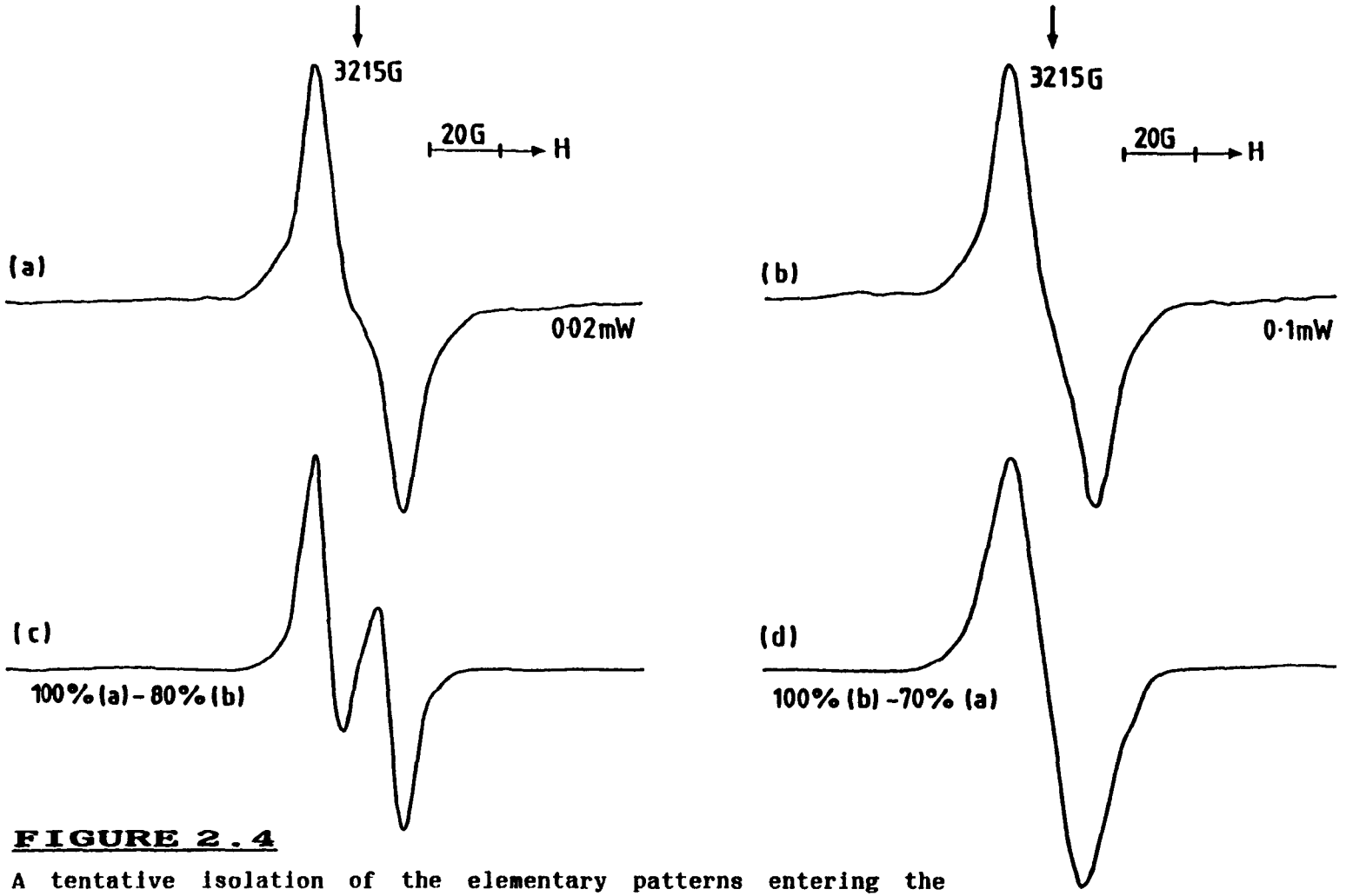

FIGURE 2.4

A tentative isolation of the elementary patterns entering the composition of the low temperature DNA spectra. Spectra (a) and (b) were recorded at different microwave powers from the same DNA sample (50 mg + 1 ml H_2O, $-O_2$) irradiated at 77 K, and annealed to 135 K. Detection at different power levels clearly reveals that spectra (a) and (b) are composite in structure. Under computer subtraction work, the component which saturates first develops into a doublet of 23-25 G p/p width, while the central component turns into a singlet-like pattern of about 17-19 G width.

sought to generate, in isolation, these elementary patterns.

The pure doublet (T_2) associated with $T^{\cdot -}$ was isolated by the successive subtraction from a spectrum of TMP (1 M in H_2O, $-O_2$), obtained on irradiation and subsequent annealing to 135 K, of overlapping $\dot{T}H$ (see above) and T_4 signals (Fig. 2.5a) (Gregoli *et al.*, 1976). The T_4 signal, strongly implicated as being the radical cation of thymine (Gregoli *et al.*, 1976), was itself generated by the successive subtraction from a spectrum of TMP (1 M in H_2O, $-O_2$) plus iodoacetamide (0.1 M), obtained on irradiation and annealing to 195 K, of overlapping $\dot{T}H$ signals and the quintet (T_5) signals associated with $\dot{T}OH$ (Fig. 2.5b). The T_5 profile was itself formed pure in the same TMP/iodoacetamide system on warming to 235 K (Fig. 2.5b).

The singlet pattern associated with $G^{\cdot +}$ was obtained by photoionization of DNA in a basic glass at 77 K (Sevilla *et al.*, 1979b). To DNA (30 mg) was added several drops of water. The gel-like mass was then added to 2 ml of $NaClO_4$ (8 M)/NaOH (2.3×10^{-2} M) (H_2O) and the solution stirred for 12-48 hr to disperse the DNA. No precipitation of DNA was noted on cooling to 77 K and clear glasses were formed. The beads were UV photolysed (254 nm) for 5½ hr at 77 K. After the photoionization the e.s.r. spectrum showed O^- features as well as the cation spectrum (Fig. 2.6a). To remove the O^- it was produced separately by photoionization (324 nm) of $K_4Fe(CN)_6$ (saturated solution) in $NaClO_4$ (8 M)/NaOH (2.3×10^{-2} M) (H_2O) at 77 K (Fig. 2.6b) and subsequently subtracted from the spectrum of the DNA (Fig. 2.6c). This final spectrum is assigned to $G^{\cdot +}$ in DNA.

The spectra of $G^{\cdot +}$, $T^{\cdot -}$, $\dot{T}H$ and $ROO^{\cdot}$ once normalized with regard to their first moment were stored on disc for use in subtraction from, or reconstruction of, experimental DNA spectra.

The e.s.r. spectrum of the histone protein electron-loss centres $(Hist)^{\cdot +}$† was generated by the irradiation and annealing to 130 K of a sample of histone (85 mg + 1 ml H_2O, $-O_2$) and $K_3Fe(CN)_6$ (5 mM) (Fig.

---

† Though $(Hist)^{\cdot +}$ denotes cationic species, the histone electron-loss centres are believed to constitute <u>both</u> neutral amide radicals and various positive ionic species, i.e. $(Tyr)^{\cdot +}$ and $(Trp)^{\cdot +}$ [see Chapter Five]. However, for the sake of clarity both these types of centres will be represented by $(Hist)^{\cdot +}$ in the text.

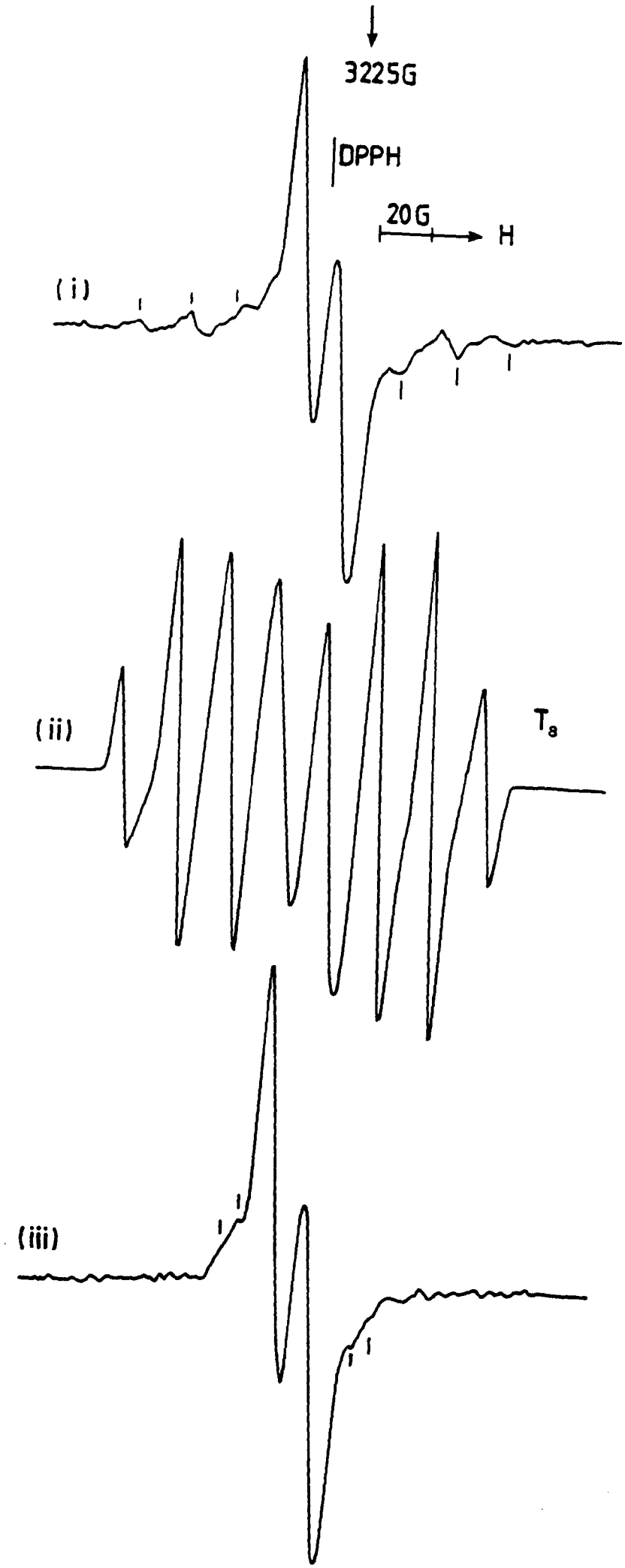
3225G
DPPH
20G
H
(i)
(ii)
T_s
(iii)

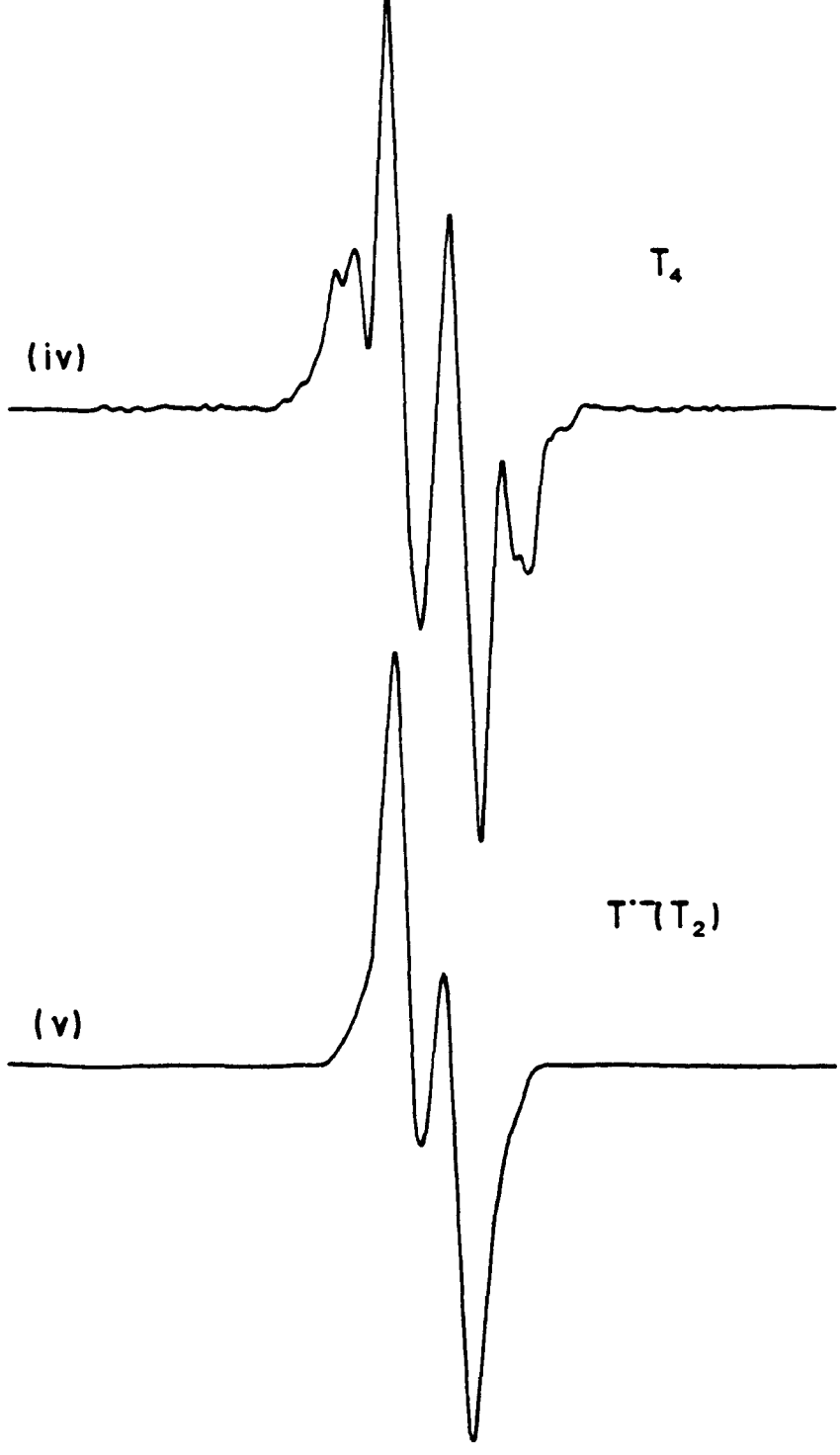

FIGURE 2.5(a)

Isolation of the pure doublet (T_2) associated with the thymine radical anion ($T^{\cdot-}$). This was obtained by successive subtractions, from the experimental spectrum (i) (arising from thermal annealing to 135 K of an irradiated frozen solution of TMP, 1 M in H_2O, $-O_2$) of the overlapping $\dot{T}H$ (ii, T_6) and T_4 (iv) signals. Profile (iii) is the product of (i) minus (ii, to best fit) [as judged by the cancellation of the outer $\dot{T}H(T_6)$ features], whilst (v) shows the pure doublet of $T^{\cdot-}$ (T_2) resulting from (iii) minus (iv, to best fit) [again as judged by the cancellation of the outer T_4 features].

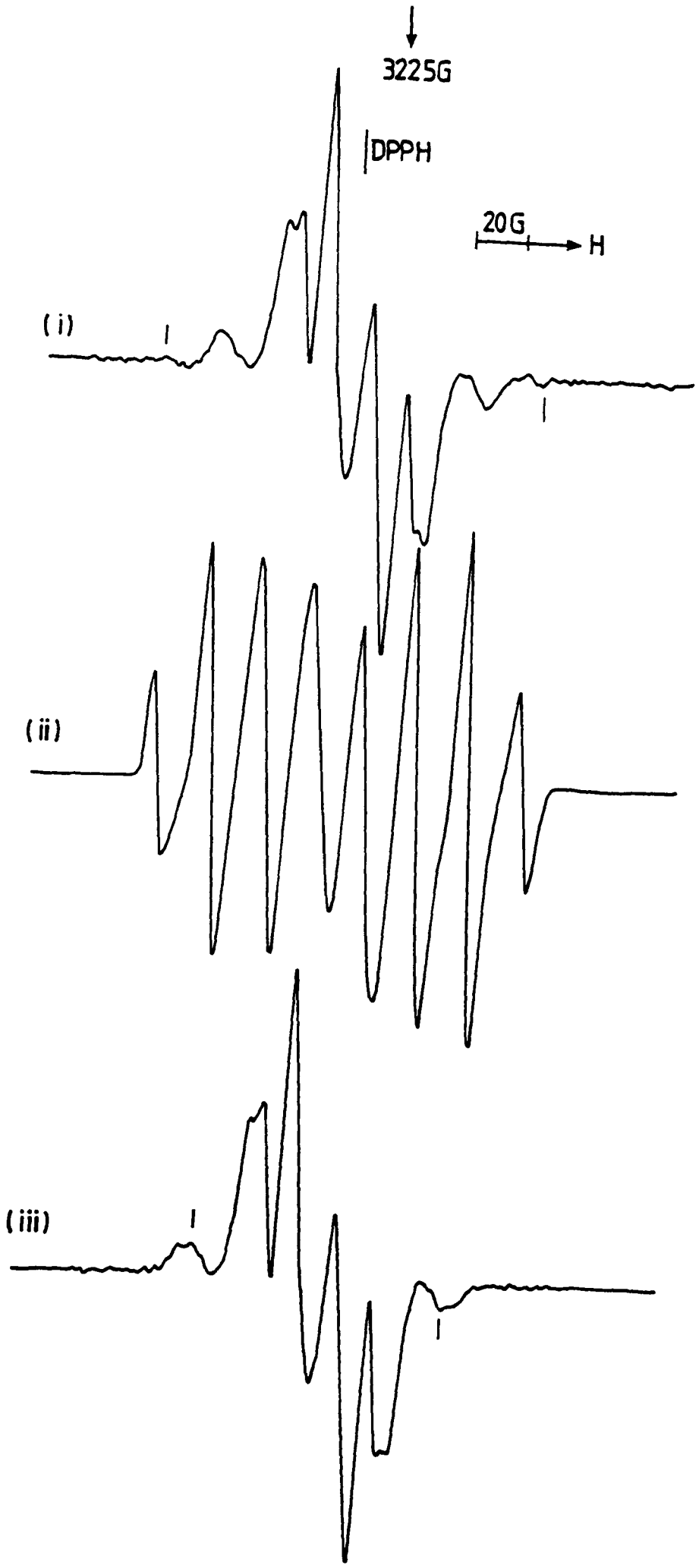
3225G
DPPH
20G
H
(i)
(ii)
(iii)

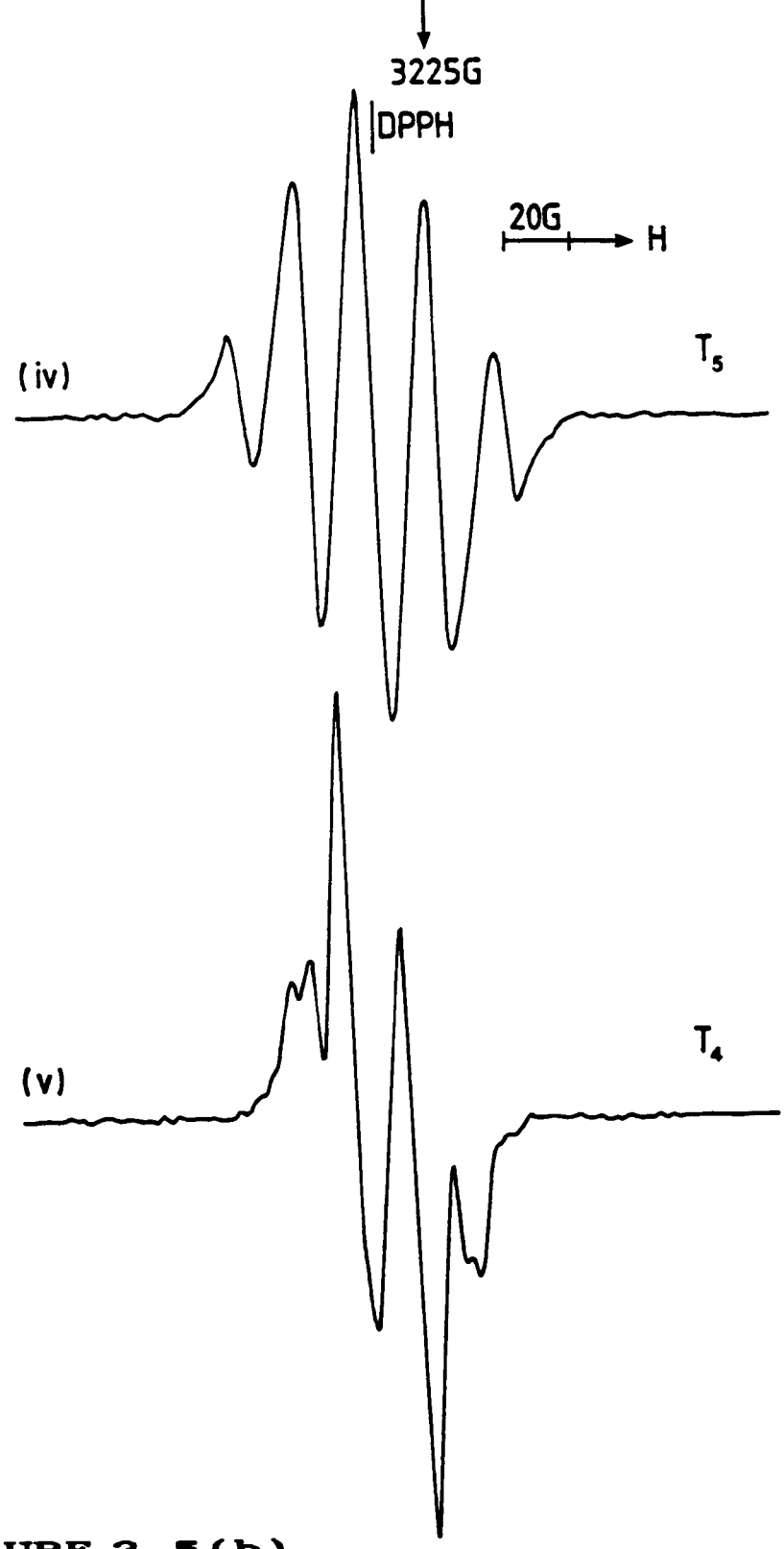

FIGURE 2.5(b)

Isolation of a pure e.s.r. profile of T_4, for use in the previous subtraction [see text and legend to Fig. 2.5a]. This was obtained by successive subtractions, from the experimental spectrum (i) (arising from thermal annealing to 195 K of an irradiated frozen solution of TMP (1 M in H_2O, $-O_2$) and iodoacetamide (0.1 M) of overlapping $\dot{T}H$ (ii, T_6) and $\dot{T}OH$ (iv, T_5) signals. Profile (iii) is the product of (i) minus (ii, to best fit) [as judged by the cancellation of the outer $\dot{T}H(T_6)$ features], whilst (v) shows the pure e.s.r. profile of T_4 resulting from (iii) minus (iv, to best fit) [again as judged by cancellation of the outer $\dot{T}OH(T_5)$ features]. The pure e.s.r. pattern of T_5 (iv) was obtained on warming the above TMP/iodoacetamide system to 235 K.

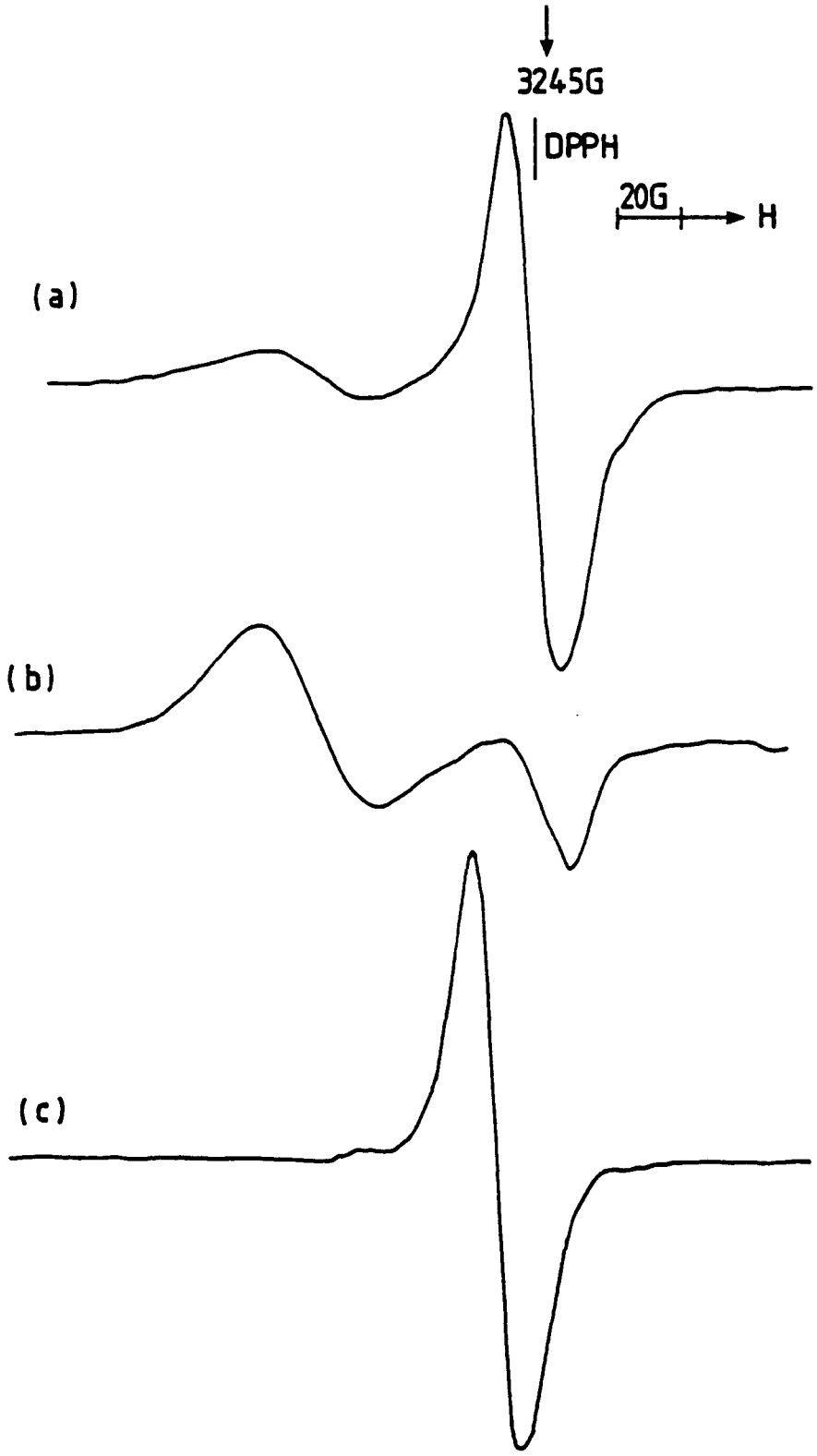

FIGURE 2.6

(a) The e.s.r. spectrum produced by the UV photoionization (254 nm) of DNA (30 mg) in 2 ml $NaClO_4$ (8 M)/NaOH (2.3×10^{-2} M) (H_2O) at 77 K. This spectrum consists of the π-cation and O^- produced by the reaction of the photo-ejected electron with perchlorate.
(b) The e.s.r. spectrum of O^- produced by photoionization (324 nm) of $K_4Fe(CN)_6$ (saturated solution) in $NaClO_4$ (8 M)/NaOH (2.3×10^{-2} M) (H_2O) at 77 K.
(c) The result of subtraction of O^- (b) from (a). This final spectrum is assigned to the guanine base π-cation in DNA.

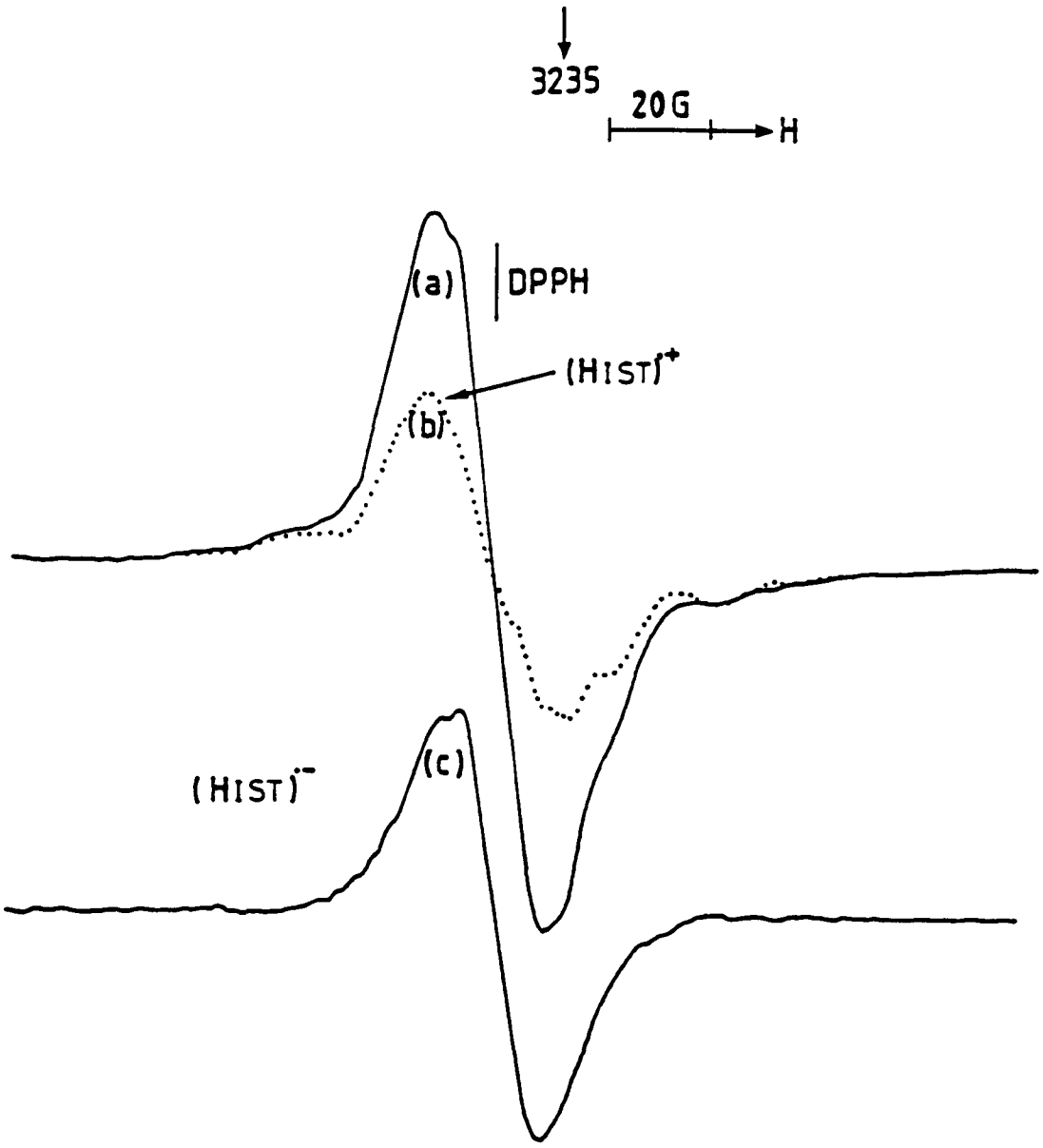

FIGURE 2.7

The generation of the e.s.r. profile of histone radical anion species $(Hist)^{\cdot -}$ (c), by subtraction of a spectrum of histone electron-loss centres $(Hist)^{\cdot +}$ (b) [generated by irradiation and annealing to 130 K of a sample of histone (85 mg + 1 ml H_2O, $-O_2$) and $K_3Fe(CN)_6$ (5 mM)] from one of pure histone (85 mg + 1 ml H_2O, $-O_2$) (a), irradiated and annealed as above.

2.7b). The e.s.r. profile for the radical anion species of histone $(Hist)^{\cdot -}$ was generated by subtraction of the $(Hist)^{\cdot +}$ spectrum from one recorded for pure histone (85 mg + 1 ml H_2O, $-O_2$), irradiated and annealed as above (see Fig. 2.7).

Assay for DNA breaks

Many physical and biochemical techniques have been used to quantify DNA chain breaks both *in vivo* and *in vitro*. Most studies conducted *in vitro* using chromosomal DNA usually rely on average molecular weight determination by hydrodynamic methods (Gillespie *et al.*, 1972; Drazil and Juaskova, 1979). A disadvantage with these assays is that many single and double strand breaks are required before an appreciable and quantifiable change occurs. Other methods include the use of single sweep voltammetry (Sequaris and Valenta, 1980) filter elution assays (Kohn, 1986) and various chromatographic techniques (Haber and Stewart, 1981; Maura *et al.*, 1981; Bryant and Blocher, 1980; Schuessler and Hartmann, 1985). However, improved methods for extracting and purifying plasmid DNA offers a further assay employing gel electrophoresis. Of the methods currently available it is both simple and accurate, and detection of low level phosphodiester bond scission can be made (van Touw *et al.*, 1985).

Plasmid DNA can exist in three different topological forms, the covalently closed superhelical Form (I), the "nicked" (relaxed) open circular Form (II), and the linear Form (III). The three Forms may be resolved by gel electrophoresis and quantifiable by staining. Chain breakage at a single site on one chain of the plasmid allows the superhelical twists of Form (I) to relax generating Form (II). Scission of both strands at a coincidental site generates Form (III) (Fig. 2.8). The simplicity of this method arises from the fact that there is no molecular weight change on the introduction of a strand break, only a conformational alteration, also the migration of Forms (II) and (III) are independent of the actual site of chain scission, i.e. all plasmids of a particular form co-migrate. Clearly, in a γ-irradiation experiment starting with Form (I), the production of Forms (II) and (III) indicates the degree to which single and double strand breaks occur respectively.

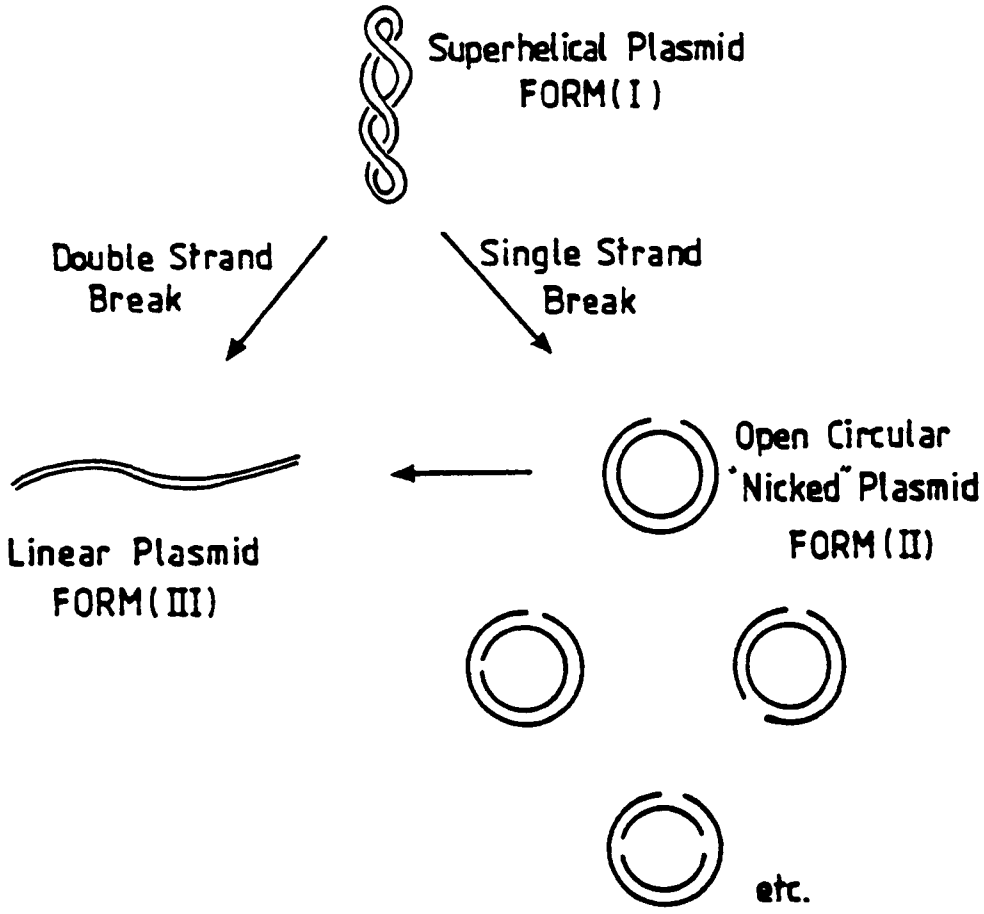

FIGURE 2.8

Protocol for the analysis of γ-irradiation induced single and double strand breaks using plasmid DNA.

The plasmid based assay used in this study was a modified procedure of that employed by Boon *et al.* (1984). Variations were introduced in order to optimise the separation of the linear Form (III) DNA from the relaxed Form (II) DNA. A solution of additive (10 μl) was added to the plasmid DNA solution (90 μl; 80 $\mu g\ ml^{-1}$) in Tris hydrochloride buffer (10 mM; pH 7.6) containing EDTA (1 mM) to give the appropriate final additive concentration. Samples with and without additive were γ-irradiated in a Vickrad ^{60}Co γ-ray source under the appropriate conditions (77 K or room temperature). Oxygenated and deoxygenated samples were prepared by gas purging with oxygen or thoroughly deoxygenated nitrogen for 60 minutes, then sealed and frozen prior to irradiation. Following irradiation and annealing to room temperature, a dye-EDTA mixture (6 μl; 56% glycerol $^{V}/v$; 50 mM EDTA; 0.05% bromophenol blue $^{W}/v$) was added and aliquots removed for analysis by agarose gel electrophoresis.

Gel Electrophoresis

Samples of irradiated plasmid DNA (0.7-1 μg) were layered onto agarose slab gels (0.65%) and subjected to electrophoresis in a horizontal gel apparatus at 40 V for *ca.* 16 hours at room temperature using Tris buffer (90 mM, pH 8.3) containing boric acid (90 mM) and EDTA (2.5 mM). After electrophoresis the gels were stained with ethidium bromide (2.5 $\mu g\ ml^{-1}$) in electrophoresis buffer for at least 15 minutes and the excess removed by washing. The stained gels were then excited with a UV transilluminator and photographed with a Polaroid MP-4 Land Camera using a red filter (Kodak Wratten filter No. 9) and Polaroid type 55 film. The photographic negatives were used for densitometric scanning.

Quantitation of Single and Double Strand Breaks

The negative films of the ethidium bromide-stained gels were scanned using a UV/visible spectrophotometer with gel scanning attachment (Pye Unicam SP8-100). The superhelical Form (I) of the plasmid takes up less ethidium bromide than the other two Forms, so a staining efficiency of 80% [as demonstrated for pBR322, (Hertzberg and Dervan, 1982)] was used to normalize the data. No further uptake of ethidium bromide was observed on prolonged incubations. All samples were analysed in duplicate and the average values reported. The results are presented as dose response curves, with the percentage of plasmid

containing single and double strand breaks indicated by the amounts of Forms (II) and (III) respectively measured. The linear semi $\log_{10}$ plots of the disappearance of Form (I) as a function of dose, are also presented. For the purpose of comparing the effects of the various additives, the slopes of the linear $\log_{10}$ plots were used to define a parameter called the additive effect ratio (a.e.r.) (Cullis *et al.*, 1985a). This is defined as the ratio of the slope of the plot for the experiment in the presence of the additive to the slope of the plot for the control experiment, where no additive is present. An a.e.r. of greater than unity corresponds to an enhancement of the irradiation dependent damage to DNA due to the additive, i.e. sensitization, while an a.e.r. of less than unity corresponds to a reduction in the damage, i.e. protection. The a.e.r. is clearly dependent on the concentration of the additive.

Control experiments to ensure that the various additives used did not effect the staining of the plasmid nor that the additives had any effect prior to irradiation, were conducted to confirm the validity of the DNA strand break assay.

Preparation of Denuded† Nuclei from Calf Thymus Tissue

Thymus glands were collected immediately after slaughter, frozen in liquid nitrogen and stored at -80°C until ready for use. Connective tissue, blood vessels and fat deposits were removed from partially thawed thymus glands and the nuclei isolated by differential centrifugation after homogenization in a Waring blender, essentially as in Panyim *et al.* (1971) but modified by the inclusion of 0.1 mM phenylmethylsulphonyl fluoride (PMSF) and a reduction of the magnesium(II) chloride to 6 mM. The nuclei were stored overnight frozen in 80 mM NaCl, 6 mM $MgCl_2$, 10 mM Tris pH 7.5, 40% glycerol at -80°C.

Once thawed, 100 ml of the nuclei was centrifuged at 600 *g* for 20 minutes and the pellet resuspended twice in 200 ml of 300 mM NaCl, 6 mM $MgCl_2$, 5 mM Tris pH 7.5, 0.2 mM PMSF. After centrifuging at 480 *g* for 10 minutes the pellet was resuspended in 150 mM NaCl, 1 mM $CaCl_2$, 5 mM Tris pH 7.5, to a total volume of 230 ml (8.0 mg DNA ml^{-1}). A portion

† With outer nuclear membrane removed and non-histone proteins (NHP) reduced.

(70 ml) of the solution was concentrated by centrifugation, as above, and resuspended in a minimum of the latter buffer (19.1 mg DNA ml^{-1}). This solution was used directly to prepare nuclei samples for irradiation in the usual way.

Isolation of Chromatin from Denuded Calf Thymus Nuclei

Chromatin was prepared from the remaining 160 ml of denuded nuclei which were suspended in digestion buffer (150 mM NaCl, 5 mM Tris pH 7.5, 1 mM $CaCl_2$, 0.1 mM PMSF) at 8 mg DNA ml^{-1}. The time course of the digestion was determined as follows. With the nuclei on ice, a 1 ml of sample was taken, to it added 50 units of micrococcal nuclease and incubated at 37°C. Aliquots (150 μl) were taken after 1, 2, 5, 10, 20 and 40 minutes and the digestion terminated with 5 μl 250 mM Na_3 EDTA. The samples were extracted once with phenol and once with chloroform. To 2 μl of each sample was added 38 μl of the buffer 30 mM Tris, 36 mM NaH_2PO_4, 0.1 mM EDTA, pH 6.8. 4 μl Aliquots were loaded onto a horizontal agarose slab gel (1%) and subjected to electrophoresis at 80 V for 1-2 hr in the latter buffer. Analysis of the gel under UV indicated that a digestion time of 15 minutes was appropriate.

To the remaining nuclei in the main sample was added 800 μl of 10 U μl^{-1} micrococcal nuclease (50 U ml^{-1} final) and the solution incubated at 37°C for 15 min. Digestion was terminated with 3.2 ml 250 mM Na_3 EDTA and the solution centrifuged at 600 *g* for 30 minutes. The supernatant was shown to contain 0.14 mg DNA ml^{-1}. The pellet was then resuspended in 120 ml of 5 mM NaCl, 5 mM Tris pH 7.5 and 0.5 mM Na_3 EDTA and again centrifuged at 600 *g* for 20 minutes. Although the nuclei had swollen, minimal DNA was found in the supernatant. The nuclei were suspended in 1 mM Na_3 EDTA, 0.1 mM PMSF and dialysed against 1 mM Na_3 EDTA (2 L) overnight. The nuclei were next centrifuged at 600 *g* for 20 minutes and the supernatant, now shown to contain significant amounts of DNA ~3 mg ml^{-1}, was put into two dialysis bags which were covered in polyethylene glycol (m.wt. 20000) dry powder for concentration. One of the bags was removed after the volume had decreased to about half of the original volume (1 hr), while the second was left longer (2-3 hr). The concentrations were 6.7 and 15.4 mg DNA ml^{-1} respectively. These samples were used directly to prepare chromatin samples for irradiation in the usual way. The

average size of the DNA was determined to be 1400 b.p. (~7 nucleosomes) and was distributed mainly between 400 and 2000 b.p.

The DNA concentrations of chromatin were measured by diluting the chromatin in water and reading the absorbance at 260 nm (1 mg DNA ml^{-1} at A_{260} = 20). For the DNA concentration of nuclei, the material was first solubilized by sonication or digestion with micrococcal nuclease and diluted with 3 M NaCl, 5 M urea.

Other physical data, kindly provided by Dr. Staynov, is shown in Table 2.I.

TABLE 2.I

Physical Data of the Chromatin and Nuclei Samples Prepared

Concentration mg ml^{-1}	Chromatin (1)	Chromatin (2)	Nuclei
[DNA]	6.7	15.4	19.1
[Hist]	6.8	15.9	19.9
[NHP]	3.0	7.1	9.5
Total wt.	16.5	38.4	48.5

CHAPTER THREE

The Role of Hydrogen Peroxide

INTRODUCTION

As discussed in Chapter One, it is generally agreed that there are two extremes of the action of radiation towards DNA. One is the indirect process in which primary damage is to the surrounding water molecules, with attack on the DNA occurring almost exclusively through hydrogen atoms ($H^{\cdot}$), hydrated electrons (e^{-}_{aq}) and especially hydroxyl radicals ($^{\cdot}OH$), and is representative of irradiative action in dilute aqueous solutions (Scholes, 1983; von Sonntag *et al.*, 1981). The other limiting mechanism is direct damage, in which primary electron-loss and electron-capture occurs within the DNA molecule, and this mechanism appears operative in frozen aqueous solutions (Boon *et al.*, 1984; Gregoli *et al.*, 1982). For reasons already discussed, this study is concerned primarily with these latter solvated systems.

Both at room temperature and under frozen conditions, the properties of water molecules are somewhat altered in the vicinity of a polar molecule such as DNA (Tait and Franks, 1971; Mathur de Vré, 1979; Texter, 1978). The polarizing effect of the DNA can perturb the water structure over several tens of angstroms. These perturbed water molecules or "hydration water" have several peculiar characteristics. Their diffusion is anisotropic and they possess an ordered structure which above 0°C shows restricted rotational and translational mobility different to that of bulk water. Conversely they are able to maintain mobility down to temperatures as low as -80°C where mobility of bulk water is restricted. Infrared (Faulk *et al.*, 1970) and n.m.r. (G. Archer and M. C. R. Symons, unpublished results) spectroscopic studies suggest that the concentration of the water of solvation in the frozen DNA phase is 10-12 molecules per base.

The fate of ionization events within the solvating water both at room temperature and under frozen conditions is unclear, with positive and negative hole production, along with concomitant dry charge transfer to the DNA, being postulated rather than hydroxyl radical formation (Bakale and Gregg, 1978; Gregoli *et al.*, 1982). Whatever the situation, $H_2O^{\cdot +}$ is expected to be one of the primary cation species formed under frozen conditions. These may either transfer protons to give $^{\cdot}OH$ radicals or gain electrons from the DNA to reform H_2O (they are not expected to be trapped as such).

The major aim of the present study was to assess the possibility and consequence of the former action ($^{\cdot}OH$ formation) occurring in the hydration water of frozen DNA systems. Although $G^{\cdot+}$ and $T^{\cdot-}$ are the only detectable paramagnetic species present after annealing to 130 K (Gregoli *et al.*, 1982; Boon *et al.*, 1984), the possibility remains that some $^{\cdot}OH$ radicals are formed from $H_2O^{\cdot+}$, and that these react with DNA to yield radicals which for various reasons make no clear contribution to the e.s.r. spectrum. Their production could have a significant effect on strand break formation if they were generated, and so reacted, in the vicinity of the DNA deoxyribose moieties. Through the addition of hydrogen peroxide (H_2O_2) it was hoped to be able to assess the effects of $^{\cdot}OH$ radicals being formed in the DNA phase by electron-capture under frozen conditions, equation [3.1].

$$H_2O_2 + e^- \rightarrow HO^{\cdot} + OH^- \qquad [3.1]$$

A second aim was to explore a possible explanation for the curious effect noted by Loman and co-workers (private communication) which may be caused by hydrogen peroxide formation. They found that, for a given dose of radiation, the extent of DNA damage was enhanced if, instead of irradiating continuously at 77 K, they interrupted the irradiation periodically and allowed the system to warm to room temperature, then recooled it to 77 K prior to continuing the irradiation. Such action might be as a consequence of the gradual accumulation in the DNA phase of H_2O_2 formed initially in the irradiated ice crystallites. This could be confirmed by the present experiments.

Finally this work may also provide some insight as to the mode of H_2O_2 mediated sensitization of near-UV induced strand breaks found for phage DNA. This effect was noted to be synergistic, with the action of the two agents being observed at concentrations at which the individual agents had little or no effect (Ananthaswamy and Eisenstark, 1976).

EXPERIMENTAL

The e.s.r. spectroscopic measurements of the DNA-H_2O_2 systems were conducted as outlined in Chapter Two, using concentrations of peroxide of between 0.04 mM and 40 mM, (additive:base pair ratio, 1:~1550 → 1:~1.55). The e.s.r. spectra of H_2O-H_2O_2 systems in the presence and

absence of glass forming promotors were studied for comparative purposes.

The plasmid assays for DNA breaks (both s.s.b's and d.s.b's) were conducted solely by Mrs. (now Dr.) M. C. Sweeney and detailed results are presented elsewhere (Sweeney, 1986). The brief results presented and discussed below are reproduced through the kind permission of Dr. M. C. Sweeney. In all cases, otherwise identical solutions containing DNA only and DNA plus peroxide were compared. Care was taken to ensure the absence of transition metal ions which might catalyse the decomposition of the peroxide. Studies of unirradiated systems proved that that was not significant.

RESULTS

It has been fully established that in the absence of H_2O_2 three radicals are detectable by e.s.r. spectroscopy following γ-irradiation of a frozen aqueous solution of DNA at 77 K (Boon *et al.*, 1984; Gräslund *et al.*, 1971; Gregoli *et al.*, 1982; Sevilla, 1977). Hydroxyl radicals are formed in the pure ice crystallites, and $G^{\cdot+}$ and $T^{\cdot-}$ in the solvated DNA phase. In the presence of H_2O_2 the central e.s.r. features, observed at low microwave powers, were considerably modified and at high powers extra features assignable to $HO_2^{\cdot}$ radicals were observed. Such changes were far better defined on annealing to 130 K, the temperature at which the obscuring $^{\cdot}OH$ radicals in the ice are lost. Typical e.s.r. spectra at both low and high powers are shown in Figures 3.1a-c.

Analysis of the e.s.r. spectra at low powers shows that as the concentration of peroxide was increased, so the concentration of DNA radicals fell and new features described as 'X' appeared (Fig. 3.1b). Such signals were similar to those noted for DNA systems irradiated in the presence of iodoacetamide (Cullis *et al.*, 1985a) and also to those observed for deoxyribose after hydrogen atom abstraction by free hydrogen atoms (Riederer *et al.*, 1981), see Table 3.I.

Features observed at high powers comprise doublets (*x*, *y* and *z*) characteristic of $HO_2^{\cdot}$ radicals. They were similar to those observed in H_2O-H_2O_2 glassy systems (Table 3.II), obtained for example by adding KBF_4, but differed surprisingly from the features obtained from polycrystalline H_2O containing H_2O_2 at concentrations similar to those

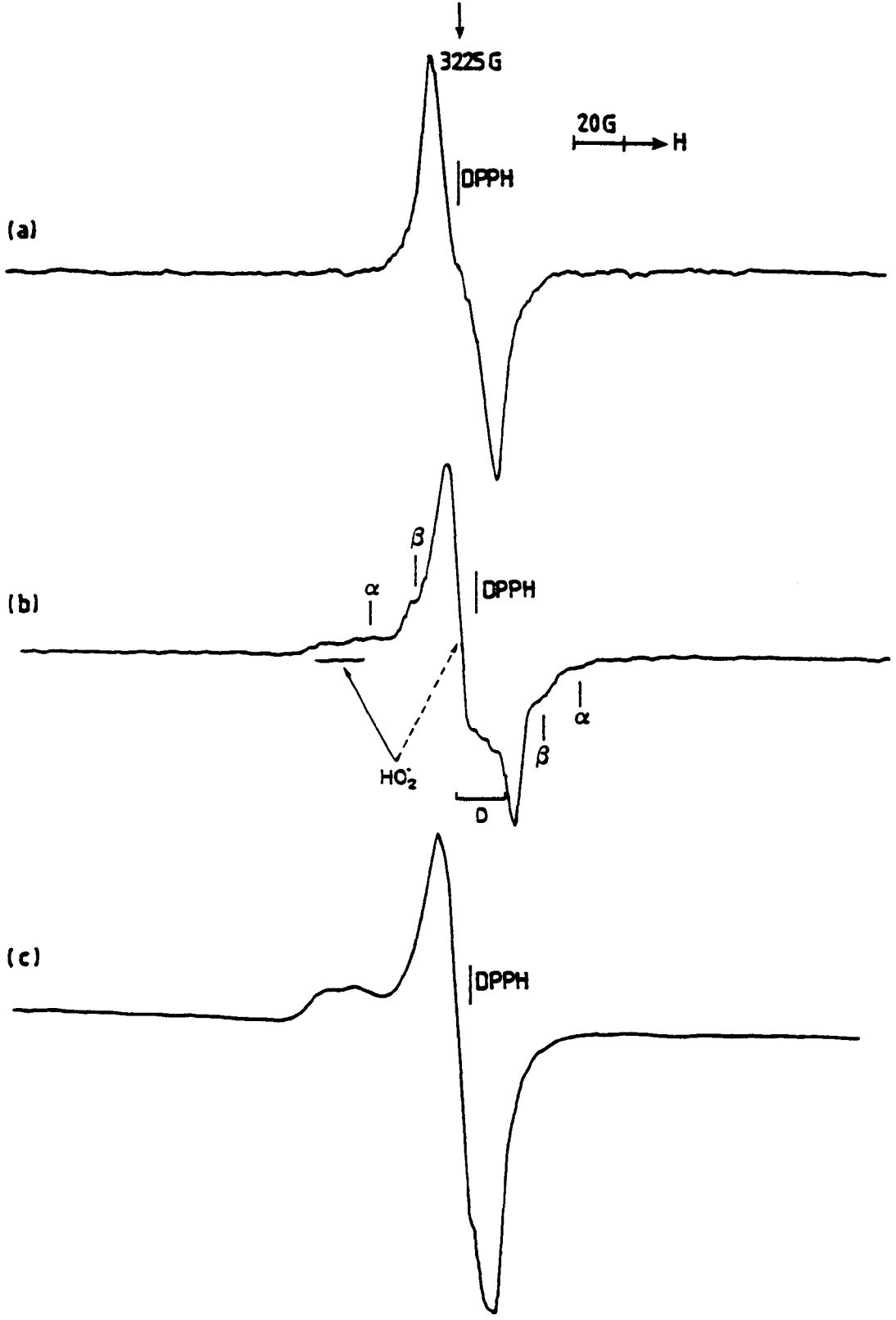

FIGURE 3.1

(a) Spectrum of an anoxic DNA solution (50 mg + 1 ml H_2O) after irradiation (dose ~1.5 Mrad.) and warming to 130 K. The spectrum shows features assigned to $G^{\cdot+}$ and $T^{\cdot-}$.
(b) Spectrum of an anoxic DNA solution (50 mg + 1 ml H_2O) in the presence of hydrogen peroxide (40 mM), after an irradiation and annealing cycle as outlined in (a), showing features α and β assigned collectively to species 'X' (see text).
(c) As in (b) with the spectrum recorded at a high microwave power (15 mW) showing parallel and perpendicular features assigned to $HO_2^{\cdot}$ radicals.

TABLE 3.I

Comparison of the Spectral E.s.r. Features of the Components of 'X' from Different Studies

Feature	Study H_2O_2[a]	Iodoacetamide[b]	$K_3Fe(CN)_6$[c]	Deoxyribose-H·[d]	Proposed Structure
α	~85 G	~85-90 G	-	~90 G	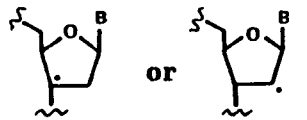
β	~55 G	~50 G	~50 G	~60 G	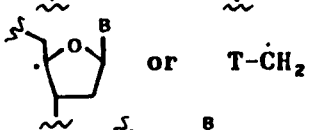
D	~20 G	~30 G	~20 G	~30 G	

[a] Present study;
[b] P. M. Cullis, M. C. R. Symons, B. W. Wren and S. Gregoli, J. Chem. Soc., Perkin Trans. 2, (1985), 1819;
[c] G. D. D. Jones and M. C. R. Symons, unpublished results;
[d] H. Riederer, J. Hüttermann and M. C. R. Symons, J. Phys. Chem., (1981), 85, 2789.

employed in the DNA experiments (Fig. 3.2).

The various effects on the e.s.r. spectra of increasing [H_2O_2] are summarized in Figure 3.3 and Table 3.III.

The effects of H_2O_2 on the yield of strand breaks are shown in Figures 3.4 and 3.5. In the absence of γ-irradiation (and transition metals), H_2O_2 does not significantly alter the yield of strand breaks. However on γ-irradiation the yield of strand breaks, both single and double, was enhanced (the latter d.s.b's were most markedly enhanced at higher concentrations of H_2O_2). The magnitude of the effect has been shown to be unequivocally dependent on the peroxide concentration (Fig. 3.5).

DISCUSSION

Formation of ·OH Radicals

An important point to note in these experiments is that the hydrogen peroxide is expected to be largely in the solvated DNA phase rather than in the ice crystals. This is because, on freezing the solution, the growing ice crystallites tend to exclude the peroxide molecules such that they generally become part of the solvated DNA phase. That the peroxide is indeed in the DNA phase is strongly supported by the fact that the e.s.r. spectrum of the $HO_2^{\cdot}$ radicals, observed under high power, was similar to that for $HO_2^{\cdot}$ radicals in aqueous glasses and was clearly distinguishable from the species formed in frozen dilute aqueous solution (Fig. 3.2, Table 3.II). The reason for the spectral differences is unknown, however the result is used empirically to establish the location of the $HO_2^{\cdot}$ radicals, and hence peroxide, as being in the vitreous frozen solvating water.

As discussed in Chapter One, damage to the ice crystals can be ignored since the hydroxyl radicals in the ice crystallites are lost on annealing without change in the nature or yield of the DNA centred radicals. The observation that $\dot{T}H$, and hence $T^{\cdot -}$, was greatly diminished in the presence of H_2O_2 (Fig. 3.3, Table 3.III) indicated that the peroxide was indeed acting as an electron trap as outlined in equation [3.1]. However the ·OH radicals proposed to be formed were not detected by the e.s.r. spectroscopy studies conducted. Reasons for this are most likely twofold. Firstly, if they are trapped, their

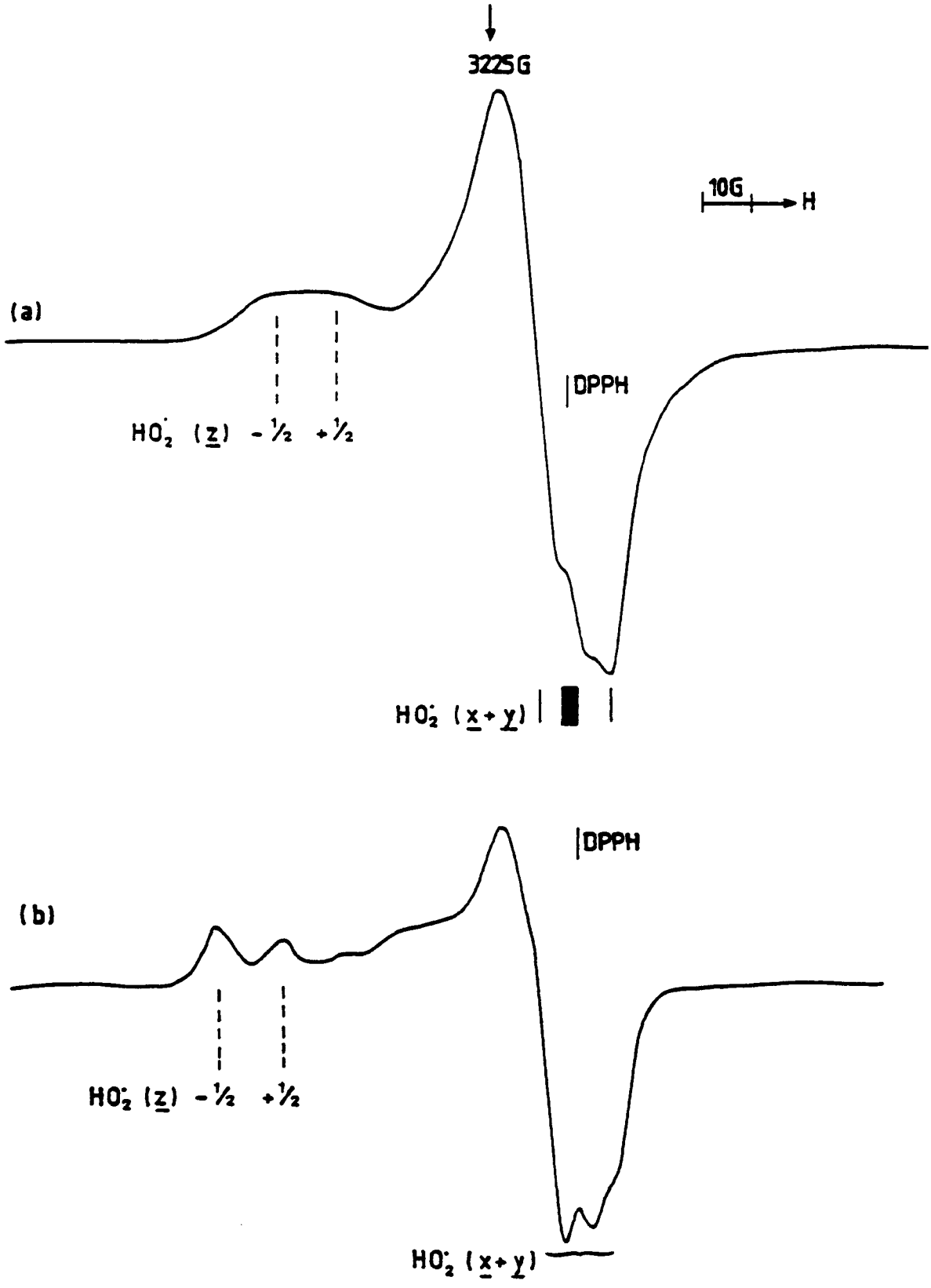

FIGURE 3.2

Comparison of e.s.r. features of $HO_2^{\cdot}$ formed in (a) frozen DNA solutions with those formed from (b) dilute frozen aqueous solutions.

TABLE 3.II

E.s.r. Parameters for $HO_2^{\cdot}$ Radicals in Various Environments

Host	^1H Hyperfine Coupling/G[a]			g-values		
	x	y	z	x	y	z
$Na^{\cdot} + O_2/H_2O$, 77 K[b]	-	av. 11.5	-	2.035,	2.0039,	2.003
H_2O_2/H_2O glass + hν/77 K[c]	13.8	3.6	15.7	2.0353,	2.0081,	2.0042
$H^{\cdot} + O_2$/Ar, u.v., 4 K[d]	13.5	8.6	8.6	2.0393,	2.0160,	2.0044
$SrCl_2.6H_2O$/77 K[e]	17.2	6	12.7	2.0355,	2.0076,	2.0031
$H_2O_2/H_2O/KBF_4$ glass 77 K + γ-rays	13.5	*f*	*f*	2.037	*f*	*f*
H_2O_2/H_2O phase separated/77 K + γ-rays	14	*f*	*f*	2.045	*f*	*f*
H_2O_2/H_2O/DNA/77 K + γ-rays	13.5	*f*	*f*	2.038	*f*	*f*

[a] G = 10^{-4} T;
[b] J. E. Bennett, B. Mile and A. Thomas, Proc. 11th. Int. Symp., Combustion, (1967), 853;
[c] S. J. Wyard, R. C. Smith and F. J. Adrian, J. Chem. Phys., (1968), 49, 2780;
[d] F. J. Adrian, E. L. Cochran and V. A. Bowers, J. Chem. Phys., (1967), 47, 5441;
[e] R. C. Catton and M. C. R. Symons, J. Chem. Soc. (A), (1969), 446;
[f] Central features hidden.

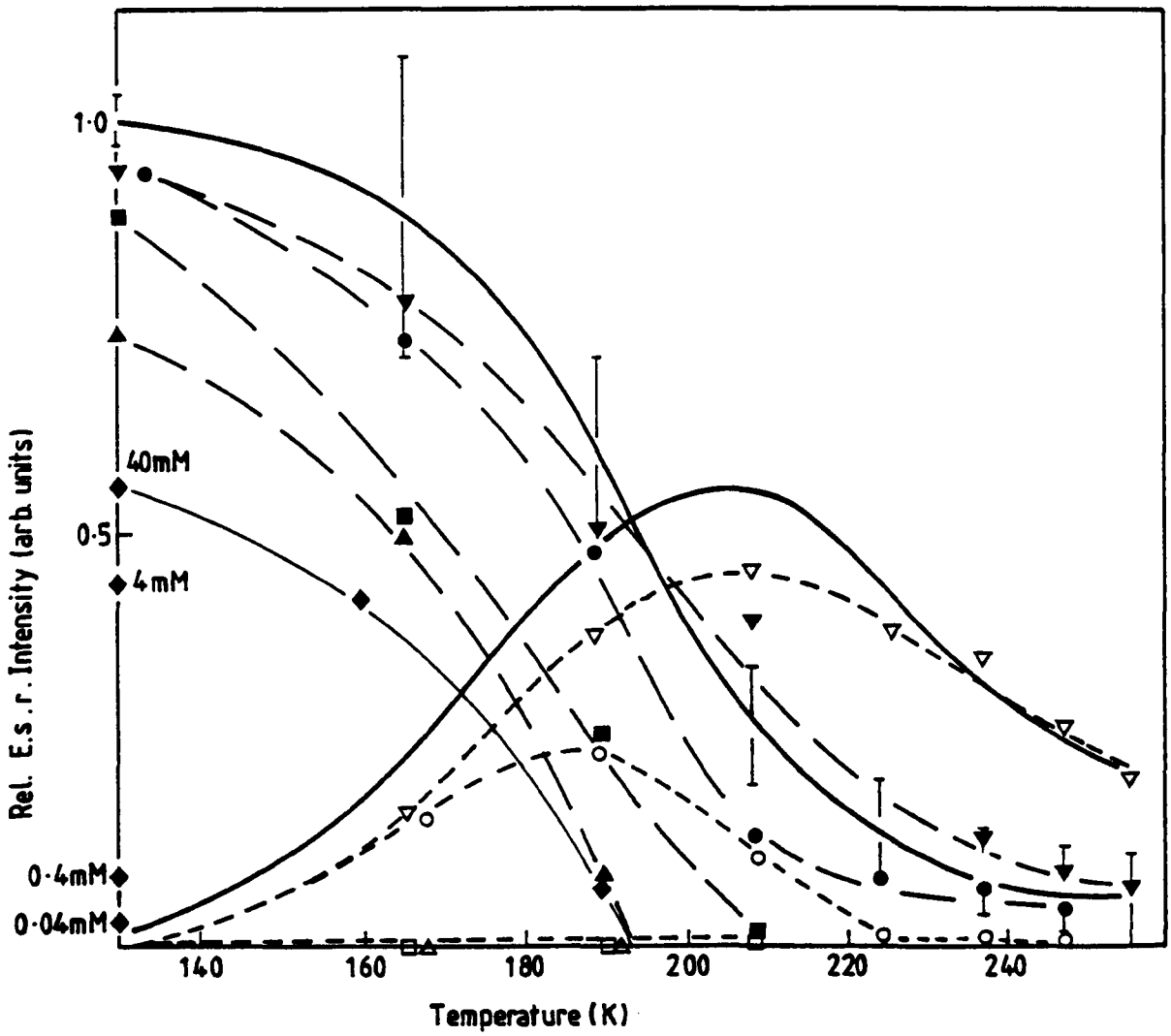

FIGURE 3.3

The temperature dependent decay of the e.s.r. spectral features of DNA after irradiation (see text and legend to Fig. 3.1) in the presence (▲,△, 40 mM; ■,□, 4 mM; ●,○, 0.4 mM; ▼,▽, 0.04 mM) and absence (thick unbroken line) of hydrogen peroxide. The plots show the decrease, with temperature, of the central features (filled symbols) of DNA ($G^{\cdot+}$, $T^{\cdot-}$, 'X') concurrent with the growth and subsequent decay of 5-thymyl radical $\dot{T}H$ (open symbols) (as measured through the relative intensity (x 5) of the seventh line of the octet, at g = 1.9731. Also shown is the temperature dependent decay of wing features (measured between g = 2.0115 and g = 1.4869) (◆) attributable to the collection of radicals previously noted as 'X' (see legend to Fig. 3.1 and text). Only 'X' feature decay in the presence of 40 mM H_2O_2 is shown.

TABLE 3.III

Summary of the Changes of the E.s.r. Spectral Features of DNA on Irradiation in the Presence of Increasing Concentrations of Peroxide

$[H_2O_2]$	A:B.P.†	Comments
0.04 mM	1:~1550	Little or no effect on the $G^{\cdot+}/T^{\cdot-}$ ratio at 130 K. $\dot{T}H$ formation largely unaffected. $HO_2^{\cdot}$ and 'X' features not apparent. DNA radicals persist to >255 K.
0.4 mM	1:~155	Little detectable effect on the $G^{\cdot+}/T^{\cdot-}$ ratio at 130 K. $\dot{T}H$ formation 25-35% of normal. $HO_2^{\cdot}$ and 'X' present but weak. A few DNA radicals persist to ≥255 K. However, a more rapid decay is evidenced.
4 mM	1:~15.5	Rapid loss of all radicals except $HO_2^{\cdot}$ by 190-210 K is noted, much faster than normal. At 130 K, a significant loss of $T^{\cdot-}$ is observed with 'X' features apparent. Near total loss of $\dot{T}H$ formation. $HO_2^{\cdot}$ and 'X' features now well established on annealing to 165 K with apparent loss of $G^{\cdot+}$. All radicals lost by ~215 K with loss of 'X' features by 195 K.
40 mM	1:~1.55	Similar rapid loss of all radicals except $HO_2^{\cdot}$ at a much accelerated rate. At 130 K a large alteration in profile is observed indicative of substantial $T^{\cdot-}$ loss with large contributions from 'X' and $HO_2^{\cdot}$. No $\dot{T}H$ observed. Features from 'X' and $HO_2^{\cdot}$ persist to 195 K with apparent loss of $G^{\cdot+}$. All radicals loss by 200 K with loss of 'X' features by 195 K.

† A:B.P. = additive:base-pair ratio

contribution to the e.s.r. spectra is expected to be poorly defined (Riederer *et al.*, 1983) and would inevitably be masked by the intense, well defined signals of the hydroxyl radicals formed in ice. Secondly, since they are formed in the DNA phase, hence in close vicinity to the DNA (and at high $[H_2O_2]$ to other peroxide molecules), they have every opportunity to react. Certainly after annealing to 130 K they must have reacted since no signals assignable to 'OH species could be detected. Also the appearance of the e.s.r. features collectively described as 'X' (see below), and the presence of $HO_2^{\cdot}$ radicals (Figs. 3.1b and 3.1c), strongly suggests that the 'OH radicals, resulting from peroxide electron capture, have reacted with the DNA or with other H_2O_2 molecules.

Radicals 'X'

Directly after loss of the 'OH radicals at 130 K, spectra of the type shown in Figure 3.1b, with strong outer e.s.r. features, were obtained. These outer lines, designated α and β, closely resembled features previously obtained from DNA irradiated in the presence of iodoacetamide, which were collectively assigned the symbol 'X'. In that study (Cullis *et al.*, 1985a) it was proposed that these signals were mainly due to sugar radicals formed by hydrogen atom abstraction (by $H_2\dot{C}CONH_2$) from various sites in the deoxyribose units. One of the reactions exhibited by 'OH at ambient temperature is such hydrogen atom abstraction (Scholes, 1983; von Sonntag *et al.*, 1981), therefore similar reactions are expected in this study. A second important reaction in fluid solutions is addition to base moieties to give the respective 'OH adducts, e.g. ĠOH (Scholes, 1983; Kasai *et al.*, 1984). These might have been expected to form in the present work, however no clear contribution to the spectra from any particular species was noted.

The 'X' component in Figure 3.1b appears to be a composite of at least three species. One with a total splitting of *ca.* 85 G (outer features α), a second species (β) for which the outer lines show a degree of asymmetry and a doublet (D) of *ca.* 20 G which proved to be the most persistent of all the secondary radicals. The extra low field signals observed in Figure 3.1b are most probably low microwave power contributions from the $HO_2^{\cdot}$ signals (Fig. 3.1c), the overlapping central feature of which results in the asymmetric appearance of the doublet. These

observations are also very similar to those obtained for radicals formed from deoxyribose by free hydrogen atom mediated hydrogen atom abstraction (Riederer *et al.*, 1981). In particular the major species, both in this and the previous iodoacetamide study, species β, is equivalent to the radical assigned Q, and α is proposed to correspond to radical Q′. These species were in turn proposed to be C_4' and C_3' (or C_2') carbon centred sugar radicals respectively (Riederer *et al.*, 1981).

The doublet noted by Riederer and coworkers was postulated as being a C_5' radical, however in that investigation and in the work involving iodoacetamide (Cullis *et al.*, 1985a) this signal had a splitting of *ca.* 30 G in comparison to one of *ca.* 20 G noted in the present peroxide study. Hence its assignment as a C_5' radical is somewhat doubtful. A second ambiguity concerns the proposed conversion of Q to Q′ noted on annealing, and hence Q being proposed as a precursor of Q′ (Riederer *et al.*, 1981). This has not been noted in the current study nor in work using a DNA-$K_3Fe(CN)_6$ system which on γ-irradiation results in remarkably strong spectra consisting predominantly of β-features (G. D. D. Jones and M. C. R. Symons, unpublished results). The conversion, Q to Q′, would involve 1-2 (or 1-3) intramolecular and/or intermolecular H· atom shifts, which are feasible in carbohydrates (Dixon *et al.*, 1977). However in the above mentioned $K_3Fe(CN)_6$ system the β-features, assigned to Q, decayed, exposing only the underlying doublet of *ca.* 20 G.

In view of the results for deoxyribose, the assignments of features 'X' to sugar radicals seems most reasonable. However a final abstraction radical should be mentioned. This is the radical formed by H· atom abstraction from the methyl group of thymine residues. This radical was previously thought to be a reasonable candidate for the β species (Cullis *et al.*, 1985a). However since it is formed only to a minor extent in the liquid phase (Scholes, 1983) its influence in the frozen system must likewise be regarded as negligible. The above observations are summarized in Table 3.I.

If the radicals responsible for 'X' are sugar radicals, this would explain the occurrence of extensive strand breaks in the presence of H_2O_2. Indeed, the fact that the number of strand breaks is enhanced by H_2O_2 strongly supports this assignment. It is important to note that sugar radicals, **when formed**, can be detected in frozen aqueous

solution. Studies with various additives, particularly iodoacetamide and H_2O_2 have shown that sugar radicals are formed under special circumstances for which one can propose reasonable mechanistic pathways.

It must however be emphasised that the features 'X' are not observed for DNA in the absence of additives. This is an important contrast since it means that these radicals are not formed significantly in the temperature range 130-190 K in the absence of additives, which in turn means that the concentration of $^{\cdot}OH$ radicals formed in the vicinity of the DNA, that is, from the solvating water, must be very low. This confirms that electron transfer to $H_2O^{\cdot+}$ is faster than proton-loss from $H_2O^{\cdot+}$ which is indicative of the proposed dry charge transfer mechanism being operative under frozen conditions.

A second important result is that features 'X' are lost at lower temperatures, *ca.* 190 K, than those at which $G^{\cdot+}/GN^{\cdot}$ and $\dot{T}H$ are lost. Hence if, as has been proposed (Cullis and Symons, 1986), sugar radicals are formed in the pathways leading from the ionic primary DNA damage ($G^{\cdot+}$ and $T^{\cdot-}$) to strand breaks, they would remain undetected by e.s.r. spectroscopy. This explains the failure to detect sugar radicals in the e.s.r. studies of γ-irradiated DNA conducted to date (Boon *et al.*, 1984; Gregoli *et al.*, 1982).

Formation of $HO_2^{\cdot}$ Radicals

As can be seen in Figure 3.1c signals from $HO_2^{\cdot}$ radicals dominate the e.s.r. spectra when recorded at high microwave power. This is as a result of the signals from the organic radicals being strongly saturated whilst saturation has not set in for the $HO_2^{\cdot}$ radicals. Their spectral data are compared with those for $HO_2^{\cdot}$ radicals formed in other matrices in Table 3.II. There is little doubt concerning their identity and, as already mentioned, the results show that these radicals are formed in the glassy DNA phase rather than in the polycrystalline ice phase. They can be produced by at least three possible mechanisms, namely direct, equation [3.2], or indirect, equation [3.3], electron-loss followed

$$H_2O_2 \rightarrow H_2O_2^{\cdot+} \rightarrow HO_2^{\cdot} + H^+ \qquad [3.2]$$

$$G^{\cdot+} + H_2O_2 \rightarrow G + HO_2^{\cdot} + H^+ \qquad [3.3]$$

$$H_2O_2 + {}^{\cdot}OH \rightarrow HO_2^{\cdot} + H_2O \qquad [3.4]$$

by proton-loss, or by attack of $^{\cdot}OH$ radicals as in equation [3.4]. Furthermore the fact that yields of $G^{\cdot+}$ were reduced (see Table 3.III) requires that reaction [3.3] is important and it is concluded that, except for relatively concentrated solutions, this reaction dominates.

The radical cation of $H_2O_2^{\cdot+}$ has not been studied by e.s.r. spectroscopy but work on the di-*t*-butyl derivative shows that this must have the expected π^* structure (Chandra *et al.*, 1983). Since H_2O_2 has a lower ionization potential than H_2O, $H_2O_2^{\cdot+}$ might well be formed indirectly from $H_2O^{\cdot+}$. On the other hand, $H_2O_2^{\cdot+}$ is expected to be a strong acid so deprotonation should be rapid, thereby inhibiting subsequent electron-transfer processes, Scheme 3.I.

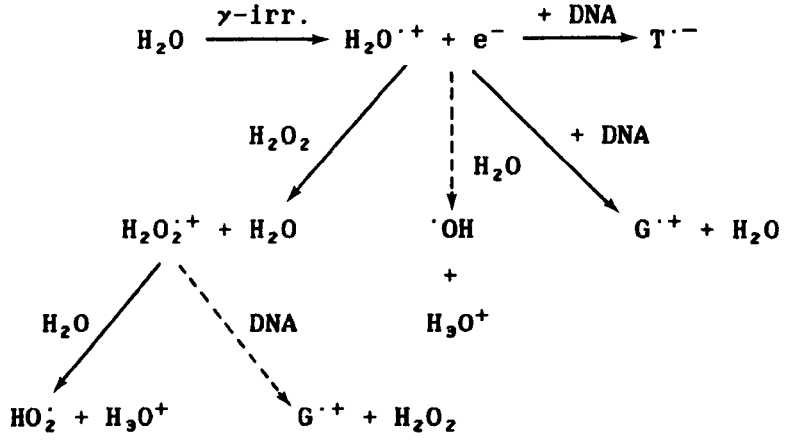

Scheme 3.I

The fact that $HO_2^{\cdot}$ radicals are lost at higher temperatures than those required for loss of species 'X' means that if, like hydroxyl radicals, they ultimately react *via* $H^{\cdot}$ abstraction to form mainly sugar radicals, these would not be detected during the hydroperoxide radical decay. That such a hydrogen abstraction should occur is expected since peroxyl intermediates ($RO_2^{\cdot}$) formed in oxygenated systems almost certainly react in this way (Boon *et al.*, 1984; von Sonntag *et al.*, 1981).

Strand Breaks

Concurrent with the e.s.r. study, reactions leading to strand breakage, both in the presence and absence of H_2O_2, have been examined (Sweeney, 1986). It has previously been established under conditions where $G^{\cdot+}$

and $T^{\cdot -}$ are the only detectable primary radicals that strand breaks occur to significant levels (Boon *et al.*, 1984), and that additives which influence the yield or nature of these primary species alter the extent to which breaks are induced (Cullis *et al.*, 1985b).

In the presence of hydrogen peroxide there is an increase in the number of both single and double strand breaks (Fig. 3.4). Exhaustive control experiments, including both pre- and post-irradiative "incubations" of plasmid with H_2O_2 show that the peroxide mediated strand break enhancement is solely radiation dependent (Sweeney, 1986) and is proportional to peroxide concentration (Fig. 3.5). The yields of d.s.b's, notably enhanced at the higher peroxide concentrations, are linear with dose up to *ca.* 300 Krad, but at higher doses cleavage of the linear fragment, Form (III) of pBR322 (see Chapter Two), into small fragments is responsible for the apparent curve.

These strand break observations are in accord with the above e.s.r. studies since $^{\cdot}OH$ and $HO_2^{\cdot}$ will, amongst other reactions, abstract hydrogen from the deoxyribose units, and the resulting sugar radicals, especially $C_4^{\prime}$, are known to result in strand breaks (Dizdaroglu *et al.*, 1975b; von Sonntag *et al.*, 1981). So the increase in strand breaks is a consequence of damage being diverted from the DNA bases (which, in the absence of additives, are the eventual sites of all damage resulting from ionizations within the DNA phase) to the sugars in a manner made more efficient by the formation of oxygen centred sugar attacking radicals. However, it is also important to note, from the comparison of relative degrees of strand break formation (Fig. 3.4), that the efficiency of the direct mechanism (*via* $G^{\cdot +}$ and $T^{\cdot -}$) is of similar magnitude to the pseudo-"indirect" mechanism mediated through $^{\cdot}OH$ and $HO_2^{\cdot}$ radicals, and so must be considered significant with regard to the indirect mechanism.

An important conclusion drawn from work using frozen aqueous solutions is that the direct mechanism causes a high degree of d.s.b's (Boon *et al.*, 1984, 1985; Cullis *et al.*, 1985a). The high incidence of d.s.b's can be explained in terms of a distribution of trapping sites for the ionic radicals $G^{\cdot +}$ or $T^{\cdot -}$ such that a significant number of these centres are trapped within *ca.* 40 Å of each other. Provided that there

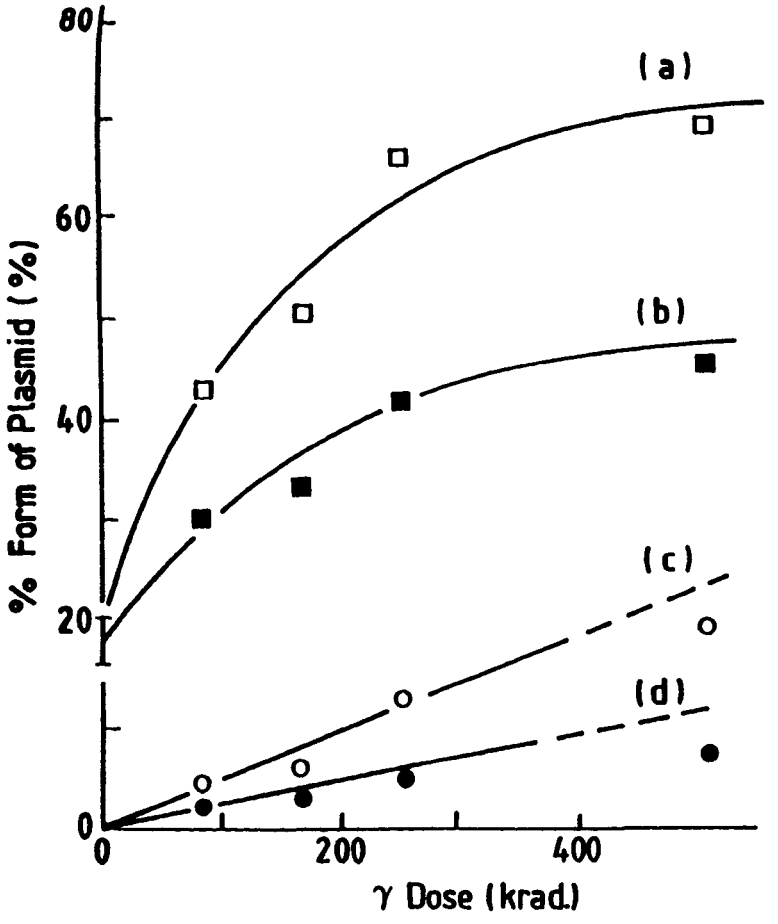

FIGURE 3.4

The effect of hydrogen peroxide on the number of strand breaks induced by γ-irradiation of plasmid DNA (pBR322) at 77 K. The percentage of Form (II) indicates single strand breaks produced (a) in the presence and (b) in the absence of H_2O_2 (4 mM). Double strand breaks formed (c) in the presence and (d) in the absence of H_2O_2 are indicated by Form (III).

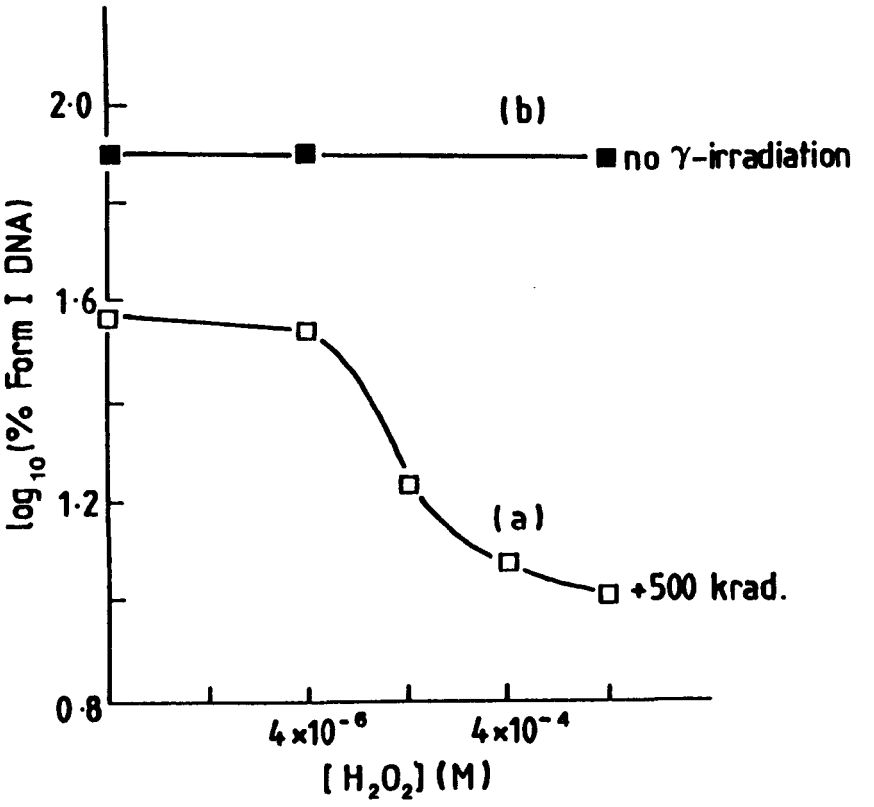

FIGURE 3.5

The effect of increasing hydrogen peroxide concentration on the radiation dependent reactions leading to strand breaks. Samples of plasmid DNA (supercoiled pBR322; *ca.* 80 μg ml^{-1}) in the presence of various concentrations of hydrogen peroxide were subjected to a constant dose of γ-irradiation (500 krad.) at 77 K (a). Control experiments (b) in which the γ-irradiation was omitted were also performed.

is a reasonable chance that both centres can lead to chain scission, it follows that d.s.b's will occur far more frequently than expected from an initial random statistical distribution of radical cations and anions. It should be emphasised that this proposal suggests that d.s.b's arise from a single ionizing event, or from a local multiple damage site (a spur), and that it is the electrons and 'holes' which are trapped closest together that are the most likely precursors of d.s.b. formation.

In the presence of moderate concentrations of H_2O_2 d.s.b's are enhanced, since under the constrained conditions imposed by frozen systems, $^{\cdot}OH$ and $HO_2^{\cdot}$ are largely trapped close to the DNA molecule. This situation contrasts with that expected for fluid systems. For higher concentrations of peroxide the direct ionization reaction, equation [3.2], may result in an enhancement of d.s.b's. Thus for example an electron ejected from H_2O_2, leaving a trapped $HO_2^{\cdot}$, could react with a nearby H_2O_2 molecule yielding an $^{\cdot}OH$ radical. These radicals are expected to react with DNA units close to the trapping sites since mobility is restricted and under the right conditions these events may lead to d.s.b's, Scheme 3.II.

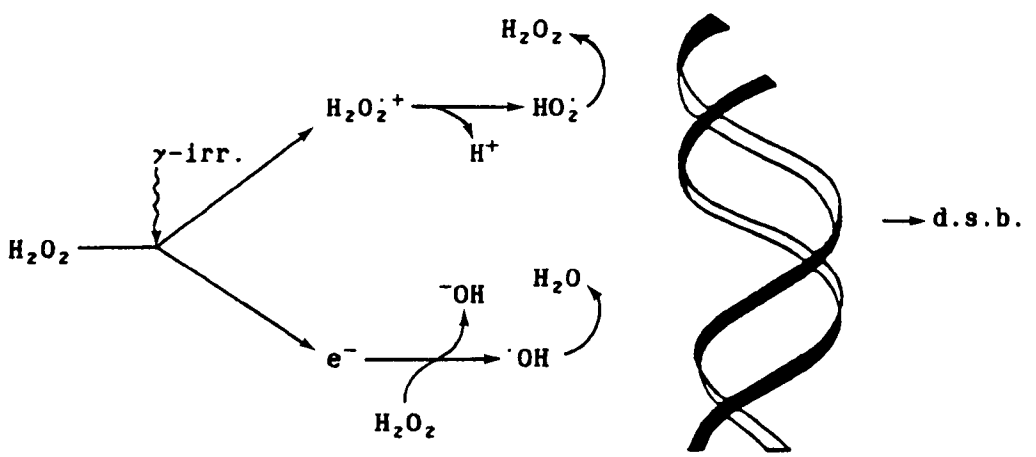

Scheme 3.II

It must be stressed that the d.s.b. enhancement primarily arises because the efficiency of strand breakage is greater, as shown by the increase in s.s.b's. However it may also reflect the fact that neutral radicals can be trapped closer together than ionic centres, since the latter can back react *via* electron transfer when they are too close.

Annealing Cycles and Near UV Sensitization

The finding that the presence of H_2O_2 enhances the overall yield of strand breaks, provides at least a qualitative explanation for the small increases in damage observed when several thermal cycles are included in radiolysis of DNA (H. Loman, private communication). Thus each time the irradiated ice crystals melt, H_2O_2 molecules formed from $^{\cdot}OH$ recombination in the ice crystals are liberated and on re-freezing these molecules will be incorporated largely into the DNA phase, as the above results have shown. Direct or indirect damage to these H_2O_2 molecules will yield $HO_2^{\cdot}$ and $^{\cdot}OH$ radicals which will attack the DNA and result in an increase in strand breaks. Similar experiments to those outlined by Loman have been conducted using the plasmid DNA assay (Chapter Two) and samples receiving the split dose freeze-thaw cycle style of irradiation showed more damage than those samples continuously irradiated at 77 K (Sweeney, 1986). Control experiments indicated that this was a radiation dependent phenomenon and not as a result of mechanical damage due to the repeated freeze-thaw cycles.

These results are also in agreement with those of Ananthaswamy and Eisenstark (1976) who have shown that hydrogen peroxide synergistically sensitizes near-UV induced breaks in phage DNA. Irradiation of H_2O_2 directly or energy transfer from the DNA to H_2O_2 could result in oxygen centred radical species similar to those discussed above and hence in an enhancement of damage. However there is some controversy as to the actual species that results in the increase in damage. As a result of superoxide dismutase activity greatly reducing T7 synergistic inactivation by near-UV and H_2O_2, it was suggested that $O_2^{\cdot -}$ and not $^{\cdot}OH$, was the virulent species in this inactivation (Ahmad, 1981, 1983). However others suggest that $O_2^{\cdot -}$ is ineffective at producing strand breaks (Blok and Loman, 1973) and that strand lesion can only occur as a consequence of hydroxyl radicals being formed (Lesko *et al.*, 1980).

CONCLUSIONS

(i) The addition of H_2O_2 to a frozen system switches the mechanism from direct damage to a pathway in part mediated through oxygen-centred radicals analogous to the indirect mechanism.

(ii) This results in an increase in the number of strand breaks and is correlated with an increase noted in e.s.r. features assignable

to sugar radicals, proposed precursors of strand breakage.

(iii) Though there is an enhancement of strand breakage under the "indirect" conditions imposed by H_2O_2 the direct mechanism is still significant in comparison to the oxygen centred radical pathway, i.e. the efficiency of conversion of $G^{\cdot+}$ and $T^{\cdot-}$ into strand breaks does not differ markedly from that of the formation of breaks *via* attack of $^{\cdot}OH$ and $HO_2^{\cdot}$.

(iv) Under the restrictive immobile conditions imposed by the frozen aqueous solution close trapping of the neutral species is important, but this is unlikely to be the case for dilute fluid solutions in which indirect damage dominates.

(v) A simple explanation for the catalytic effects of freeze-thaw cycles during exposure to ionizing radiation is that the H_2O_2 formed in ice crystallites is repeatedly transferred to the DNA phase and hence can increase the extent of damage by the proposed pathway.

(vi) The sensitization of near-UV induced strand breakage by H_2O_2 can be explained by the present results as direct or indirect production, from the peroxide, of the more efficient strand break mediating radicals $^{\cdot}OH$, $HO_2^{\cdot}$ and/or $O_2^{\cdot-}$.

CHAPTER FOUR

The Role of Thiols in Chemical Repair

INTRODUCTION

The lethal and mutagenic effects of ionizing radiation on cellular systems are assumed to be associated with the radical induced chemical changes to key biological macromolecules, particularly DNA, that accompanies exposure to such radiation (Greenstock, 1981). Many different radiation dependent alterations to DNA have been characterised ranging from various base modifications through to single and double strand breaks (Hüttermann *et al.*, 1978). The latter lesion must be considered to be a very serious form of damage since the informational content of the macromolecule cannot be easily restored. It is therefore not surprising throughout the extensive research centred on the problem of protecting living systems from the deleterious effects of ionizing radiation, that a great deal of interest has been focused at the DNA-molecular level.

At the most fundamental level of protection it is generally accepted that various small molecules play important rôles as radical scavengers, particularly with respect to the reactive hydroxyl radical, thereby preventing their interaction with DNA and other macromolecules (Sanner and Pihl, 1969; Okada, 1970; Goldstein and Czapski, 1984). Clearly this is of importance with respect to the indirect mechanism. At the next level of protection, it has been suggested that radicals formed within the DNA may be "repaired" (Copeland *et al.*, 1967; Henriksen, 1968; Adams, 1970; O'Neill, 1983). Such action, pertinent to both direct and indirect damage, may serve to intercept such radicals before they react further to give strand breaks and other forms of damage. Finally living systems can utilize a variety of complex biochemical means when dealing with the hazards associated with ionizing radiation, in particular, there are a number of efficient enzymatic repair pathways that can specifically recognise and excise a range of radiation induced modifications to DNA (Hanawalt *et al.*, 1979).

Radioprotective Action of Thiols

The ability to protect mammals against the harmful effects of ionizing radiation by pre-treatment with certain chemical compounds has been known for many years and the aminothiols, or compounds possessing (or that can give rise to) free thiol moieties, were found to be the most protective. In fact the vast majority of antiradiation agents are

aminoalkyl thiols, the prototype of which is the sulfur-containing amino acid cysteine [4.1].

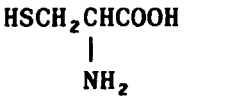

[4.1]

This compound protected 75-89% of rats subjected to 8 Gy (800 rad) when administered 5 minutes prior to X-irradiation at 175-575 mg kg^{-1} whilst only 19% of the irradiated control rats survived (Patt *et al.*, 1949). Mice given 1000 mg kg^{-1} of cysteine intravenously were protected to the extent of 50% from the lethal effects of ionizing radiation (Doherty *et al.*, 1957; Klayman *et al.*, 1969), and it was also found that chromosome damage in irradiated human bone-marrow cells was reduced 58% by cysteine (Romito, 1969).

The decarboxylated form of cysteine, namely 2-mercaptoethylamine [4.2] (MEA), more commonly called cysteamine, was an even more promising anti-radiation agent (Bacq *et al.*, 1951).

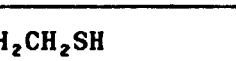

[4.2]

MEA as the free base is readily air oxidized to its disulfide form, however the hydrochloride is less susceptible to air oxidation and is the form in which it is generally stored and administered. Due to its structural simplicity, MEA hydrochloride is one of the most studied antiradiation agents. It is the compound that not only serves as a model for the design of other agents, but generally is also the standard by which the activity of other agents are judged. The antiradiation properties of MEA were optimized in mice if it was administered 10 minutes prior to irradiation (Bacq and Beaumariage, 1965), whereas in rats, best results were obtained by administration 45 minutes before irradiation (Smoliar, 1962). MEA protected mouse (Mandl, 1959; Luning *et al.*, 1961) and rat (Starkie, 1961; Fedorov, 1965) spermatozoa, and in the rat foetus it prevented foot deformities and gait defects in the progeny if administered to mothers prior to irradiation on the fourteenth day of pregnancy (Ershoff *et al.*, 1962). Also, it reduced learning deficiency in surviving rats irradiated in utero (Roberts, 1972).

That the mechanism of thiol protection was, in part, chemical (involving fast chemical reactions) rather than biochemical (involving slow reactions of protecting agents with biologically important targets prior to or after irradiation) was shown by rapid mixing of cysteine with bacteria or lysozyme. With a pre-irradiation mixing time as short as 4 ms protection was found, but with mixing 5 ms after irradiation no protection was observed. Theories concerning their mode of action are based at the molecular level and classically include radical scavenging (Sanner and Pihl, 1969; Okada, 1970), hydrogen transfer (Copeland *et al.*, 1967; Henriksen, 1968; Adams, 1970) and the mixed disulphide hypothesis (Eldjarn and Pihl, 1956; Eldjarn *et al.*, 1956). Since DNA has no -SH or -SS- moieties it would seem that the latter mixed disulphide hypothesis, which requires temporary disulphide bond formation between added thiol and target, does not apply to the protection of what is considered to be the most important target.

The most generally accepted mechanism by which sulphydryl compounds act in biological systems is by hydrogen atom donation (Adams *et al.*, 1968, 1969; Ward, 1971). The chemical reaction for this "transfer" process was first described by Alexander and Charlesby (1955) to explain -SH protection against radiation induced cross linking of polyvinyl-alcohol in anoxia, equation [4.3], though at the time there was no agreement that such a process could explain radiobiological protection.

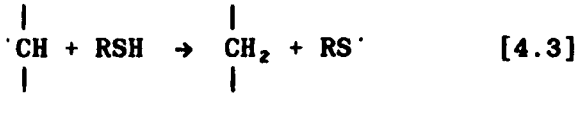

$$\begin{array}{l} | \\ \cdot CH \\ | \end{array} + RSH \rightarrow \begin{array}{l} | \\ CH_2 \\ | \end{array} + RS\cdot \qquad [4.3]$$

This repair mechanism was again suggested by Scholes and Weiss (1959) who postulated that the reaction would be in competition with oxygen fixation of the damage,† equation [4.4].

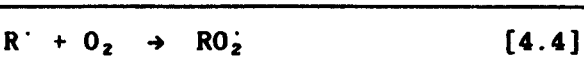

$$R\cdot + O_2 \rightarrow RO_2\cdot \qquad [4.4]$$

Later, working at the biomolecular level, Hutchinson (1961) was able to show radioprotection by sulphydryl compounds of enzymes and nucleic acids irradiated in dilute aqueous solutions. It was clear from this

† This topic still constitutes an exceedingly important area of radiation biology and has since been further expounded on at length by others (Howard-Flanders, 1960; Held *et al.*, 1981; Willson, 1983).

work that the glutathione scavenged a considerable amount of aqueous free radicals. However the data, particularly the oxygen effect observed in the presence of -SH groups, were consistent with hydrogen atom transfer to the biomolecule.

One of the clearest and earliest investigations of the hydrogen atom transfer reaction in model systems were those conducted by Ormerod, Riesz and coworkers (1966, 1967). They irradiated solids *in vacuo*, recorded the e.s.r. spectra of the radicals produced and determined their concentrations. The samples could then be exposed to a selected atmosphere and the e.s.r. spectra followed. When hydrogen sulphide was used, the radical e.s.r. signal disappeared. If the H_2S was labelled with tritium, covalently bound tritium was found in the exposed material. When the material was a protein (Riesz *et al.*, 1966) the label could be traced into the constituent amino acids following hydrolysis. The yield of free radicals as measured by e.s.r. was in close agreement with the measurement of incorporated tritium, clear evidence of H' atom transfer to the protein radical sites. However when the same experiment was conducted with dry DNA (Ormerod and Riesz, 1967), the degree of tritium incorporation was far greater than the yield of free radicals. This was thought to be indicative of a chain reaction propagated by thiyl radicals ($RS^{\cdot}$) adding to unsaturated DNA bases. Alternatively, it could also be as a consequence of $RS^{\cdot}$ mediated $H^{\cdot}$ abstraction from the deoxyribose moiety, as recently discussed by Akhlaq *et al.* (1987). However, it was proposed that the bimolecular radical termination step, equation [4.5], would predominate in aqueous solution (Ormerod and Riesz, 1967).

$$RS^{\cdot} + RS^{\cdot} \rightarrow RSSR \qquad [4.5]$$

The intense transient absorption spectrum of the radical anion $RS\dot{S}R^{-}$ ($\lambda_{max} \approx 410$ nm) produced by pulse radiolysis of cysteamine solutions *via* reaction [4.6] (Adams *et al.*, 1967) was used to measure the

$$RS^{\cdot} + RS^{-} \rightleftharpoons RS\dot{S}R^{-} \qquad [4.6]$$

kinetics of $H^{\cdot}$ transfer reactions from the sulphydryl group to a number of organic radicals (Adams *et al.*, 1968, 1969). For organic radicals it was found that the rates varied from 4.2×10^{6} M^{-1} s^{-1}, for the radical

resulting from H· abstraction from isopropyl alcohol, to $\leq 10^7$ M^{-1} s^{-1} for radicals formed on thymidine. It was also shown that oxygen could compete with the sulphydryl for the radical site and that with the radical from methanol it reacts over thirty times faster than MEA.

Action of Thiols Towards Sugar Radicals

Deoxycytidylic acid (dCMP) irradiated in aqueous solution has been employed as a model system for examining mechanisms of strand break formation in DNA (Ward, 1971). It has been proposed that the reaction leading to the formation of strand breaks was the abstraction of a hydrogen atom from the deoxyribose portion of the molecule, equation [4.7] (von Sonntag *et al.*, 1981; Dizdaroglu *et al.*, 1975b).

Base-sugar-phosphate + ·OH →
base-sugar· + phosphate (Pi) + H_2O [4.7]

With inorganic phosphate (Pi) release being equated to strand break formation in DNA, it was reasoned that if hydrogen atom donation from an -SH compound could take place, i.e. chemically repairing the sugar damage, then the yield of released phosphate should be decreased. Figure 4.1 shows the yield of phosphate release as a function of MEA concentration (Ward, 1971). Obviously with a mixture of solutes, competition exists for the primary free radicals (·OH) so that a reduction in the yield of Pi was expected. This anticipated reduction was calculated using known rate constants and is indicated by the broken line in Figure 4.1. It was observed that the measured yield of Pi release was much lower and could be explained by the occurrence of the chemical repair process.

Nucleoside, nucleotide and DNA radicals have been shown to react with cysteine with rates of the order of 10^8 M^{-1} s^{-1} (Greenstock and Dunlop, 1975). It was assumed that this rate predominately represents reaction with the sugar component of the molecules. This assumption is consistent with the observation that the -SH compound dithiothreitol (DTT) reacts with 2'-deoxyribose and some related sugars in a manner consistent with two time components. The rates for the slow component ranged from 0.5 to 9 x 10^7 M^{-1} s^{-1}, depending on the sugar, and the rates for the fast component were approximately tenfold greater (Held *et al.*, 1985).

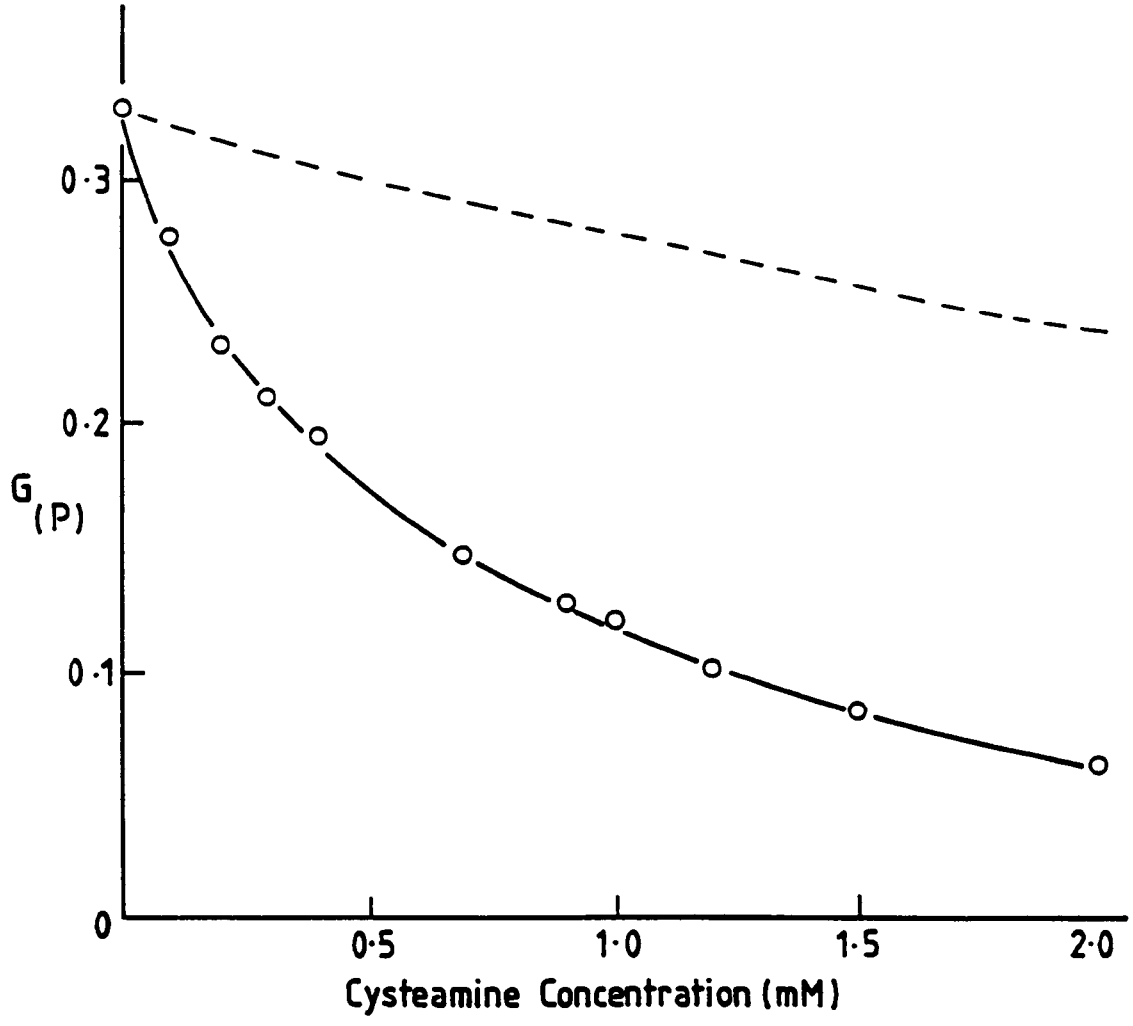

FIGURE 4.1

Effect of cysteamine concentration on the γ-radiation yield of total (inorganic + labile) phosphate from aqueous solutions of deoxycytidylic acid (10^{-2} mol dm^{-3}) at pH 4 in the absence of oxygen. (O) Experimental data. Dashed curve calculated for reduction of yield expected when allowance is made for hydroxyl radical scavenging. From Ward, (1971).

Thiol mediated hydrogen transfer to a carbon centred sugar radical can result in either inversion or retention of configuration at that centre. Repair that proceeds with inversion of an optically active centre, i.e. at C_4' (Fig. 4.2) has been termed a "pseudo repair" because the repair is configurationally incorrect (Akhlaq *et al.*, 1987). Though there is some evidence that inversion on repair occurs in model compounds (Cadet and Berger, 1985), it is conceivable that in double stranded DNA, the base-pairing constraints introduce a bias for the sugar radical to undergo proper repair rather than pseudo repair, which most likely constitutes serious damage.

Action of Thiols Toward Base Radicals

While the chemical repair by thiols is easily applied to free radicals formed on the deoxyribose moieties of DNA, the repair of base radicals needs further consideration. Most of the product radicals formed between the free radicals of water radiolysis and the DNA bases are *via* addition (Ward, 1975; Scholes *et al.*, 1969). In equation [4.8] the reaction of ·OH with cytosine is indicated.

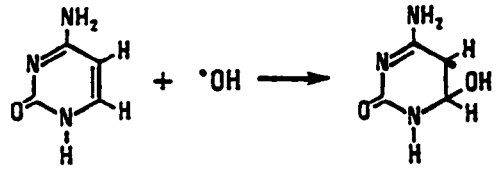

[4.8]

Donation of a hydrogen atom to such a radical centre does not constitute repair but rather the formation of a hydrate, equation [4.9].

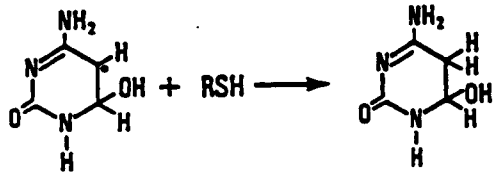

[4.9]

Hydrogen atom donation by cysteine to the hydrogen atom adduct of cytosine to form the dihydro-derivative was observed by Holian and Garrison (1969). They followed the reaction *via* the release of ammonia caused by the spontaneous hydrolysis of the dihydro-compound. Similarly, the 5,6-dihydrothymidine, formed from the parent nucleoside by irradiation in the presence of cysteine and glutathione, was accounted for by H· donation to the 5,6-dihydrothymid-5-yl and 6-yl radicals (Cadet and Berger, 1983).

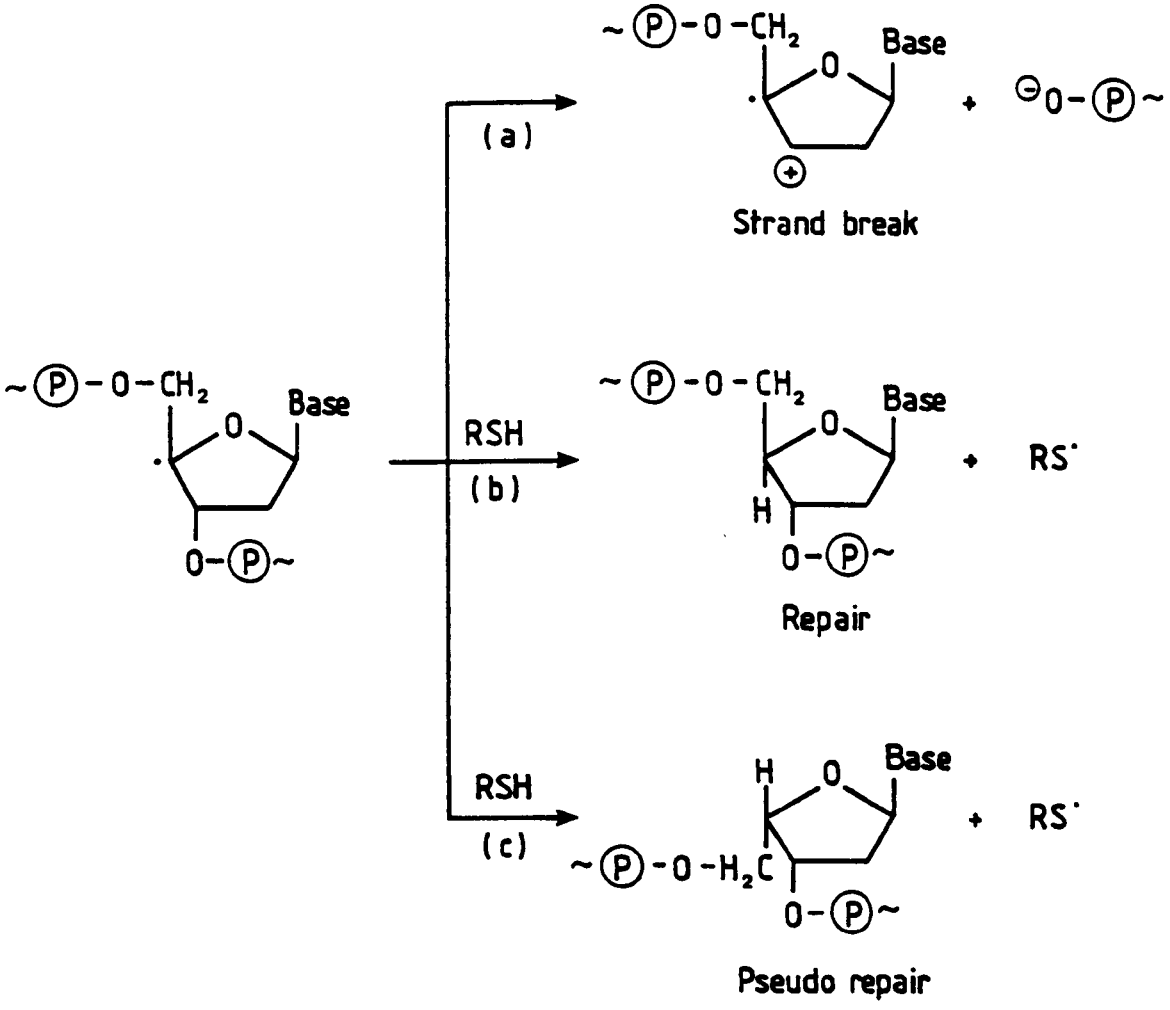

FIGURE 4.2

A scheme showing the C_4' radical of DNA either yielding a strand break, *via* a β-elimination, (reaction a) or its repair (reaction b) or pseudo repair (reaction c) by thiol.

Hydrogen donation to pyrimidine OH adduct radicals by thiols occurs with rate constants in the vicinity of 10^6 M^{-1} s^{-1} (Adams *et al.*, 1968; Nucifora *et al.*, 1972), approximately one order of magnitude slower than their reaction with sugar radicals. These values are in good agreement with the rate constant for repair by DTT of poly(U) (1.7×10^6 M^{-1} s^{-1}; Bothe and Schulte-Frohlinde, 1982), so in the case of poly(U) it was concluded that the major part of thiol repair occurs by hydrogen atom donation to the base radicals (Akhlaq *et al.*, 1987).

For poly(U) the major contribution to strand breakage and its repair is due to base radicals. However, in DNA G(strand breakage) is much lower than for poly(U) (Lemaire *et al.*, 1984; von Sonntag *et al.*, 1981) and it may be that DNA base radicals contribute relatively less and hence primary sugars relatively more to this process. This may account for the apparent differences in the reaction rates noted for thiol action towards DNA and poly(U) radicals.

There has been a recent upsurge of interest in these repair reactions particularly with respect to the rôle of the tripeptide glutathione (GSH) in modifying the response of cells to ionizing radiation (Revesz and Malaise, 1983; Ward, 1983; Michael *et al.*, 1983), where efficient repair of damaged DNA is strongly implicated.

The present study investigates the chemistry involved when thiols interact with the primary and secondary DNA radicals produced under conditions of direct damage. The majority of the studies outlined above have concentrated on the rôle of thiols under conditions of indirect damage. However, it has been argued that in the cells of eukaryotes the nuclear DNA is not well modelled by a dilute aqueous solution and that because there is not a substantial amount of bulk water present in the nucleus, the direct damage pathway will make a significant contribution (Boon *et al.*, 1984; Gregoli *et al.*, 1982).

Studies of nucleic acid-thiol systems under direct conditions have been previously conducted. Most recently, Schulte-Frohlinde and coworkers (1985b) showed that the thiols, glutathione and dithiothreitol, prevented poly(U) single strand breakage by reacting with a "poly(U)

intermediate", generated directly by laser-flash photolysis. The repair reaction rate constants were 0.16 x 10^6 M^{-1} s^{-1} and 1.2 x 10^6 M^{-1} s^{-1} for GSH and DTT respectively. Surprisingly, in contrast to the data given above, these authors explained that the reaction rate constant of 1.2 x 10^6 M^{-1} s^{-1} noted for DTT was as a consequence of the repair of C_4' and/or C_2' sugar radicals rather than uracil radicals, even though they quote the rate constant for the reaction of DTT with ribose radicals as 1.2 x 10^7 M^{-1} s^{-1} and the rate constant for its reaction with uracil OH adducts as 1 x 10^6 M^{-1} s^{-1}. They substantiate their claim by stating that with radicals from poly(U) the corresponding reaction rate constants, in comparison to uracil, are expected to be smaller by up to one order of magnitude due to steric factors and a lower collision factor caused by the polymeric nature of poly(U).

Other studies of DNA-thiol systems under direct conditions have almost exclusively dealt with dry solid samples, often under vacuum (Ormerod and Alexander, 1963; Milvy, 1971). For reasons already discussed (Chapter One) these systems are not believed to typify direct damage expected *in vivo*. The results from such studies (mainly e.s.r.) are, however, consistent with a transfer of spin from the DNA to the thiol in accordance with hydrogen atom donation, though several ambiguous points necessitate re-examination. Also, comparatively recent evidence that thiols can act as reducing agents (*via* electron transfer) towards DNA radicals that are proposed direct damage centres (Willson *et al.*, 1974; O'Neill, 1983) can be investigated.

EXPERIMENTAL

The e.s.r. spectroscopic measurements, both at X- and Q-band frequencies, of the DNA-RSH, RSSR and RSMe (glutathione, cysteamine, cysteine, dithiothreitol, cystamine and S-methyl-L-cysteine) systems were conducted as outlined in Chapter Two using additive concentrations of 0.1-140 mM (additive to base-pair ratio, 1:~620-~0.44). The spectrum of 5,6-dihydro-5-thymyl radicals (ṪH) for computer subtraction was obtained from a wet DNA sample (100% relative humidity), γ-irradiated and annealed as described in Chapter Two.

The plasmid assays for DNA s.s.b's and d.s.b's were conducted in collaboration with Mrs. (now Dr.) M. C. Sweeney. Samples of plasmid DNA

at a concentration of 100 μg/ml in the presence and absence of MEA (5 mM or 40 mM) were purged with oxygen or thoroughly deoxygenated nitrogen for 30-60 minutes prior to irradiation. Quantitation of strand breaks was carried out as described in Chapter Two. The average of duplicates is given.

RESULTS

It is now generally accepted that γ-irradiation of DNA, either as frozen aqueous solutions or as dry films, at 77 K, gives rise to a remarkably simple pattern of primary damage with the initial ionic radicals being exclusively the guanine radical cation ($G^{\cdot+}$) and the thymine radical anion ($T^{\cdot-}$) in approximately equal yields (Boon *et al.*, 1984; Gregoli *et al.*, 1982; Hüttermann *et al.*, 1984). On thermal annealing in the presence or absence of oxygen these ionic centres convert to neutral secondary radical species and in so doing yield DNA e.s.r. spectra dominated by peroxyl radical features (Fig. 4.3c) or 5-thymyl radical signals (Fig. 4.3a) respectively.

The inclusion of a variety of thiols (1 mM to 40 mM) in the frozen aqueous solutions of DNA did not alter the relative or absolute proportions of $G^{\cdot+}$ and $T^{\cdot-}$. However, on annealing, the normal e.s.r. patterns were abruptly modified, with all e.s.r. signals being lost at temperatures well below those at which they are normally stable, i.e. for a cysteamine concentration of 40 mM all signals were lost by 210±10 K (Fig. 4.3b and 4.3d). Figures 4.4 and 4.5 profile the decay of DNA e.s.r. radical features on warming, in the presence of 10 mM MEA, under anoxic and oxic conditions respectively, and Table 4.I summarizes the effects on the DNA e.s.r. spectra of the various water soluble thiols investigated.

Concurrent with the loss of the DNA radical signals, the growth and decay of e.s.r. signals attributable to sulphur-containing species was observed. Under anoxic conditions the broad features of the $RS\dot{S}R^{-}$ radical anions were well defined at Q- (Fig. 4.6a) and X-band† (Fig. 4.6b) frequencies, and a comparison of spectral data with those from the

† At X-band frequencies, the e.s.r. features of $RS\dot{S}R^{-}$ were observed after subtraction of overlapping TH signals (see legend to Fig. 4.6b).

literature and from previous studies (G. D. D. Jones, J. S. Lea and M. C. R. Symons, unpublished results) (Table 4.II) supports this assignment. At a cysteamine concentration of 40 mM, the e.s.r. features of $RS\dot{S}R^-$ were lost by 210 K, the temperature at which <u>all</u> the signals were lost (Fig. 4.7).

Under oxic conditions strong, sharp features at g = 2.017 and 2.025 were observed amongst residual $RO_2^{\cdot}$ signals (Fig. 4.8a). These were identical to the features assigned to the aminothiol sulphur peroxyl radical ($RSO_2^{\cdot}$) observed in a spectrum of γ-irradiated *E.coli* B/r plus 0.1M mercaptopenthylamine (MPA) by Copeland (1975) (Fig. 4.8b and Table 4.II). Further work from a related study (G. D. D. Jones, J. S. Lea and M. C. R. Symons, unpublished results) concerning the addition of O_2 to $RS^{\cdot}$ (from glutathione) confirms this assignment (Table 4.II).

As a consequence of the dramatic influence that thiols have on the direct DNA radiolysis pathways, a study was conducted to judge the effect of MEA on strand break induction under similar conditions using the plasmid assay described in Chapter Two. The data concerning the percentage formation of pBR322 Form (II) (s.s.b.) and Form (III) (d.s.b.) and loss of Form (I) (as $\log_{10}$), with dose, under oxic and anoxic conditions, in the presence (and absence) of MEA (40 mM), is shown in Table 4.III, and depicted in Figures 4.10a and 4.10b. Similarly for 5 mM MEA ($\pm O_2$) data for percentage formation of Form (II) and (III), and loss of Form (I), with dose, is given in Table 4.IV and plotted in Figures 4.11a and 4.11b.

For comparative purposes DNA in the presence of RSMe (S-methyl-cysteine, 40 mM) and RS^- (MEA [10 mM] + 10 mM/100 mM NaOH) were studied and their temperature dependent e.s.r. decay patterns are shown in Figures 4.12b, 4.12c and 4.13b.

Also a DNA-RSSR (cystamine, 40 mM) system was examined and the spectrum recorded after warming to 130 K is shown in Figure 4.14.

DISCUSSION

The γ-irradiation of frozen aqueous solutions of DNA at 77 K results in the surprisingly simple initial damage of $G^{\cdot+}$ and $T^{\cdot-}$ in equal yields.

On annealing, in the absence of oxygen, the thymine radical anion protonates on carbon (C6) to yield the 5-thymyl radical $\dot{T}H$ that is unambiguously characterised by its well established eight-line e.s.r. spectrum (Fig. 4.3a). $G^{\cdot+}$ decays without accumulation of any secondary radical that can be easily distinguished from the parent cation by e.s.r. spectroscopy under the conditions used in the present study. However, a recent investigation involving oriented DNA fibres, suggests that $G^{\cdot+}$ decays at 220 K *via* loss of a proton from nitrogen to give a neutral radical (symbolized as $G\dot{N}$) with a high spin-density on nitrogen (N3) (HUttermann and Voit, 1986).

Effects of Thiols (E.s.r. Studies of Anoxic Systems)

The addition of moderate concentrations of a range of thiols (MEA, cysteine, glutathione and dithiothreitol) (1-40 mM) to frozen aqueous solutions of DNA did not alter the initial relative or absolute amounts of either $G^{\cdot+}$ or $T^{\cdot-}$. However, at higher concentrations of MEA (>40-140 mM) a slight decrease in the yield of $T^{\cdot-}$ was noted. This was probably due to traces of oxidized MEA (RSSR) present in the commercial material or formed during incubation with DNA. The disulphide is an effective electron scavenger (see below).

On annealing irradiated frozen aqueous DNA solutions in the presence of a variety of thiols all e.s.r. signals were abruptly lost at temperatures well below those at which they normally decay (see Figs. 4.3b and 4.4 and Table 4.I). Concurrent with this sudden loss of DNA radical features, the growth and subsequent decay of signals from sulphur-centred species, derived from transient thiyl radicals ($RS^{\cdot}$), was observed (see below). The loss of all DNA radicals at temperatures below those at which they normally decay was demonstrated under anoxic conditions at thiol concentrations as low as 1 mM (1:62 base pairs). Below this concentration some radicals did survive to higher temperatures.

Effect of Thiols (E.s.r. Studies of Oxic Systems)

Under oxic conditions, in the absence of thiols, the DNA radicals ($\dot{T}H$ and probably $G\dot{N}$) are efficiently converted to peroxyl radicals ($RO_2^{\cdot}$) at *ca.* 190±10 K, these radicals being characterised by a broad singlet with $g_{\parallel}$ ~2.033 and $g_{\perp}$ ~2.000 (Fig. 4.3c). When thiols were included, the $RO_2^{\cdot}$

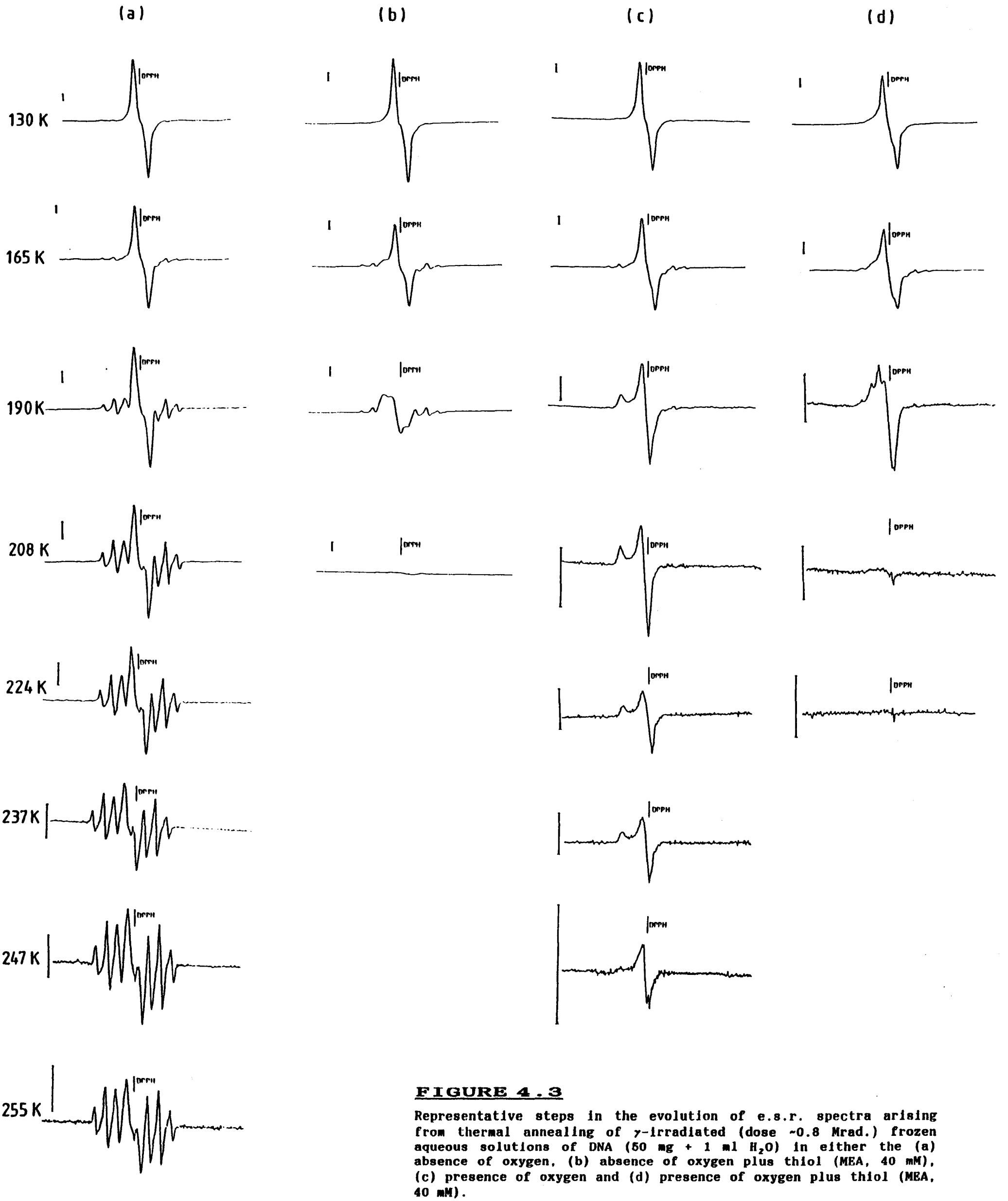

FIGURE 4.3

Representative steps in the evolution of e.s.r. spectra arising from thermal annealing of γ-irradiated (dose ~0.8 Mrad.) frozen aqueous solutions of DNA (50 mg + 1 ml H_2O) in either the (a) absence of oxygen, (b) absence of oxygen plus thiol (MEA, 40 mM), (c) presence of oxygen and (d) presence of oxygen plus thiol (MEA, 40 mM).

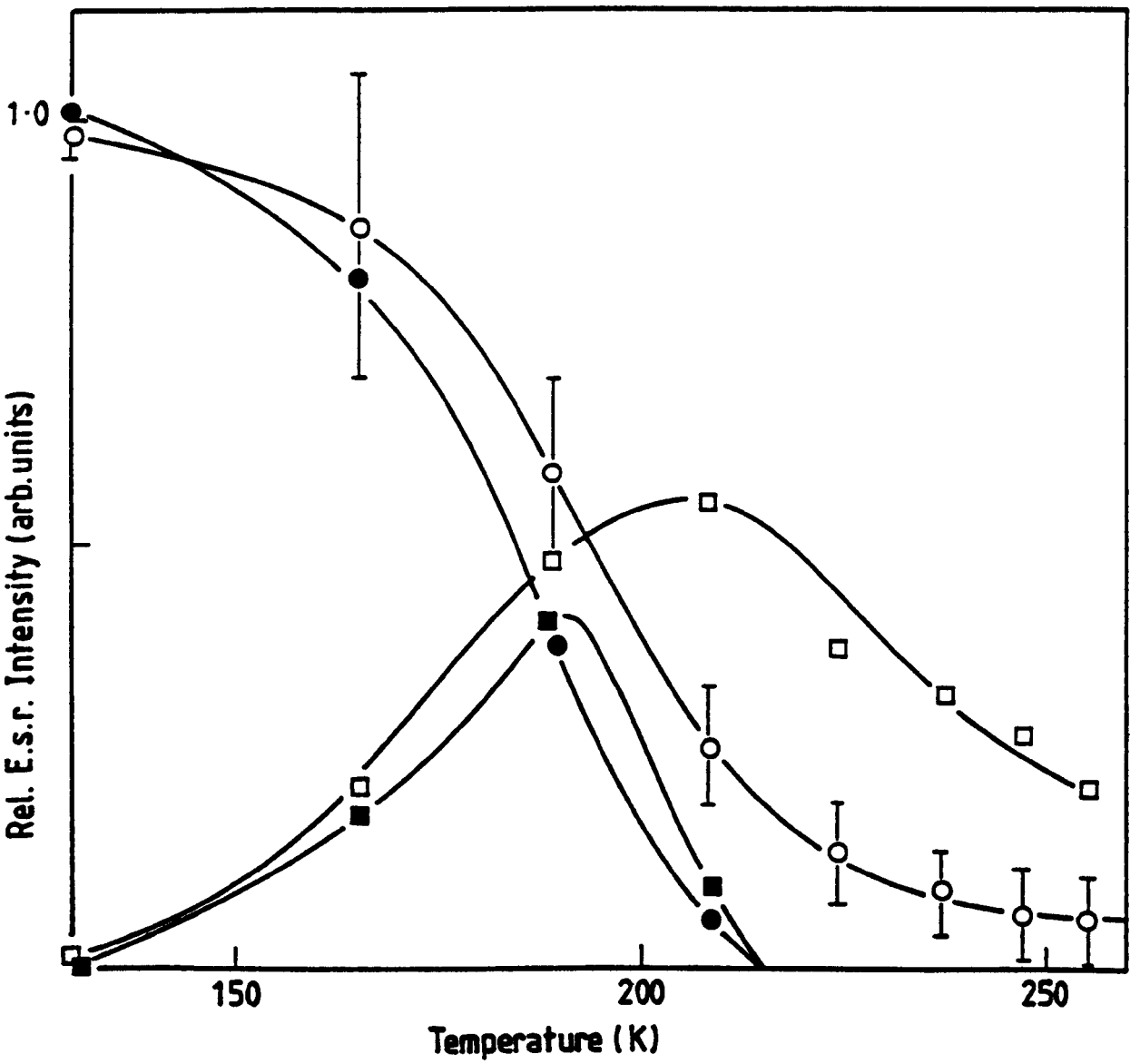

FIGURE 4.4

Temperature dependent decay of the e.s.r. features of anoxic DNA solutions (50 mg + 1 ml H_2O) following irradiation (dose ~0.8 Mrad.). The intensities of the central features ($G^{\cdot+}$ and $T^{\cdot-}$) of the DNA spectra in the presence (●) and absence (○) of MEA (10 mM) are shown as a function of annealing temperature together with the growth and decay of the TH signals (as measured through the relative intensity (x 5) of the seventh line of the TH octet at *ca.* g = 1.9731) in the presence (■) and absence (□) of thiol.

TABLE 4.I

Summary of the Changes to the E.s.r. Spectral Features of Anoxic Frozen Aqueous Solutions of DNA on Irradiation in the Presence of a Variety of Water Soluble Thiols (40 mM)†

Mercaptoethylamine (MEA) $NH_2-CH_2-CH_2-SH$	No effect on $G^{\cdot+}$ and $T^{\cdot-}$ formation at 130 K. Onset of $RS\dot{S}R^-$ features and associated yellow colouration (λ_{max} 410 nm) noted by *ca.* 190 K. $\dot{T}H$ reduction over 190-208 K, 70-~0% of norm. Last radical observed at *ca.* 210 K.
Dithiothreitol (DTT) $HS-CH_2-[CH(OH)]_2-CH_2-SH$	No effect on $G^{\cdot+}$ and $T^{\cdot-}$ formation at 130 K. Onset of $RS\dot{S}R^-$ features and yellow colouration noted by *ca.* 190 K. $\dot{T}H$ reduction over 190-208 K, 90%-50% of norm. Last radical observed at ~>208-224 K.
Cysteine 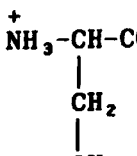	No effect on $G^{\cdot+}$ and $T^{\cdot-}$ formation at 130 K. Onset of $RS\dot{S}R^-$ features and yellow colouration noted by *ca.* 190 K. $\dot{T}H$ reduction over 190-208 K, 60-40% of norm. Last radical observed at >208-224 K.
Glutathione (GSH) 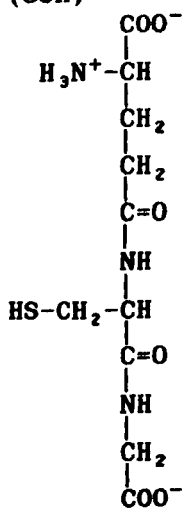	No effect on $G^{\cdot+}$ and $T^{\cdot-}$ formation at 130 K. Onset of yellow colour noted by 208 K concurrent with appearance of a doublet of 26 G. $\dot{T}H$ reduction over 190-208 K ~10% of norm. Last radicals observed at 224 K.

† RSH : base-pair, 1:~1·55.

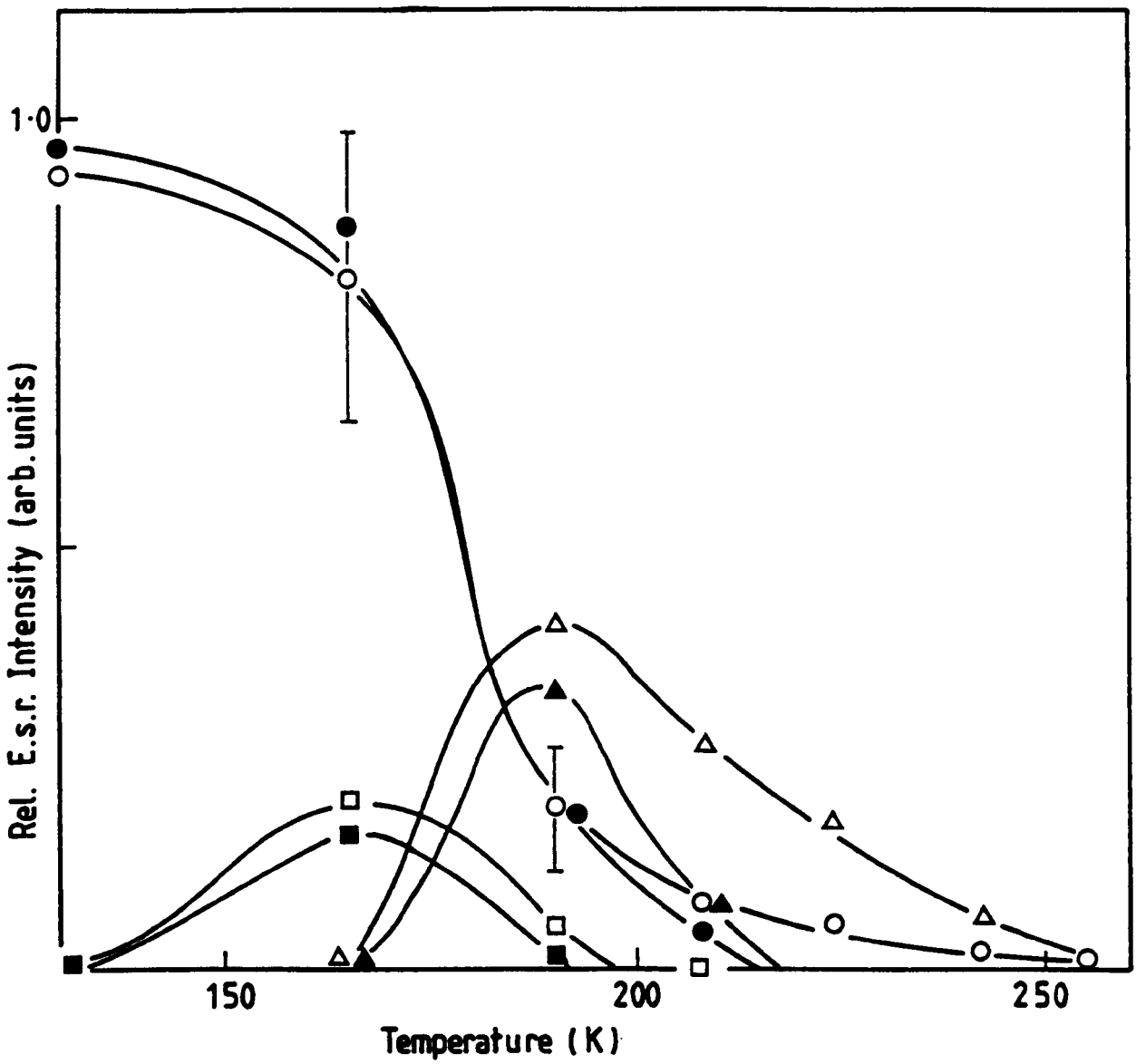

FIGURE 4.5

Temperature dependent decay of the e.s.r. features of oxic DNA solutions (50 mg + 1 ml H_2O) following irradiation (dose ~0.8 Mrad.). The intensities of the central features ($G^{\cdot+}$ and $T^{\cdot-}$) of the DNA spectra in the presence (●) and absence (○) of MEA (10 mM) are shown as a function of annealing temperature together with the growth and decay of the $\dot{T}H$ signals (as measured through the relative intensity (x 5) of the seventh line of the octet at *ca.* g = 1.9731) in the presence (■) and absence (□) of thiol. Also shown is the temperature dependent growth and decay of the $RO_2^{\cdot}$ radical features in the presence (▲) and absence (△) of MEA (10 mM) (as measured by the relative intensity (x 5) of the $g_{\parallel}$ peroxyl feature at *ca.* g = 2.033).

radical yields were reduced and they again abruptly decayed at much lower temperatures than normal (see Figs. 4.3d and 4.5). However at concentrations below 10 mM some residual $RO_2^{\cdot}$ radicals were noted to persist to higher temperatures.

Sulphur Radicals

At the temperature at which the DNA radicals decayed as a result of thiol action (under anoxic conditions), new e.s.r. features appeared which are characteristic of $RS\dot{S}R^-$ radical anions. Features for these anions were well defined at Q- and X-band frequencies (Figs. 4.6a and 4.6b respectively). An intense yellow colour appeared together with these features, this colour being also characteristic of $RS\dot{S}R^-$ radical anions ($\lambda_{max} \approx 410$ nm). A comparison of the spectral data with those for $RS\dot{S}R^-$ from previous studies (G. D. D. Jones, J. S. Lea and M. C. R. Symons, unpublished results) and the literature (Table 4.II), supports this assignment. At a concentration of 40 mM MEA, the e.s.r. signals for $RS\dot{S}R^-$ species are themselves lost by *ca.* 210 K (Fig. 4.3b), the temperature at which <u>all</u> spins are lost (Fig. 4.7).

The RS$^{\cdot}$ radicals, thought to be formed directly as a result of reaction with DNA radicals ($R'^{\cdot}$), equation [4.10], have not been detected by e.s.r. spectroscopy.

$$R'^{\cdot} + RSH \rightarrow R'^{\cdot} + RS^{\cdot} \qquad [4.10]$$

This is not surprising since their spectra are controlled by the environment (as a result of hydrogen-bonding which lifts the degeneracy of the 3p(π) orbitals) which is itself expected to be variable in the systems employed in this study (Nelson *et al.*, 1977). However, reaction [4.11] is facile and so the radical $RS\dot{S}(H)R$ was carefully looked for (Nelson *et al.*, 1977; Symons, 1974).

$$RS^{\cdot} + RSH \rightleftharpoons RS\dot{S}(H)R \qquad [4.11]$$

Surprisingly, no sign of this species was observed, only the conjugate base $RS\dot{S}R^-$ was detected. It seems, therefore, that reaction [4.11] is facile but that, under the present conditions, the effective pH is such that deprotonation occurs. Indeed our own studies (G. D. D. Jones, J. S. Lea and M. C. R. Symons, unpublished results) together with those of others (Wu *et al.*, 1984; Chan *et al.*, 1974; Faraggi *et al.*, 1975)

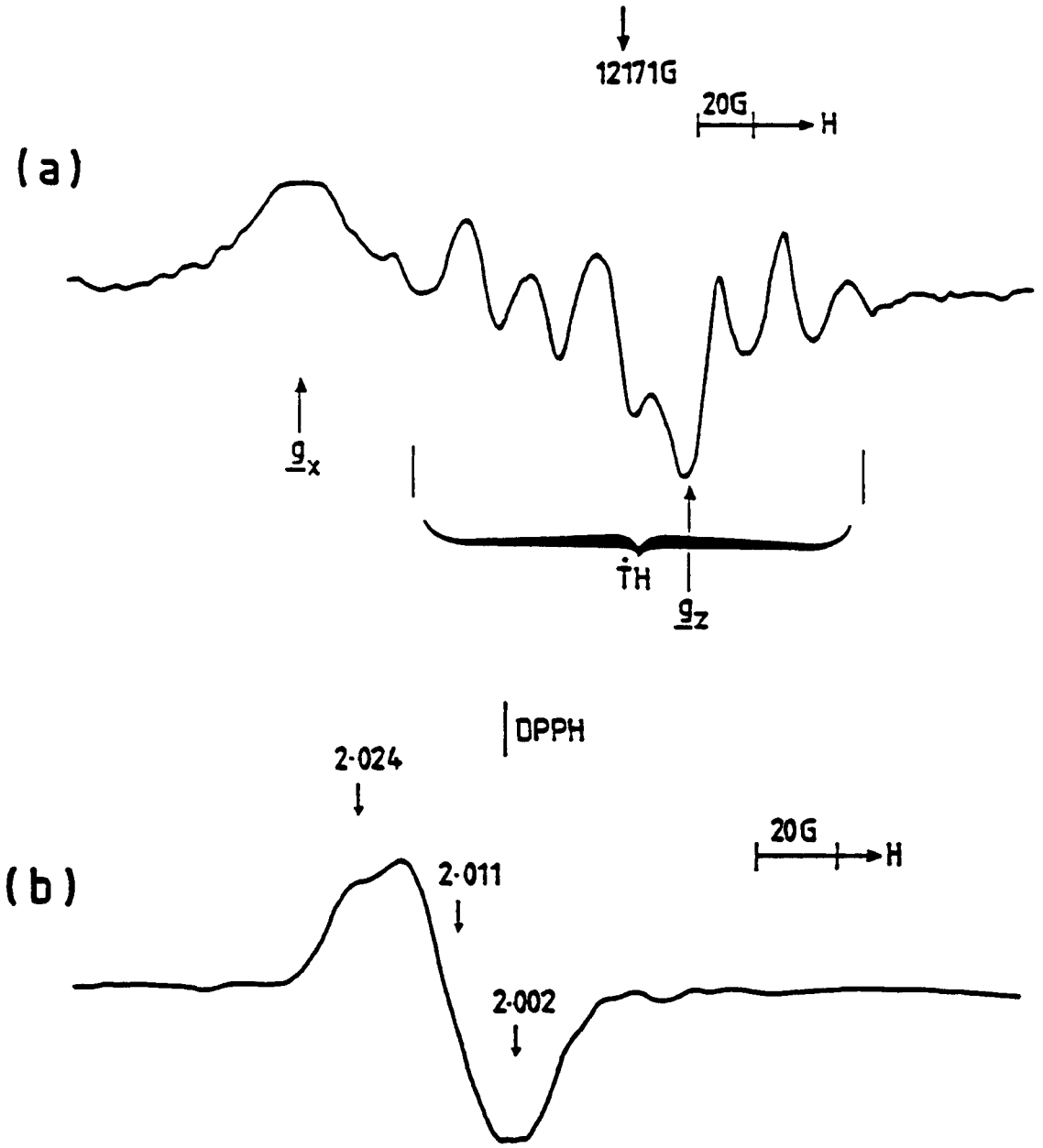

FIGURE 4.6

(a) First derivative Q-band e.s.r. spectrum at *ca.* 100 K for a anoxic solution of DNA (50 mg + 1 ml H_2O) containing MEA (40 mM), after exposure to ^{60}Co γ-rays (dose 1-4 Mrad.) and annealing to 195 K showing g_x and g_z features for $RSSR^-$ radicals, together with features for residual TH radicals. Microwave power 1.1 uW.
(b) The resultant X-band first derivative e.s.r. spectrum at 77 K for a anoxic DNA solution (50 mg + 1 ml H_2O) containing MEA (40 mM), on exposure to ^{60}Co γ-rays (dose ~0.8 Mrad.) and annealing to 190 K (i.e. Fig. 4.3b 190 K), after computer subtraction of overlapping signals from TH (as judged by cancellation of the octet features). g-Tensor components for $RSSR^-$ radicals can be seen and are compared with other experimental and literature values (Table 4.II).

TABLE 4.II

Comparison of E.s.r. Parameters of the Sulphur-Containing Radicals formed in Oxic and Anoxic DNA-MEA Binary Systems after Annealing to 190-208 K, with Experimental[d] and Reported Data for $RSS\dot{R}^{-}$[b,c,e,f,g] and $RSO_2^{\cdot}$[h]

	g-Tensor Components		
	g_x	g_y[i]	g_z
DNA/MEA/-O_2[a]	2.024	2.011	2.002
Cystine HCl/Crystal[b]	2.0178	2.0174	2.002
Glutathione oxidized/D_2O-CD_3OD[c] (*ca.* 4:1 $^{v}/_{v}$)	2.017	2.017	2.002
Dithiothreitol/D_2O-CD_3OD/-O_2 pH 10[d] (*ca.* 4:1 $^{v}/_{v}$)	2.022	2.011	2.003
Dithiodiglycolic Acid/Crystal[e]	2.021	2.017	2.001
Dimethylsulphide/Crystal[f]	2.020	2.020	2.001
Cyclotetramethylene Disulphide/Oxidation of Thiol Ti(III) + H_2O_2/H_2O, R.T.[g]		2.013(iso)	
DNA/MEA/+O_2	2.025	2.017[j]	2.002
D_2O/Glutathione/+O_2[d]	2.026	2.016[j]	2.000
Mercaptopentylamine/+O_2[h]	2.026	2.017[j]	2.000
E. Coli B/r/0.1M MPA/+O_2[h]	2.02	2.017[j]	2.002

[a] Parameters measured after computer subtraction of $\dot{T}H$ and residual $G^{\cdot+}$ and $T^{\cdot-}$;

[b] H. C. Box and H. G. Freund, J. Chem. Phys. (1964), **41**, 2571;

[c] D. N. R. Rao, M. C. R. Symons and J. M. Stephenson, J. Chem. Soc., Perkin Trans. 2, (1983), 727;

[d] G. D. D. Jones, J. S. Lea and M. C. R. Symons, unpublished results;

[e] H. C. Box, T. Freund and G. W. Frank, J. Chem. Phys., (1968), **48**, 3825;

[f] T. Gillbro, Chem. Phys., (1974), **4**, 476;

[g] B. C. Gilbert, H. A. H. Laue, R. O. C. Norman and R. C. Sealy, J. Chem. Soc., Perkin Trans. 2, (1975), 892;

[h] E. S. Copeland, J. Magn. Resonance, (1975), **20**, 124;

[i] In most cases, g_z and g_y were not sufficiently defined to draw a clear distinction.

[j] These do not represent true g_y features (which occur at g ~2.014[h]) but are, in fact, prominent first derivative maxima for $RSOO^{\cdot}$.[h]

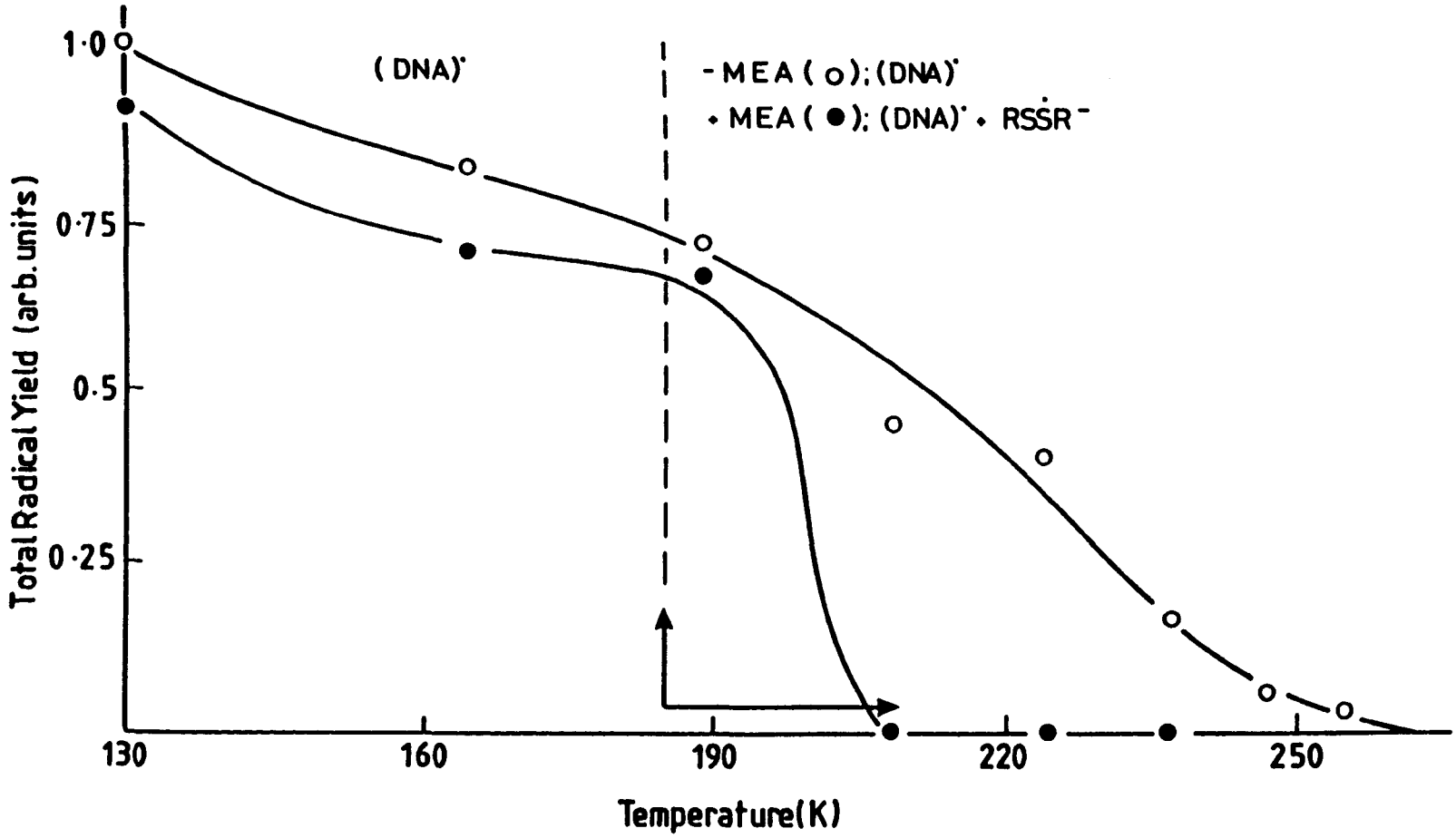

FIGURE 4.7

The temperature dependence of the total radical yield of an irradiated (dose ~0.8 Mrad.) anoxic DNA solution (50 mg + 1 ml H_2O) in the presence and absence of MEA (40 mM). At temperatures <130 K, both the DNA-located $(DNA)^{\cdot}$ and the H_2O-located $(H_2O)^{\cdot}$ free radicals contribute to the total radical yield. At temperatures ≥130 K all H_2O radicals have already reacted and the total yield corresponds to the yield of $(DNA)^{\cdot} \pm RSSR^{\cdot-}$. Temperatures for the onset and duration of the $RSSR^{\cdot-}$ radicals existence are shown (↑ →).

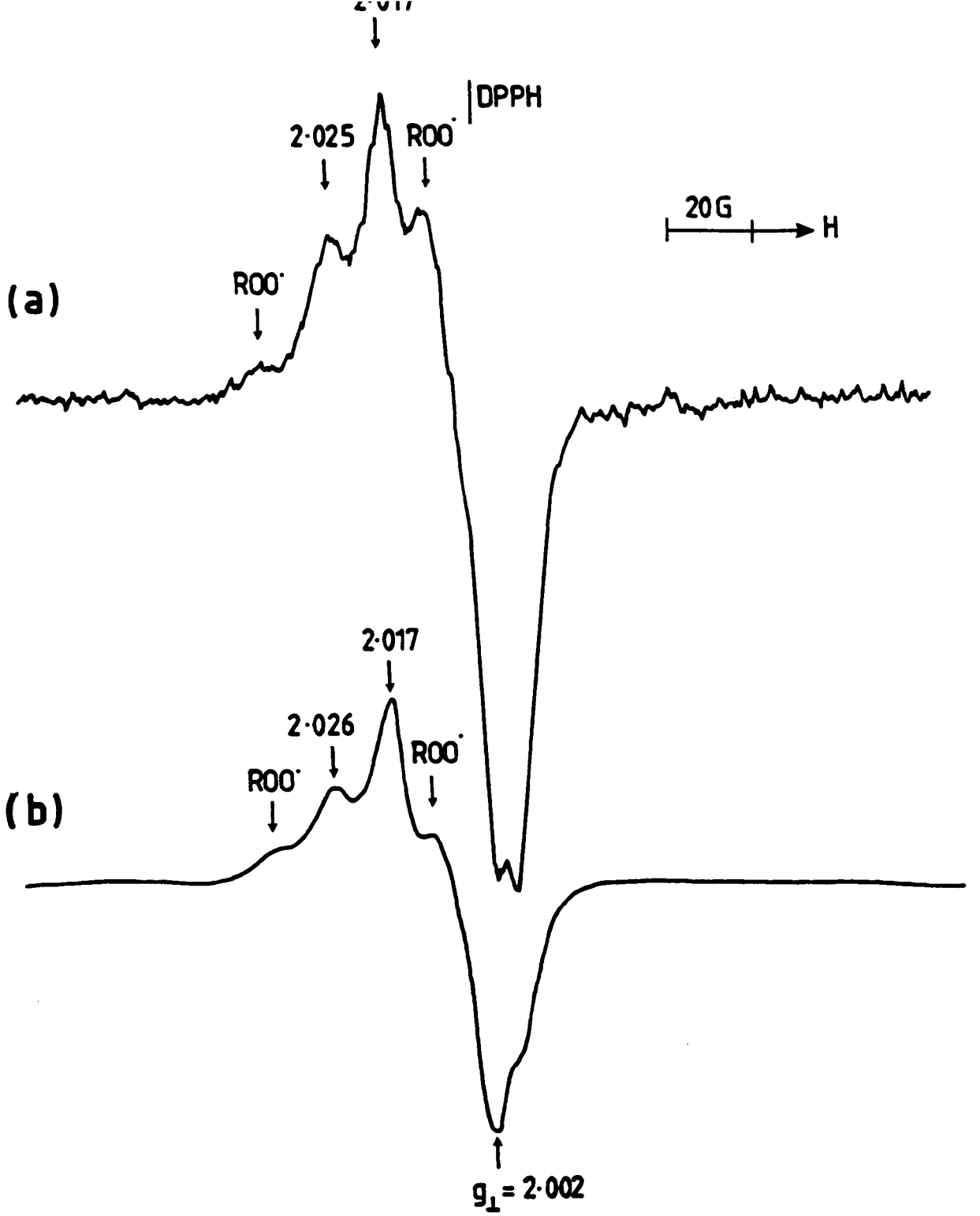

FIGURE 4.8

(a) First derivative X-band spectrum for a oxic solution of DNA (50 mg + 1 ml H_2O) containing MEA (40 mM), after exposure to ^{60}Co γ-rays (dose ~0.8 Mrad.) and annealing to 190 K, showing g-tensor components of RSOO· radicals [see Table 4.II for comparisons with other experimental and literature values].
(b) The observed e.s.r. spectrum recorded at 77 K, after warming to 193 K, of a solution of *E. coli* B/r plus 0.1 M MPA, equilibrated in oxygen before freezing and γ-irradiation (77 K) [from Copeland (1975)].

indicate the pK of disulphide radical anions to be ~5.5. Such a value would allow the deprotonation, equation [4.12], to be favourable.

$$RS\dot{S}(H)R + B \rightleftharpoons RS\dot{S}R^- + H^+B \qquad [4.12]$$

(B is any local base material)

Under oxic conditions, in addition to the normal $RO_2^\cdot$ signal which appear at 190 K (but to a diminished extent), clear features at g = 2.025 and 2.017 were observed rather than $RS\dot{S}R^-$ (Fig. 4.8a). These are similar to the g_x and g_y features assigned by Copeland (1975) to the aminothiol sulfur peroxyl radical ($RSO_2^\cdot$) observed in a spectrum of *E.coli* B/r plus 0.1M MPA equilibrated in oxygen prior to freezing, γ-irradiation and annealing to 193 K (Fig. 4.8b and Table 4.II). Spectral data from work conducted in this laboratory, involving the addition of oxygen to $RS^\cdot$ (from glutathione) confirms this assignment (G. D. D. Jones, J. S. Lea and M. C. R. Symons, unpublished results) (Table 4.II). At an MEA concentration of 40 mM the $RSO_2^\cdot$ signals were again abruptly lost at ~210-220 K (Fig. 4.3d).

Strand Break Analysis

It has previously been shown that under both oxic and anoxic conditions single and double strand breaks occur at significant levels (Boon *et al.*, 1984). In order to account for this it was proposed that a significant number of the base radicals react *via* an intramolecular hydrogen atom abstraction from an appropriately positioned deoxyribose moiety (Cullis and Symons, 1986) as shown in Figure 4.9. Further reactions of the sugar radicals thus formed, to give strand breaks, presumably occurs *via* mechanisms analogous to those described for the hydroxyl radical initiated reaction (von Sonntag *et al.*, 1981). Immediate decay of the sugar radicals must occur since under normal conditions no further radicals are detected. In support of this it has been observed that when sugar-centred radicals are generated at lower temperatures they are indeed detectable (see Chapter Three and Cullis *et al.*, 1985a) and decay to give non-radical products at lower temperatures than those for the normal DNA radicals. Similar base mediated intramolecular hydrogen atom abstractions have been proposed as steps in the reactions of H and OH base radical adducts leading to strand breaks and base release in dilute aqueous solutions of poly(U) (Lemaire *et al.*,

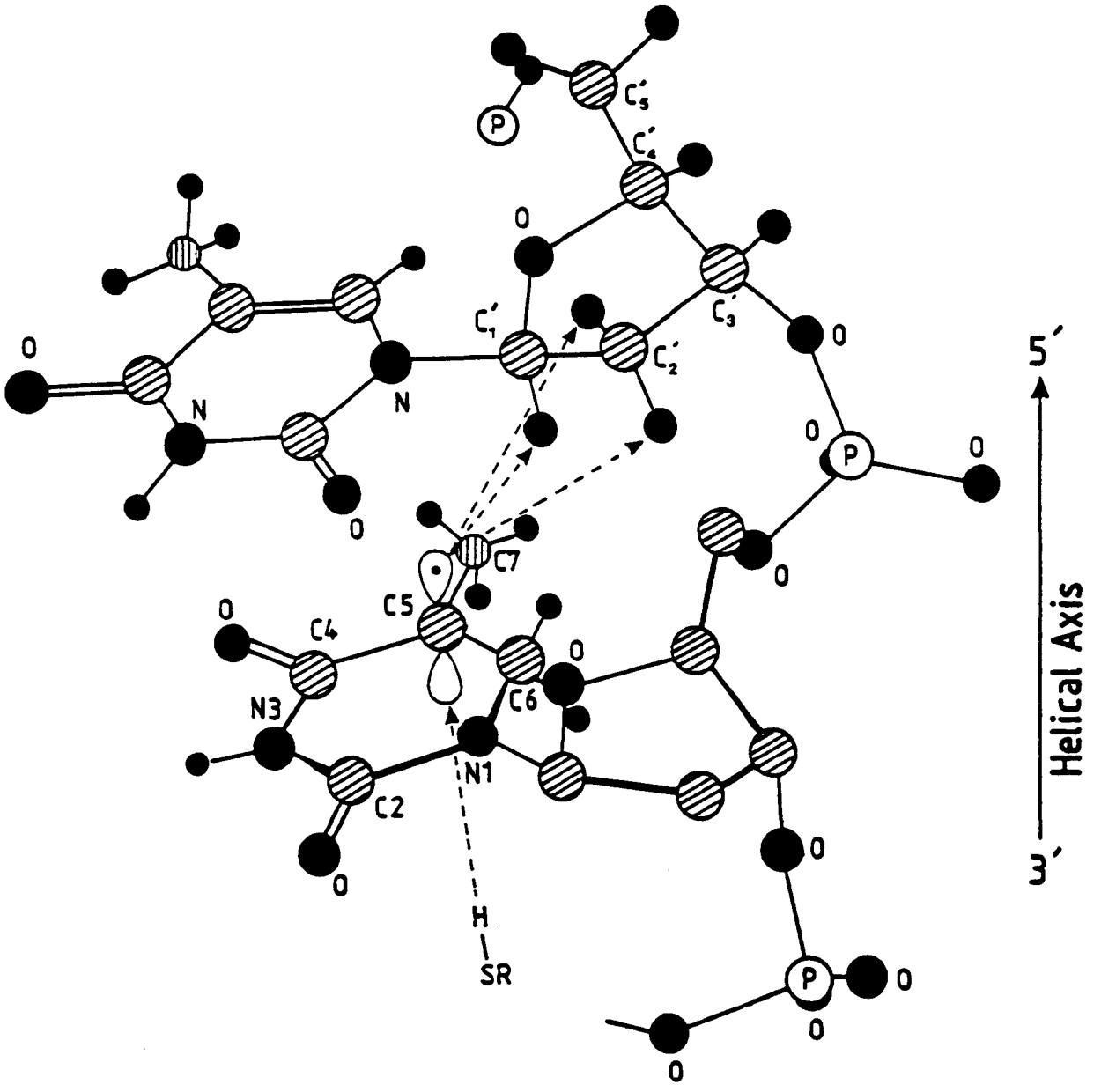

$$\dot{T}H + H\text{-}5'\text{-}dR \longrightarrow (R)TH_2 + 5'\text{-}dR^{\cdot}$$

$$\dot{T}H + H\text{-}SR \longrightarrow (S)TH_2 + RS^{\cdot}$$

FIGURE 4.9

A dinucleotide fragment of B-DNA showing the close proximity of the C_1' and C_2' 5′-ribosyl-hydrogens to the $\dot{T}H$ radical centre. $\dot{T}H$ mediated abstraction of these sugar hydrogens would result in R-conformer of TH_2 about C5, whilst $H^{\cdot}$ donation from a thiol, occurring unhindered from major groove, would result in the C5 S-conformer of TH_2.

1984; Deeble and von Sonntag, 1984).

Assuming that hydrogen atom abstraction would be most favourable from the nearest available site on the adjacent sugar, a B-DNA structure has been inspected using computer molecular graphics (Chem-X, Chemical Designs Ltd., Oxford). For the 5-thymyl radical $\dot{T}H$ the hydrogens attached to C_1' and C_2' of the deoxyribose unit 5' to the 5-thymyl bearing nucleoside are significantly closer than other alternative centres (Fig. 4.9). Also, from this work, it can be predicted that the TH_2 (reduced thymine) formed by the intramolecular hydrogen atom abstraction, under anoxic conditions, would have the R-configuration about C5 (Fig. 4.9). Subsequent to this prediction Furlong *et al.* (1986) have recently shown that this is indeed the case.

The above also predicts that strand breaks occurring under conditions of direct damage arise through a mechanism that is distinct from the indirect pathway in which hydroxyl radicals predominately abstract the C_4' hydrogen atoms (von Sonntag *et al.*, 1981). [However those strand breaks in DNA (if any) that are a result of OH or H base radical adduct mediated hydrogen atom abstraction would, of course, occur by a mechanism more or less analogous to the direct mechanism.] This will be further discussed in Appendix B.

The presence of MEA (40 mM) was demonstrated to protect plasmid DNA (pBR322) against both single and double strand breaks arising as a result of irradiation at 77 K. The degree of damage and extent of protection by MEA (40 mM) was largely unaffected by the presence of oxygen (a.e.r., 40, $\pm O_2$ = 0.45) (Table 4.III) (Figs. 4.10a and b). At lower concentrations of MEA (5 mM) the extent of protection under anoxic conditions was reduced (a.e.r., 5, $-O_2$ = 0.54) (Table 4.IV) (Figs. 4.11a and b) and this was further reduced in the presence of oxygen (a.e.r., 5, $+O_2$ = 0.78), suggesting opposing, competitive reactions of thiols and of oxygen at the lower thiol concentrations.

It is noteworthy that even at high relative concentrations of thiol a significant number of strand breaks were detected (Figs. 4.10a and b). This possibly correlates with results shown in Figure 4.7 which show a gradual loss of radicals as the temperature increases from 130 to

TABLE 4.III

The Effect of 40 mM MEA on Radiation Induced Strand Breaks in Plasmid DNA (pBR322)

Conditions	Dose Mrad.	% Form (II) (○)	% Form (III) (□)	Log_{10} % Form (I) (○)
No MEA	0	12.1	0	1.94
+ N_2	0.2	39.9	3.5	1.75
	0.4	56.5	3.5	1.60
	0.6	67.1	3.8	1.46
	0.8	66.8	6.9	1.41
		(●)	(■)	(●)
40 mM MEA	0	16.8	0	1.92
+ N_2	0.2	28.0	2.5	1.86
	0.4	36.2	1.5	1.78
	0.6	44.0	1.8	1.73
	0.8	40.9	1.7	1.75
		(▽)	(△)	(▽)
No MEA	0	12.0	0	1.94
+ O_2	0.2	44.7	2.2	1.72
	0.4	53.3	4.5	1.62
	0.6	62.8	8.0	1.46
	0.8	60.9	8.9	1.48
		(▼)	(▲)	(▼)
40 mM MEA	0	14.5	0	1.93
+ O_2	0.2	28.9	1.6	1.84
	0.4	33.5	1.1	1.81
	0.6	42.8	2.1	1.74
	0.8	49.7	1.7	1.68

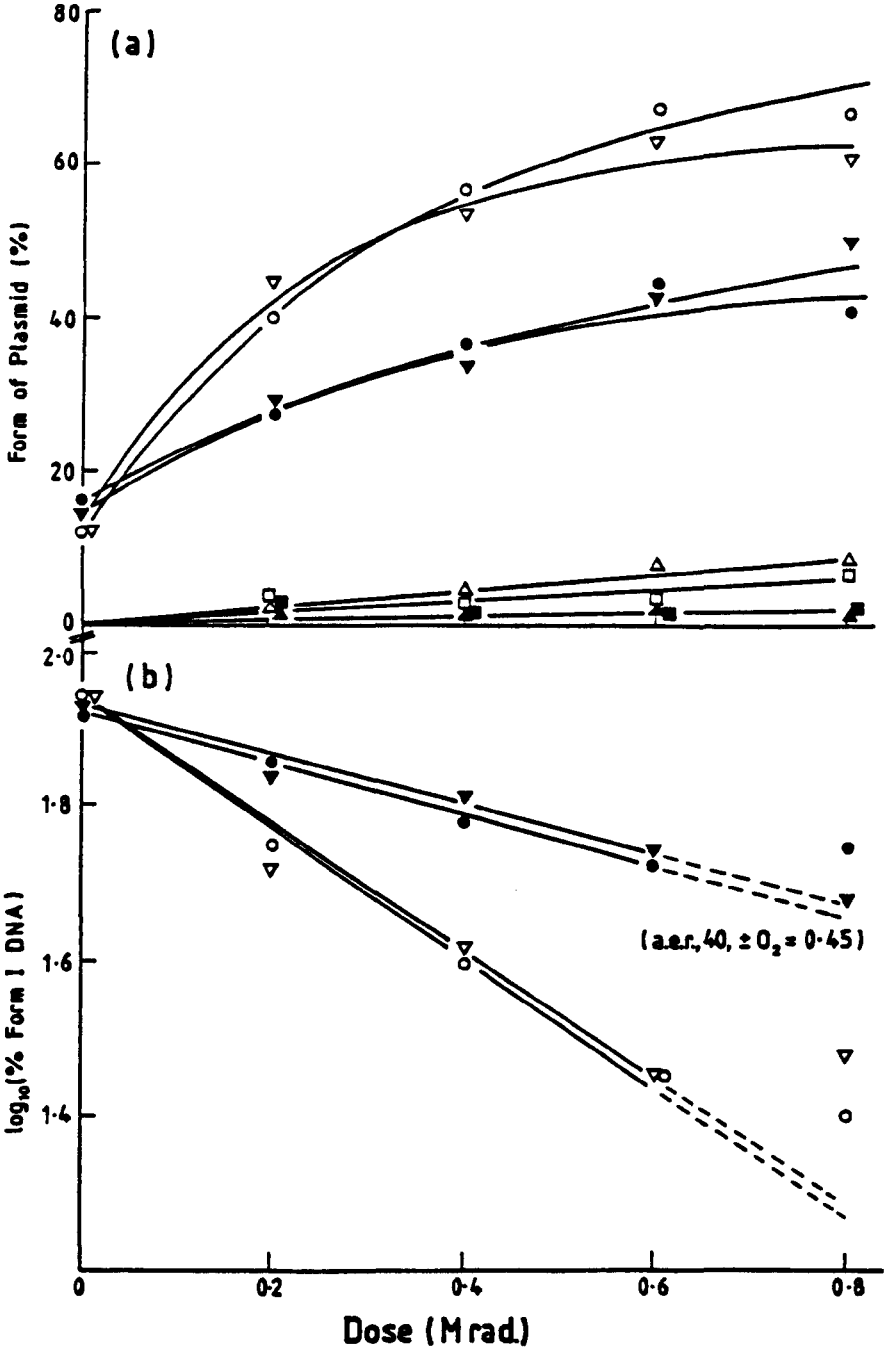

FIGURE 4.10

(a) The effect of MEA (40 mM) on strand breaks induced by γ-irradiation of plasmid (pBR322) at 77 K under oxygenated and deoxygenated atmosphere. The percentage of Form (II) indicates single strand breaks produced (▼ +MEA $+O_2$, ● +MEA $-O_2$, ▽ $+O_2$ and ○ $-O_2$). Double strand breaks formed are indicated by Form (III) (▲ +MEA $+O_2$, ■ +MEA $-O_2$, △ $+O_2$ and □ $-O_2$).
(b) Semi-log plot of the loss of Form (I) plasmid DNA (pBR322) following irradiation as in (a) (▼ +MEA $+O_2$, ● +MEA $-O_2$, ▽ $+O_2$ and ○ $-O_2$).

TABLE 4.IV

The Effect of 5 mM MEA on Radiation Induced Strand Breaks in Plasmid DNA (pBR322)

Conditions	Dose Mrad.	% Form (II)	% Form (III)	Log_{10} % Form (I)
		(○)	(□)	(○)
No MEA	0	15	0	1.93
+ N_2	0.2	47.2	2.6	1.78
	0.4	61.4	4.3	1.59
	0.6	66.7	7.0	1.53
	0.8	73.2	7.2	1.45
		(●)	(■)	(●)
5 mM MEA	0	14.7	0	1.92
+ N_2	0.2	37.5	1.2	1.82
	0.4	44.0	2.4	1.74
	0.6	56.6	3.0	1.64
	0.8	58.7	3.7	1.62
		(▽)	(△)	(▽)
No MEA	0	14.7	0	1.93
+ O_2	0.2	45.0	3.0	1.76
	0.4	56.1	6.5	1.61
	0.6	67.1	12.2	1.45
	0.8	71.3	12.8	1.41
		(▼)	(▲)	(▼)
5 mM MEA	0	19.7	0	1.91
+ O_2	0.2	42.6	0.9	1.80
	0.4	53.4	3.3	1.65
	0.6	62.0	3.0	1.59
	0.8	64.0	5.2	1.51

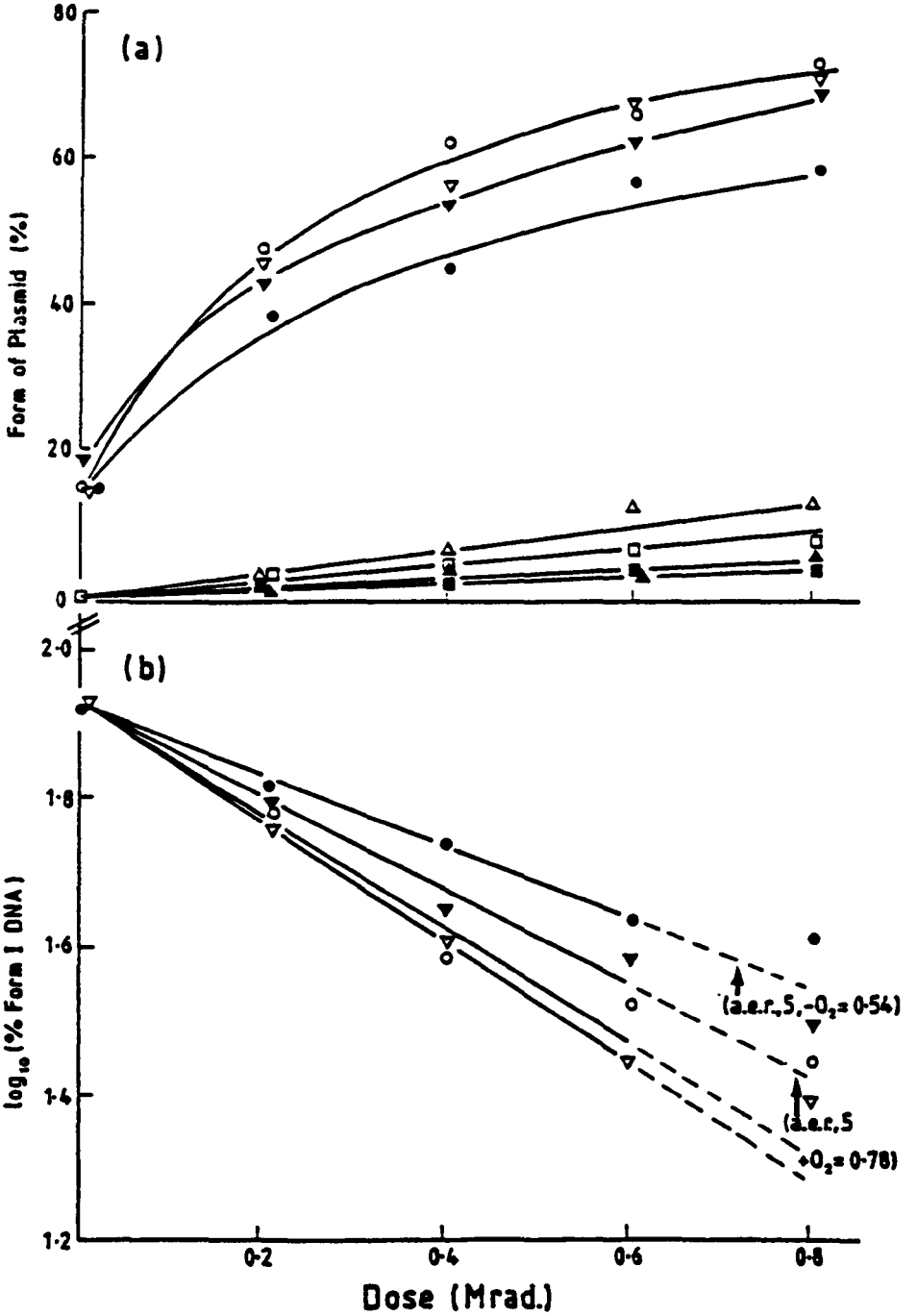

FIGURE 4.11

(a) The effect of MEA (5 mM) on strand breaks induced by γ-irradiation of plasmid (pBR322) at 77 K under oxygenated and deoxygenated atmosphere. The percentage of Form (II) indicates single strand breaks produced (▼ +MEA $+O_2$, ● +MEA $-O_2$, ▽ $+O_2$ and ○ $-O_2$). Double strand breaks formed are indicated by Form (III) (▲ +MEA $+O_2$, ■ +MEA $-O_2$, △ $+O_2$ and □ $-O_2$).
(b) Semi-log plot of the loss of Form (I) plasmid DNA (pBR322) following irradiation as in (a) (▼ +MEA $+O_2$, ● +MEA $-O_2$, ▽ $+O_2$ and ○ $-O_2$).

~190 K, that is, prior to the onset of reaction with the thiol molecules. This is an artefact of the frozen system and reflects the unreactivity of RSH below 190 K.

Mechanism of Thiol Action (i)

That thiols are acting as efficient repair agents in the frozen system is shown by the dramatic and sudden loss of the DNA base radicals at temperatures well below those at which they normally decay, and the dependence of such action on the presence of a -S<u>H</u> functionality (see below) indicates that thiols are acting as efficient hydrogen atom donors towards the base radicals, i.e. reaction [4.10].

However, there are some important liquid phase results which suggest that whilst this reaction ($H^{\cdot}$ donation) does occur under most circumstances for DNA, in the particular case of $G^{\cdot+}$ formation, electron transfer dominates with the thiolate anion being the active species (Wilson *et al.*, 1974; O'Neill, 1983), equation [4.13].

$$G^{\cdot+} + RS^- \rightarrow G + RS^{\cdot} \overset{RS^-}{\rightleftharpoons} RS\dot{S}R^- \qquad [4.13]$$

It is unlikely that this type of reaction can occur with RSH rather than RS^-. However, to check this, a study of the effect of S-methyl-L-cysteine (RSMe), which is likely to be a better electron donor than RSH, was conducted. In fact, this compound, when included at 40 mM in an anoxic frozen system, had only a small effect on the course of DNA damage (Fig. 4.12b) <u>in comparison</u> with that noted for an equivalent concentration of RSH (Fig. 4.3b). However with no $R\dot{S}Me^+$ radicals (Rao *et al.*, 1984) being detected and with similar activity being noted at low thiol concentrations (0.1-0.5 mM) the observed action was most likely due to contaminating thiol.

Therefore an investigation of the reaction described in equation [4.13] was attempted *via* study of DNA-RSH samples prepared in alkali, so generating RS^- *in situ*. The temperature dependent e.s.r. profiles of DNA-MEA (10 mM) in 10 mM† and 100 mM NaOH are shown in Figures 4.12c and 4.13b respectively. Unfortunately, the higher pH, especially of the

† Actual [NaOH] employed was 20 mM, however presumably half of this reacted with the HCl present in MEA hydrochloride.

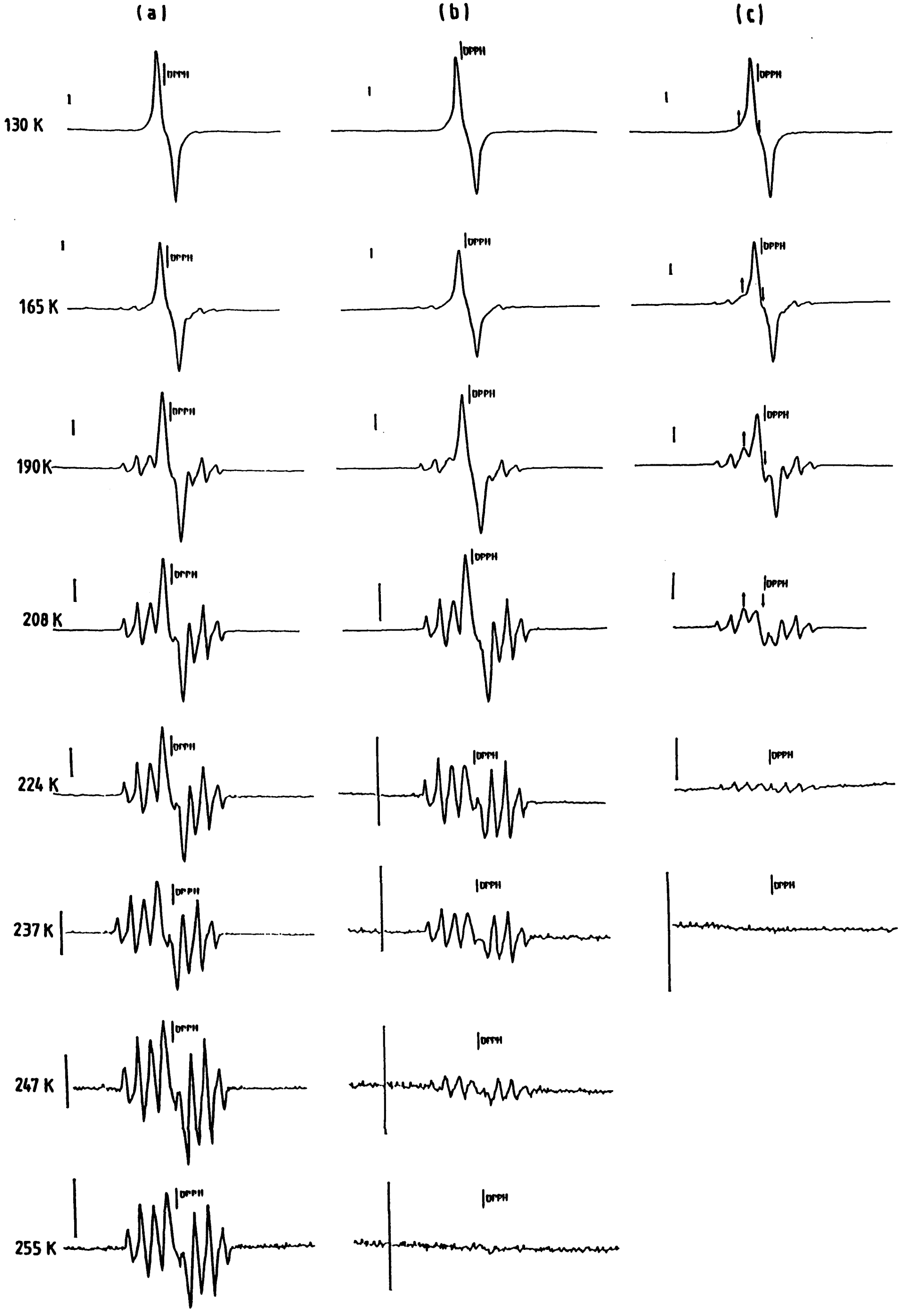

FIGURE 4.12

Representative steps in the evolution of e.s.r. spectra arising from the thermal annealing of γ-irradiated (dose ~0.8 Mrad.) frozen aqueous solutions of DNA (50 mg + 1 ml H_2O) in either the (a) absence of oxygen (b) absence of oxygen plus S-methyl-L-cysteine (40 mM) and (c) absence of oxygen plus MEA (10 mM)/NaOH (10 mM).

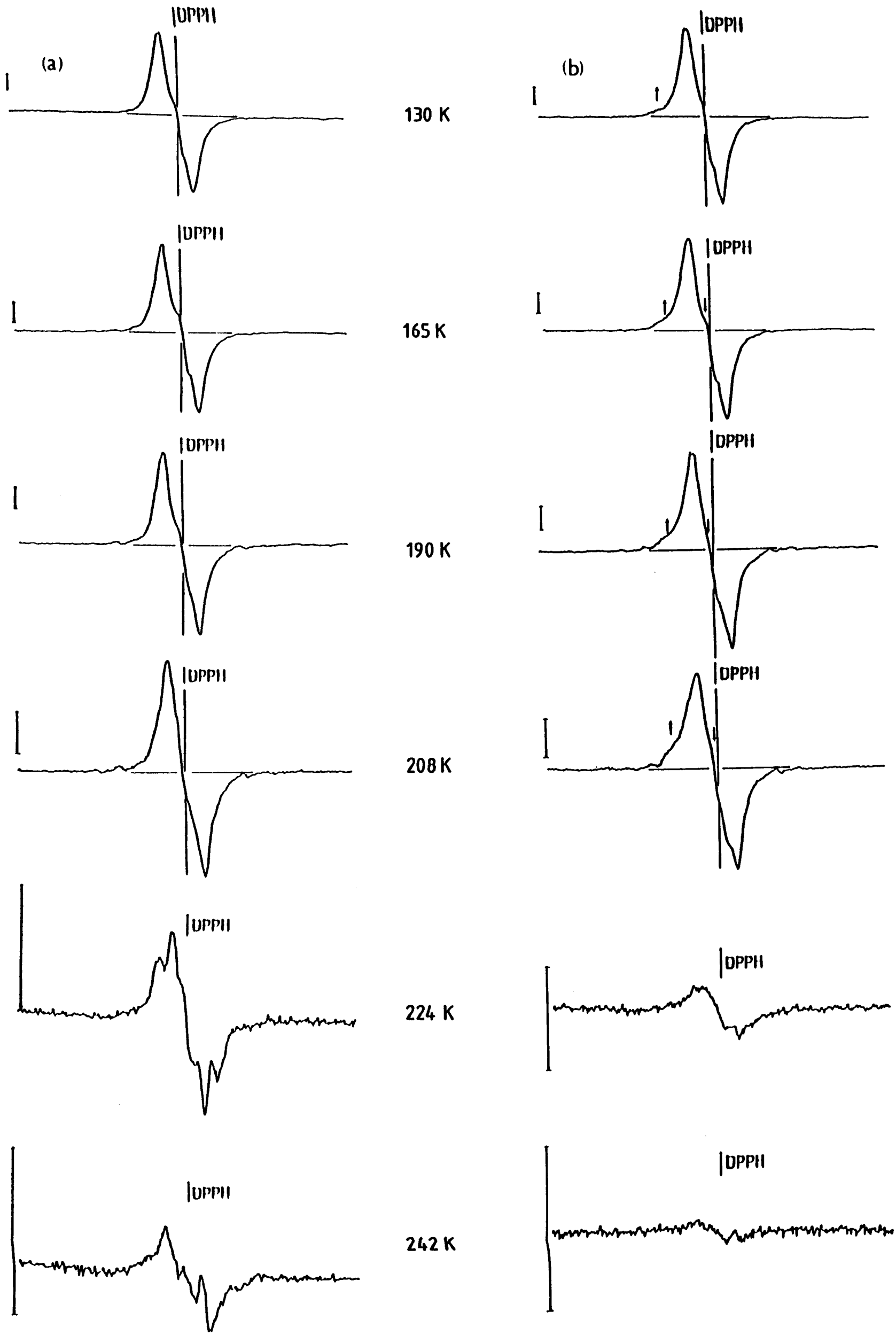

FIGURE 4.13

Representative steps in the evolution of e.s.r. spectra arising from the thermal annealing of γ-irradiated (dose ~0.8 Mrad.) frozen aqueous solutions of DNA (50 mg + 1 ml H_2O) in either the (a) absence of oxygen plus NaOH (100 mM) and (b) absence of oxygen plus MEA (10 mM)/NaOH (100 mM).

latter system, modifies the DNA and course of radiolytic damage (Gregoli *et al.*, 1982). So for comparison, DNA in the presence of 100 mM NaOH is shown in Figure 4.13a. In both cases, although there was no alteration in primary damage at 130 K, there was an earlier onset of $RS\dot{S}R^-$ (↑) formation (>130-165 K) than in the neutral systems, concurrent with a loss of a central feature ($G^{\cdot+}$) (↓) indicative of reaction [4.13] (coupled with reactions [4.11/4.12]) occurring.

$$G^{\cdot+} + RS^- \rightarrow G + RS^{\cdot} \underset{}{\overset{RS^-}{\rightleftharpoons}} RS\dot{S}R^-$$
$$RSH \searrow \quad \nearrow B$$
$$RS\dot{S}(H)R \qquad \ldots\ [4.13\ [4.11/.12]]$$

In the DNA-MEA-10 mM NaOH system (Fig. 4.12c) the decay of $\dot{T}H$ over the temperature range 208-237 K could be as a consequence of residual unionized RSH, though the thiolate anion mediated reaction [4.14] cannot be discounted, (cf. Fujita and Steenken, 1981).

$$TH^{\cdot} + RS^- \rightarrow TH^- + RS^{\cdot}(RS\dot{S}R^-) \qquad [4.14]$$

Similarly, the high temperature loss of signals noted over 208-242 K for the 10 mM MEA/100 mM NaOH system (Fig. 4.13b) could be due to analogous reactions, although in the absence of thiols the DNA signals are lost almost as rapidly under these very alkaline conditions (Fig. 4.13a). Overall these results support [4.13] in so much that, **when present**, RS^- does appear to act by quenching $G^{\cdot+}$.

However, since no such low temperature action (i.e. $RS\dot{S}R^-$ appearing at >130-165 K) was noted in neutral systems (in which $RS\dot{S}R^-$ was not noted till *ca.* ~180-190 K), coupled with the fact that at pH 6.5 RS^- cannot constitute more than *ca.* ~2.5% of the total thiol present and that efficient e.s.r. repair was noted at thiol concentrations as low as 1 mM, it is concluded that thiol mediated electron transfer does not have a major rôle to play in the repair of DNA direct damage in neutral frozen aqueous systems. This, together with the evidence that a compound of the type RSMe does not influence the DNA radical decay to anything like the extent for that noted with free thiols, substantiates the claim that RS**H** is essential to the efficient repair of directly induced DNA damage.

In summary, the most dramatic effects on DNA radicals in the frozen aqueous systems have been observed at neutral pH's in the presence of free thiols. This observation is best understood in terms of hydrogen atom transfer reactions occurring between free thiols and the DNA base radicals. Hydrogen atom transfer to the base radicals from the thiols clearly competes favourably with the base mediated intramolecular hydrogen atom abstraction from neighbouring deoxyribose moieties, postulated above. Since the latter reaction is thought to give rise to strand breaks, thiols should protect DNA against strand breaks under conditions of direct damage and, as discussed above, this is indeed the case.

Mechanism of Thiol Action (ii)

Under oxic conditions and low thiol concentrations, the principal sulphur-containing radical detected by e.s.r. spectroscopy is $RSO_2^{\cdot}$ which arises from addition of O_2 to the thiyl radical ($RS^{\cdot}$). As noted above, at lower concentrations of thiol, the effect of RSH on strand breaks is competitive with the influence of oxygen. These observations are consistent with the reactions shown in Scheme 4.I.

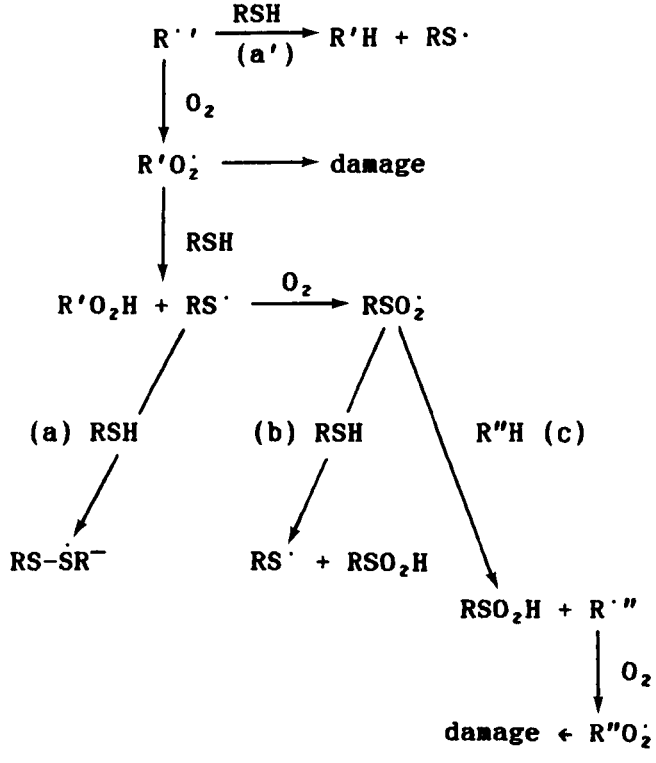

Scheme 4.I

According to this, hydrogen atom donation by RSH to the base peroxyl radicals initially occurs to give RS$^{\cdot}$ radicals. These combine with oxygen to give $RSO_2^{\cdot}$ rather than giving $RS\dot{S}R^{-}$. As the relative concentration of thiol increases pathway (b) begins to dominate, oxygen is consumed and the DNA protected. Reactions to give $RS\dot{S}R^{-}$ will also occur as thiol concentration increases *via* repair reactions (a') and (a). At low concentrations of thiol, however, it is the thiol which is effectively consumed and, therefore, pathways (a) and (b) are prevented. The alternative pathway (c) in which the $RSO_2^{\cdot}$ radical abstracts a hydrogen atom helps to account for the attenuation by oxygen of the protection afforded by thiols at low concentration.

The precise chemical nature of the DNA "repair" product is of major importance in relation to biological function, which may depend on further enzymatic repair. Under anoxic conditions, the quenching of $\dot{T}H$ by thiols leads to TH_2 (reduced thymine) rather than restoration of the thymine base. That TH_2 is a major identifiable product under conditions of direct irradiation supports the above proposals (Cadet *et al.*, 1983a). With the TH_2 product from DNA irradiated alone being noted to be in the R-configuration about C5 (see above), it is interesting to speculate as to what would be the configuration of thiol repaired TH_2. As depicted in Figure 4.9, $\dot{T}H$ mediated hydrogen atom abstraction from the ribose 5' to the thymyl bearing nucleoside (i.e. from "above"), results in the R-conformer. Assuming that the close approach of a thiol molecule to the radical site is a prerequisite of repair, examination of the B-DNA topography by computer graphics reveals that H$^{\cdot}$ donation from a thiol would be least hindered if it occurred from "below" (from the major groove) and so yield the C5 S-conformer.

Concerning $G^{\cdot+}$, there is less direct evidence. However, if the principal decay pathway for $G^{\cdot+}$ is by loss of a proton to give $G\dot{N}$ as proposed by Hüttermann and Voit (1986) then hydrogen atom donation to $G\dot{N}$ by RSH should restore the guanine base (though a base-catalysed rearrangement would be required prior to full integrity being restored). Under oxic conditions H$^{\cdot}$ donation reactions lead to organic peroxides (RO_2H). The reactive nature of these latter products must represent a further danger to the integrity of the DNA.

Dialkyl Disulphides

Incidental to the primary study of sulphydryl derivatives, a brief study of the effects of disulphides on DNA damage has been made. As expected (Lenherr and Ormerod, 1968), these molecules proved to be efficient electron scavengers, features due to $RS\dot{S}R^-$ anions being clearly present after irradiation (Fig. 4.14) at the expense of $T^{\cdot -}$ ($\dot{T}H$) formation. In this respect these RSSR molecules protect DNA from electron damage, but there was no suppression of $G^{\cdot +}$ formation, and no appearance of e.s.r. features for $RS\dot{S}R^+$ π-radical cations (Rao *et al.*, 1984).

CONCLUSIONS

It is concluded that under the conditions of this study, thiols act as efficient repair agents. Although this might be seen to be an expected result, there are several reasons why it is considered to be significant:

(i) Most previous studies on pure DNA have involved working with dilute fluid systems, under these conditions attack on DNA is largely by $^{\cdot}OH$ radicals. The present study shows that repair by hydrogen atom transfer is remarkably effective under conditions of direct damage and involves the base radicals. Such action has been noted to lead to a significant reduction of directly-induced biologically important lesions.

(ii) It is concluded that repair by electron donation does not have a major rôle to play in thiol mediated repair of directly induced damage in the neutral systems employed. However under conditions that induce RS^- formation positive hole repair does occur, but it is distinguishable from repair in the neutral system.

(iii) In the presence of oxygen the situation is more involved but our results support the contentious idea that $RS^{\cdot}$ radicals can combine with oxygen to give the sulphur peroxyl radical ($RSO_2^{\cdot}$) (Schafer *et al.*, 1978; Al-Thannon *et al.*, 1974; Quintiliani *et al.*, 1977) and that these can lead to further damage, or are themselves repaired.

(iv) The results show that in the absence of oxygen, $RS^{\cdot}$ radicals, even at temperatures well below the freezing point of water are able to locate and react with other RSH molecules, and that the initial adducts are efficiently deprotonated to give stable $RS\dot{S}R^-$ radical anions. It is not possible to comment on the recent proposal that $RS^{\cdot}$ radicals may be able to induce strand

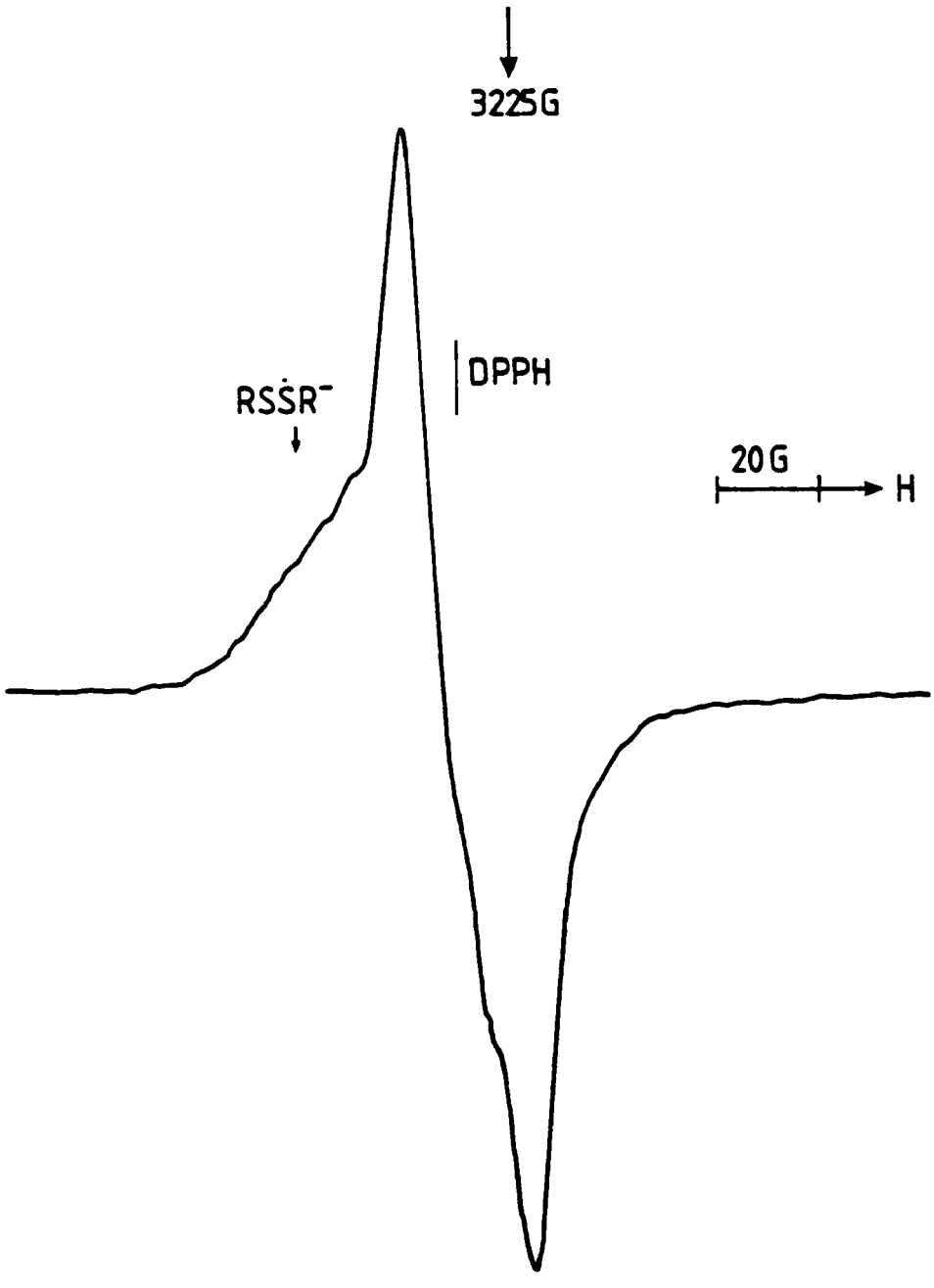

FIGURE 4.14

E.s.r. spectrum of a frozen anoxic solution of DNA (50 mg + 1 ml H_2O) plus cystamine (40 mM), after γ-irradiation (dose ~0.8 Mrad.) and annealing to 130 K.

break formation by abstraction of hydrogen from the deoxyribose moiety (Akhlaq *et al.*, 1987). However, such action may, in part, be responsible for the observation that even at high thiol concentrations there is still a significant number of strand breaks persisting.

CHAPTER FIVE

The Direct Effects of Ionizing Radiations on the Higher Order Structures of DNA

INTRODUCTION

The structure of DNA in its functional state in cells is modified through protein binding and the introduction of superhelix density. Whilst this is probably true for the majority of natural DNA molecules, it is especially so for eukaryotic DNA. Here at least an equal weight of protein serves to contract about one metre of nucleic acid, by approximately five orders of magnitude into a nucleus of diameter ~5 μm, whilst still allowing access by enzymes involved in all aspects of nucleic acid metabolism. The resulting DNA-protein complex, i.e. the nucleoprotein material, is called chromatin. Discrete chromatin molecules, containing DNA of between 10^4 and 10^6 kilobase-pairs (Kb.p.) in length, are further organized within the nucleus into morphologically and genetically distinct units called chromosomes.

Many studies of chromatin structure have focused on the nucleoprotein subunit, the nucleosome. Starting with this one certain structural element, investigators have worked in two directions, either examining the internal structure of the nucleosome or speculating on ways of assembling arrays of nucleosomes to give the higher orders of structure and DNA compaction that are characteristic of chromatin in the nucleus.

Nucleosome Structure

The structure of the nucleosome has been reviewed extensively (Kornberg, 1977; Felsenfeld, 1978; Chambon 1978; Lilley and Pardon, 1979) and the major features of the prevailing model (Finch *et al.*, 1977) are summarized in Figure 5.1a. Three structural domains have been distinguished by nuclease digestion, a protected nucleosome core, a chromatosome, and an exposed linker DNA segment of variable length. The nucleosome core consists of 146 base-pairs of DNA coiled around a central protein octamer containing two each of the slightly lysine-rich histones H2A (m.wt. 13960) and H2B (m.wt. 13774) and the arginine-rich histones H3 (m.wt. 15273) and H4 (m.wt. 11236). Histone H1 (m.wt. ~21000), which contains both lysine and to a lesser extent arginine, associates with a further 20 base-pairs of DNA adjoining the core, to complete two full superhelical turns of 83 base-pairs each around the histone octamer (Thoma *et al.*, 1979; Simpson, 1978).

Within the octamer core particle the two pairs of histones H2A, H2B and

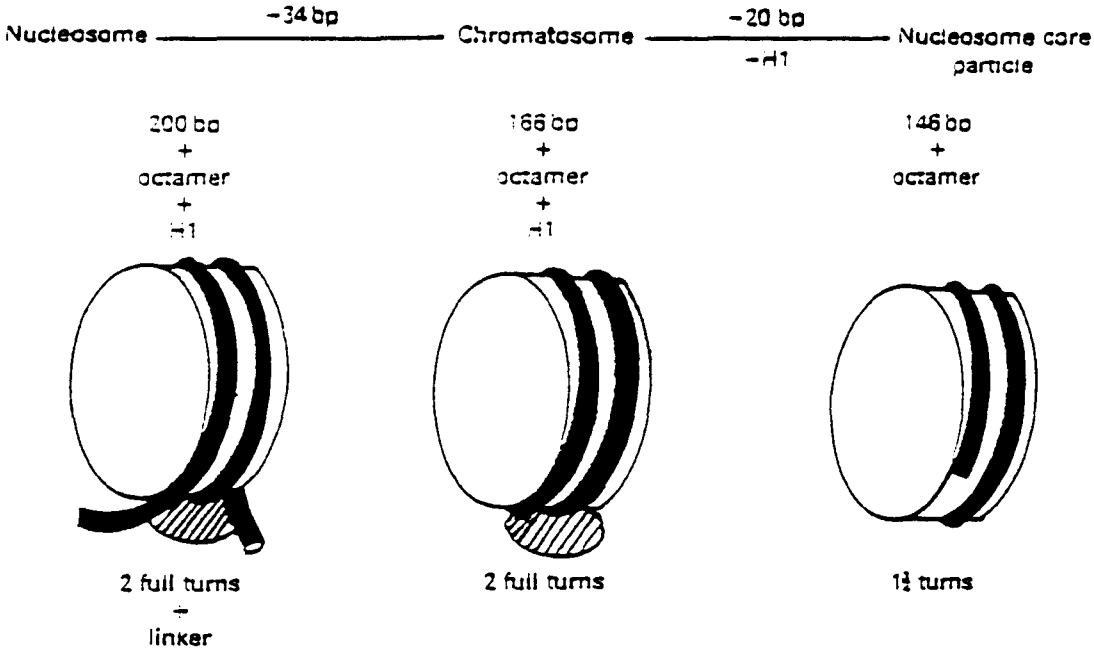

FIGURE 5.1a

The relationship between the nucleosome, and the chromatosome and core particle generated from it by 'trimming' with micrococcal nuclease.

H3, H4 occur as specific oligomeric complexes: a tetramer of arginine-rich histones $(H3)_2 \cdot (H4)_2$ and probably a dimer H2A·H2B (or polymer of dimers) of lysine-rich proteins (Thomas and Kornberg, 1975). There is an asymmetric distribution of the basic residues within these polypeptides, with H2A, H2B, H3 and H4 having relatively basic N-termini (and to a lesser extent the C-terminus) whereas H1 has a basic region towards the C-terminus. The remainder of the chains are dominated by hydrophobic and acidic amino acids (Elgin and Weintraub, 1975). The basic regions are undoubtedly responsible for the strong charge interactions involved when histones complex DNA.

The availability of reliable reconstitution methods makes it possible to examine the rôle of each histone component in the organization of the nucleosome, by systematically omitting one or more from the reconstitution procedure. In this way it was found that the arginine-rich histones, H3 and H4, were essential for the formation of nucleosomes, and were in themselves sufficient for the generation of nucleosome-like (subnucleosomal) complexes (Oudet *et al.*, 1977). No combination of histones that omits either H3 or H4 gave any indication of an ability to induce structure (Camerini-Otero and Felsenfeld, 1977). The subnucleosomal particles formed between H3, H4 and DNA have properties similar to those noted for normal nucleosomes, and though there is some debate about whether a tetramer (Bina-Stein and Simpson, 1977) or an octamer (Camerini-Otero *et al.*, 1977) of H3-H4 is associated in such a particle, it is clear that the arginine-rich histone pair play a central rôle in nucleosome formation. The importance of the arginine-rich histones is reflected in the fact that their amino acid sequence is the most strictly conserved during evolution. They are also the most tightly bound of all the histones. More specifically, the tetramer, believed to be horseshoe shaped (see below) (Klug *et al.*, 1980) is thought to organize the central turn of about 80 base-pairs of DNA, leaving the two H2A-H2B dimers each to stabilize a further half-turn of DNA above and below the plane of the tetramer (Thomas, 1983).

The earliest physical studies of nucleosome core structure suggested a particle spherical in shape, about 10 nm in diameter. However a detailed study of the neutron and X-ray scattering behaviour of nucleosomes in solution led investigators at Searle (Pardon *et al.*, 1977;

Richards *et al.*, 1977) to conclude that the nucleosome could not be spherical. Their data better fitted a flattened cylindrical structure about 11 nm in diameter and 5 nm in height, with the DNA wrapped around it to form a pair of rings at the top and bottom. X-ray diffraction of single crystals, combined with electron microscopy (e.m.) (Finch *et al.*, 1977, 1981), and neutron diffraction (Bentley *et al.*, 1981) have subsequently shown the core particle to be a slightly wedge-shaped disc, 11 nm in diameter and 5.5 nm high.

While there is general agreement that the configuration of DNA in chromatin is of the B-type (Cotter and Lilley, 1977; Goodwin and Brahms, 1978) the question of how the DNA helix is deformed to allow folding about the nucleosome core is still a matter for discussion. The hand of the superhelix was originally deduced from nuclease digestion studies which, on the assumption that the double helix was right-handed, gave positions of cutting only compatible with a left-handed superhelix (negative supercoiling) (Lutter, 1978). Later, image reconstruction of the isolated histone octamer (Klug *et al.*, 1980) showed it to have a shape suitable for acting as a spool for a left-handed DNA superhelix (Fig. 5.1b). X-ray data obtained from nucleosome core crystals has only just begun to yield detailed information concerning the path of DNA, and the assumption is still that the helix is smoothly bent about the histone core in a regular superhelix (Levitt, 1978; Sussman and Trifonov, 1978). Additional evidence in favour of a smooth deformation of DNA around the octamer comes from circular dichroism studies (MacDermott, 1985). These studies propose a secondary structure for DNA, differing from standard B-form only by an increase in the base normal tip angle.

As an alternative to the smooth deformation model, kinks have been suggested as a means by which DNA may form superhelices (Crick and Klug, 1975; Sobell *et al.*, 1976). In this instance the DNA is highly deformed but only over a few base-pairs per superhelical turn. However though the path of the spiral may not be completely uniform (Simpson and Shindo, 1979) there is no convincing evidence for the presence of kinks in nucleosomal DNA.

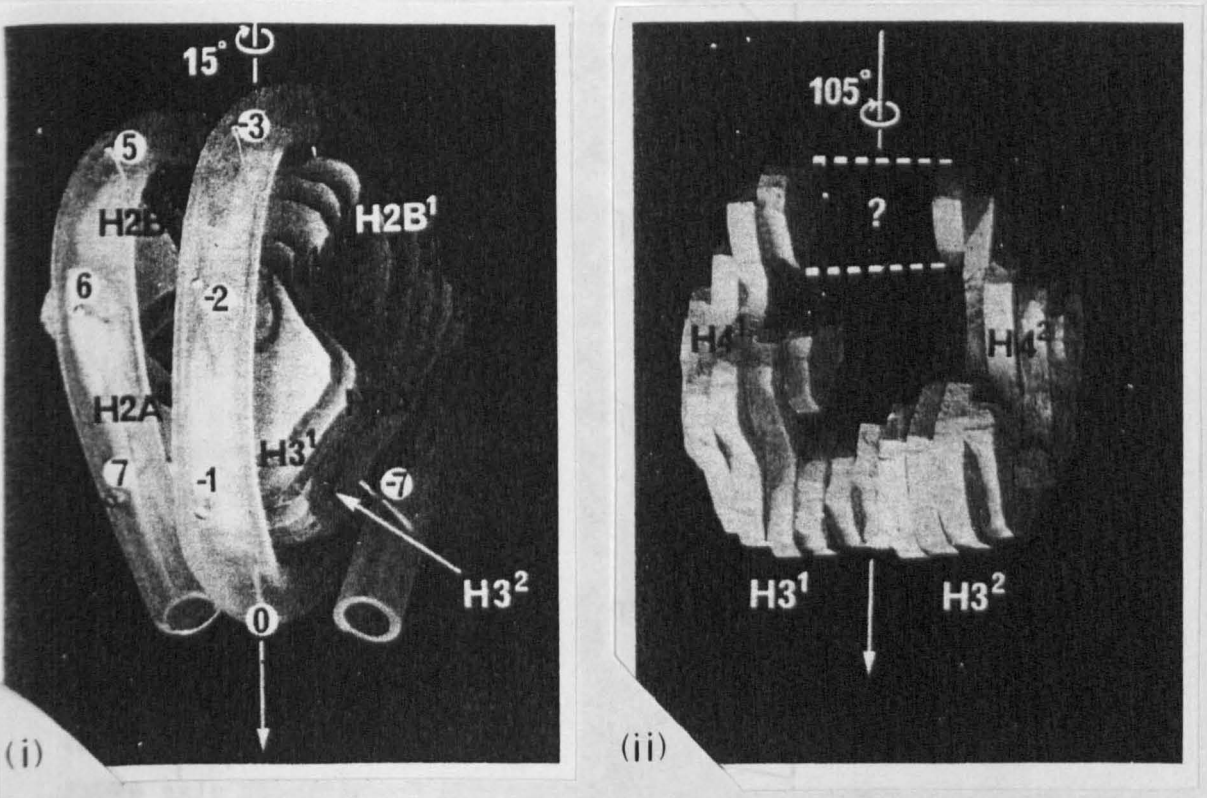

FIGURE 5.1b

(i) The structure of the nucleosome core particle obtained by image reconstruction analysis showing the histone octamer with two turns of a DNA superhelix wound on it. [The DNA diameter is slightly larger than indicated.] Distances along the DNA are indicated by numbers -7 to +7, taking the dyad axis as origin, to mark the 14 repeats of the double helix contained in the 146 b.p. of DNA in the nucleosome core particle, which correspond to the sites of DNase I attack.

(ii) The $(H3)_2.(H4)_2$ tetramer dissected out of the octamer model. The region marked '?' cannot be assigned unambiguously to one or other of the H4 and H2B molecules bordering it. The periphery of the tetramer constitutes about one turn, or somewhat less, of a flat left-handed helix. The views in (i) and (ii) are related by rotation about the dyad axis as indicated [from Thomas (1983)].

Higher Order Structure

The nucleosome must also be involved with the higher orders of structure that fold the DNA into the extremely compact form found in the nucleus. Much attention has been focused on the first two levels of organization, a 'thin' chromatin filament 10 nm in diameter and a thicker fibre, with a diameter of 20-30 nm. The thin fibre is almost certainly a linear array of nucleosome cores in contact with one another. The thick fibre seems to be generated by coiling of the thin fibre.

Within the thin fibre it is not certain how the cores are arranged relative to the fibre axis. Individual core particles show a tendency to stack with their cylindrical axes parallel to the fibre axis (Finch *et al.*, 1977; Dubochet and Noll, 1978), but this cannot be assumed to be true for connected nucleosomes with H1 present. As an alternative arrangement, core particles may associate edge-to-edge thereby giving an approximately 11 nm centre-to-centre spacing (Fig. 5.2) (Thoma *et al.*, 1979).

The term higher order structure is taken to mean the path of the 10 nm fibre axis resulting in possible interactions between nucleosomes that are not adjacent neighbours on the DNA. Models have been proposed in which the axis is coiled to form a regular superhelix or solenoid of chromatin, or constrained to form discrete globular assemblies of nucleosomes, sometimes called superbeads. The solenoid structure, only observed in the presence of magnesium and H1, was depicted as a continuous thread of nucleosomes that describes a helix of 11 nm pitch and 30 nm diameter, thus having about six nucleosomes per turn. On the basis of cross-striations seen in electron micrographs (Finch and Klug, 1976) and the 11 nm reflection in the X-ray pattern of folded chromatin fibres (Sperling and Klug, 1977), it has been proposed that the nucleosomes are arranged in edge-to-edge contact in the solenoid, with their faces projecting radially from the solenoid axis, and aligned roughly parallel to the axis as shown in Figure 5.2 (Thoma *et al.*, 1979). Higher order structures that are more discontinuous in appearance have been proposed by others. Renz *et al.* (1977) and Stratling *et al.* (1978) have presented micrographs of 20 nm diameter superbeads spaced along chromatin which require both H1 and relatively high ionic strength to be visualized. These beads can contain 6-16 nucleosomes. It is entirely

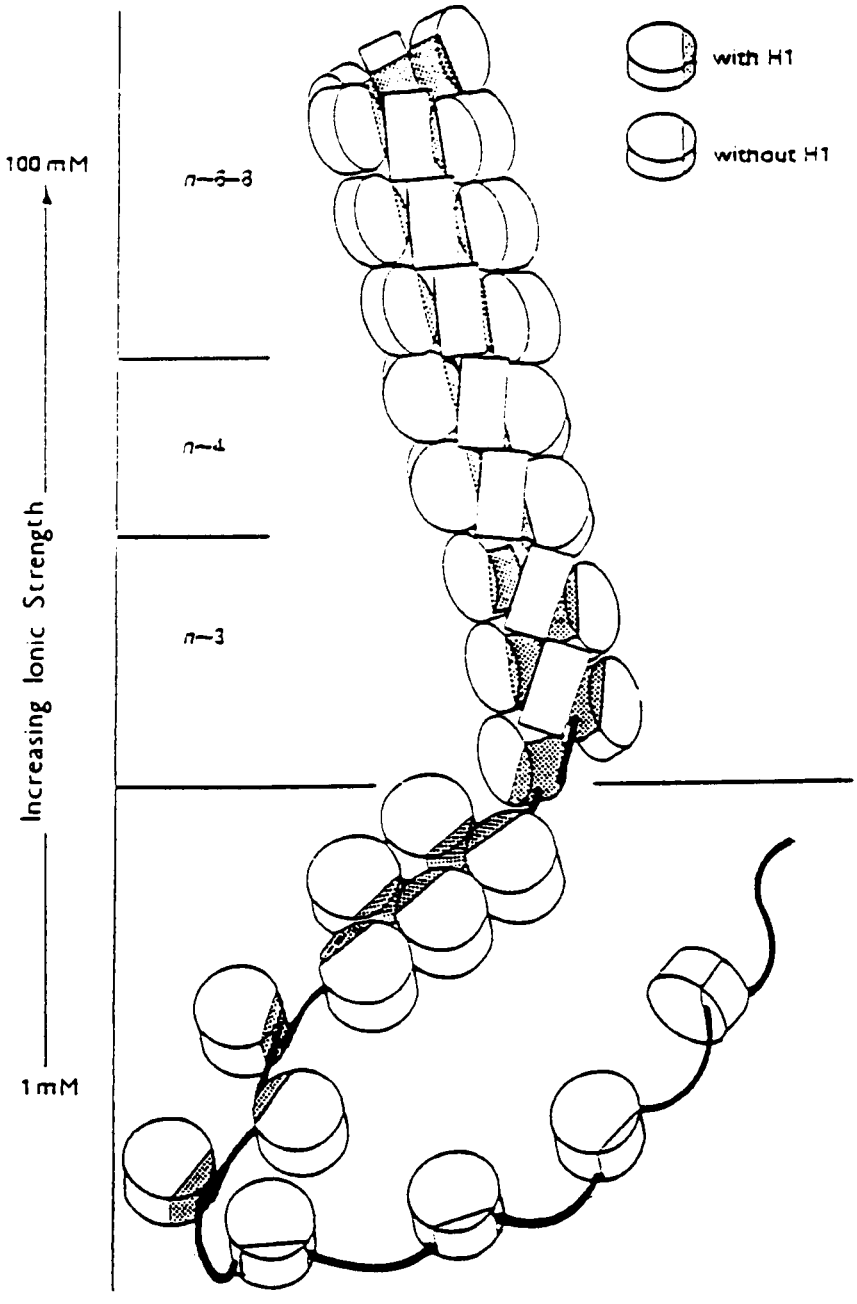

FIGURE 5.2

A model for chromatin condensation. An idealized drawing of helical superstructures formed by chromatin containing H1 with increasing ionic strength. The open zig-zag of nucleosomes (bottom left) closes up to form helices with increasing numbers of nucleosomes per turn (n). The solenoid formed at high ionic strength probably has six nucleosomes per turn. When H1 is absent (bottom right), no zig-zag or definite higher order structures are formed [from Thoma *et al.* (1979)].

possible that superbeads and helical structures may co-exist, possibly in an interconvertible situation. In some micrographs both types of assembly are visible (Olins, 1978), each having the internal appearance of close-packed arrangements of nucleosomes.

Two common points emerge from the above observations. Firstly, chromatin seems to possess the capacity for further levels of coiling, be it continuous or discontinuous, and secondly H1 is likely to be involved in the adoption of these structures. The exact rôle of H1 is difficult to determine beyond a general compaction. However to this end H1 may form bridges between superhelical turns, for it has been shown that when H1 was added to H1-depleted SV40 minichromosomes, some H1 molecules linked non-adjacent nucleosomes (Christiansen and Griffith, 1977). H1 may also connect spacer regions on either side of a single nucleosome (Gaubatz *et al.*, 1978) and interestingly it has been proposed that the amino-acid variability noted for H1, in terms of basic residue content, may in some way determine the length of the internucleosomal spacer region (Morris, 1976; Noll, 1976).

Chromosome Structure

The gross macroscopic characteristics of whole chromosomes have been appreciated for some time. Whole mount electron micrographs of chromosomes (Dupraw, 1970) indicate that they consist of discrete elongated structures with a basic fibrular structure, and have distinct functional domains such as the centromere and the telomere. There is still, however, a considerable need for more information to bridge the gap between the structure at the level of the chromatin fibre and that of the whole chromosome.

It seems highly likely that the basic thread of nucleosomes, even within the 30 nm fibre, is coiled once or several more times to form a reasonably organized structure for the chromosome. Scanning e.m. images of whole metaphase chromosomes (Sedat and Manuelidis, 1978; Wray *et al.*, 1978) show compact structures with uneven knobbly surfaces, and high voltage e.m. studies of nuclei show 200 nm tubes in parallel or orthogonal arrays (Sedat and Manuelidis, 1978). These thicker fibres could represent further stages of coiling of the chromatin thread.

From the observations of Cook and Brazell (1975) it was implied that the DNA of the chromosome has linkage, that is, points of topological constraint, such that it has potential superhelix density. By a study of target size for γ-radiation damage they were able to estimate sizes of 1500 Kb.p. for the superhelical units. Other authors in equivalent observations also predict loops but of smaller size, i.e. 85 Kb.p. (Benyajati and Worcel, 1976) and 34 Kb.p. (Igo-Kemenes and Zachau, 1978). Perhaps the most convincing demonstration of chromosome loops comes from Paulson and Laemmli (1977). They have presented electron micrographs of histone depleted metaphase HeLa chromosomes which show a central core (or scaffold)† of similar shape to the intact chromosome, from which DNA loops of between 30 and 90 Kb.p. emanate. They also observe that the loop ends occur very closely together at the core.

Overall it would appear that the entire length of DNA in a single chromosome is segmented into domains or loops, which may have important functional significance, and may be related to the banding of chromosomes by stains and to banding and puffing phenomena in polytene chromosomes.

Initial Radiolytic Damage

Due to their high abundance and dramatic influence on DNA organization within the nucleus it is important to determine what effects the packaging proteins of chromatin have upon DNA radiolytic pathways. In dilute fluid aqueous solutions (indirect damage) the chromosomal proteins act protectively towards the DNA component, by simply providing alternative targets for the damaging water radicals (Robinson *et al.*, 1966; Mee *et al.*, 1978). Also biological repair of chain lesions, including d.s.b's, could be facilitated with the DNA 'anchored' to the protein.†† On the other hand there exists the opportunity for detrimental DNA-protein cross links which would undoubtedly interfere with transcription and replication†† (Mee and Adelstein, 1979). However, as discussed in Chapter One, systems which favour indirect damage are not considered to be good models for the study of DNA radiolysis *in vivo*, whilst 'dry' and frozen aqueous systems which favour direct damage, are thought to better represent the *in vivo* situation.

---

† Non-histone high molecular weight protein stabilized by metal protein interactions forms only 3-4% of total chromosome protein.

†† Also relevant to direct damage.

One of the earliest studies that investigated the effects of direct ionizing radiation on nucleoprotein complexes was conducted by Alexander *et al.* (1961). They reported that the e.s.r. spectrum from γ-irradiated lyophilised salmon sperm heads closely resembled that of native DNA, and differed from the spectrum obtained from a mechanical mixture of their constituents (65% DNA and 35% salmine protein). The close resemblance between the spectrum of irradiated spermheads and DNA was ascribed to an energy transfer occurring in the nucleoprotein, at -196°C, from the protein constituent to the DNA (i.e. increase in G(radicals) for the DNA component). At room temperature Ormerod (1965), Singh (1968) and Kuwabara *et al.* (1973) observed the 5-thymyl radical $\dot{T}H$ originating from the DNA of irradiated spermheads and deoxyribonucleoprotein, and these three groups also concluded that spin transfer in nucleoprotein occurred from protein to DNA. This idea was further supported by the luminescence studies of Lillicrap and Fielden (1972) who reported that excitation energy formed in the protein component of a nucleohistone sample was transferred to DNA, following irradiation with electron pulses of 1.6 μs duration.

Contrary to the above, an e.s.r. study conducted by van der Vorst *et al.* (1965) showed the spectrum of irradiated calf-thymus deoxyribonucleoprotein to be similar to that of histone rather than DNA. From this they concluded that free radicals in the deoxyribonucleohistone were mainly formed in the protein moiety. Alternatively, Kirby-Smith (1960), from earlier studies of the UV action spectra for chromosome breaks and e.s.r. spectra for irradiated chromosomes, had concluded that little migration of energy occurred between nucleic acids and protein.

More recently Kuwabara and Yoshii (1976) from e.s.r. studies of γ-irradiated deoxyribonucleoprotein-proflavine complexes observed that stable free radicals were not formed at random on the complex but were preferentially located on proflavine. Since proflavine intercalated to DNA bases serves as a final acceptor of electron liberation by ionization (Gregoli *et al.*, 1970b), the result of the above experiment was regarded as suggesting that it was electron transfer from the protein moiety to the DNA moiety that occurred in irradiated deoxyribonucleoprotein. In support of this, Fielder *et al.* (1982) and Stanger *et al.* (1982) reported that the e.s.r. spectra of irradiated natural nucleo-

histone complexes (chromatin) were apparently much poorer in the histone pattern than expected, whilst being richer in the DNA radical component $\dot{T}H$.

Chemical Damage

When solid deoxyribonucleoprotein was irradiated with γ-rays Lucke-Huhle *et al.* (1970) found that single strand breaks of DNA were produced more frequently in the nucleoprotein than in pure DNA, whilst double strand breaks occurred with a similar probability in both systems. Intermolecular cross linking of the DNA double strand occurred much less frequently in nucleoprotein than in pure DNA. No detailed mechanism for these reactions were proposed.

Protein-protein and DNA-protein cross links have been noted in liquid phase irradiations involving isolated histone octamer complexes and nucleosomes respectively. In the former case (Deeg *et al.*, 1984) calf thymus histone octamer complexes were irradiated in their native state in N_2O saturated dilute aqueous solution with 50 or 100 ns pulses of 16 MeV electrons or γ-rays. Time resolved laser light scattering measurements and optical absorption measurements indicated that the octamers underwent a volume contraction due to intra-complex cross linking induced by the attack of $\dot{O}H$ radicals. Cross linking proceeded to a certain extent *via* a 2,2'-biphenol coupling as inferred from product analysis. Protein-DNA cross links were reported by Mee and Adelstein (1981) on irradiating chromatin and nucleosome core particles (H2A, H2B, H3, H4 and DNA) prepared from chinese hamster cells. A comparison of the formation of cross links in the two systems studied demonstrated that the core histones were the specific proteins involved in cross linking. The removal of the H1 histone and non-histone chromosomal protein (possibly consisting of as many as 100 structural, enzymic and regulatory proteins), which together represent *ca.* 45% of the protein in chromatin, produced no significant reduction in cross linking.

In the solid state (i.e. under conditions of direct radiation), as a consequence of the proposed electron transfer from protein to DNA it was suggested that damage to the protein component of irradiated nucleoprotein complexes would arise primarily from the electron-loss centres ('holes') and to a lesser extent from deposited electrons (Kuwabara *et*

al., 1977). Extensive e.s.r. studies on a large number of model peptides (Sevilla *et al.*, 1979a) indicates that the dominant long-lived radicals observed in irradiated proteins (Gordy and Shields, 1958; Riesz and White, 1970) originating from electron-loss centres are the α-carbon radicals, equation [5.1]

$$R\text{-}CO\text{-}NH\text{-}\dot{C}(R')\text{-}R'' \qquad [5.1]$$

or radicals resulting from specific side group radical cations, i.e. phenoxyl radical formation. Combination of these long-lived radicals in irradiated proteins yields high molecular weight aggregate products (Haskill and Hunt, 1967; Friedberg, 1969a). However from work concerning simple amides (Rao and Symons, 1982; Eastland *et al.*, 1986) it is expected that electron-loss should result <u>initially</u> in radical cations with their semi occupied molecular orbitals (SOMO's) largely centred on nitrogen. This point is considered in detail below.

The outcome of electron deposition and trapping within histone, by those electrons that are not transferred to the DNA, most probably results in main chain cleavage by the reactions shown in equations [5.2-5.4].

$$e^- + RCONHCHR_2 \rightarrow R\dot{C}(\bar{O})NHCHR_2 \xrightarrow{H^+} R\dot{C}(OH)NHCHR_2 \qquad [5.2]$$

$$R\dot{C}(OH)NHCHR_2 \rightarrow RCONH_2 + \dot{C}HR_2 \qquad [5.3]$$

$$\dot{C}HR_2 + RCONHCHR_2 \rightarrow CH_2R_2 + RCONH\dot{C}R_2 \qquad [5.4]$$

Though the formation of amide functions dictates that chain scission occurs, this does not necessarily mean that lower molecular weight products will be observed. The average number molecular weight of solid polyamino acids and fibrous proteins does indeed decrease on irradiation in the solid state (Friedberg, 1969b). However globular proteins show a much lower yield of molecular fragments even after reduction of intramolecular disulphide bonds (Friedberg, 1969b; Ray and Hutchinson, 1967; Stevens *et al.*, 1967). The reason for this difference is that radical combination within the hydrated globule would be favoured by the constraints imposed by the secondary and tertiary structures. With the polyamino acids and fibrous proteins such constraints are minimal and the separation of radical fragments on dissolution would be competitive with combination (Friedberg, 1969b; Garrison, 1972).

In the present study both a qualitative and quantitative investigation of the effects of direct ionizing radiation on the higher ordered structures of DNA is undertaken, with special interest being paid to any transfer of damage between DNA and protein. The nature of the systems investigated covers the extremes of DNA-histone association discussed above. Firstly nucleohistone (Sigma) is described simply as a crude complex of DNA and histone. Secondly chromatin, isolated from calf thymus (1400 b.p. ~7 nucleosomes) can be assumed to be a linear array of nucleosomes typical of the 10 nm fibre. Finally, using isolated calf thymus nuclei allows a study of the effects that the gross chromosomal structure has on the radiolysis of DNA and can be taken to typify DNA in an *in vivo* eukaryotic system.

In a parallel study, damage to the protein component of nucleohistone was investigated with special attention being paid to the structural nature and fate of histone electron-loss centres.

EXPERIMENTAL

The isolation of calf thymus chromatin and cell nuclei was conducted with the assistance of Dr. Staynov (Portsmouth Polytechnic) and a detailed procedure along with physical data of the isolated materials is given in Chapter Two.

The e.s.r. spectroscopic measurements of irradiated DNA (6.7-50 mg + 1 ml H_2O), histone (50-85 mg + 1 ml H_2O), nucleohistone (50-135 mg + 1 ml H_2O) (all Sigma preparations) and of the isolated calf thymus chromatin (6.7 and 15.4 mg DNA ml^{-1}) and nuclei (19.1 mg DNA ml^{-1}) were conducted as outlined in Chapter Two. Care was taken to ensure that the DNA concentration of the co-irradiated standards matched that of the DNA-histone complex under study.

Work concerning the identification of the electron-loss centres of a range of proteins and certain polyamino acids was conducted in collaboration with Mr. F. A. Taiwo and Mr. (now Dr.) J. S. Lea. The central region (g = 2) of a range of irradiated proteins and polyamino acids were studied in frozen aqueous solutions (77 K). For systems lacking inherent electron scavenging centres, i.e. FeO_2 or Cu^{II} or -S-S- moieties, low concentrations (1-5 mm) of $K_3Fe(CN)_6$ were introduced to

scavenge the electrons.

Finally work referred to as S. Gregoli unpublished results has been adapted from spectra donated to this laboratory.

RESULTS

Under frozen aqueous conditions, where only $G^{\cdot+}$ and $T^{\cdot-}$ are detected by e.s.r. spectroscopy, both DNA s.s.b's and d.s.b's have been noted to occur to significant levels on raising the temperature. Additives that have interfered with the production of these ionic radicals (or their subsequent radiolytic pathways) have also been shown to alter the extent of strand break formation (Cullis and Symons, 1986; Cullis *et al.*, 1985b). Hence any histone mediated transfer of electrons either to or from the DNA that alters the extent of $G^{\cdot+}$ and $T^{\cdot-}$ formation, will likewise be expected to influence the degree of strand breakage.

In Figure 5.3 the e.s.r. spectra of irradiated DNA (50 mg + 1 ml H_2O), histone (85 mg + 1 ml H_2O) and nucleohistone (135 mg + 1 ml H_2O) are compared. It can be clearly seen that the outer features noted for histone alone (Fig. 5.3a) [collectively assigned as A (g ~2.0451- ~2.0223) and B (g ~1.9815- ~1.9497)] were also present to an equivalent extent in the nucleohistone spectrum (Fig. 5.3c, solid line). The central feature, C, (g ~2.0031) noted for DNA alone (Fig. 5.3b) was also present in the nucleohistone spectrum but was absent from a spectrum resulting from computer addition of the DNA and histone spectra (Fig. 5.3c, broken line). Similar results (though not identical) were noted for a sample consisting of a mechanical mixture of DNA and histone (Fig. 5.3d).

In both of the above cases the 'composed' spectra (i.e. Figs. 5.3c, broken line, and 5.3d) had slightly greater integrated intensities than the experimentally derived nucleohistone spectrum (Fig. 5.3c, solid line). This matches the data given in Table 5.I where the G-values derived for the individual components (histone and DNA) are employed to yield a calculated G-value for nucleohistone, and this compared with an experimentally derived value. In both the cases given in Table 5.I G(nucleohistone, calc.) was greater than G(nucleohistone, exp.) by between 5-15%.

The temperature dependent e.s.r. profiles of irradiated nucleohistone (135 mg + 1 ml H_2O) and DNA (50 mg + 1 ml H_2O) are shown in Figure 5.4 and a plot of the decay of the e.s.r. features with temperature in Figure 5.5. From these results it can be clearly deduced that there is an increase in $\dot{T}H$ (hence $T^{\cdot -}$) formation in irradiated nucleohistone in comparison with that of DNA.

The outer features of A and B for irradiated histone (Fig. 5.3a) are shown in greater detail in Figure 5.6a and several salient signals noted. These signals persist to an equivalent extent in samples of histone irradiated in the presence of the efficient electron capture agent $K_3Fe(CN)_6$ (1-5 mM) (Fig. 5.6b-d). Some further signals, namely A_0 and B_4, were also revealed through the addition of $K_3Fe(CN)_6$. A summary of the above results is given in Table 5.II. The intensity of the spectrum of histone in the presence of 5 mM $K_3Fe(CN)_6$ (Fig. 5.6d) was judged, by the integration of its absorption curve, to be approximately half that of the spectrum of histone irradiated alone (Fig. 5.6a) and was therefore assigned to the electron-loss species of histone protein, denoted as $(Hist)^{\cdot +}$.

Only the most prominent of the $(Hist)^{\cdot +}$ features noted in Figure 5.6d (i.e. A_1, A_2, A_4 and B_1) could be observed, amongst low temperature $\dot{T}H$ signals, in the spectrum of irradiated nucleohistone (Fig. 5.7b). However these, along with the other $(Hist)^{\cdot +}$ features, were better resolved in spectra of nucleohistone irradiated in the presence of 2.5 mM and 5 mM $K_3Fe(CN)_6$ (Figs. 5.7c and 5.7d respectively) (Table 5.II). From careful measurements of the intensities of these $(Hist)^{\cdot +}$ features, it was determined that the histone electron-loss centres were present in the spectra of irradiated nucleohistone (Fig. 5.7b-d) to an extent the same as that expected for a proportional amount of histone irradiated in the absence of DNA.

Computer subtraction of a spectrum of $(Hist)^{\cdot +}$ from one obtained of histone irradiated alone, as shown in Figure 5.8, gave a spectrum for the histone protein radical anion species, denoted as $(Hist)^{\cdot -}$.

The $(Hist)^{\cdot +}$ and $(Hist)^{\cdot -}$ spectra, and those for $G^{\cdot +}$ and $T^{\cdot -}$ (see Chapter Two), were used in a semi-quantitative analysis of the nucleo-

histone 130 K spectrum. The procedure and results of this analysis are given in Figure 5.9 and Table 5.III. From the results it is clear that the protein radical anions were reduced (~20%) in comparison to the protein 'hole' component. Furthermore the final spectrum obtained on computer subtraction was a clean doublet with a good fit to an authentic spectrum of $T^{\cdot -}$. The yield of $T^{\cdot -}$ was enhanced by ~60% relative to that found for the same concentration of DNA in the absence of histone. The integrated intensity of the histone electron-loss species spectrum used in the subtraction was, within experimental error, the same as that of the 'hole' component obtained on irradiation of isolated histones.

Figures 5.10a, b and c respectively show the temperature dependent growth and decay of the 5-thymyl radical $\dot{T}H$ for irradiated calf thymus chromatin [6.7 mg ml^{-1} (1) and 15.4 mg ml^{-1} (2)]† and cell nuclei (19.1 mg ml^{-1}).† In all cases, as with the nucleohistone, the extent of $\dot{T}H$ (hence $T^{\cdot -}$) formation was greater for the DNA-protein complex than the co-irradiated DNA standard of equal concentration. However when comparing the plots corresponding to the higher concentration of chromatin (Fig. 5.10b) and the nuclei (Fig. 5.10c), the increase of $\dot{T}H$ appears to be proportionally far greater for the nuclei.

This point is further demonstrated in Figure 5.11 which shows the extent of $\dot{T}H$ formation by 170 K (prior to the onset of $ROO^{\cdot}$ formation, see below) for the chromatin samples, the nuclei and the corresponding DNA standards. For both the chromatin samples the increase in $\dot{T}H$ was approximately 1.75-1.85 times greater than that noted in DNA. For the nuclei however a greater enhancement of $\dot{T}H$, approximately double what was expected, was observed.

Because the irradiations involving chromatin and nuclei were conducted under ambient conditions there was loss of $\dot{T}H$ above 170 K, rather than above 210 K as was noted for the deoxygenated systems. Control experiments involving mechanical mixtures of DNA and protein, at concentrations equivalent to the chromatin and nuclei showed only a slight increase in [$\dot{T}H$], relative to the DNA standards, at 170 K. This dictates that the $\dot{T}H$ enhancements observed for DNA-protein complexes

---

† Represents DNA concentration only, see Table 2.I for full physical data of isolated calf-thymus materials.

were real and not as a consequence of the ambient 'atmospheric' oxygen 'scavenging' TH in the lower DNA concentration standards.

Semi-quantitative analysis of the damage centres in chromatin (15.4 mg ml^{-1}) and nuclei 130 K spectra, are shown in Figures 5.12 and 5.13 respectively and the results are given in Table 5.III. For the chromatin, delineation to a clean residual signal was not achieved due to the appearance of obscuring signals similar to those ascribed to features 'X' (see Chapter Three). However the amount of protein 'hole' component $(Hist)^{\cdot +}$ present was the same as that expected for a proportional amount of pure histone irradiated alone.

For the nuclei, the protein radical anion component $(Hist)^{\cdot -}$ was approximately 40% of that expected from a proportional amount of irradiated histone and the final spectrum obtained was a clean $T^{\cdot -}$ profile with an excellent fit to an authentic spectrum (Fig. 5.13). The yield of $T^{\cdot -}$ was enhanced by more than 100% relative to that formed in the same concentration of DNA in the absence of protein. Surprisingly there was also an increase in the amount of the protein 'hole' component present (as measured by the amount subtracted) relative to that expected from an equivalent amount of pure histone irradiated alone (46% increase). Possible reasons for this shall be discussed.

A parallel investigation into the nature and fate of protein electron-loss centres has been conducted through study of the g = 2 region of a range of irradiated proteins and certain polypeptides in frozen aqueous solutions (77 K). For proteins lacking inherent electron scavenger centres, low concentrations of $K_3Fe(CN)_6$ were introduced. Under these conditions spectra were obtained which were better assigned to nitrogen centred rather than carbon centred radicals (although in some of the polyamino acids both sorts of centre were formed). Typical spectra are shown in Figures 5.14 and 5.17.

DISCUSSION

Irradiation of dry or fully hydrated frozen DNA systems (conditions of direct damage) has been shown by e.s.r. spectroscopy to give rise to electron-gain centres localised on thymine ($T^{\cdot -}$) and electron-loss

centres ('holes') localised on guanine ($G^{\cdot+}$) in approximately equal yield (Gregoli *et al.*, 1982; Huttermann *et al.*, 1984; Boon *et al.*, 1984). Parallel studies on the development of both single and double strand breaks under comparable conditions provide good evidence that these radical centres are the precursors to such damage (Boon *et al.*, 1984, 1985; Cullis and Symons, 1986), and it has been argued that this may be of relevance to the damage pathways *in vivo*. The present study reports the findings of an investigation of the direct effects of ionizing radiation on systems constituting higher ordered structures of DNA, representative of the nucleic acid *in vivo*, and in particular details what effects the associated histone proteins have on the DNA radiolytic pathways.

Nucleohistone

A comparison of the e.s.r. spectra of γ-irradiated DNA and histone with one of nucleohistone, as in Figure 5.3, shows that the nucleohistone spectrum contains both histone (A and B) and DNA (C) features. However DNA feature C was present to an extent greater than that expected from a simple superimposition of the two individual component spectra, whilst the features A and B [later to be identified as belonging to histone protein electron-loss species, $(Hist)^{\cdot+}$] were present to an extent equivalent to that noted for histone irradiated alone. These initial observations of the nucleohistone spectrum being richer in DNA features than expected does suggest that there is a transfer of damage to the DNA, and since features A and B are not diminished, coupled with the fact that feature C arises from $T^{\cdot-}$ and not $G^{\cdot+}$, it can be proposed that the transfer is predominately *via* electron migration to DNA. Similar results were noted with a sample consisting of a DNA and histone mechanical mixture. In the spectrum of the mixture (Fig. 5.3d) DNA feature C was present, though not to the extent with which it was noted in the authentic nucleohistone spectra. This indicates that some transfer occurs even in a prepared mixture of DNA and histone, though not to the degree with which it is found for nucleohistone.

That both the 'composed' spectra (Figs. 5.3c broken line and 5.3d) had slightly greater intensities than that of the nucleohistone spectrum agrees with the data outlined in Table 5.I. Here calculated G-values for nucleohistone (derived through the addition of G-values determined

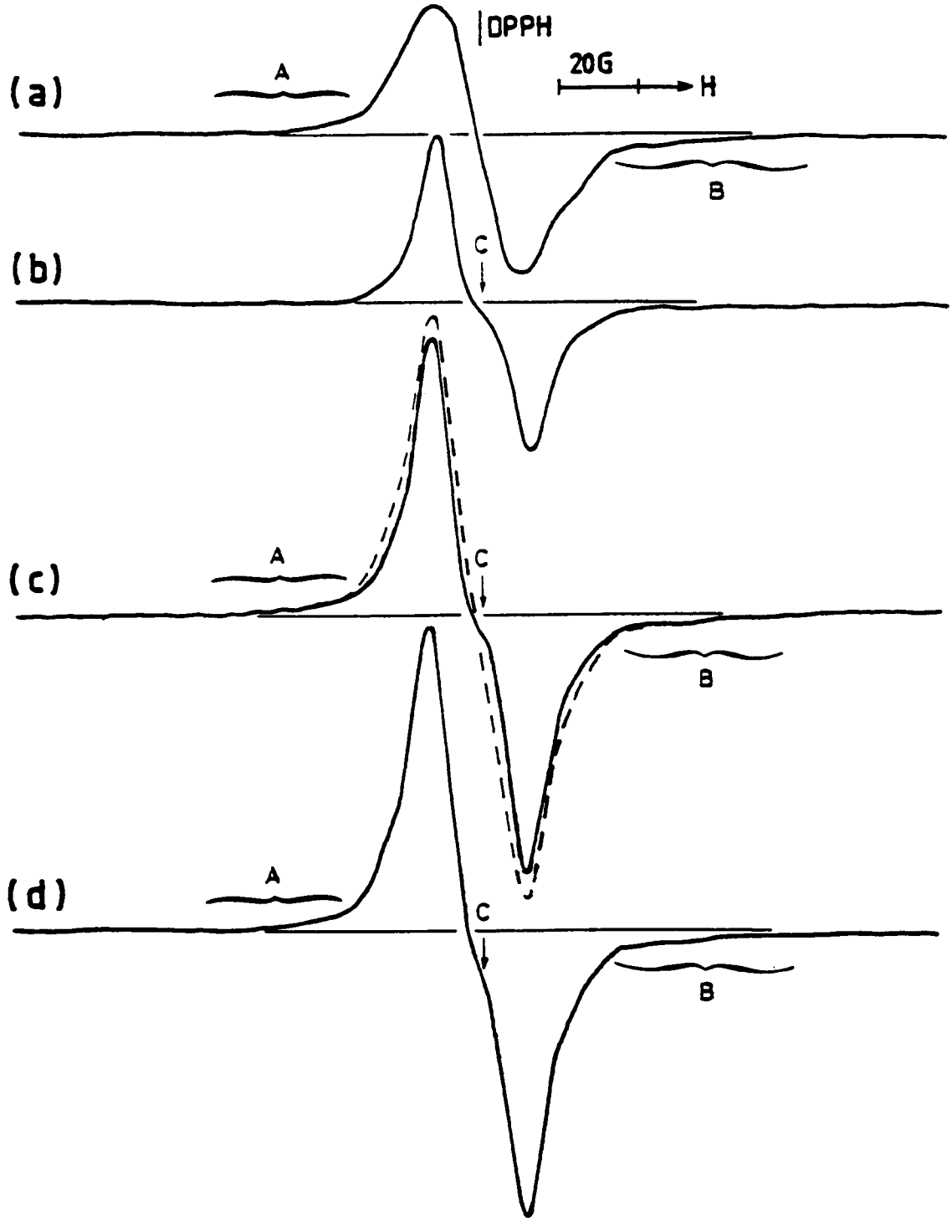

FIGURE 5.3

A comparison of the e.s.r. spectra for irradiated (dose ~1.2 Mrad.) frozen anoxic solutions of (a) histone (85 mg + 1 ml H_2O), (b) DNA (50 mg + 1 ml H_2O) and (c) (solid line) nucleohistone (135 mg + 1 ml H_2O). All spectra were recorded after warming to 130 K. (c) (Broken line) shows the profile resulting from the computer addition of (a) and (b). (d) Shows an e.s.r. spectrum resulting from a sample consisting of a mechanical mixture of DNA (50 mg) and histone (85 mg) in 1 ml H_2O, irradiated and annealed as above. The histone 'outer' features, A and B, and the DNA central feature, C, are, where present, shown in the other spectra.

TABLE 5.I

Comparison of G-values for DNA, Histone and Nucleohistone[a]

DNA	Histone	Nucleohistone	
G_{so}	G_{so}	$G_{(calc)so}$[b]	$G_{(exp)so}$
1.5	1.65	1.59	1.35
1.5[c]	2.17[c]	1.92[c]	1.84[c]

[a] All samples (50 mg + 1 ml H_2O) were γ-irradiated at 77 K and annealed to 130 K for 2 minutes prior to their spectra being recorded;
[b] DNA:histone = 1:1.7;
[c] S. Gregoli, unpublished results.

for each of the components in isolation) were between 5-15% greater than the G-values determined experimentally for nucleohistone. One possibility that could account for this was that a charge recombination event occurred concurrent with the proposed electron transfer. Alternatively the respective G-values of the two components, DNA and protein, may differ relative to one another when together in the DNA-protein complex from their values in isolation, possibly due to an alteration in the degree of solvation of the two components on association. Overall, the amount by which G(exp.) is less than G(calc.) for nucleohistone is small and is not considered a major factor in DNA-protein complex irradiation.

That the proposed transfer of damage in nucleohistone concerns electrons migrating from protein to DNA is further supported by the observation that $\dot{T}H$ (hence $T^{\cdot -}$) formation was ~60-95% enhanced on warming a sample of γ-irradiated nucleohistone, relative to that noted for a proportional amount of DNA (Figs. 5.4 and 5.5).

When a more detailed study of the outer e.s.r. histone features, A and B, was conducted several salient signals were noted (Fig. 5.6a). These features were observed to persist in the presence of the electron capture agent $K_3Fe(CN)_6$ (Fig. 5.6b-d) and so were assigned to histone protein electron-loss species, $(Hist)^{\cdot +}$ (Table 5.II). Identical features were observed during a similar detailed examination of γ-irradiated nucleohistone (Fig. 5.7b) and these were again found to persist in the presence of $K_3Fe(CN)_6$ to an extent the same as that noted for an equivalent amount of histone irradiated alone (Fig. 5.7c,d) (Table 5.II). These results indicate that in nucleohistone 'hole' transfer, to or from the DNA, does not occur.

A spectrum consisting solely of histone protein electron-loss species was obtained by irradiation of the histone proteins in the presence of $K_3Fe(CN)_6$ (5 mM) (Fig. 5.6d). Subtraction of this spectrum from one of the proteins irradiated alone, as in Figure 5.8, yields a spectrum of the histone protein radical anions, $(Hist)^{\cdot -}$. The nature of the radical species that gave rise to these spectra, in particular the protein electron-loss centres, will be discussed later.

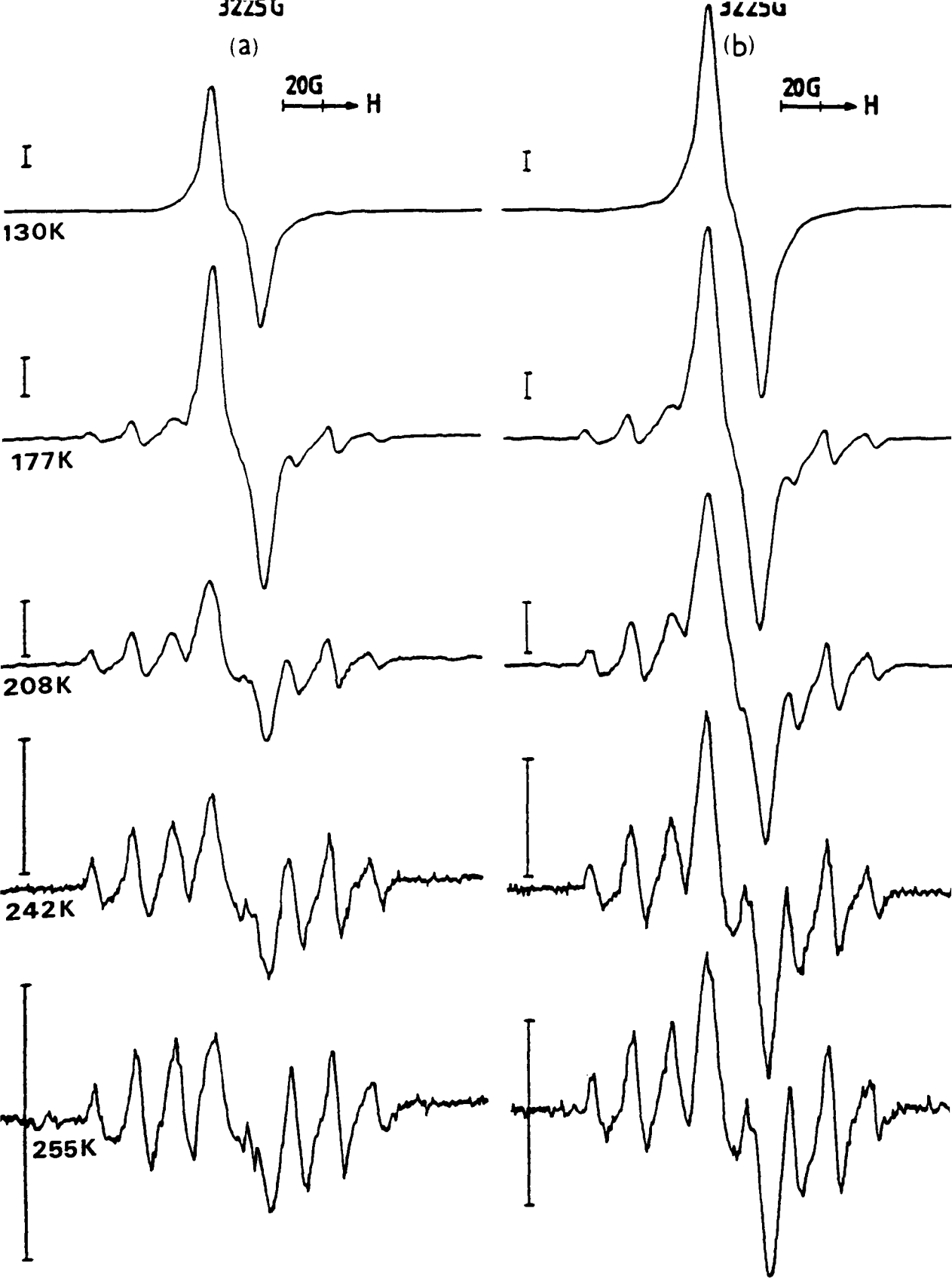

FIGURE 5.4

Representative steps in the evolution of e.s.r. spectra arising from thermal annealing of irradiated (dose ~1.2 Mrad.) frozen anoxic solutions of (a) DNA (50 mg + 1 ml H_2O) and (b) nucleohistone (135 mg + 1 ml H_2O).

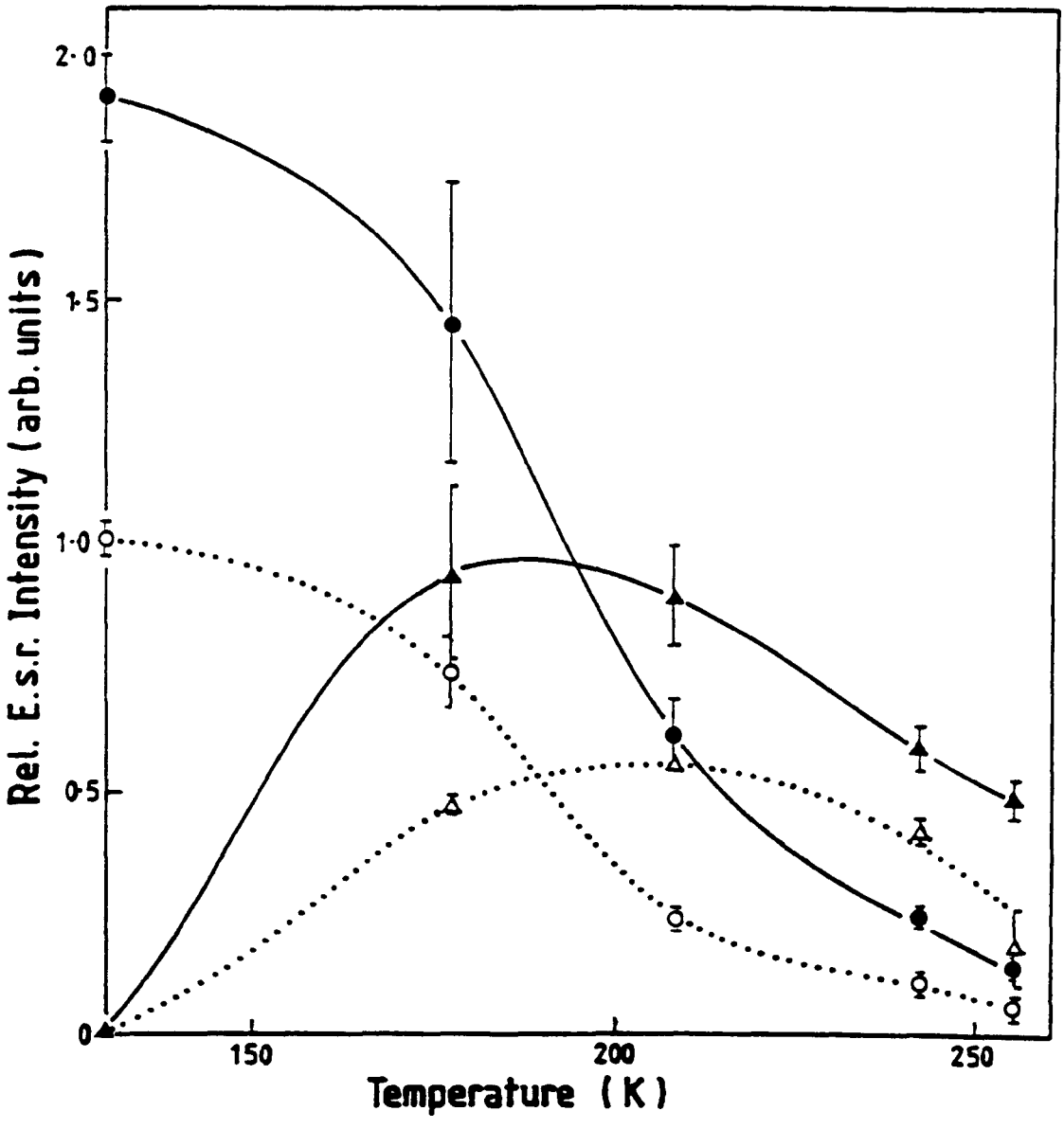

FIGURE 5.5

The temperature dependent decay of the e.s.r. spectral features for frozen anoxic solutions of nucleohistone (135 mg + 1 ml H_2O) and DNA (50 mg + 1 ml H_2O) following irradiation (dose ~1.2 Mrad.). The intensity of the central features (●) and (○) are shown together with the growth and decay of the 5-thymyl TH signals (▲) and (△) [as measured through the relative intensity (x 5) of the seventh line of the octet, at g = 1.9731] for nucleohistone and DNA respectively. Error bars indicate a 99% confidence limit for duplicate samples.

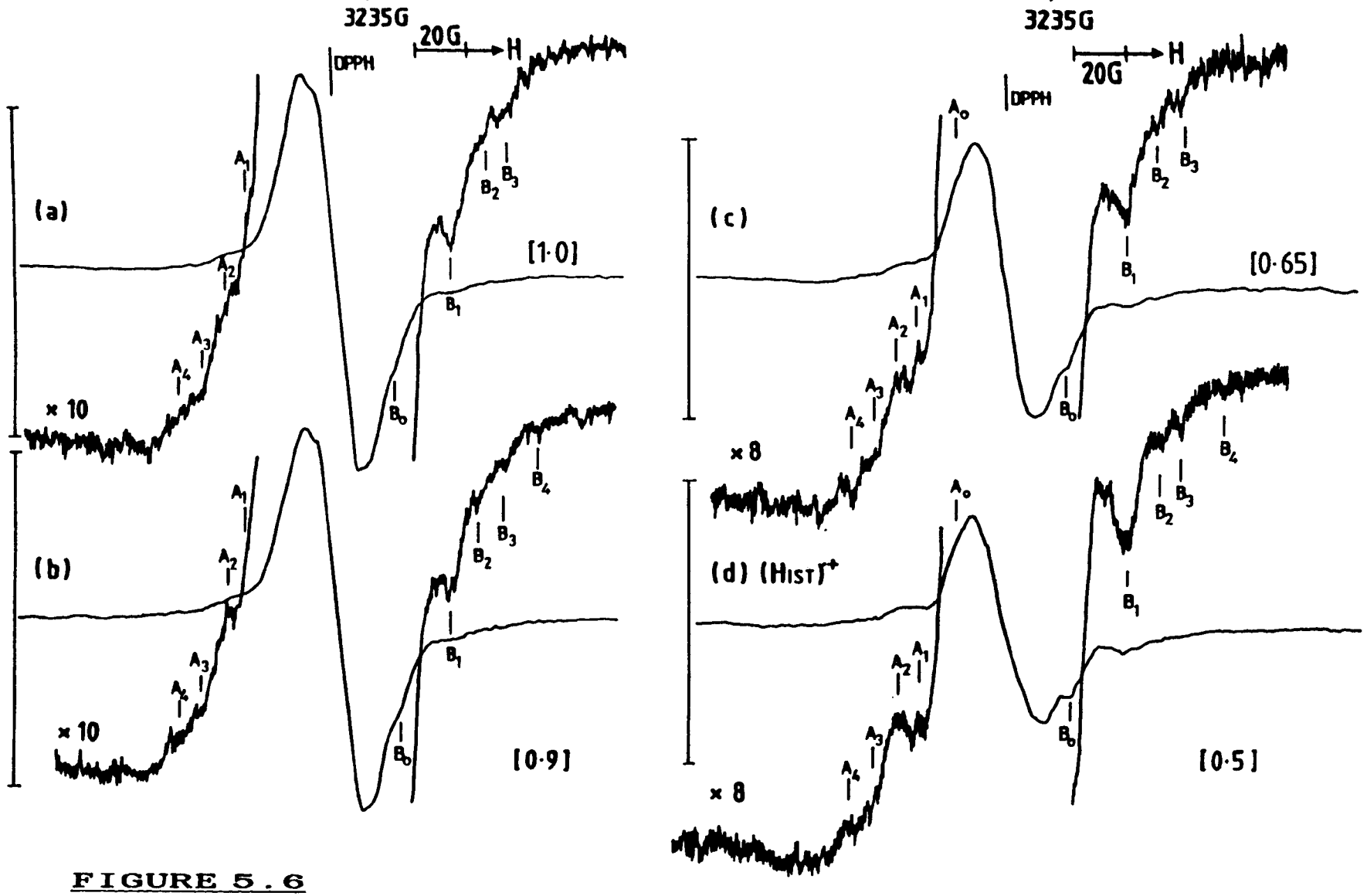

FIGURE 5.6

The e.s.r. spectra for frozen anoxic solutions of histone (85 mg + 1 ml H_2O) irradiated (a) alone, and in the presence of (b) 1 mM, (c) 2.5 mM and (d) 5 mM $K_3Fe(CN)_6$, after brief annealing to 130 K. The intensity standard corresponds to the magnified wing traces, the unmagnified spectra all being recorded at the same gain. The relative integrated intensities are given in square parenthesis [ ], and signals salient to features A (A_0,A_1 ...) and B (B_0,B_1 ...) shown.

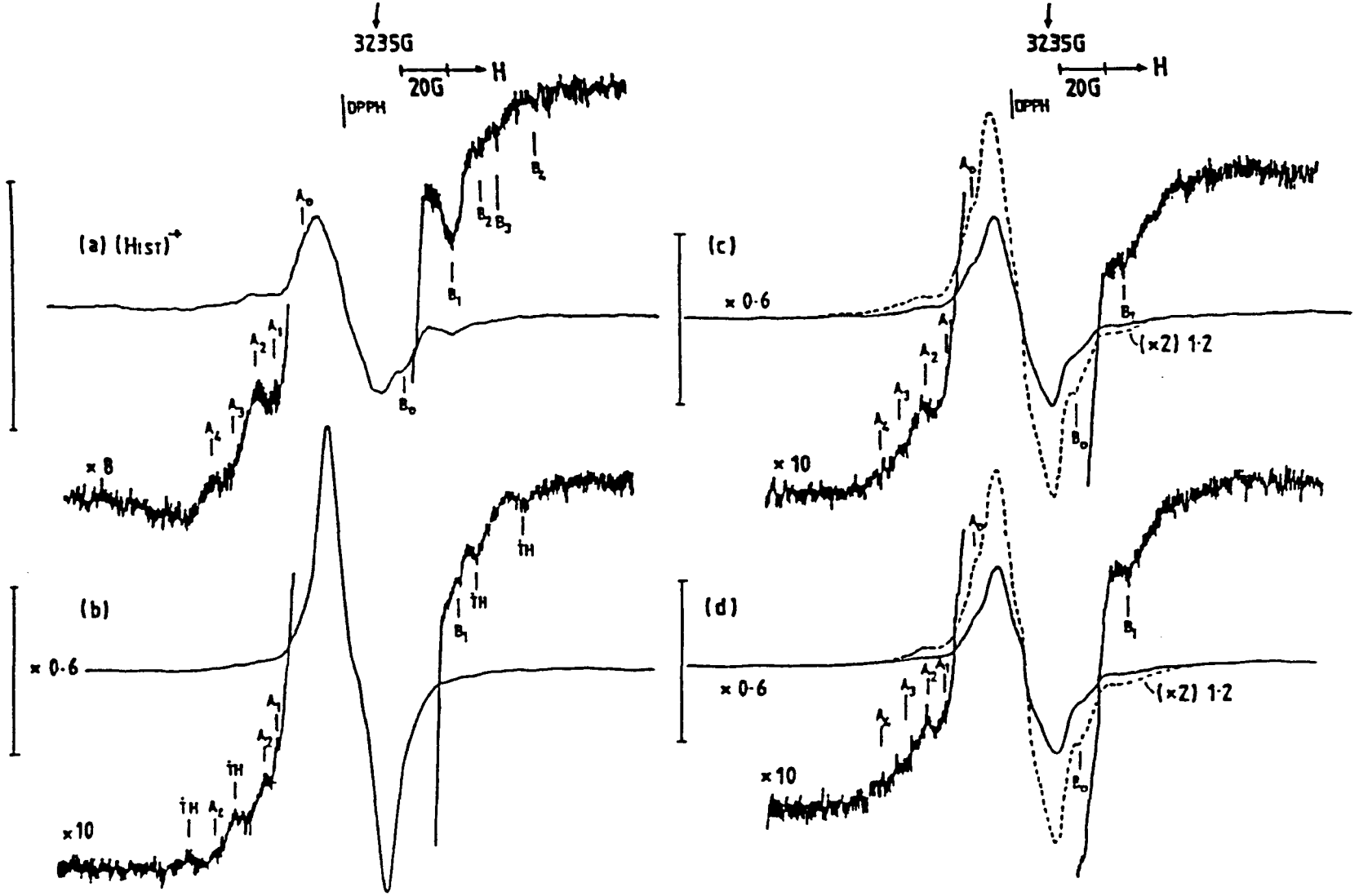

FIGURE 5.7

The e.s.r. spectra for frozen anoxic solutions of nucleohistone (135 mg + 1 ml H_2O) irradiated (b) alone and in the presence of (c) 2.5 mM and (d) 5 mM $K_3Fe(CN)_6$, after brief annealing to 130 K [profile (a), assigned to $(Hist)^{\cdot+}$ (Fig. 5.6d), is shown for comparison]. The intensity standard corresponds to the magnified wing traces, the unmagnified spectra being recorded at gains of approximately 0.6 of that employed in (a). Signals salient to histone features A (A_0,A_1 ...) and B (B_0,B_1 ...) are shown. The broken line profiles in (c) and (d) represent the unmagnified spectra at a gain of x 2.

TABLE 5.II

A Comparison of the Signals that Constitute Features A and B for Histone Irradiated Alone with those noted for Histone Irradiated in the Presence of $K_3Fe(CN)_6$, and Nucleohistone Irradiated in the Presence and Absence of $K_3Fe(CN)_6$

A(g ~2.0451- ~2.0223)	B(g ~1.9815- ~1.9497)
A_0 g ~2.0157	B_0 g ~1.9893
A_1 g ~2.0235	B_1 g ~1.9767
A_2 g ~2.0277	B_2 g ~1.9683
A_3 g ~2.0337	B_3 g ~1.9635
A_4 g ~2.0391	B_4 g ~1.9533

	A_0	A_1	A_2	A_3	A_4	B_0	B_1	B_2	B_3	B_4
Histone[a]	-	++	+++	+	+	++	+++	+	+	-
Histone 1mM-$K_3Fe(CN)_6$	-	++	+++	+	+	++	+++	+	+	+
Histone 2.5 mM-$K_3Fe(CN)_6$	++	++	+++	+	+	++	+++	+	+	-
Histone 5 mM-$K_3Fe(CN)_6$	++	++	+++	+	+	++	+++	+	+	+
Nucleohistone[b]	-	++	+++	-	+	-	++	-	-	-
Nucleohistone 2.5 mM $K_3Fe(CN)_6$	++	++	+++	+	+	++	+++	-	-	-
Nucleohistone 5 mM $K_3Fe(CN)_6$	++	++	+++	+	+	++	+++	-	-	-

+++ V. Prominent
++ Present
+ Present but weak
- Absent or obscured by overlapping features

[a] 85 mg + 1 ml H_2O, $-O_2$
[b] 135 mg + 1 ml H_2O, $-O_2$

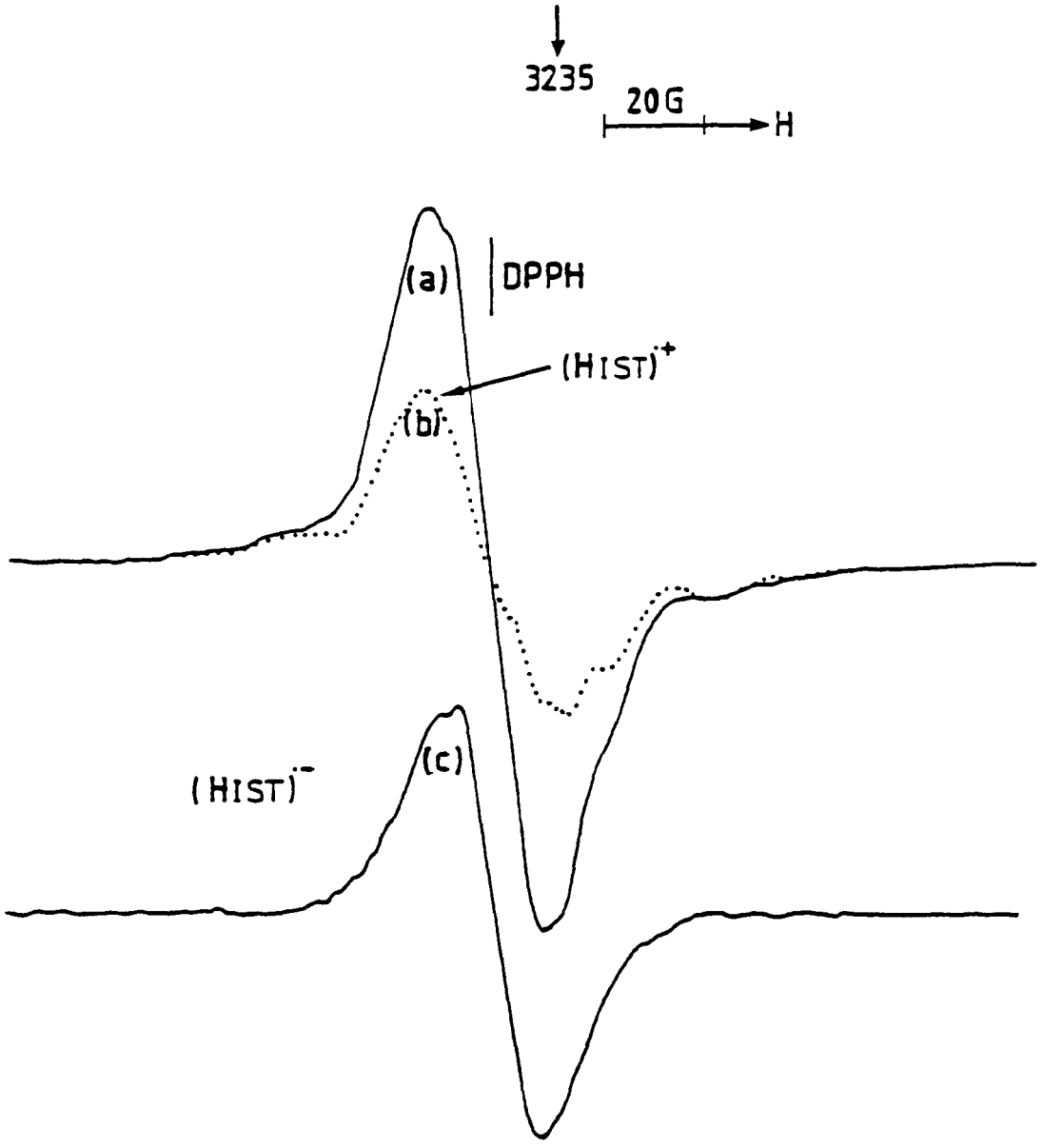

FIGURE 5.8

The generation of the radical anion species, $(Hist)^{\cdot -}$, e.s.r. profile (c), by the subtraction of a spectra of $(Hist)^{\cdot +}$ (b) from one of histone irradiated alone (a).

The $(Hist)^{\cdot+}$ and $(Hist)^{\cdot-}$ spectra, together with those for $G^{\cdot+}$ and $T^{\cdot-}$ (see Chapter Two), were used in analysis of the nucleohistone 130 K spectrum by progressive subtraction of the various components (Fig. 5.9) (Table 5.III). It is clear that the protein radical anion component was ~20% reduced in comparison to the protein 'hole' component, providing direct evidence for electron transfer from the protein. In addition the final spectrum obtained on subtraction was a clean doublet (23 G splitting) with a good fit to an authentic $T^{\cdot-}$ spectrum, thus indicating that the electron transfer was indeed to the DNA. The yield of $T^{\cdot-}$ was 60% enhanced relative to that formed in the same concentration of DNA in the absence of histones, and accounts for the noted increase in $\dot{T}H$ (Fig. 5.5). In contrast to this no evidence was found for any transfer of the positive 'hole' from histone to DNA in that the integrated intensity of the histone electron-loss component used in the subtraction was, within experimental error, the same as the 'hole' component obtained on irradiation of isolated histone. This was in agreement with findings reported above concerning the measurement of the outer $(Hist)^{\cdot+}$ features of nucleohistone and their similarity in intensity to those observed for histone irradiated alone.

With the Sigma prepared nucleohistone being described as a crude complex of DNA and protein, it was important that this study be extended to encompass better defined examples of DNA-histone association, prepared under mild biochemical conditions to preserve nucleosome integrity. To this end calf thymus chromatin and cell nuclei were isolated as outlined in Chapter Two.

Chromatin

As with nucleohistone, the irradiated chromatin (6.7 and 15.4 mg DNA ml^{-1}) showed on warming a substantial increase in $\dot{T}H$ ($T^{\cdot-}$) formation relative to DNA (Figs. 5.10a and 5.10b). The increase in $\dot{T}H$ noted by 170 K was similar for both chromatin samples (75-85%) (Fig. 5.11) and comparable with that noted for nucleohistone. Above 170 K the intensity of $\dot{T}H$ for the two DNA standards and the 6.7 mg DNA ml^{-1} chromatin sample decreased, whilst for the higher concentration of chromatin the $\dot{T}H$ e.s.r. intensity continued to increase up to ~190 K, before decaying. This was as a consequence of all these irradiations having been conducted under ambient 'atmospheric' conditions where, above 170 K, $\dot{T}H$

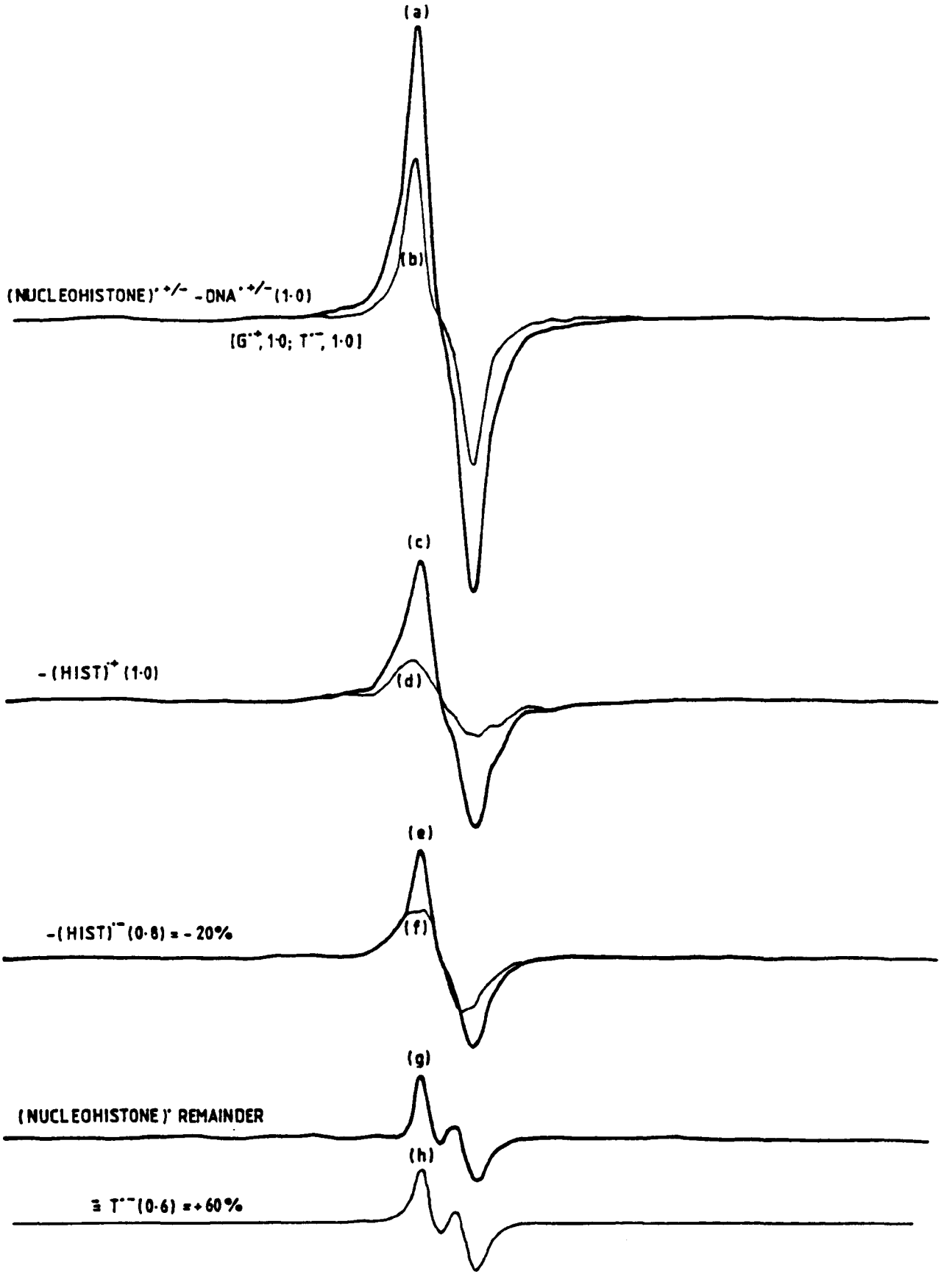

FIGURE 5.9

The e.s.r. spectra of: (a) calf thymus nucleohistone (135 mg + 1 ml H_2O) after irradiation and brief annealing to 130 K; (b) DNA at a concentration equivalent to the DNA concentration of the nucleohistone treated under identical conditions; (c) the result of subtraction of (b) from (a); (e) the result of the subtraction of the histone electron-loss centre spectrum (d) from (c); (g) the result of the subtraction of the histone radical anion spectrum (f) from (e), and (h) authentic $T^{\cdot -}$ for comparison.

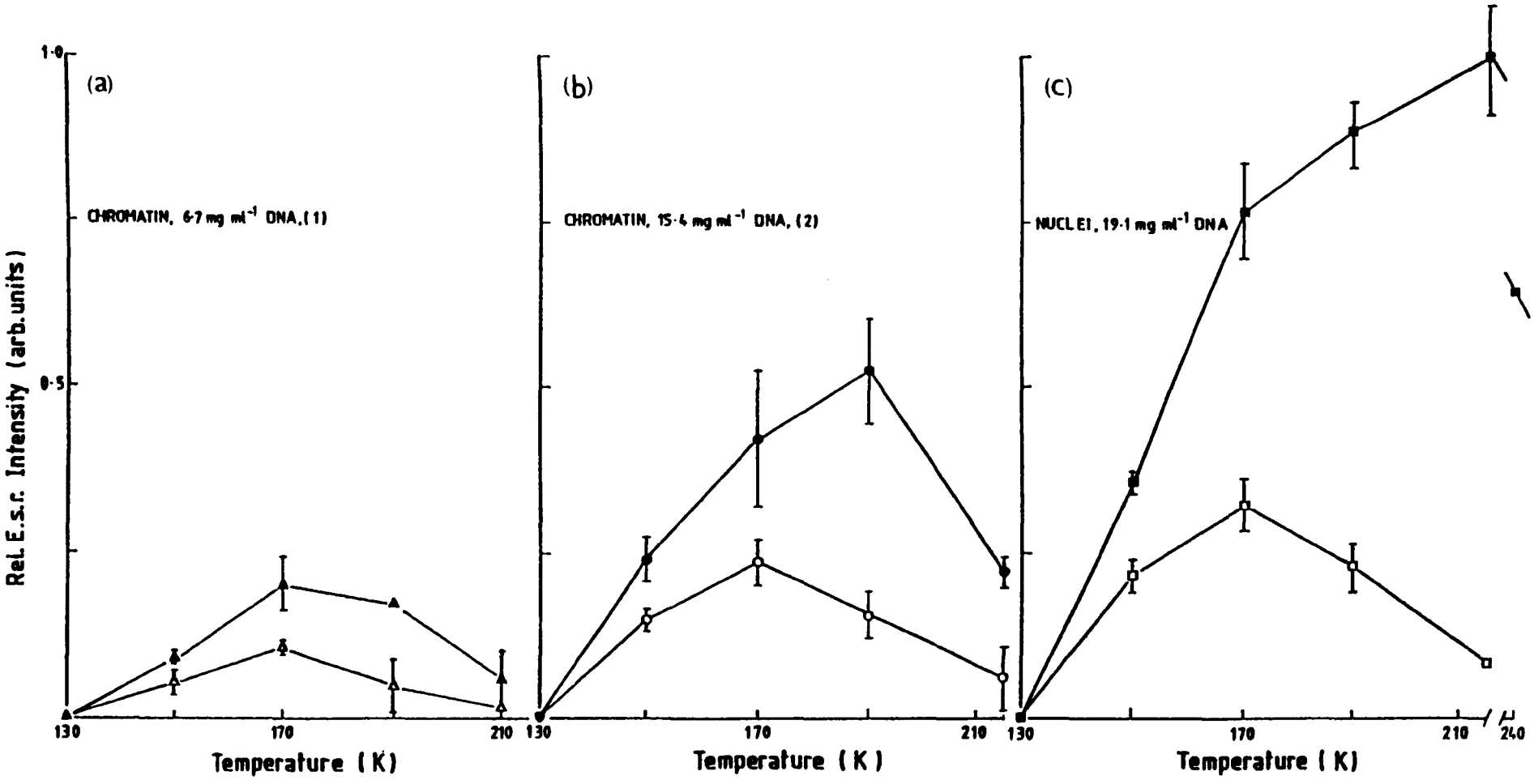

FIGURE 5.10

A comparison of the temperature dependent growth and decay of the 5-thymyl $\dot{T}H$ e.s.r. signals for irradiated frozen solutions of (a,b) isolated calf thymus chromatin [▲] 6.7 mg DNA ml^{-1}, [●] 15.4 mg DNA ml^{-1}, and (c) nuclei [■] 19.1 mg DNA ml^{-1}. The intensities of the $\dot{T}H$ signals for the corresponding DNA standards are also shown (open symbols). The degree to which $\dot{T}H$ was formed was estimated from the relative intensity of the seventh line of the octet (g = 1.9731). The error bars indicate a 99% confidence limit for duplicate samples.

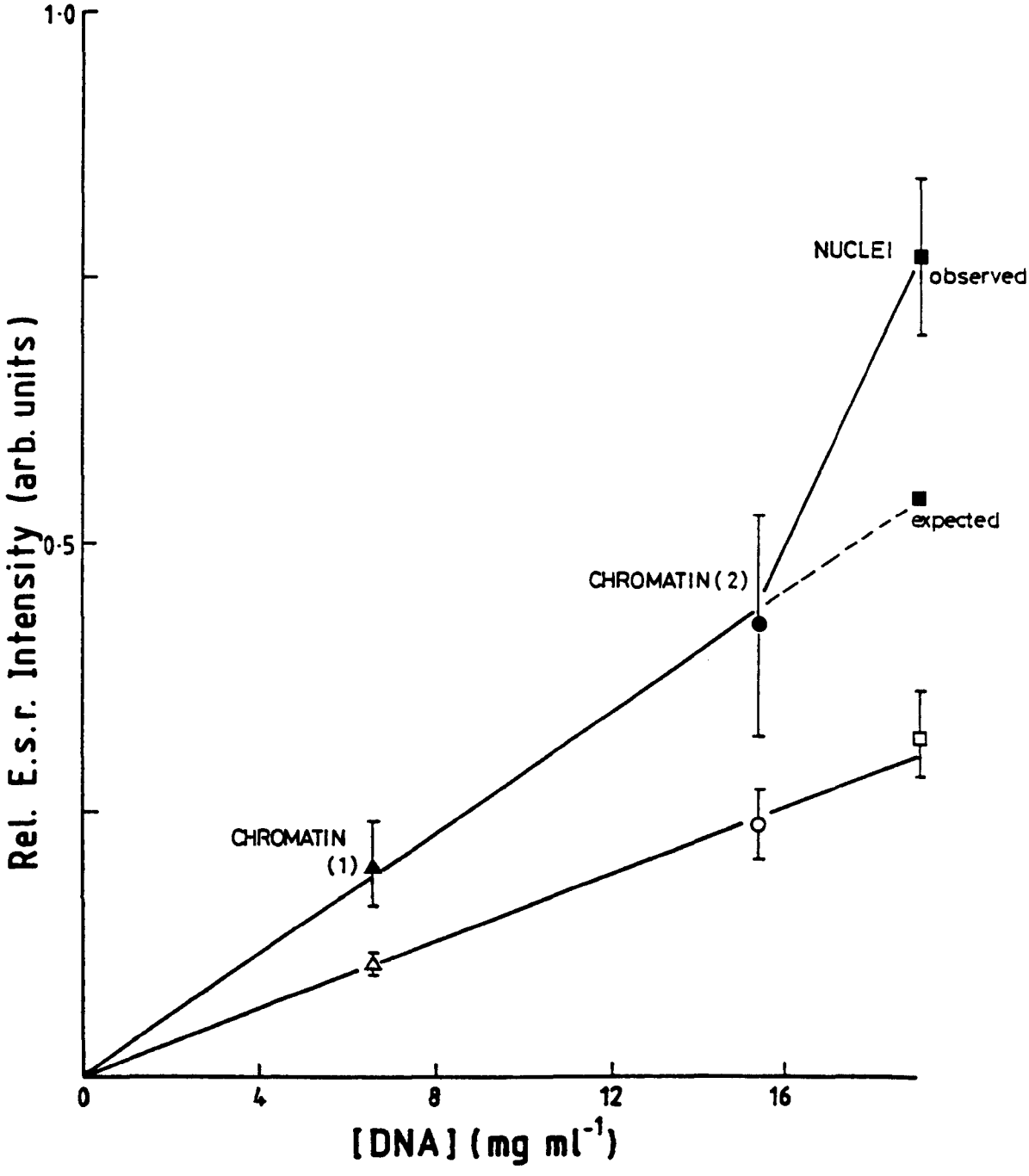

FIGURE 5.11

The relative e.s.r. intensities of TH at 170 K for the chromatin samples, 6.7 mg DNA ml^{-1} (▲) and 15.4 mg DNA ml^{-1} (●), and the nuclei, 19.1 mg DNA ml^{-1} (■), after irradiation. The intensity of TH in the corresponding DNA standards are also shown (open symbols).

converts to the peroxyl radical THOO·(ROO·), the e.s.r. features of which ($g_{\parallel}$ 2.033, $g_{\perp}$ 2.0025) appeared above this temperature. However, for the higher concentration of chromatin it would seem that the oxygen present was limiting, thus allowing ṪH to survive and persist to higher temperatures, prior to decaying. Similar trends were observed in control experiments employing DNA and histone mixed together at concentrations equivalent to the above chromatin samples.

A full analysis of the chromatin 130 K spectrum was not possible due to the appearance of obscuring features similar to those assigned to radicals 'X' (see Chapter Three; Cullis *et al.*, 1985a). These features were not observed in either the nucleohistone or nuclei studies (see below) and it is difficult to rationalize their appearance. It is most likely to be due to a buffer constituent acting in a manner similar to iodoacetamide (Cullis *et al.*, 1985a) or H_2O_2 (see Chapter Three) and so be an artifact. However, the partial analysis conducted with the chromatin 130 K spectrum (Fig. 5.12) did allow a determination of the extent to which $(Hist)^{\cdot +}$ was formed, and like nucleohistone it was found to be equivalent to the 'hole' component formed in a proportional amount of histone irradiated alone, thus negating 'hole' transfer either to or from the DNA.

The above results indicate that the isolated calf thymus chromatin acts analogously to the nucleohistone in terms of the magnitude of electron transfer to DNA and the absence of any positive 'hole' transfer.

Nuclei

With the chromatin being taken to represent the 10 nm fibre (linear array of nucleosomes) the isolated calf thymus nuclei were regarded as being representative of the gross structure that typifies chromosomal DNA. Figure 5.10c shows the temperature dependent growth of the ṪH e.s.r. signal for calf thymus nuclei (19.1 mg DNA ml^{-1}) after irradiation at 77 K. The enhancement of ṪH by 170 K was *ca.* ~140% relative to that formed in the same concentration of DNA, and was approximately double the ṪH enhancement noted for chromatin (Fig. 5.11). The reason for the continuing increase in the intensity of the ṪH signal above 170 K must, in part, be due to a situation similar to that which arose with the higher concentration of chromatin. That is, the oxygen present

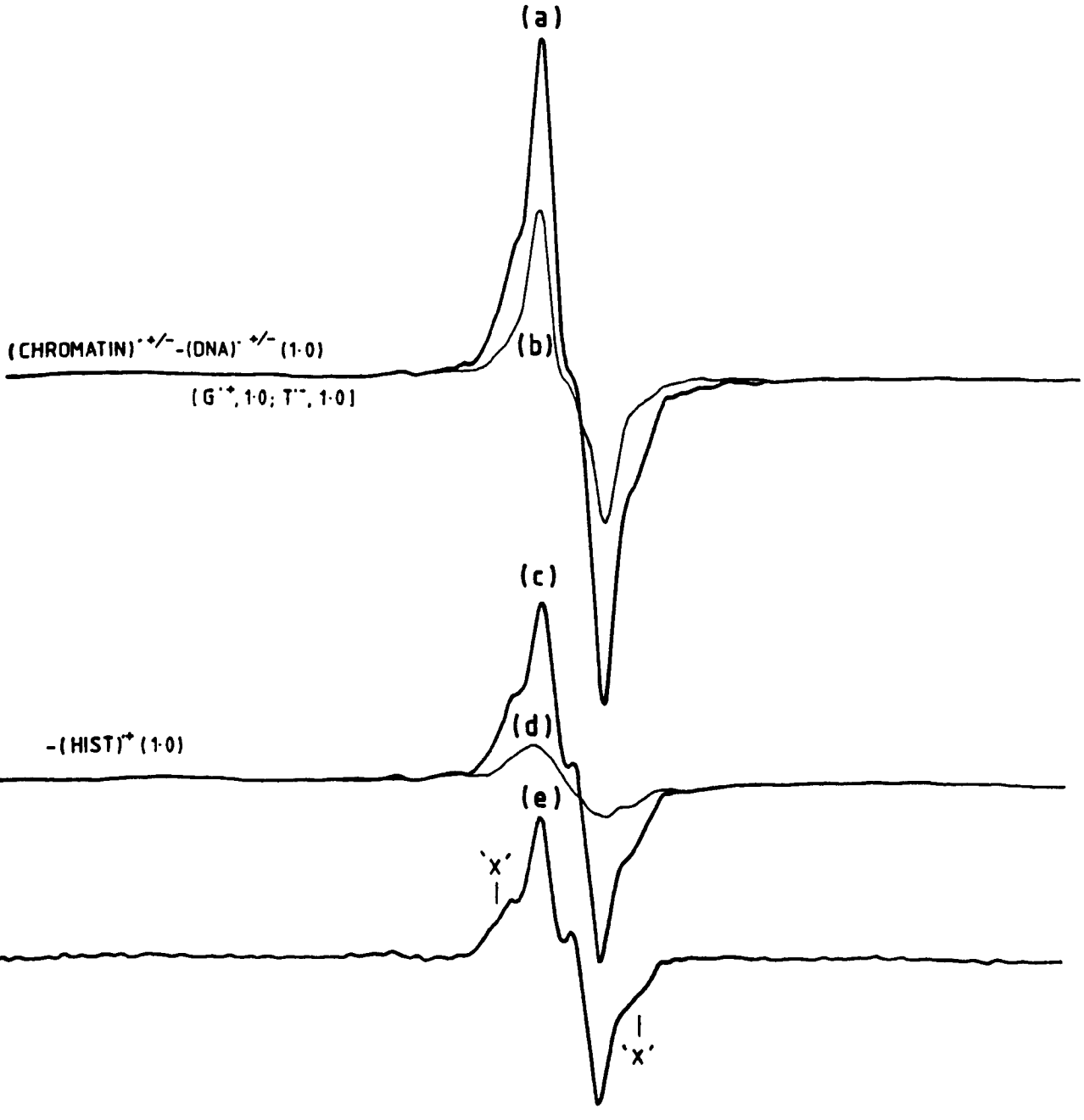

FIGURE 5.12

The e.s.r. spectra of: (a) calf thymus chromatin (15.4 mg DNA ml^{-1}) after irradiation and brief annealing to 130 K; (b) DNA at a concentration equivalent to the DNA concentration within the chromatin treated under identical conditions; (c) the result of the subtraction of (b) from (a); (e) the result of subtraction of the histone electron-loss centre spectrum (d) from (c). No further subtractions were conducted due to the appearance of obscuring 'X' features, see text.

in these higher concentration samples was limiting and with protein radicals competing with $\dot{T}H$ for O_2, the nuclear $\dot{T}H$ remains largely 'unscavenged' and so persisted to a higher temperature. However the large increase in $\dot{T}H$, both above and below 170 K, was proportionally far higher than expected (Fig. 5.10 and 5.11) and must be due to a greater degree of electron migration to DNA occurring in the nuclei than in chromatin.

This in turn is supported by analysis of the 130 K e.s.r. spectrum of the irradiated nuclei (Fig. 5.13) (Table 5.III). The protein radical anion component, $(Hist)^{\cdot -}$, was approximately 40% (60% reduced) of that expected for an equivalent amount of histone irradiated alone, thus indicating that a far greater degree of electron transfer occurred from the protein for nuclei, than for nucleohistone (where the $(Hist)^{\cdot -}$ was only 20% reduced) and presumably chromatin.† Similarly the residual clean $T^{\cdot -}$ signal, which had an excellent fit to an authentic signal, was enhanced by more than 100%, approximately double that noted for nucleohistone. This confirms that in nuclei, as with the other DNA-protein complexes studied, electron transfer is indeed to the DNA, with the final electron 'sink' being the thymine base.

The greater degree of electron transfer from protein to DNA noted for the nuclei, over that of chromatin and nucleohistone, could be accounted for by the presence of additional higher ordered structures in the nuclei. Within these structures possible additional internucleosomal protein-DNA contact could facilitate the greater transfer. Such structures would undoubtedly be absent in the isolated chromatin filaments (~7 nucleosomes in length) and nucleohistone samples.

Somewhat surprisingly the e.s.r. features corresponding to the protein electron-loss centres, $(Hist)^{\cdot +}$, were noted to be of greater intensity in the nuclei samples (+46%) than expected (Fig. 5.13) (Table 5.III). This was initially thought to support the notion of positive 'hole' transfer occurring in nuclei from DNA to histone. However no apparent loss of $G^{\cdot +}$ was detected. Alternatively, the increase in $(Hist)^{\cdot +}$ was considered to be as a consequence of the large electron migration to the

---

† Inferred from an increase in $\dot{T}H$ ($T^{\cdot -}$) that was similar to that of nucleohistone.

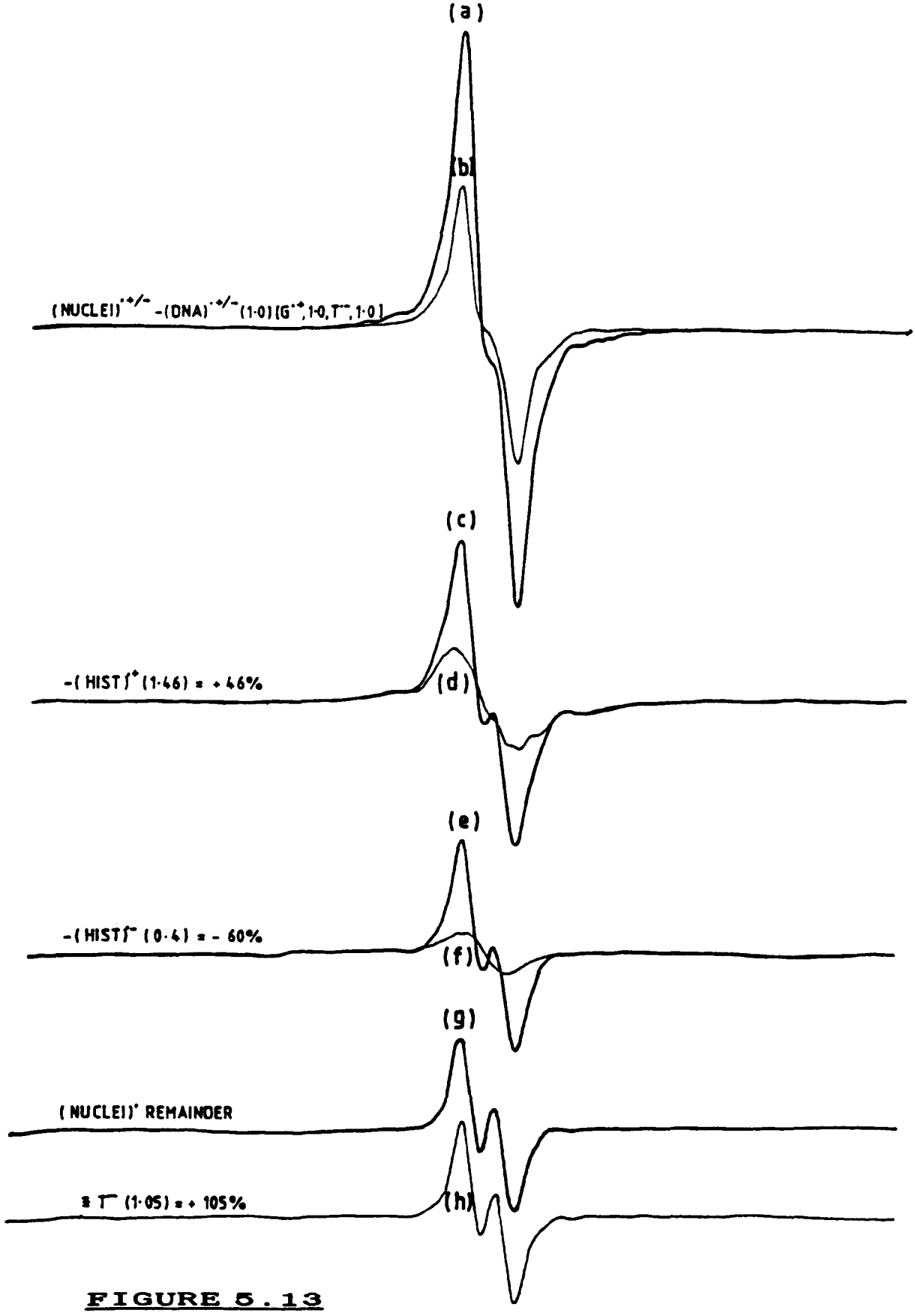

FIGURE 5.13

The e.s.r. spectra of: (a) calf thymus cell nuclei (19.1 mg DNA ml^{-1}) after irradiation and brief annealing to 130 K; (b) DNA at a concentration equivalent to the DNA concentration within the nuclei treated under identical conditions; (c) the result of subtraction of (b) from (a); (e) the result of subtraction of the histone electron-loss centre spectrum (d) from (c); (g) the result of subtraction of the histone radical anion spectrum (f) from (e), and (h) authentic $T^{\cdot-}$ for comparison.

TABLE 5.III

A Comparison of the Results from the Semi-Quantitative Analyses Conducted on the 130 K Spectra of γ-Irradiated Nucleohistone, Chromatin and Nuclei, and the $\dot{T}H$ Enhancements noted on Annealing

	$G^{\cdot+}$	$(Hist)^{\cdot+}$	$T^{\cdot-}$	$(Hist)^{\cdot-}$	$\dot{T}H$
DNA	1.0	-	1.0	-	-
Histone		1.0	-	1.0	-
Nucleohistone	≤1.0[a]	1.0	1.6(+60%)	0.8(-20%)	(+60-95%)
Chromatin	≤1.0[a]	1.0	?(>50%[c,d])	?[c]	(+75-85%)
Nuclei	≤1.0[a]	1.46[b](+46%)	2.05(+105%)	0.40(-60%)	(+~140%)

[a] Possible recombinational event on e^- transfer (see text);
[b] Possible hole transfer, or non-recombined hole (see text);
[c] Absolute values not determined due to obscuring 'X' type features;
[d] $T^{\cdot-}$ enhancement deduced from $\dot{T}H$ enhancement.

DNA interrupting a protein based charge recombination event. However no such increase in $(Hist)^{\cdot+}$ was noted when $K_3Fe(CN)_6$ was employed to efficiently scavenge electrons from either nucleohistone or histone. At present no satisfactory answer can be given to account for this increase in $(Hist)^{\cdot+}$.

Protein Damage

As well as indicating an enhancement of DNA anionic damage, the e.s.r. spectra of the various DNA-protein complexes showed clear signals corresponding to protein electron-loss centres. A study of these species within a variety of irradiated proteins and certain polypeptides in frozen aqueous solutions (77 K), yielded spectra which were better assigned to nitrogen-centred radicals (-CON$\dot{}$-CHR-) than to carbon-centred radicals (-CONH-C$\dot{}$R-), although with some aliphatic polyamino acids the latter were also formed at 77 K. Typical spectra are shown in Figures 5.14 and 5.17.

If, as is anticipated, the primary cations, (-CO$\overset{+}{\dot{N}}$H-CHR-) readily deprotonate *via* their hydrogen bonds to give (-CON$\dot{}$-CHR-) radicals, the following e.s.r. features are expected by comparison with a wide range of nitrogen-centred π-radicals (Rao and Symons, 1982; Eastland *et al.*, 1986):-

(a) Relatively weak $M_I(^{14}N) = \pm 1$ 'parallel' features together with an intense nearly isotropic $M_I = 0$ line.

(b) Each of these should split into nearly isotropic doublets by coupling to the unique β-proton of the adjacent -CHR- unit. The difficulty with this prediction is that the magnitude of the coupling to the β-proton is a function of the angle Θ defined in Figure 5.15 and could take any value from *ca.* 50 G to zero, depending on this angle.

For values of Θ close to 90° unsplit features of significant intensity are expected, but unless there are a large number of units with nearly equal values for Θ the signals will extensively broaden over the available range. Fortunately, as can be judged from Ramachandran-plots for many proteins (Schulz and Schirmer, 1979), values of Θ do tend to cluster and, in particular, for α-helix units, values around 30° are expected. A computer synthesised spectrum is shown in Figure 5.16 which illustrates these points using Θ = 30° and 90°, which is an upper limit.

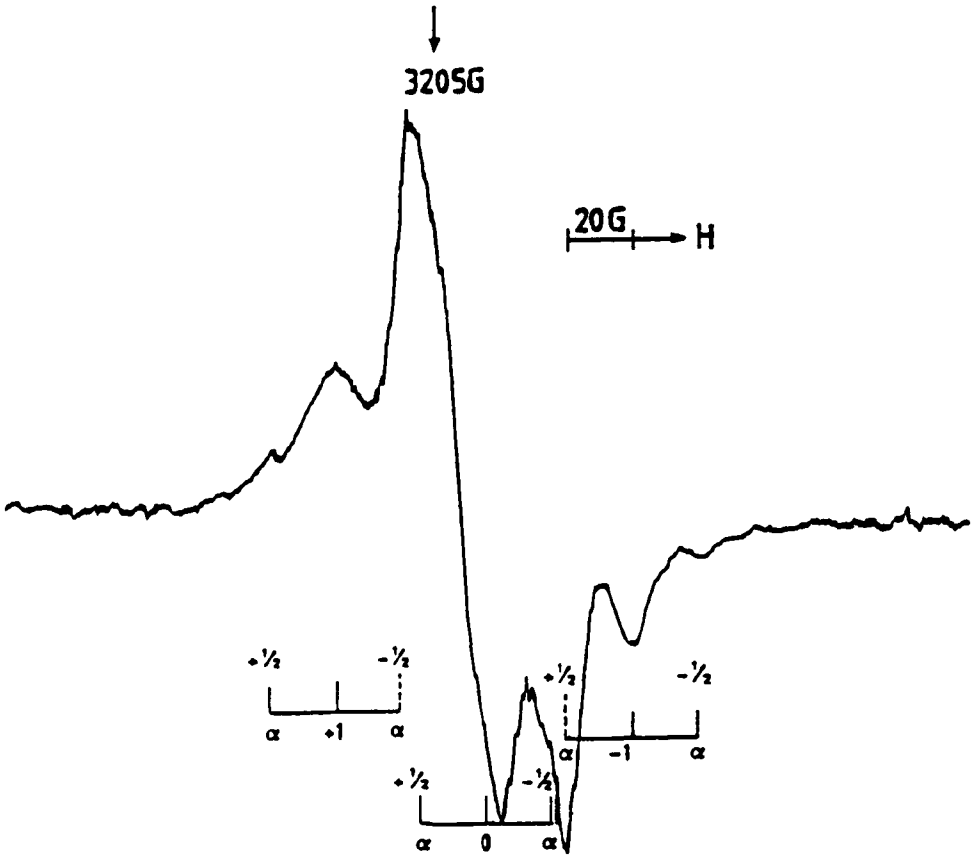

FIGURE 5.14

First derivative e.s.r. spectrum for met-haemoglobin after exposure and annealing to 140 K, showing features assigned to electron-loss centres. [Ejected electrons were captured at Fe(III), as indicated by a marked decrease in the Fe(III) feature at g = 6.] One species [$M_I(^{14}N)$ = +1, 0, -1] has $A_{\parallel}$ = 43 G, $A_{\perp}$ ~0, and no resolved proton splitting. A second species (α) has similar ^{14}N parameters with $A(^1H)$ ~38 G. [The $|+1, -^1/_2\rangle$ and $|-1, +^1/_2\rangle$ lines for α, indicated by dashed lines, are concealed beneath the main spectrum.]

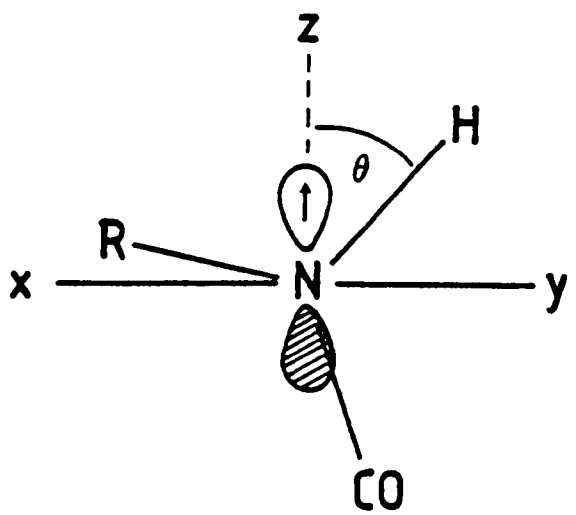

FIGURE 5.15

View along the N-C bond with the amide unit in the *x-y* plane, showing the angle Θ between the $2p_z$ orbital on N and the C-H bond.

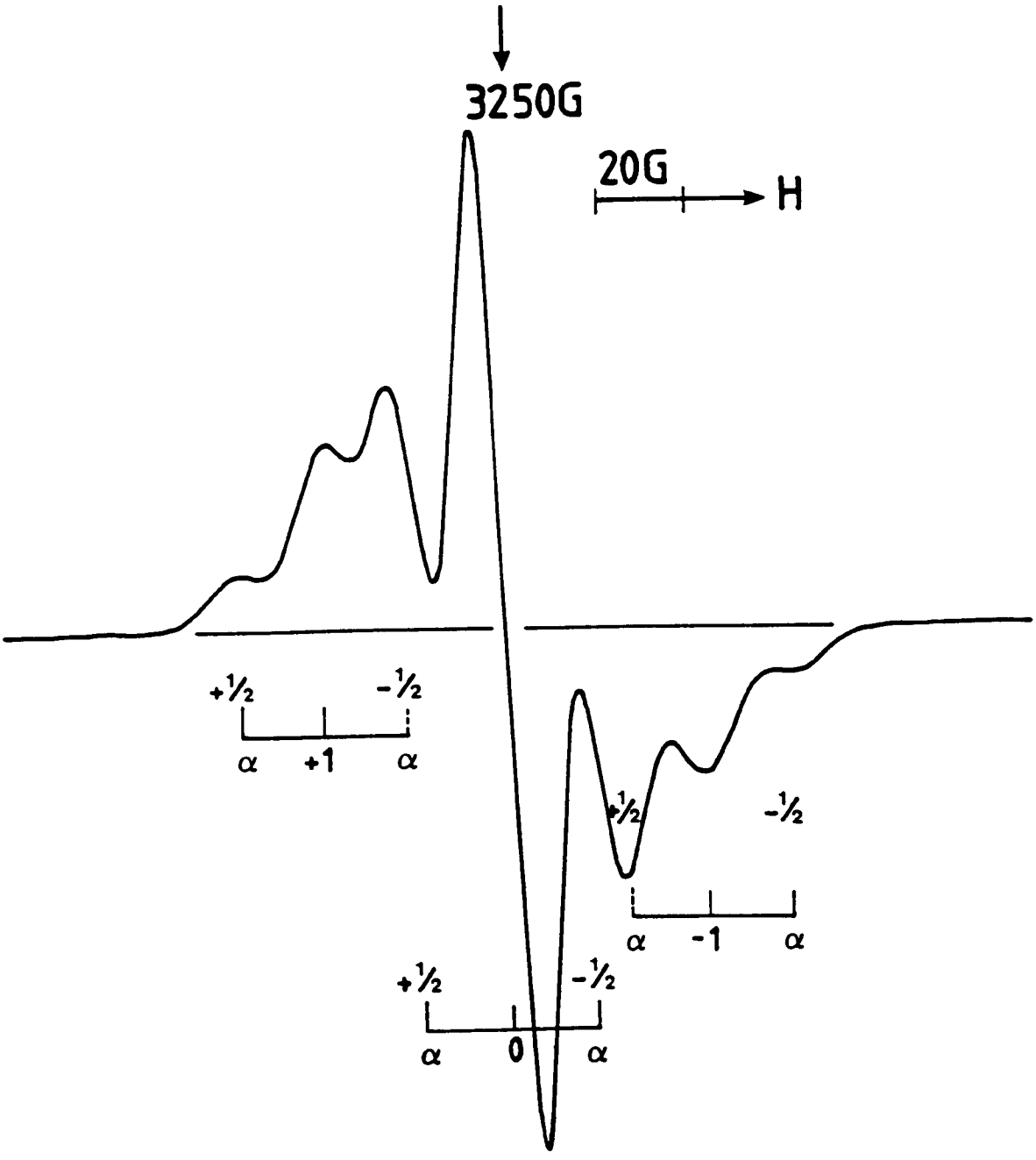

FIGURE 5.16

Computer synthesised e.s.r. spectrum for two sets of amide radicals, both having $A(^{14}N)$ = 43 G, one, comprising 60% of the total, has $A(^{1}H)$ = 0 and the other (40%) (α) has $A(^{1}H)$ = 38 G, with $g_{\parallel}$ = 2.002 and $g_{\perp}$ = 2.004. This idealized spectrum shows the weakness of the $|\pm1\rangle$ lines relative to the $|0\rangle$ lines, and it also shows how the inner parallel features of the $A(^{1}H)$ = 38 G species are hidden under the central lines, and how the presence of such species is clearly defined.

Results for oxy- and met-haemoglobin are in satisfactory agreement with the predictions (Fig. 5.14). For these proteins electrons are efficiently captured by the iron units, so that the g = 2 region of the spectra should be dominated by the electron-loss centres. The results show that the major species have a large ^{14}N parallel splitting (*ca.* 43 G) with a small β-proton coupling (0±5 G) ($\Theta \approx 90°$) for one and *ca.* ~38 G ($\Theta \approx 30°$) for another. The latter accords well with expectation since much of the protein is α-helical. A central ($M_I = 0$) doublet with $A(^1H)$ *ca.* ~38 G can also be seen. The intense lines corresponding to $\Theta \approx 90°$ are close to the limit allowed by the Ramachandran plots. Definite turning points are expected at the limits.

It seems that electron-loss from the peptide backbone dominates. However, additional unresolved central e.s.r. features suggest the presence of delocalized organic radicals such as $(Tyr)^{\cdot+}$ or $(Trp)^{\cdot+}$.

Similar results were noted for histones irradiated in the presence of $K_3Fe(CN)_6$ (Fig. 5.17). These proteins contain α-helical regions and gave clear parallel features from ^{14}N splittings [$A(^{14}N)_{\parallel} = 43$ G] with $A(^1H)$ ~39 G, ($\Theta \approx 28°$) for amide radicals formed in the α-helical regions (features A_4 and B_3 representing the $\alpha|+1,+^1/_2>$ and $\alpha|-1,-^1/_2>$ lines respectively). Other features corresponding to specific ^1H splittings were also found, which could be assigned to radicals in less highly organized regions of the protein, i.e. for features A_3/A_1 and B_2 (corresponding to $\beta|+1,+^1/_2,-^1/_2>$ and $\beta|-1,-^1/_2>$ lines respectively) $A(^1H)$ values of *ca.* ~23 G were noted corresponding to $\Theta \approx 47°$. The intense features of [$A(^{14}N)_{\parallel} = 43$ G] and $A(^1H)$ ~0, i.e. features A_2 and B_1, ($M_I \pm 1$) again correspond to upper limits for α-helices where definite turning points are expected.

It seems that these centres are trapped rapidly, before significant 'hole' migration can occur. For example, when deoxyhaemoglobin was irradiated [with $Fe(CN)_6^{3-}$ to scavenge the electrons], (F. A. Taiwo, unpublished results) there was no appearance of signals at g = 6, characteristic of Fe(III) haeme centres. Thus none of the electron-loss centres were able to migrate to iron. However with the met Fe(III) form, the majority of the ejected electrons were able to reach the iron prior to trapping out within the protein. Similarly, whilst

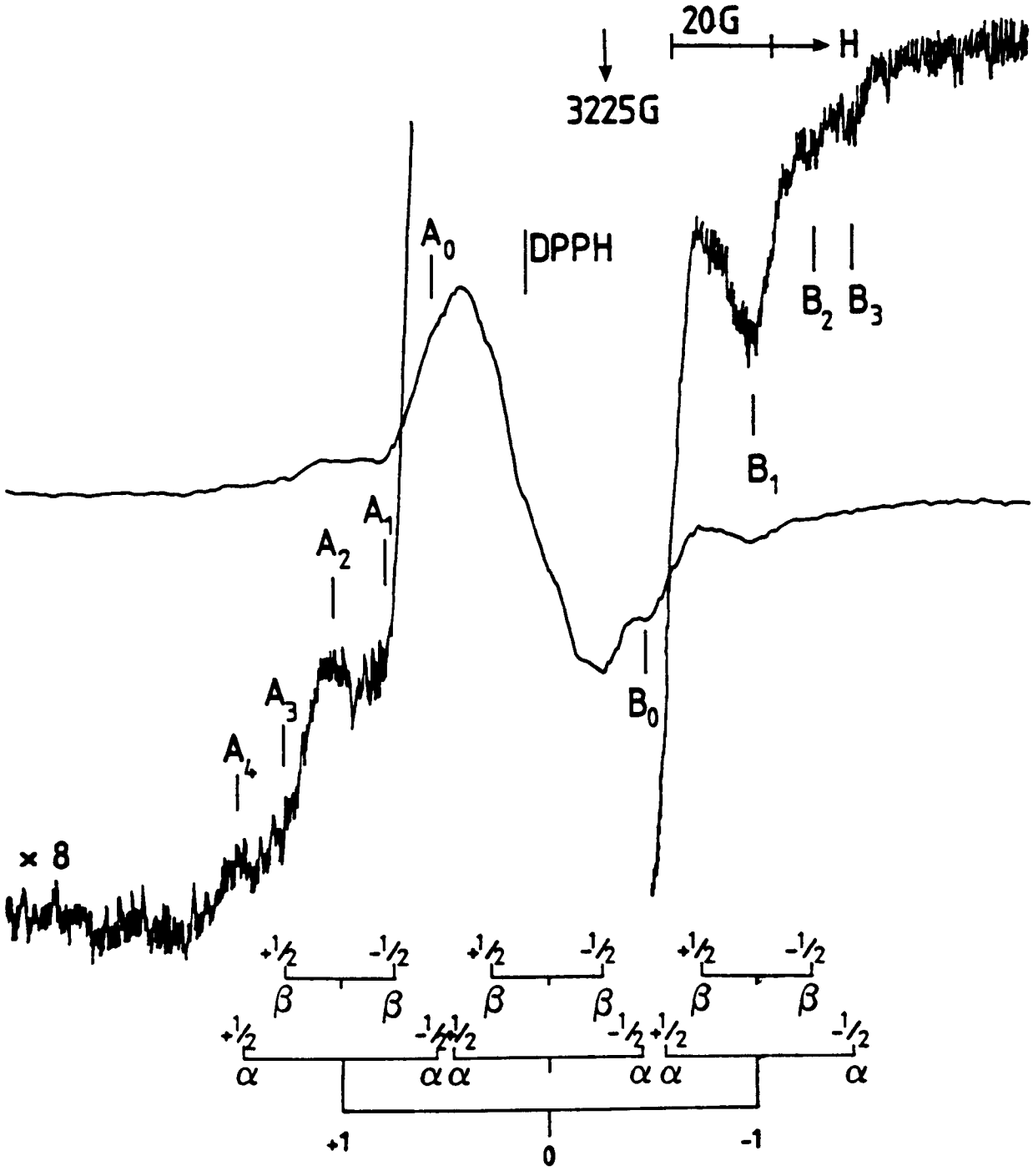

FIGURE 5.17

First derivative spectrum for histone protein (85 mg + 1 ml H_2O, $-O_2$), in the presence of $K_3Fe(CN)_6$ (5 mM), after exposure and annealing to 130 K, showing clear features assigned to electron-loss centres. One species (denoted by features A_2 and B_1) [$M_I(^{14}N)$ = +1, 0, -1] has $A_{\parallel}$ = 43 G, $A_{\perp}$ ~ 0, and no resolved proton splitting. A second species (α) (denoted by features A_4, A_0 and B_3) has similar ^{14}N parameters with $A(^1H)$ ~39 G. A third species (β) (denoted by features A_3, A_1 and B_2) has again similar ^{14}N parameters but with a $A(^1H)$ ~23 G. The other features indicated by the stick diagram are less well defined but can be seen to contribute to the fine structure noted for the central portion of the spectrum.

$RS\dot{S}R^{-}$ are major centres in proteins containing disulphide bridges, $RS\dot{S}R^{+}$ centres are not detected.

These observations are in agreement with the above irradiated DNA-histone studies. That is, the electrons are mobile and can migrate to the sites of higher electron affinity (which in the case of a DNA-histone complex is the thymine bases), whilst the protein electron-loss centres are not mobile because they are centred on simple amide units of the backbone and are trapped there by loss of the N-H proton.

Of the histone proteins, it can be speculated that the prime contenders for the source of the transferable electrons are histones H3 and H4, for it is these two proteins, present as two pairs in a tetramer, that are intimate and essential for nucleosome formation (Felsenfeld, 1978; Camerini-Otero and Felsenfeld, 1977; Oudet *et al.*, 1978; Jorcano and Ruiz-Carrilo, 1979) and are also amongst the histones that are specifically involved in DNA-protein cross links (Mee and Adelstein, 1981). However there is indirect evidence to suggest an inter-H3 disulphide bridge being present in the $(H3)_2.(H4)_2$ nucleosome tetramer (Garrard *et al.*, 1977). Such a moiety as an electron affinic R-S-S-R bridge (see Chapter Four) could act competitively with the protein to DNA electron transfer and may account for the transfers having efficiencies of less than 100% (Table 5.III) whilst the scavenging of electrons from isolated histones by $K_3Fe(CN)_6$ was noted to be complete.

CONCLUSIONS

(i) It is concluded that histones actually sensitize DNA to ionizing radiation, since $T^{\cdot -}$ ($\dot{T}H$) radicals can lead to strand breaks (Boon *et al.*, 1984, 1985; Cullis and Symons, 1986) as well as other forms of damage such as TH_2 units (J. Cadet personal communication; Furlong *et al.*, 1986). This represents an overall sensitization which is most likely to occur also on room temperature irradiation and suggests that nuclear DNA is more sensitive to ionizing radiation than isolated purified DNA.

(ii) Also it is concluded that the protein damage noted within directly irradiated DNA-histone complexes will arise predominately from initial positive electron-loss centres which are amide cations, readily trapped by loss of the NH proton.

(iii) The results provide an explanation for the reported increase in DNA single strand breaks due to the presence of complexed histone (Luckle-Huhle *et al.*, 1970) as a consequence of their enhancing the DNA anionic damage.

APPENDIX A

Electron Spin Resonance

APPENDIX A

Electron Spin Resonance

The following discussion is not concerned with the rigorous mathematical theory of electron spin resonance which can be found, explained in detail, in Ayscough (1967), Hecht (1967), Wertz and Bolton (1986) and Ingram (1958). A more general treatment of electron spin resonance and its applications may be found in Symons (1978).

Of the spectroscopic techniques, electron spin resonance (e.s.r.), sometimes known as electron paramagnetic resonance (e.p.r.), is a particularly informative means of studying radiation induced free radicals. E.s.r. takes advantage of the fact that electrons have an intrinsic magnetic moment quantized into one of two states. In diamagnetic materials all electrons are paired, that is for each electron there is a partner in the other state. However, in paramagnetic materials, there are one or more unpaired electrons. In the absence of an applied magnetic field the two states (referred to as spin states α and β) are doubly degenerate (they are equal in energy, and therefore a transition between states requires no energy).† In an applied magnetic field the degeneracy is lifted, and the energy levels (electron Zeeman levels) are obtained using the spin Hamiltonian,

$$H = \beta H.g.S \qquad [A1]$$

which symbolizes the interaction between the applied magnetic field H and the spin magnetic moment of the electron, where β is the Böhr magneton (the intrinsic magnetic moment of a free electron), S is the quantum mechanical spin operator and g is a tensor which rotates H into S (g.H is often referred to as the effective field H_e). S can take up values of $\pm^1/_2$, and therefore, the energy level separation in an applied magnetic field (Zeeman splitting) is,

$$\Delta E = g_e \beta H \qquad [A2]$$

† There may be various magnetic interactions in the molecule (such as the dipolar interaction between spins or spin orbit coupling) that create local magnetic fields. The local fields can remove the degeneracy and cause a splitting of the electron-spin energy levels even in the absence of applied magnetic field. These local fields are termed zero fields, and the resulting splitting is called zero field splitting (z.f.s.).

where g_e is isotropic (independent of orientation) in the case where the spin system is tumbling fast enough for the anisotropic terms in g_e to average out. The fundamental characteristic which must be pointed out here is that the separation between the Zeeman levels increases linearly with the magnetic field as is shown in Figure A.1.

Since the energy levels are populated according to Boltzman statistics, there is a temperature dependent population difference of the spin states equal to,

$$\frac{N\alpha}{N\beta} = e^{-\Delta E/kT} \qquad [A3]$$

$$= e^{-g\beta H/kT} \qquad [A4]$$

and therefore at resonance,

$$h\nu = g\beta H \qquad [A5]$$

there can be a net absorption of energy dependent on the intensity of the exciting radiation field ($h\nu$). This continues until saturation (equalization of spin state populations) is reached. Equation [A5] also helps one to understand the meaning of g-value which is defined as,

$$g = \frac{h\nu}{\beta H} \qquad [A6]$$

and gives a fingerprint of the magnetic environment of the unpaired electron. The g-value is used to characterize the position of the resonance and it is a measure of the local magnetic field experienced by the electron.

If only the electron Zeeman interaction was observed, then all e.s.r. spectra would consist of a single absorption peak. The intensity of the absorption would be directly related to the concentration of the unpaired spins and the only structural information contained in the spectrum would relate to the orbital electronic environment of the electron as reflected by the g-value. If the only source of magnetism arose from a free electron spin, $g_e = 2.0023$. When the electron is in an orbital far removed from other levels, g will approximate to the "free-spin" value (g_e). Any shifts occurring in the g-value from free-spin are often small and are due to the presence of orbital

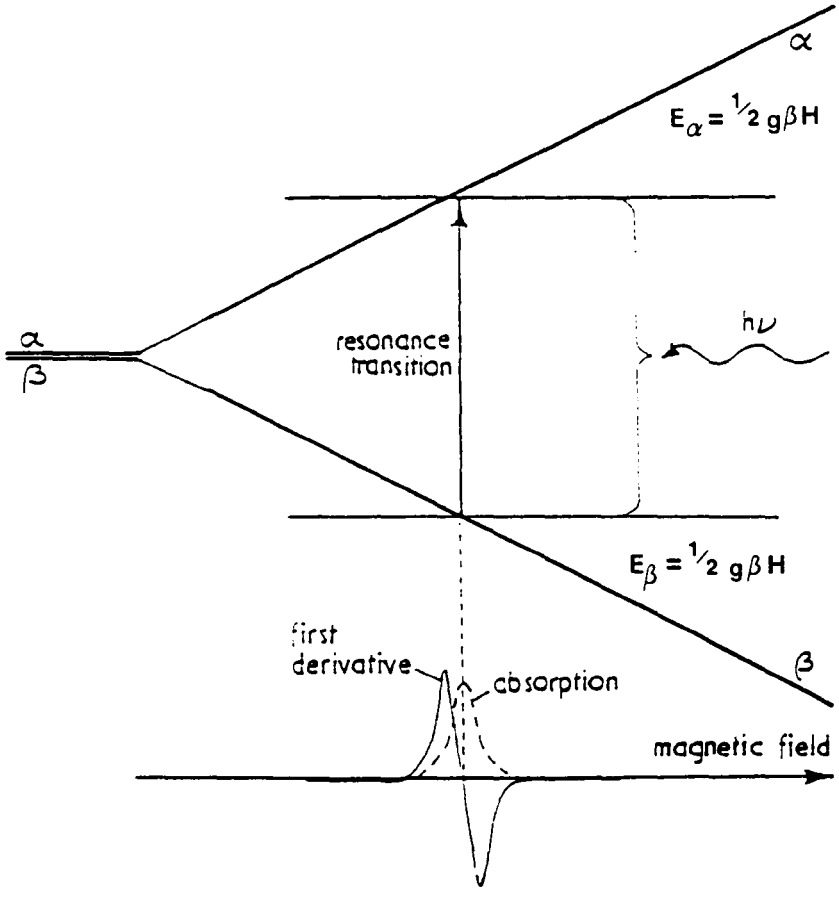

FIGURE A.1

The electron spin resonance transition, and the resulting spectrum.

magnetism (induced by the applied magnetic field in most cases) which adds to or subtracts from the spin magnetism giving rise to a negative or positive shift. Shifts in g-value above the free spin value indicate an admixture of the lone electron orbital with a filled orbital of lower energy. Shifts to lower g-values indicate admixture with an unoccupied orbital of higher energy. For organic free radicals, spin delocalization onto heteroatoms often leads to small g-shifts.

The g-value need not be isotropic and in general it is anisotropic and has three principal values along three orthogonal axes (given symbols g_x, g_y and g_z or g_{xx}, g_{yy} and g_{zz}). When the values along the x and y axes are equal the g-tensor is axial and the values $g_{\parallel}$ and $g_{\perp}$ are obtained from the spectrum.

Fortunately, in addition to just the g-value, further information detailing the unpaired electron environment appears in e.s.r. spectra as a consequence of the electron's magnetic moment interacting with the intrinsic magnetic moment of surrounding nuclei, giving rise to a second term in the spin Hamiltonian, called the hyperfine term [A7],

$$hS.A.I \qquad [A7]$$

where h is Planck's constant, I is the nuclear magnetic moment and A is the hyperfine tensor, which describes the interaction of nuclear and electron magnetic moments. Although this term is generally much weaker (10^{-2}) than the Zeeman term, it is of great importance. To a first approximation, the single absorption peak due to the Zeeman interaction is split into (2I+1) peaks by the hyperfine interaction (or for n equivalent nuclei into (2nI+1) lines) as depicted in Figure A.2. Thus, by inspection, one can usually identify the spin quantum number of the nucleus giving rise to the hyperfine splitting, and the number of nuclei present. As with g, the hyperfine tensor consists of an isotropic and anisotropic component as shown in equation [A8],

$$A = A_0 1 + T \qquad [A8]$$

where A_0 is the isotropic component, 1 is the unit tensor, and T is the anisotropic component.

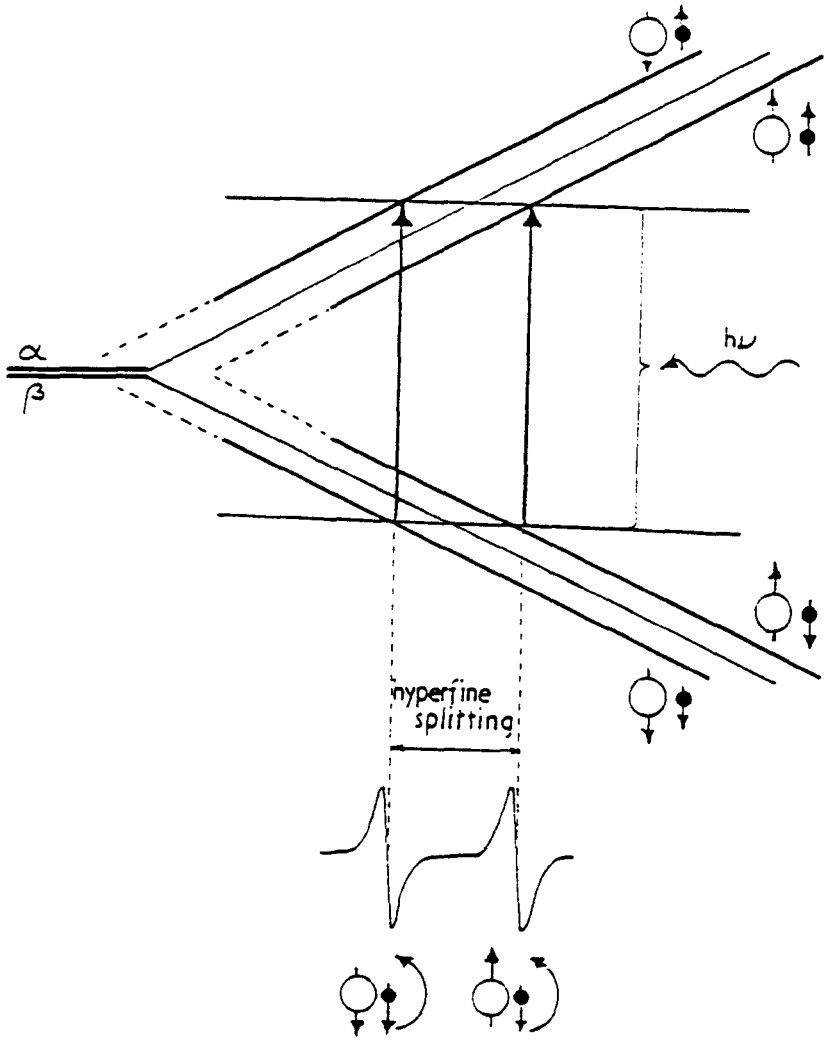

FIGURE A.2

The source of hyperfine splitting in a radical containing one spin ½ nucleus (denoted by the larger circle).

The isotropic component (easily measured in systems where rapid tumbling of the free radicals averages out the anisotropic components) is a measure of the "contact interaction" because it is due to the finite density of the unpaired electron at the nucleus (Fermi contact), and is characteristic of the s-orbital character of the electron. The anisotropic component of A provides information about the p-electron character of the orbital containing the unpaired electron and arises from the dipole-dipole interaction between the electron and nuclear spins, and is therefore orientation dependent. As with the g-tensor the A-tensor is characterized by three principal values: A_{xx}, A_{yy} and A_{zz}. In the case of axial symmetry, $A_{\parallel} = A_{zz}$ and $A_{\perp} = A_{xx} = A_{yy}$. For p-orbitals the direction of minimum T corresponds to a situation where the field is perpendicular to the axis of the orbital and due to its dispersion is reversed and takes a value of -B. When the field is parallel to the axis of the orbital the field at the electron takes a value of 2B. The values for $A_{\parallel}$ and $A_{\perp}$ are given in equations [A9] and [A10].

$$A_{\parallel} = A_{iso} + 2B \qquad [A9]$$

$$A_{\perp} = A_{iso} - B \qquad [A10]$$

A third term in the spin Hamiltonian is the nuclear Zeeman term. It arises from the interaction between the external magnetic field and the nuclear magnetic moment (I),

$$g_n \beta_n H.I \qquad [A11]$$

where β_n and g_n are the nuclear counterparts to the electron constants. In a typical e.s.r. experiment the change in nuclear spin quantum number (ΔM_I) is zero and to a first approximation this term can be ignored. In electron nuclear double resonance (ENDOR), however, a ΔM_I=1 transition is brought about by applying a strong radio frequency (n.m.r.) field that satisfies the nuclear resonance condition. This transition restores some of the population difference eliminated by saturation and causes an increase in the e.s.r. absorption. Two additional terms in the spin Hamiltonian describe organic free radicals. They are the quadrupole term, equation [A12],

$$hI.Q.I \qquad [A12]$$

where Q is the quadrupole coupling tensor, and the spin-spin term, equation [A13],

$$S.D.S. \qquad [A13]$$

where D is a tensor similar to T (equation [A8]).

The nuclear electric quadrupole term is important when a nucleus with an appreciable quadrupole moment interacts with the gradient of the electric field of the surrounding electrons. If this distribution is cubic, the electric field gradient is zero. However, if there is a polarized bond between two atoms, this gradient is non-zero and the quadrupole coupling is a measure of the electron polarization of the bond. The spin-spin term, sometimes called the fine structure term, describes the dipole-dipole interaction between the spins of a system with $S > {}^1/_2$ (triplet state). In such systems the effects of the ligand interaction and the spin-orbit coupling may produce a ground state in which the levels are not degenerate in zero magnetic field. When such z.f.s's are present, the levels will no longer be equally spaced in an external magnetic field, so that the various magnetic transition no longer coincide and a series of lines are observed.

The full spin Hamiltonian is given in equation [A14],

$$H_{e.s.r.} = \beta H.g.S + hS.A.I - g_n\beta_n H.I + hI.Q.I + S.D.S \qquad [A14]$$

where g, A, g_n, Q and D are tensors that couple the indicated vectors H, S and I. Depending on the system under study all or part of this Hamiltonian is used, and in many cases certain terms may be ignored.

Use of E.s.r. on Biological Systems

The above discussion indicates that e.s.r. detects only paramagnetic species. Therefore, in a typical biological system, e.s.r. provides the necessary selectivity to differentiate between the bulk material and the species of interest. The sensitivity of modern e.s.r. instruments is sufficient to detect about 10^{-9}M. While these advantages are impressive there are several features inherent in the technique which tends to limit its usefulness. One drawback is the inability of e.s.r. to identify the diamagnetic end product of a free radical reaction. This often deprives an investigator of vital information regarding free

radical reaction pathways. A second disadvantage follows from difficulty in interpreting the e.s.r. spectrum. Often information regarding the structure of the paramagnetic species under study is masked by spectral complexity or lack of resolution and even with current techniques the data is difficult to extract. A third difficulty with the technique follows from sample preparation. The more informative e.s.r. studies come from orientated systems, where one can usually distinguish between several free radical species, estimate their relative magnitudes and determine their structure. Often, however, single crystals of interesting samples are difficult, if not impossible, to obtain. In this case the study must be conducted on a disordered system, where data is generally more difficult to extract.

However one advantage using a disordered "powdered" system, either glassy or polycrystalline, is that it is a much more convenient method both in terms of sample preparation and in mode of study. Analysis of powder spectra is discussed by Atkins and Symons (1967) and Kneubuhl (1960).

If more than one paramagnetic species is present the spectrum often cannot be assigned unambiguously due to its complexity. In these circumstances various parameters can be adjusted such as altering the microwave power so that lines which belong to one radical can be saturated out leaving the remaining lines to be more readily interpreted. Other variables are temperature, γ-dose and use of Q- and S-band (i.e. changing the microwave frequency and applied magnetic field), thus enabling the features arising from each radical to be recognized and interpreted.

Finally computer assisted analysis of temperature dependent e.s.r. spectra, including their reconstruction *via* addition of previously isolated single-component patterns, as outlined by Gregoli *et al.* (1976, 1977a,b, 1979, 1982) can reveal the relative and absolute abundance of each radical species in a powder sample containing a number of radicals.

APPENDIX B

Mechanism of Strand Breakage: A Computer Graphics Study

APPENDIX B

Mechanism of Strand Break Formation: A Computer Graphics Study

The work described in this thesis comprises a study of the effects of ionizing radiation on DNA under direct (frozen aqueous) conditions, where the initial ionic species formed, at 77 K, from ionizations within the DNA phase, are $G^{\cdot+}$ and $T^{\cdot-}$ (Boon *et al.*, 1984; Gregoli *et al.*, 1982; Hüttermann *et al.*, 1984). On warming, in the absence of oxygen, these ionic centres yield the neutral radicals GṄ and ṪH by deprotonation and protonation respectively (Lenherr and Ormerod, 1968; Hüttermann and Voit, 1986). It has been proposed that a significant number of these neutral centres can give rise to strand breaks by intramolecular hydrogen atom abstraction from appropriately positioned deoxyribose moieties (Cullis and Symons, 1986) and that the sugar radicals thus formed react *via* mechanisms analogous to those described for the hydroxyl radical initiated strand breakage reaction (von Sonntag *et al.*, 1981).

On the assumption that hydrogen atom abstraction would be most favourable from the nearest ribosyl-hydrogens, the B-DNA structure has been inspected using molecular graphics (Chem-X, Chemical Designs Ltd.) to determine the proximity of these sites. Figures B.1 and B.2 show computer graphic images of a section of B-DNA about the radical centres of ṪH and GṄ respectively, and in each case depict the five closest ribosyl-hydrogens. Tables B.I-IV catalogue the inter-atom distances from the radical centres C5 and N3 of ṪH and GṄ respectively, to the ribosyl-hydrogens of the sugars positioned 5′ and 3′ to the radical bearing nucleotide and also to the C′-H groups of the deoxyribose directly attached to the base radical.†

For ṪH, the closest hydrogens to its 5-yl radical centre are from C_1' and C_2' of the deoxyribose 5′ to the radical bearing nucleotide and from C_1' and C_2' of the sugar directly attached (N′) to the base radical (Fig. B.1 and Tables B.I and B.II). The sixth closest ribosyl-hydrogen is on C_5' of the deoxyribose N′ to the base radical, as is the seventh, which is again from C_2'. It should however be pointed out that, on stereo-electronic grounds, the N′ ribosyl-hydrogens may not be ideal

† The ribose directly attached to the base radical is designated as the N′ deoxyribose.

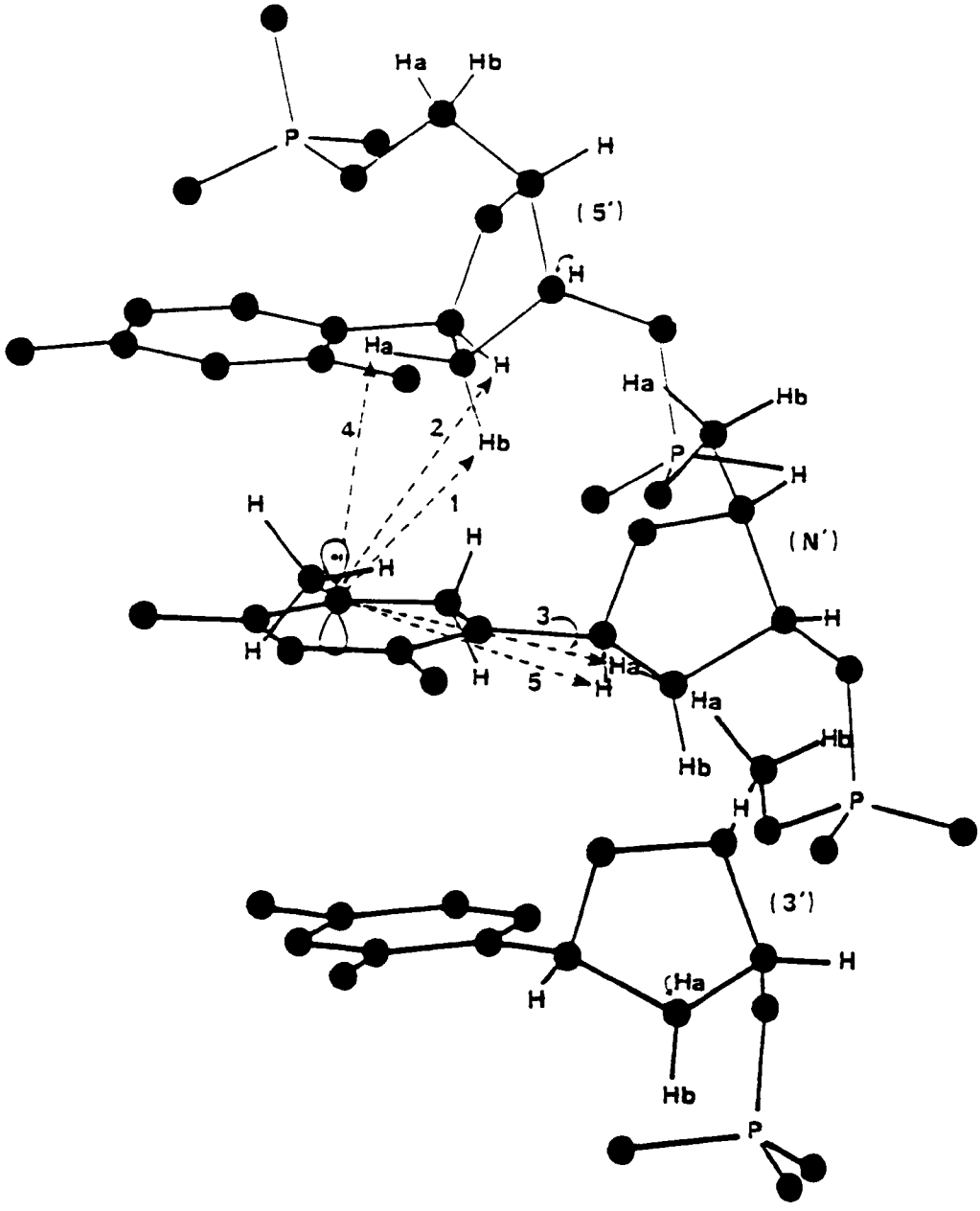

FIGURE B.1

A pyrimidine trinucleotide fragment (CTC) of B-DNA about a ṪH base radical. The distances to the nearest five hydrogen atoms that could be candidates for hydrogen atom abstraction by the base radical are indicated by arrows.

TABLE B.I

Distances, in angstroms, from the 5-thymyl (C5) radical site of TH to the C_n'-H groups of the deoxyribose sugars 5′ and 3′ to the radical bearing nucleotide, and also to the C_n'-H groups of the sugar (N′) that is directly attached to the 5-thymyl base

5′ deoxyribose	
C5 to C_1'-H	3.487 Å
" to C_2'-Ha	3.931 Å
" to C_2'-Hb	3.292 Å
" to C_3'-H	5.794 Å
" to C_4'-H	6.688 Å
" to C_5'-Ha	6.973 Å
" to C_5'-Hb	7.517 Å
N′ deoxyribose	
C5 to C_1'-H	4.400 Å
" to C_2'-Ha	3.731 Å
" to C_2'-Hb	4.779 Å
" to C_3'-H	5.810 Å
" to C_4'-H	6.045 Å
" to C_5'-Ha	4.721 Å
" to C_5'-Hb	5.823 Å
3′ deoxyribose	
C5 to C_1'-H	7.855 Å
" to C_2'-Ha	7.509 Å
" to C_2'-Hb	8.756 Å
" to C_3'-H	9.046 Å
" to C_4'-H	8.437 Å
" to C_5'-Ha	6.298 Å
" to C_5'-Hb	7.714 Å

[For C_2', Ha is assigned to the hydrogen atom above the ribosyl plane, i.e. on the same side as the base residue and the C_5' moiety, and Hb to the hydrogen below the ribosyl plane.]

[For C_5', Ha is assigned to the hydrogen atom closest to the stacked base interior of the DNA, and Hb to the hydrogen further away.]

TABLE B.II

The order of proximity of the 5′, N′ and 3′ deoxyribosyl C_n'-H groups to the 5-thymyl radical site of TH, and likely configuration about C5 of TH_2 on abstraction

1.	5′ C_2'-Hb	3.292 Å	R-config.
2.	5′ C_1'-H	3.487 Å	R-config.
3.	N′ C_2'-Ha	3.731 Å	S-config.
4.	5′ C_2'-Ha	3.931 Å	R-config.
5.	N′ C_1'-H	4.400 Å	R/S-config. [same plane]
6.	N′ C_5'-Ha	4.721 Å	R-config.
7.	N′ C_2'-Hb	4.779 Å	S-config.
8.	5′ C_3'-H	5.794 Å	R-config.
9.	N′ C_3'-H	5.810 Å	R/S-config. [same plane]
10.	N′ C_5'-Hb	5.823 Å	R-config.
11.	N′ C_4'-H	6.045 Å	R-config.
12.	3′ C_5'-Ha	6.298 Å	R/S-config. [same plane]
13.	5′ C_4'-H	6.688 Å	R-config.
14.	5′ C_5'-Ha	6.973 Å	R-config.
15.	3′ C_2'-Ha	7.509 Å	S-config.
16.	5′ C_5'-Hb	7.517 Å	R-config.
17.	3′ C_5'-Hb	7.714 Å	R/S-config. [same plane]
18.	3′ C_1'-H	7.885 Å	S-config.
19.	3′ C_4'-H	8.437 Å	S-config.
20.	3′ C_2'-Hb	8.756 Å	S-config.
21.	3′ C_3'-H	9.046 Å	S-config.

[For C_2', Ha is assigned to the hydrogen atom above the ribosyl plane, i.e. on the same side as the base residue and the C_5' moiety, and Hb to the hydrogen below the ribosyl plane.]

[For C_5', Ha is assigned to the hydrogen atom closest to the stacked base interior of the DNA, and Hb to the hydrogen further away.]

candidates for abstraction, thus making the 5′ ribosyl-hydrogens, which which are more ideally positioned, i.e. more in line with the p-orbital (and closer), the preferred target. $\dot{T}H$ mediated abstraction of these sugar bound hydrogens will result in reduced thymidine (TH_2) having mostly the R-configuration about C5. Subsequent to this prediction Furlong *et al.* (1986) have recently shown that this is indeed the case.

The sugar radicals resulting from $\dot{T}H$ mediated abstraction would therefore be predominately centred on C_1' and C_2' of the deoxyribose 5′ to the radical bearing nucleotide. The various subsequent reactions of these sugars are shown in Figure B.3.

For $G\dot{N}$ the closest hydrogens to the radical site, N3, are from C_1' and C_2' of the deoxyribose N′ to the base radical and from C_5' and C_1' of the sugar 3′ to the radical bearing nucleotide (Fig. B.2 and Tables B.III and B.IV). The sixth and seventh closest hydrogens are from C_4' and C_5' of the 3′ deoxyribose. With $G^{\cdot+}$ decaying *via* loss of a proton, $G\dot{N}$ mediated hydrogen atom abstraction should result in the quasi-repair of the guanine base (a further tautomerisation being required to fully restore the guanine moiety).

Again from stereoelectronic considerations the 3′ ribosyl hydrogens (particularly that of 3′C_1'-H) are more ideally placed for abstraction than those of N′. However the N′ hydrogens are much closer (especially N′C_1'-H at 2.671 Å) and it is unclear as to which of these factors will prevail in dictating the likely site of abstraction. Hence it is tentatively concluded that the sugar radicals resulting from $G\dot{N}$ mediated abstraction will consist of mostly C_1' and possibly C_5' centred species on the sugar 3′ to the $G\dot{N}$ bearing nucleotide and possibly C_1' and C_2' centred species on the deoxyribose N′ to the base radical. Though it must be stressed that these latter hydrogens including those on 3′C_5' are almost in the node of the p-orbital and hence may be quite unsuitable for abstraction. Subsequent reactions of these sugar radicals are also shown in Figure B.3.

In the presence of oxygen, $\dot{T}H$ and probably $G\dot{N}$ convert to peroxyl base radicals ($RO_2^{\cdot}$) on warming. For the peroxyl radical $THO_2^{\cdot}$, the radical centre on the terminal oxygen can describe an arc some 2.3-2.5 Å from

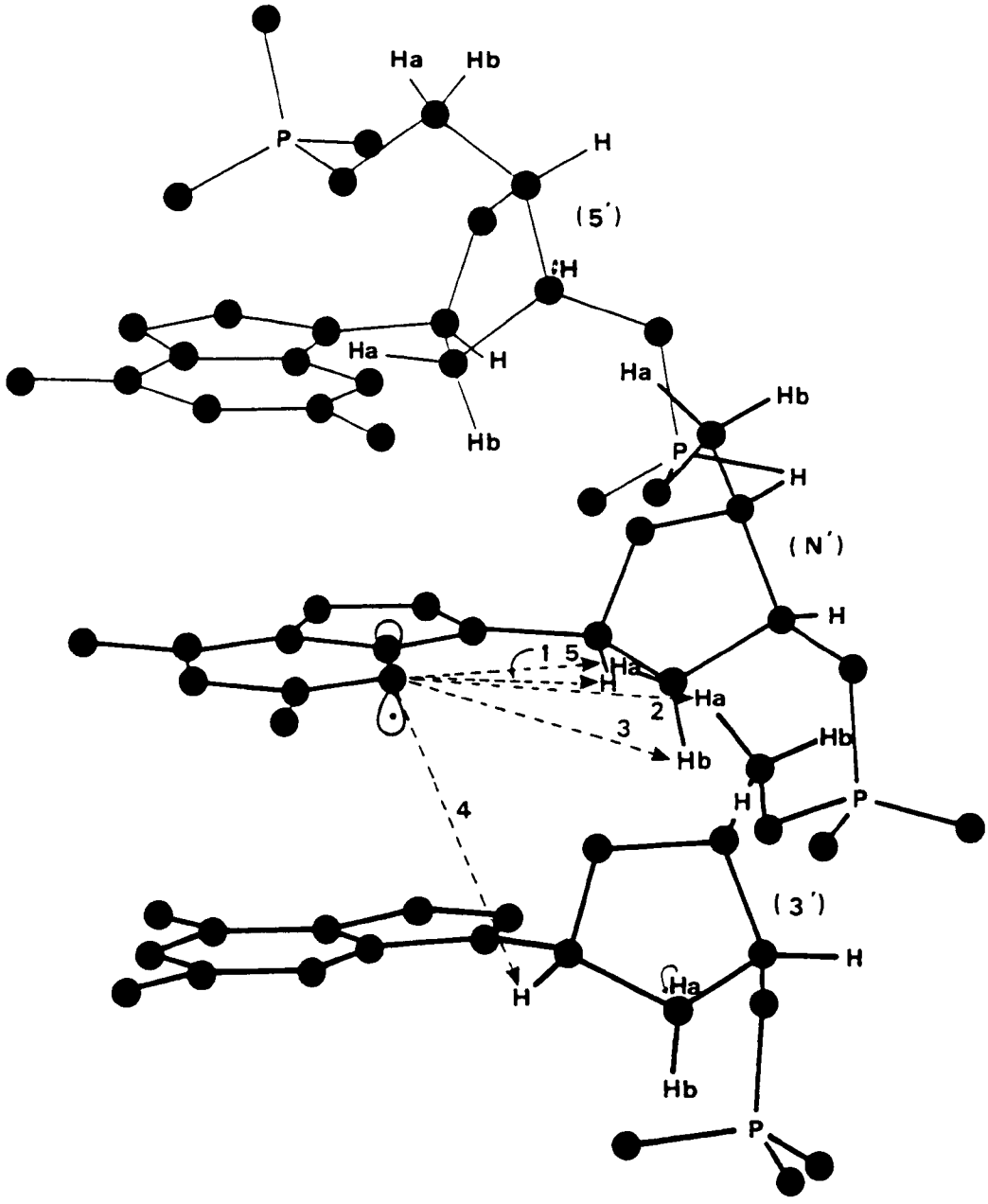

FIGURE B.2

A purine trinucleotide fragment (GGG) of B-DNA about a GṄ base radical. The distances to the nearest five hydrogen atoms that may be candidates for hydrogen atom abstraction by the base radical are indicated by arrows.

TABLE B.III

Distances, in angstroms, from the N3 radical site of GṄ to the C_n'-H groups of the deoxyribose sugars 5′ and 3′ to the radical bearing nucleotide, and also to the C_n'-H groups of the sugar (N′) that is directly attached to the guanine base radical

5′ deoxyribose	
N3 to C_1'-H	5.441 Å
" to C_2'-Ha	7.357 Å
" to C_2'-Hb	6.490 Å
" to C_3'-H	8.904 Å
" to C_4'-H	8.895 Å
" to C_5'-Ha	9.430 Å
" to C_5'-Hb	10.292 Å
N′ deoxyribose	
N3 to C_1'-H	2.671 Å
" to C_2'-Ha	4.755 Å
" to C_2'-Hb	4.518 Å
" to C_3'-H	6.247 Å
" to C_4'-H	5.630 Å
" to C_5'-Ha	5.713 Å
" to C_5'-Hb	6.827 Å
3′ deoxyribose	
N3 to C_1'-H	4.668 Å
" to C_2'-Ha	5.343 Å
" to C_2'-Hb	6.166 Å
" to C_3'-H	6.454 Å
" to C_4'-H	5.138 Å
" to C_5'-Ha	3.713 Å
" to C_5'-Hb	5.315 Å

[For C_2', Ha is assigned to the hydrogen atom above the ribosyl plane, i.e. on the same side as the base residue and the C_5' moiety, and Hb to the hydrogen below the ribosyl plane.]

[For C_5', Ha is assigned to the hydrogen atom closest to the stacked base interior of the DNA, and Hb to the hydrogen further away.]

TABLE B.IV

The order of proximity of the 5′, N′ and 3′ deoxyribosyl C_n'-H groups to the N3 radical centre of GN

1.	N′ C_1'-H	2.671 Å
2.	3′ C_5'-Ha	3.713 Å
3.	N′ C_2'-Hb	4.518 Å
4.	3′ C_1'-H	4.668 Å
5.	N′ C_2'-Ha	4.755 Å
6.	3′ C_4'-H	5.138 Å
7.	3′ C_5'-Hb	5.315 Å
8.	3′ C_2'-Ha	5.343 Å
9.	5′ C_1'-H	5.441 Å
10.	N′ C_4'-H	5.630 Å
11.	N′ C_5'-Ha	5.713 Å
12.	3′ C_2'-Hb	6.166 Å
13.	N′ C_3'-H	6.247 Å
14.	3′ C_3'-H	6.454 Å
15.	5′ C_2'-Hb	6.490 Å
16.	N′ C_5'-Hb	6.827 Å
17.	5′ C_2'-Ha	7.357 Å
18.	5′ C_4'-H	8.895 Å
19.	5′ C_3'-H	8.904 Å
20.	5′ C_5'-Ha	9.430 Å
21.	5′ C_5'-Hb	10.292 Å

[For C_2', Ha is assigned to the hydrogen atom above the ribosyl plane, i.e. on the same side as the base residue and the C_5' moiety, and Hb to the hydrogen below the ribosyl plane.]

[For C_5', Ha is assigned to the hydrogen atom closest to the stacked base interior of the DNA, and Hb to the hydrogen further away.]

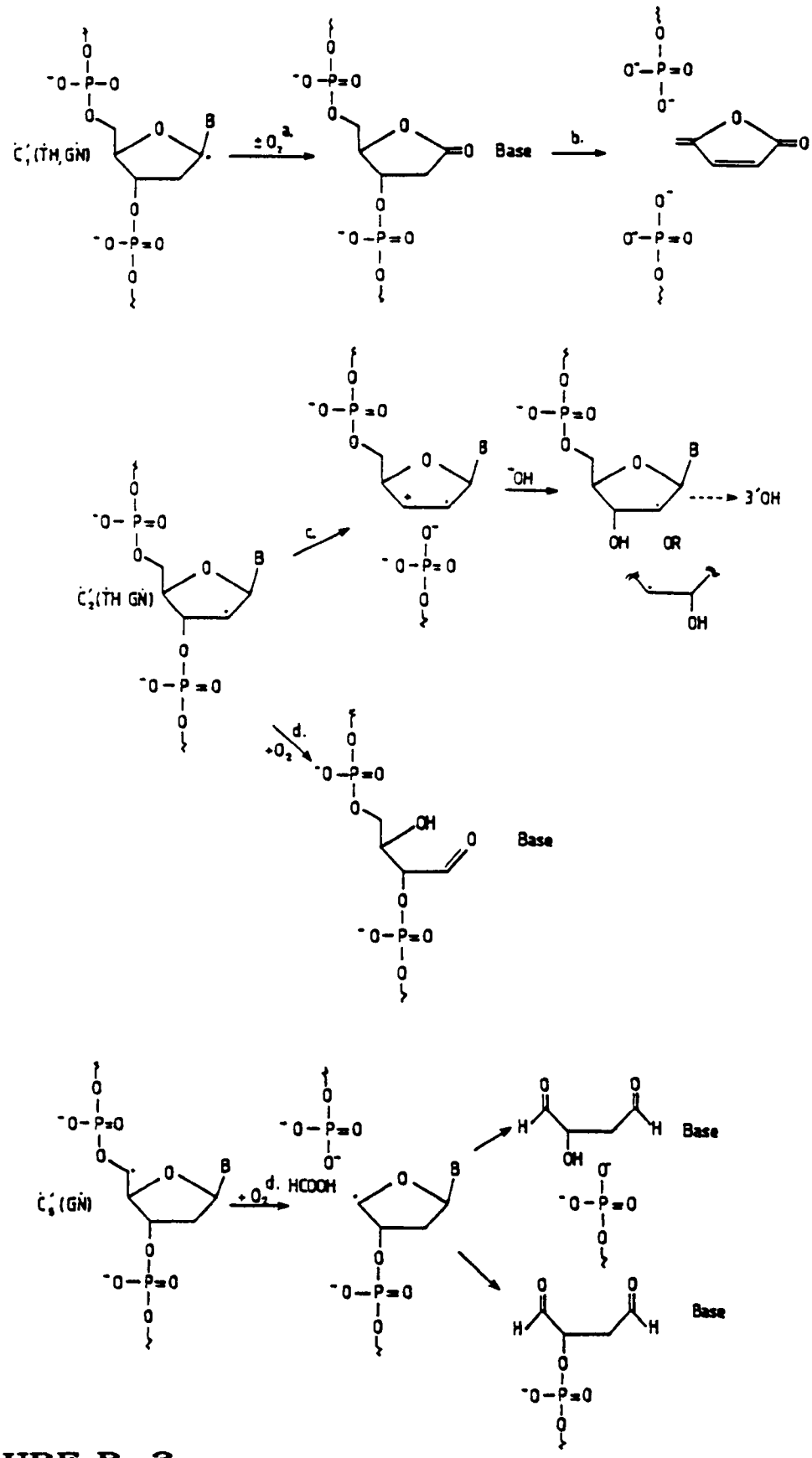

FIGURE B.3

Reactions of C_1', C_2' and C_5' centred deoxyribose radicals.

a. C. von Sonntag, Int. J. Radiat. Biol., (1984), 46, 507.

b. adapted from T. E. Goyne and D. S. Sigman, J. Am. Chem. Soc., (1987), 109, 2846.

c. $-O-PO_3^{2-}$ β-elimination cf. C_4' degradation.

d. C. von Sonntag, U. Hagen, A. Schön-Bopp and D. Schulte-Frohlinde, Adv. Radiat. Biol., (1981), 9, 109.

( ) denotes likely base radical precursor.

its original position either above or below the base plane, depending on the direction from which the oxygen adds to the C5 centred radical (Fig. B.4). Addition of oxygen from above the base plane (5′→3′), yielding the C5 S-conformer of $THO_2^{\cdot}$, generally results in the radical site being *ca.* 2.1-2.4 Å closer to the abstractable hydrogens of the deoxyribose 5′ to the radical bearing nucleotide (Fig. B.5). But as with the parent radical it is still the hydrogens on C_1' and C_2' that are the closest.

However, if, as is proposed for H$^{\cdot}$ donation from thiols (Chapter Four), oxygen preferentially adds to $\dot{T}H$ from below the base plane (3′→5′), i.e. from the less hindered major groove, the peroxyl radical centre of the R-$THO_2^{\cdot}$ formed will project into the major groove and will not result in any significant reduction of the abstraction distances involving N′ and 5′ located ribosyl-hydrogens (Fig. B.5). There is some lessening of the abstraction distances involving 3′ located hydrogens, however these are still too far away to be of any consequence.

For $G\dot{N}$ it is unlikely that oxygen addition direct to the N3 radical centre will occur and addition to C5, resulting in a carbon based peroxyl radical, is more reasonable (Fig. B.6). This will, like $THO_2^{\cdot}$, result in the radical centre being able to describe an arc some 2.3-2.5 Å from its "parent" position (when on C5) either above or below the base plane, depending on the direction of O_2 addition (Fig. B.6). The approach of oxygen from above the base plane (5′→3′), giving the C5 S-conformer of $GN(O_2^{\cdot})$, results in the radical centre being some 3.15-3.65 Å closer to the 5′ located ribosyl-hydrogens whilst the inter-atom abstraction distances to the 3′ deoxyribose hydrogens are generally increased to an equivalent extent (Fig. B.7). Similar, though less dramatic, trends are noted for the R-conformer of $GN(O_2^{\cdot})$ (Fig. B.7), which results from oxygen addition from below the base plane (3′→5′), i.e. from the less hindered major groove. Overall for both R- and S-$GN(O_2^{\cdot})$ there is no significant reduction in any abstraction distance to a value below 2.671 Å (i.e. the lowest value, noted with N′C_1'-H, for $G\dot{N}$, see Table B.IV), even though sweeping changes of over 3 Å occur for individual centres. However on stereoelectronic grounds there is some improvement, with peroxyl radical formation allowing those hydrogens that are in ideal positions, though too far away, to now be accessible. As with the parent $G\dot{N}$ radical the closest hydrogens, for both R- and

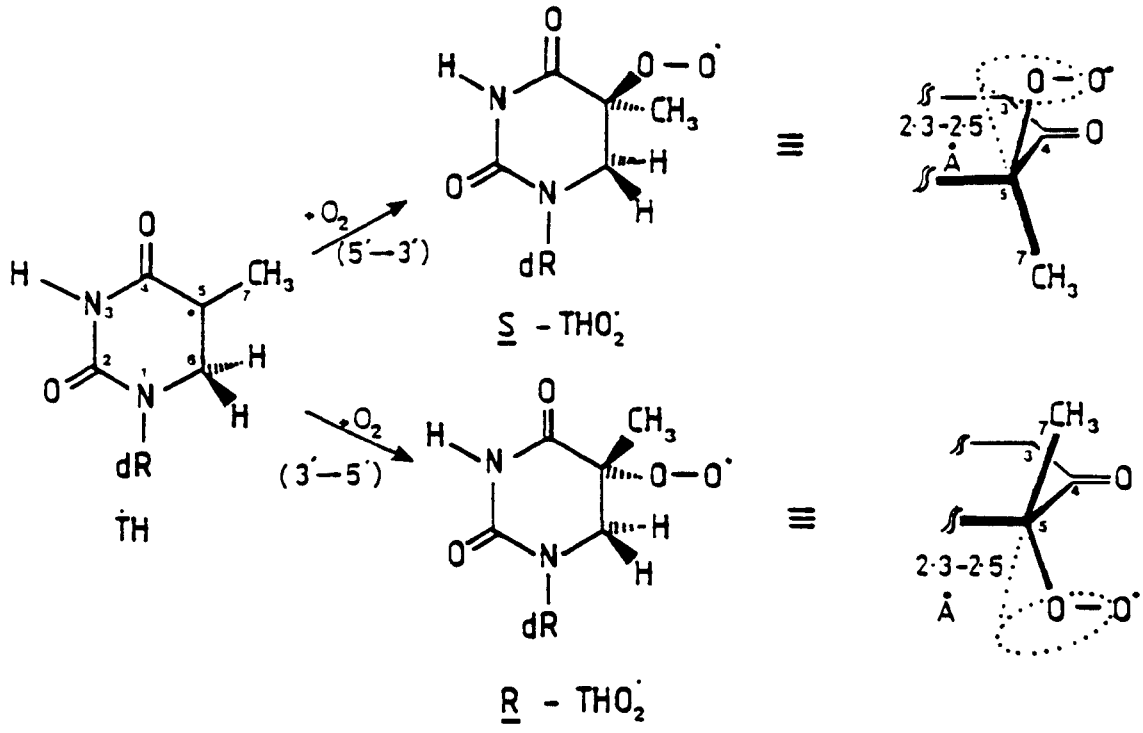

FIGURE B.4

Formation of the S- and R-conformers of $THO_2^{\cdot}$ *via* O_2 addition (5′ → 3′ and 3′ → 5′ respectively) to the C5 radical centre of $\dot{T}H$.

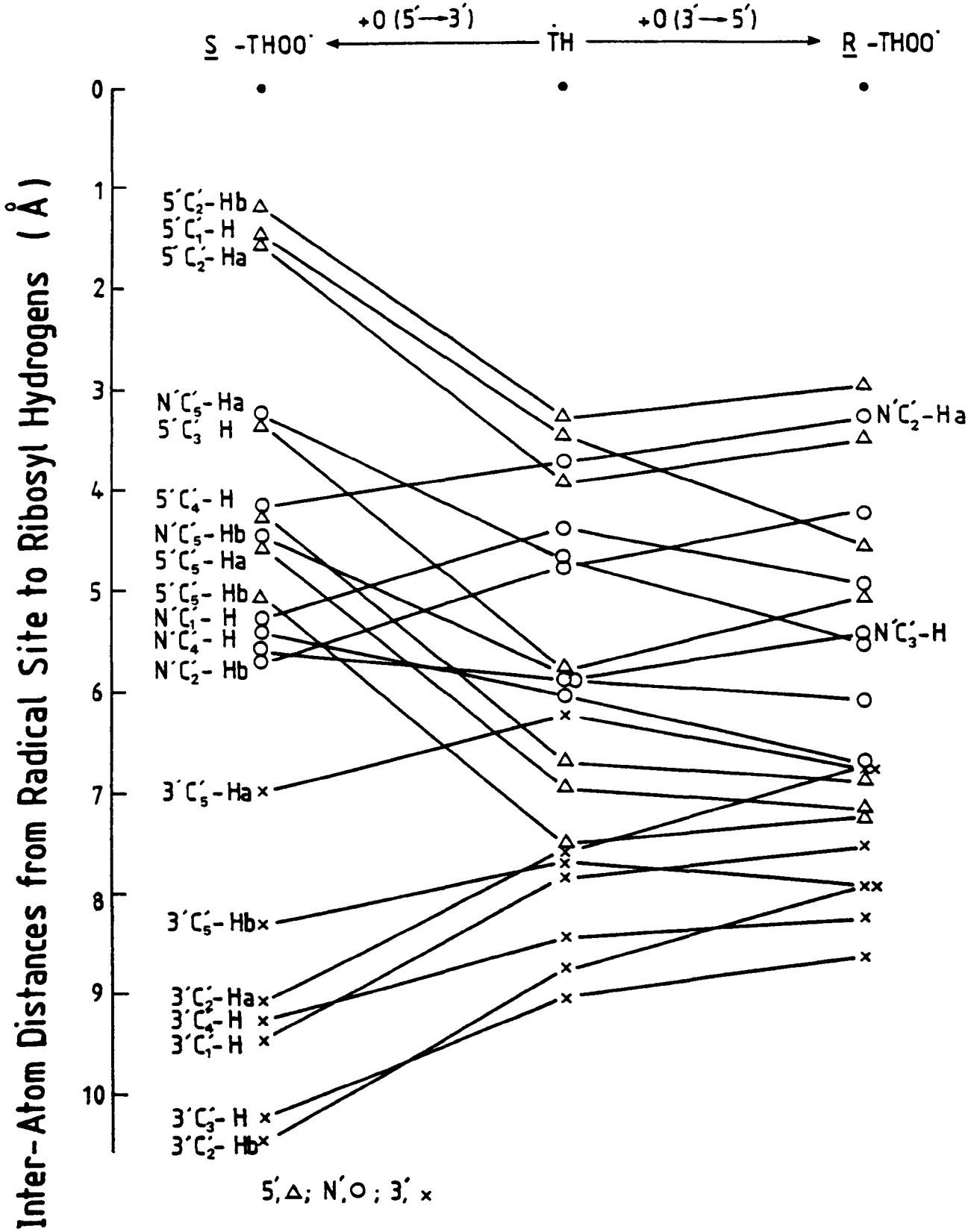

FIGURE B.5

The alterations on forming the two conformers of $THO_2^{\cdot}$ of the inter-atom distances between the base radical centre and the various deoxyribosyl hydrogens located 5′ (△), N′ (○) and 3′ (×) to the base radical moiety.

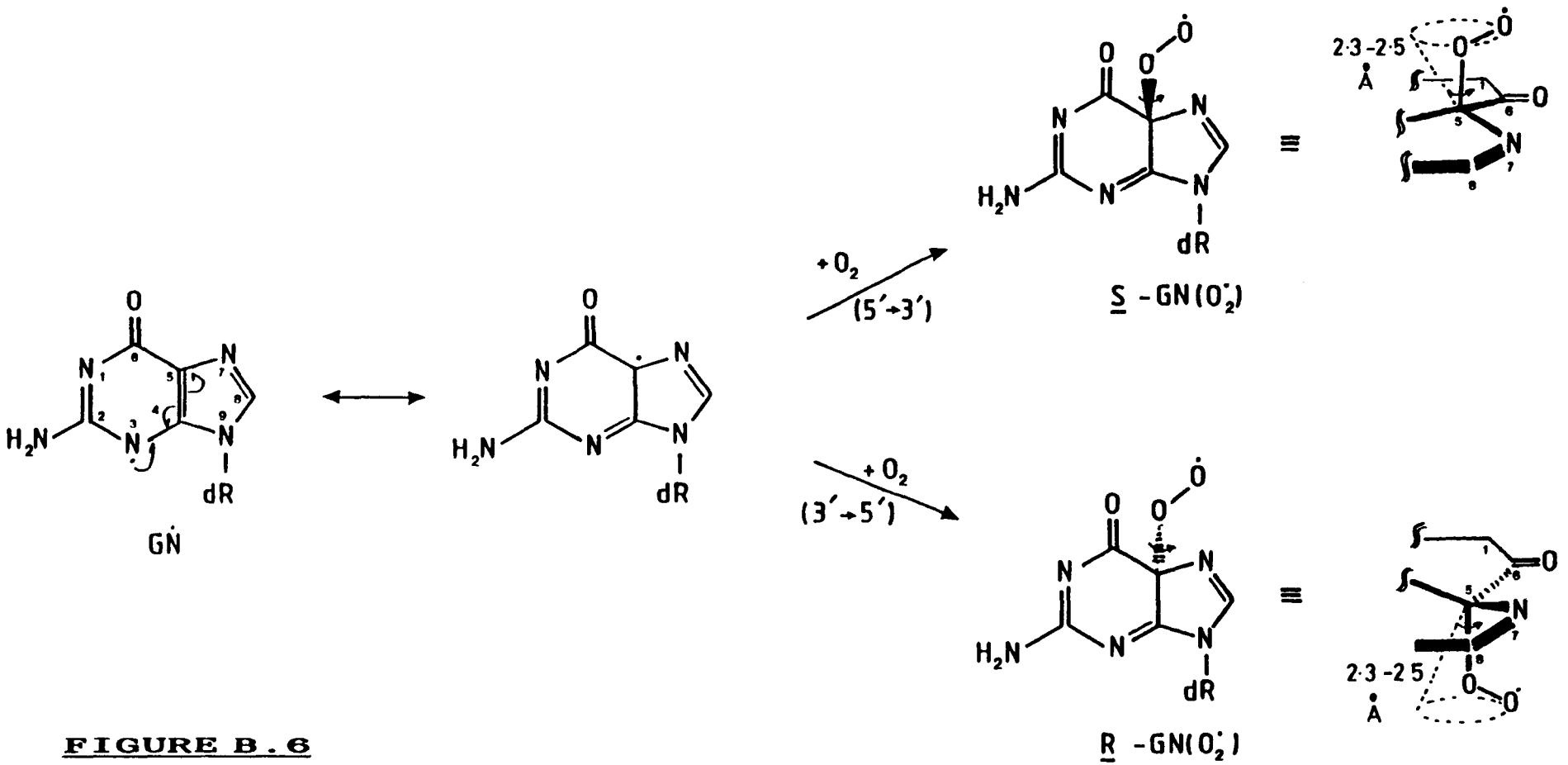

FIGURE B.6

Formation of the S- and R-conformers of GN($O_2^{\cdot}$) *via* O_2 addition (5′ → 3′ and 3′ → 5′ respectively) to the C5 radical centre of GN.

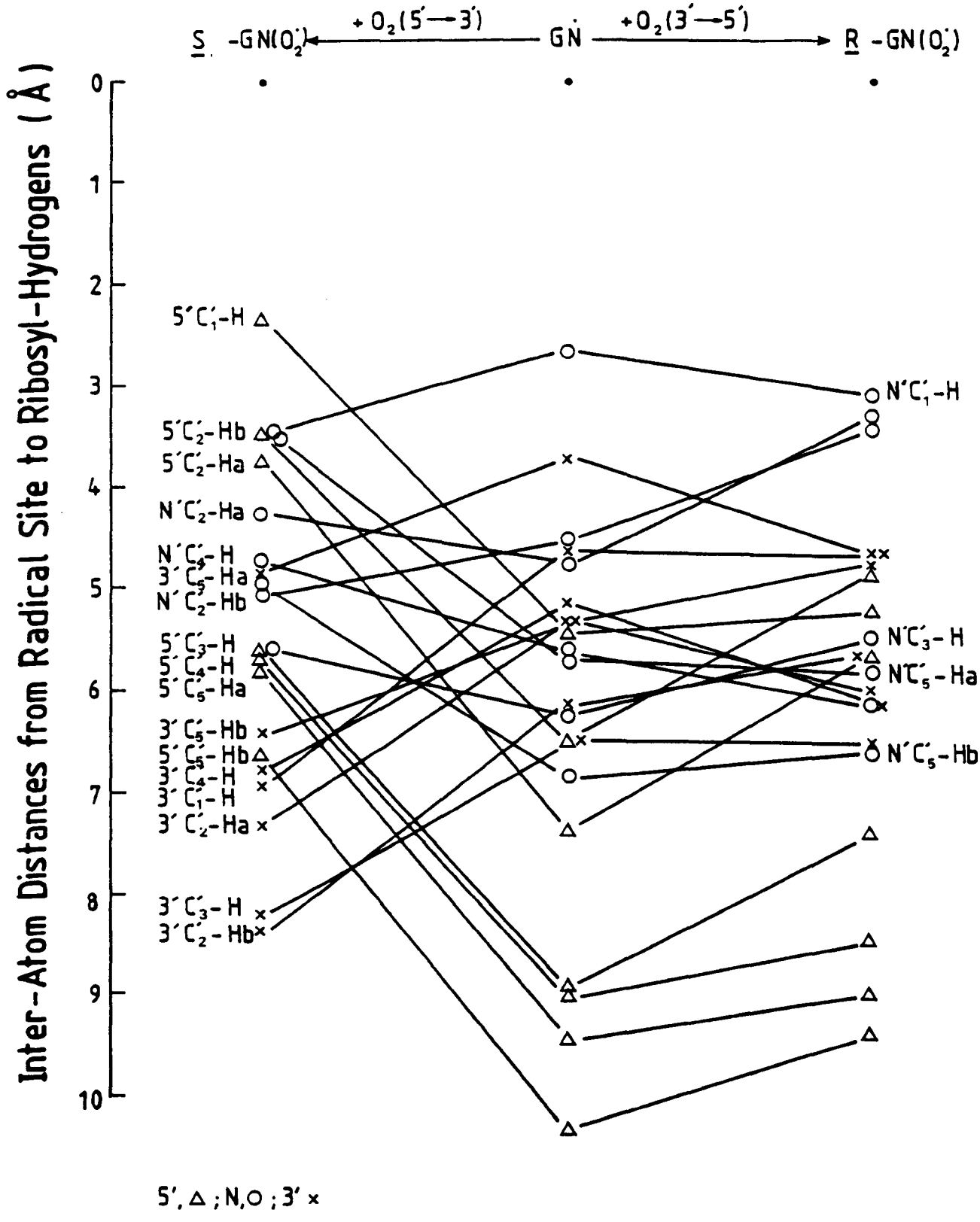

FIGURE B.7

The alterations on forming the two conformers of $GN(O_2^{\cdot})$ of the inter-atom distances between the base radical centre and the various deoxyribosyl hydrogens located 5′ (△), N′ (○) and 3′ (×) to the base radical moiety.

S-GN($O_2^{\cdot}$), are still from C_1', C_2' and C_5' and these will again be the sugar radicals most likely formed.

From the above it can be predicted that strand breaks occurring under conditions of direct damage arise through mechanisms that are distinct from those of the indirect pathway in which hydroxyl radicals predominately abstract the C_4' hydrogen atom (von Sonntag *et al.*, 1981). In none of the above situations is it likely that C_4'-H is abstracted by the base radicals and the addition of oxygen to either GṄ or ṪH does nothing to improve the likelihood of this being the case.

If, under direct damage conditions, strand breaks arise from the initially formed sugar radicals (*via* base radical H$^{\cdot}$ abstraction), then they could occur *via* the mechanims depicted in Figure B.3. Support for these reactions comes from several studies involving end group analysis of directly induced strand breaks. In particular studies of frozen aqueous solutions and 'dry' films of DNA irradiated (77 K, 220 K or R.T.) under ambient 'atmospheric' conditions, have shown that both the 5′ and 3′ end groups are predominately simple phosphate monoesters (Sweeney, 1986). Mechanisms depicting C_1', C_2' and C_5' sugar radicals yielding strand breaks with these particular end group functions are given in Figure B.3. Also a reduction in the amount of phosphoglycolate noted as a 3′ end group, when DNA was irradiated under such conditions (Sweeney, 1986), supports the notion that under direct conditions a sugar radical other than the C_4' centred species is the strand break precursor.

Other studies have reported far more 3′-OH end groups being detected on irradiation of DNA either *in vivo* or dry than when irradiated in dilute aqueous solution (Lennartz *et al.*, 1975). Such end groups could be formed from the subsequent reactions of the 3′ sugar radical resulting from base mediated H$^{\cdot}$ abstraction from C_2', followed by β-elimination of the 3′ phosphate moiety and $^{-}$OH addition (Fig. B.3). In addition DNA irradiated dry *in vitro* has been reported to yield few 5′ OH end groups (Coquerelle *et al.*, 1973).

Also proposed by the mechanisms in Figure B.3 is base release and the generation of a gap in the irradiated molecule resulting from release of

both base and an altered sugar. This has important implications for repair which, in the case of a gap, would require the combined action of a phosphatase, polymerase and a ligase.

Though it has been stated above that the mechanisms leading to strand breaks under direct conditions are expected to be distinct from those of indirect damage (where it is proposed that ·OH radicals initiate reactions leading to chain lesion by C_4'-H abstraction) a second major action of ·OH radicals with DNA is addition to the unsaturated base moieties (Scholes, 1983). This predominately results in OH-pyrimidine and purine radical adducts, with spin localized at C6 and C5 for the pyrimidines (Fujita and Steenken, 1981) and on N7, C4 and C5 for the purines (O'Neill, 1983; van Hemmen and Bleichrodt, 1971). For thymidine, a radical formed by ·OH mediated H· abstraction from the C7 methyl moiety is reported, but it is formed to less than 10% (Scholes, 1983; Fujita and Steenken, 1981). Tables B.V and B.VI catalogue the inter-atom distances from these radical centres to the ribosyl-hydrogens of the sugars positioned 5′ and 3′ to the radical bearing nucleotide and to the deoxyribose N′ to the base radical. For none of these centres does the C_4' hydrogen appear as a prime contender for abstraction. From this it can be concluded that strand breaks arising, under indirect conditions, from OH base radical adduct mediated H· atom abstraction, occur *via* mechanisms analogous to those of direct damage and are unlikely to involve abstraction of the C_4' hydrogen.

TABLE B.V

Distances, in angstroms, from the C5, C6 and C7* radical sites of pyrimidines to the deoxyribosyl C_n'-H units of the sugars 5′ and 3′ to the radical bearing nucleotide, and also to the C_n'-H groups of the sugar (N′) that is directly attached to the pyrimidine base radical

FROM / TO	C5	C6	C7
5′ C_1'-H	3.487 Å (2)	3.041 Å (2)	3.753 Å (3)
5′ C_2'-Ha	3.931 Å (4)	4.219 Å (7)	3.121 Å (2)
5′ C_2'-Hb	3.292 Å (1)	3.097 Å (3)	2.823 Å (1)
5′ C_3'-H	5.794 Å (8)	5.655 Å (12)	5.100 Å (5)
5′ C_4'-H	**6.688 Å (13)**	**6.355 Å (13)**	**6.422 Å (11)**
5′ C_5'-Ha	6.973 Å (14)	7.104 Å (16)	6.519 Å (12)
5′ C_5'-Hb	7.517 Å (16)	7.559 Å (19)	6.893 Å (14)
N′ C_1'-H	4.400 Å (5)	3.263 Å (4)	5.633 Å (7)
N′ C_2'-Ha	3.731 Å (3)	2.476 Å (1)	4.388 Å (4)
N′ C_2'-Hb	4.779 Å (7)	3.556 Å (5)	5.667 Å (8)
N′ C_3'-H	5.810 Å (9)	4.493 Å (8)	6.395 Å (10)
N′ C_4'-H	**6.045 Å (11)**	**4.776 Å (10)**	**6.861 Å (13)**
N′ C_5'-Ha	4.721 Å (6)	3.759 Å (6)	5.212 Å (6)
N′ C_5'-Hb	5.823 Å (10)	4.725 Å (9)	6.197 Å (9)
3′ C_1'-H	7.855 Å (18)	7.299 Å (17)	9.155 Å (18)
3′ C_2'-Ha	7.509 Å (15)	6.614 Å (15)	8.620 Å (16)
3′ C_2'-Hb	8.756 Å (20)	7.985 Å (20/21)	9.909 Å (20)
3′ C_3'-H	9.046 Å (21)	7.985 Å (20/21)	10.222 Å (21)
3′ C_4'-H	**8.437 Å (19)**	**7.451 Å (18)**	**9.752 Å (19)**
3′ C_5'-Ha	6.298 Å (12)	5.177 Å (11)	7.551 Å (15)
3′ C_5'-Hb	7.714 Å (17)	6.506 Å (14)	8.896 Å (17)

( ) value in parenthesis indicates the order of proximity of the hydrogen in question to the radical site.

* C7 corresponds to the radical formed from thymine by ·OH mediated H· abstraction from the C7 methyl moiety. C6-C7 = 1.384 Å 'aromatic'.

[For C_2', Ha is assigned to the hydrogen atom above the ribosyl plane, i.e. on the same side as the base residue and the C_5' moiety, and Hb to the hydrogen below the ribosyl plane.]

[For C_5', Ha is assigned to the hydrogen atom closest to the stacked base interior of the DNA, and Hb to the hydrogen further away.]

TABLE B.VI

Distances, in angstroms, from the N7, C5 and C4 centred radicals of purines, to the deoxyribose C_n'-H units of sugars 5′ and 3′ to the radical bearing nucleotide, and also to the C_n'-H groups of the sugar (N′) that is directly attached to the purine base radical

FROM / TO	N7	C5	C4
5′ C_1'-H	3.683 Å (1)	4.432 Å (2)	4.416 Å (5)
5′ C_2'-Ha	4.287 Å (5)	5.504 Å (7)	6.087 Å (13)
5′ C_2'-Hb	3.686 Å (2)	4.931 Å (4)	5.220 Å (7)
5′ C_3'-H	6.178 Å (12)	7.395 Å (15)	7.691 Å (18)
5′ C_4'-H	**6.965 Å (13)**	**7.866 Å (17)**	**7.920 Å (19)**
5′ C_5'-Ha	7.203 Å (14)	8.040 Å (19)	8.437 Å (20)
5′ C_5'-Hb	7.818 Å (18)	8.833 Å (21)	9.206 Å (21)
N′ C_1'-H	4.279 Å (4)	3.941 Å (1)	2.645 Å (1)
N′ C_2'-Ha	3.903 Å (3)	4.496 Å (3)	3.880 Å (2)
N′ C_2'-Hb	4.825 Å (6)	5.005 Å (5)	4.069 Å (3)
N′ C_3'-H	5.987 Å (8)	6.496 Å (10)	5.654 Å (10)
N′ C_4'-H	**6.117 Å (10)**	**6.314 Å (9)**	**5.315 Å (8)**
N′ C_5'-Ha	4.889 Å (7)	5.447 Å (6)	4.942 Å (6)
N′ C_5'-Hb	6.042 Å (9)	6.694 Å (12)	6.092 Å (14/15)
3′ C_1'-H	7.595 Å (16)	6.634 Å (11)	5.638 Å (9)
3′ C_2'-Ha	7.362 Å (15)	6.870 Å (13)	5.792 Å (11)
3′ C_2'-Hb	8.556 Å (20)	7.881 Å (18)	6.847 Å (16)
3′ C_3'-H	8.903 Å (21)	8.365 Å (20)	7.099 Å (17)
3′ C_4'-H	**8.219 Å (19)**	**7.437 Å (16)**	**6.092 Å (14/15)**
3′ C_5'-Ha	6.147 Å (11)	5.623 Å (8)	4.247 Å (11)
3′ C_5'-Hb	7.606 Å (17)	7.185 Å (14)	5.822 Å (12)

( ) value in parenthesis indicates the order of proximity of the hydrogen in question to the radical site.

[For C_2', Ha is assigned to the hydrogen atom above the ribosyl plane, i.e. on the same side as the base residue and the C_5' moiety, and Hb to the hydrogen below the ribosyl plane.]

[For C_5', Ha is assigned to the hydrogen atom closest to the stacked base interior of the DNA, and Hb to the hydrogen further away.]

APPENDIX C

An Alternative Mode of E.s.r. Analysis

APPENDIX C

An Alternative Mode of E.s.r. Analysis

As an alternative to the normal mode of e.s.r. analysis undertaken throughout this study (where usually frozen aqueous samples of DNA, irradiated at 77 K, were annealed to particular temperatures for approximately 2 minutes, then recooled to 77 K prior to their e.s.r. spectra being recorded; see Chapter Two), a second method was sometimes employed, which was a modified procedure of that reported by Gräslund *et al.* (1975) who used e.s.r. to measure the kinetics of free radical conversions in γ-irradiated oriented DNA. In those studies, the kinetics experiments were conducted by having spectrometer's magnetic field set corresponding to a particular point in the spectrum so that (with the field sweep set to zero) once the temperature was rapidly altered to a pre-calibrated value using variable temperature apparatus, the ensuing decay of the relevant signal could be monitored with time.

A procedure similar to this was used to follow the decay of DNA signals with temperature in the presence and absence of particular additives. With the spectrometer's magnetic field set on the DNA central feature A (Fig. C.1) and the field sweep set to zero, the liquid nitrogen was decanted from the finger Dewar (see Chapter Two) and the decay of the signal followed with time, which *via* a time/temperature calibration curve (cf. Fig. 2.1) was equated to temperature.

Figure C.1 shows the decay profiles, as produced directly from the e.s.r. spectrometer, of DNA samples (50 mg + 1 ml H_2O, $-O_2$) in (a) the presence and (b) the absence of MEA (40 mM), after γ-irradiation at 77 K (and annealing to 130 K to remove $^{\cdot}OH$ features) and analysis as outlined above. It can be clearly seen that the presence of MEA causes the e.s.r. signal to be lost at a temperature well below that at which it is normally stable. These results are analogous to those described in Chapter Four.

The principle advantage of this technique over the more conventional method of producing a decay profile is the much shorter time required to conduct the experiments. The procedure of annealing a sample to a required temperature, then recooling it prior to recording the e.s.r. spectra at 77 K, and subsequently plotting the data requires many hours,

especially with a large sample number. It is also expensive in terms of resources. However the above procedure requires only ~20 minutes per sample and the data is automatically plotted.

One disadvantage of the alternative technique is that the decaying e.s.r. intensities are recorded at the elevated temperatures and so the signals will obey the Curie law (signal intensity $\propto T^{-1}$). This may result in the secondary neutral radicals, i.e. $\dot{T}H$, being difficult to detect and quantify. However such problems could be overcome by irradiating the samples for longer periods of time and using higher spectrometer gains. A second problem is that a temperature gradient occurs across the sample during the "free" anneal described above, which results in a spread of reactions occurring at any particular time within the sample during warming. However this could be eliminated, in any future development of this work, by incorporating a variable temperature system that would allow a more gradual controlled increase in temperature to take place. Also the use of a variable temperature accessory would permit rapid alterations of temperature, so allowing kinetic experiments of the type discussed by Gräslund to be conducted on fibrous solid samples of DNA, in which not so much of a temperature gradient is expected.

A gas-flow variable temperature unit would be ideal for this sort of work for it would also minimize frequency shifts that may be encountered as the cavity warms and hence lessen the problems of detuning. Overall though more accurate measurement and control of ν and H_o (than is presently available) is required since only fairly small shifts in the latter would result in quite erroneous measurements of intensity.

REFERENCES

REFERENCES

ADAMS, G.E., (1970), in "Radioprotection and Sensitization", Morrison, H.L. and Quintiliani, M. eds. (Taylor and Francis, London) p.3.

ADAMS, G.E., (1972), Adv. Radiat. Chem., 3, 125.

ADAMS, G.E., ARMSTRONG, R.C., CHARLESBY, A., MICHAEL, B.D. and WILLSON, R.L., (1969), J. Chem. Soc., Faraday Trans., 65, 732.

ADAMS, G.E. and COOKE, M.S., (1969), Int. J. Radiat. Biol., 15, 457.

ADAMS, G.E. and JAMESON, D.G., (1980), Radiat. Environ. Biophys., 17, 95.

ADAMS, G.E., McNAUGHTON, G.S. and MICHAEL, B.D., (1967), in "Chemistry of Ionization and Excitation" (Proc. Newcastle Conf., 1966), Johnson, G.R.A. and Scholes, G. eds. (Taylor and Francis, London) p.281.

ADAMS, G.E., McNAUGHTON, G.S. and MICHAEL, B.D., (1968), J. Chem. Soc., Faraday Trans., 64, 902.

AHMAD, S.I., (1981), Photochem. Photobiophys., 2, 173.

AHMAD, S.I., (1983), Inorg. Chimica Acta, 79, 300.

AKABOSHI, M., KAWAI, K., MAKI, H. and HONDA, Y., (1985), Annu. Rep. Res. Reactor Inst. Kyoto Univ., 18, 44.

AKHLAQ, M.S., SCHUCHMANN, H.-P. and VON SONNTAG, C., (1987), Int. J. Radiat. Biol., 51, 91.

ALEXANDER, P. and CHARLESBY, A., (1955), in "Radiobiology Symposium Liege, 1954", Bacq, Z. and Alexander, P. eds.

(Butterworths Scientific Publications, London) p.49.

ALEXANDER, P., LETT, J.T. and ORMEROD, M.G., (1961), Biochim. Biophys. Acta, 51, 207.

ALPER, T., (1955), Radiat. Res., 2, 119.

ALPER, T., (1979), "Cellular Radiobiology" (Cambridge University Press, Cambridge).

AL-THANNON, A.A., BARTON, J.P., PACKER, J.E., SIMS, R.J., TRUMBORE, C.N. and WINCHESTER, R.V., (1974), Int. J. Radiat. Phys. Chem., 6, 233.

ALTMAN, P.L. and KATZ, D., (1976), in "Cell Biology" FASEB, Bethesda, MD, p.383.

ANANTHASWAMY, H.N. and EISENSTARK, A., (1976), Photochem. Photobiol., 24, 439.

ARNOTT, S., DOVER, S.D. and WONACOTT, A., (1969), Acta Cryst. sect. B, 25, 2192.

ARNOTT, S. and HUKINS, D.W.L., (1973), J. Mol. Biol., 81, 93.

ATKINS, P.W. and SYMONS, M.C.R., (1967), "The Structure of Inorganic Radicals" (Elsevier, Amsterdam).

AUERBACH, C., (1976), "Mutation Research" (Chapman and Hall, London).

AYSCOUGH, P.B., (1967), "Electron Spin Resonance in Chemistry", (Methuen, London).

BACQ, Z.M. and BEAUMARIAGE, M.L., (1965), Arch. Int. Pharmacodyn. Ther., 153, 457.

BACQ, Z.M., HERVE, A., LECOMPTE, J., FISCHER, P., BLAVIER, J., DECHAMPS, G., LE BIHAN, H. and RAYET, P., (1951),

Arch. Int. Physiol., 59, 442.

BAKALE, G. and GREGG, E.C., (1978), Br. J. Cancer, 37, Suppl. III, 24.

BEESK, F., DIZDAROGLU, M., SCHULTE-FROHLINDE, D. and VON SONNTAG, C., (1979), Int. J. Radiat, Biol., 36, 565.

BEHRENS, G., KOLTZENBERG, G., RITTER, A. and SCHULTE-FROHLINDE, D., (1978), Int. J. Radiat. Biol., 33, 163.

BEHRENS, G., KOLTZENBERG, G. and SCHULTE-FROHLINDE, D., (1982), Z. Naturforsch., 37c, 1205.

BELFI, C.A., ARAKALI, A.V., PAUL, C.R. and BOX, H.C., (1986), Radiat. Res., 106, 17.

BENTLEY, G.A., FINCH, J.T. and LEWITT-BENTLEY, A., (1981), J. Mol. Biol., 145, 771.

BENYAJATI, C. and WORCEL, A., (1976), Cell, 9, 393.

BERGER, M., CADET, J. and ULRICH, J., (1985), Can. J. Chem., 63, 6.

BERNHARD, W.A., (1981), Adv. Radiat. Biol., 9, 199.

BERNHARD, W.A., CLOSE, D.M., MERCER, K.R. and CORELLI, J.C., (1976), Radiat. Res., 66, 19.

BIAGLOW, J.E., (1981), J. Chem. Educ., 58, 144.

BINA-STEIN, M. and SIMPSON, R.T., (1977), Cell, 11, 609.

BIRNBOIM, H.C. and DOLY, J., (1979), Nucl. Acids Res., 7, 1513.

BLOK, J. and LOMAN, H., (1973), Curr. Top. Radiat. Res. Q., 9, 165.

BLOOMFIELD, V.A., CROTHERS, D.M. and TINOCO, I., (1974), "Physical Chemistry of Nucleic Acids" (Harper and Row,

New York).

BOAG, J.W., (1963), in "Actions Chimiques et Biologiques des Radiations", Haissinsky, M. ed., Vol. 6, (Masson, Paris) p.4.

BOON, P.J., CULLIS, P.M., SYMONS, M.C.R. and WREN, B.W., (1984), J. Chem. Soc. Perkin Trans. 2, 1393.

BOON, P.J., CULLIS, P.M., SYMONS, M.C.R. and WREN, B.W., (1985), J. Chem. Soc. Perkin Trans. 2, 1057

BOPP, A. and HAGEN, U., (1970), Biochim. Biophys. Acta, 209, 320.

BOTHE, E., BEHRENS, G., BOHM, E., SETHURAM, B. and SCHULTE-FROHLINDE, D., (1986), Int. J. Radiat. Biol., 49, 57.

BOTHE, E. and SCHULTE-FROHLINDE, D., (1982), Z. Naturforsch., 37c, 1191.

BOTHE, E., SCHULTE-FROHLINDE, D. and VON SONNTAG, C., (1978), J. Chem. Soc., Perkin Trans. 2, 416.

BOX, H.C. and BUDZINSKI, E.E., (1975), J. Chem. Phys., 62, 197.

BRAM, S., KOUPRACH, S. and BAUDY, P., (1978), Cold Spring Harb. Symp. Quant. Biol., 42, 23.

BRUSTAD, T. and WOLD, E., (1976), Radiat. Res., 66, 215.

BRYANT, P.E. and BLOCHER, D., (1980), Int. J. Radiat. Biol., 38, 335.

CADET, J. and BERGER, M., (1983), in "Proc. 7th. Int. Cong. Radiat. Res. Amsterdam," Vol. A. pt. A3-09.

CADET, J. and BERGER, M., (1985), Int. J. Radiat. Biol., 47, 127.

CADET, J., DUCOLOMB, R. and TEOULE, R., (1974), C. R. Hebd. Seances Acad. Sci., Ser. C, 279, 549.

CADET, J., SHAW, A., VOITURIEZ, L. and GREGOLI, S., (1983a), in "Proc. 7th. Int. Cong. Rad. Res. Amsterdam," Vol. A. pt. A3-11.

CADET, J., VOITURIEZ, L. and BERGER, M., (1983b), J. Chromatogr., 259, 111.

CAMERINI-OTERO, R.D. and FELSENFELD, G., (1977), Nucl. Acids Res., 4, 1159.

CAMERINI-OTERO, R.D., SOLLNER-WEBB, B., SIMON, R.H., WILLIAMSON, P., ZASLOFF, M. and FELSENFELD, G., (1978). Cold Spring Harb. Symp. Quant. Biol., 42, 57.

CHAMBON, P., (1978), Cold Spring Harb. Quant. Biol., 42, 1209.

CHAN, S.W., CHAN, P.C. and BIELSKI, B.H.J., (1974), Biochim. Biophys. Acta, 338, 213.

CHANDRA, H., RAO, D.N.R. and SYMONS, M.C.R., (1983), J. Chem. Res. (S), 68.

CHAPMAN, J.D. and GILLESPIE, C.J., (1981), Adv. Radiat. Biol., 9, 143.

CHATTERJEE, A. and MAGEE, J.L., (1985), Radiat. Prot. Dosim., 13, 137.

CHRISTIANSEN, G. and GRIFFITH, J., (1977), Nucl. Acids Res., 4, 1837.

COOK, P.R. and BRAZELL, I.A., (1975), J. Cell Sci., 19, 261.

COPELAND, E.S., (1975), J. Magn. Reson., 20, 124.

COPELAND, E.S., SANNER, T. and PIHL, A., (1967), Eur. J.

Biochem., 1, 312.

COQUERELLE, T., BOPP, A., KESSLER, B. and HAGEN, U., (1973), Int. J. Radiat. Biol., 24, 397.

COTTER, R.I. and LILLEY, D.M.J., (1977), FEBS Lett., 82, 63.

CRICK, F.H.C. and KLUG, A., (1975), Nature, 255, 530.

CULLIS, P.M. and SYMONS, M.C.R., (1986), Radiat. Phys. Chem., 27, 93.

CULLIS, P.M., SYMONS, M.C.R., WREN, B.W. and GREGOLI, S., (1985a), J. Chem. Soc. Perkin Trans. 2, 1819.

CULLIS, P.M., WREN, B.W., BOON, P.J., SYMONS, M.C.R., JONES, G.D.D. and CONDOR, M., (1985b), Int. J. Radiat. Biol., 47, 221.

DEEBLE, D.J., SCHULZ, D. and VON SONNTAG, C., (1986), Int. J. Radiat. Biol., 49, 915.

DEEBLE, D.J. and VON SONNTAG, C., (1984), Int. J. Radiat. Biol., 46, 247.

DEEBLE, D.J. and VON SONNTAG, C., (1986), Int. J. Radiat. Biol., 49, 927.

DEEG. K.-J., KATSIKAS, L. and SCHNABEL, W., (1984), Z. Naturforsch., 39c, 1075.

DERTINGER, H. and JUNG, H., (1969), "Molekulare Strahlenbiologie" (Springer, Berlin-Heidelberg-New York) p.76.

DEWEY, W.C., SEDITA, B.A. and HUMPHREY, R.M., (1967), Int. J. Radiat. Biol., 12, 597.

DICKERSON, R.E. and DREW, H.R., (1981), J. Mol. Biol., 149, 761.

DISCHE, S. and SAUNDERS, M.I., (1978), Br. J. Cancer, 37, Suppl. III, 311.

DIXON, W.T., FOXALL, J., WILLIAMS, G.H., EDGE, D.J., GILBERT, B.C., KAZARIANS-MOGHADDAM, H. and NORMAN, R.O.C., (1977), J. Chem. Soc. Perkin Trans. 2, 827.

DIZDAROGLU, M., NEUWALD, K. and VON SONNTAG, C., (1976), Z. Naturforsch., 31b, 227.

DIZDAROGLU, M., SCHULTE-FROHLINDE, D. and VON SONNTAG, C., (1975a), Z. Naturforsch., 30c, 826.

DIZDAROGLU, M., SCHULTE-FROHLINDE, D. and VON SONNTAG, C., (1977a), Int. J. Radiat. Biol., 32, 481.

DIZDAROGLU, M., SCHULTE-FROHLINDE, D. and VON SONNTAG, C., (1977b), Z. Naturforsch., 32c, 1021. ;

DIZDAROGLU, M., VON SONNTAG, C. and SCHULTE-FROHLINDE, D., (1975b), J. Am. Chem. Soc., 97, 2277.

DOHERTY, D.G., BURNETT, W.T. and SHAPIRA, R., (1957), Radiat. Res., 7, 13.

DRAZIL, V. and JUASKOVA, V., (1979), Fortochr. Onko., 15.

DREW, H.R., WING, R.M., TAKANO, T., BROKA, C., TANAKA, S., ITAKURA, K. and DICKERSON, R.E., (1981), Proc. Nat. Acad, Sci., USA, 78, 2179.

DUBOCHET, J. and NOLL, M., (1978), Science, 202, 280.

DUCOLOMB, R., CADET, J. and TEOULE, R., (1974), Int. J. Radiat. Biol., 25, 139.

DUPRAW, E.J., (1970), "DNA and Chromosomes" (Holt, Rhinehart and Winston, New York).

EASTLAND, G.W., RAO, D.N.R. and SYMONS, M.C.R., (1986), J.

Chem. Soc., Faraday Trans. 1, 82, 2833.

ELDJARN, L. and PIHL, A., (1956), in "Progress in Radiobiology," Mitchell, J.S., Holmes, B.E. and Smith C.L. eds., (Oliver and Bond, London) p.249.

ELDJARN, L., PIHL, A. and SHAPIRO, B., (1956), Proc. Int. Conf. Peaceful Uses Atom. Energy, 11, 335.

ELGIN, S.C.R. and WEINTRAUB, H., (1975), Annu. Rev. Biochem., 44, 725.

ERSHOFF, B.H., STEERS, C.W. and KRUGER, L., (1962), Proc. Soc. Exp. Biol. Med., 111, 391.

FARAGGI, M., REDPATH, J.L. and TAL, Y., (1975), Radiat. Res., 64, 452.

FAULK, M., POOLE, A.G. and GROYMOUR, C.G., (1970), Can. J. Chem., 48, 1536.

FEDOROV, B.A., (1965), Med. Radiol., 10, 42; (1966), Chem. Abstr., 64, 8613.

FELSENFELD, G., (1978), Nature, 271, 115.

FIEDLER, E., STANGER, H.K. and GRILLMAIER, R.E., (1982), Proc. 8th Symp. Julich, Federal Republic of Germany, Commission of the European Comunities, Radiation Protection, Microdosimetry, p.671.

FINCH, J.T., BROWN, R.S., RHODES, D., RICHMOND, T., RUSHTON, B., LUTTER, L.C. and KLUG, A., (1981), J. Mol. Biol., 145, 757.

FINCH, J.T. and KLUG, A., (1976), Proc. Natl. Acad. Sci. USA., 73, 1897.

FINCH, J.T., LUTTER, L.C., RHODES, D., BROWN, R.S., RUSHTON,

B., LEVITT, M. and KLUG, A., (1977), Nature, 269, 29.

FOSTER, J.L. and WILLSON, R.L., (1973), Br. J. Radiol., 46, 234.

FRANKLIN, R.H. and GOSLING, R.G., (1953), Acta. Cryst., 6, 678.

FREIFELDER, D., (1965), Proc. Nat. Acad. Sci. USA, 54, 128.

FRIEDBERG, F., (1969a), Radiat. Res. Rev., 2, 131.

FRIEDBERG, F., (1969b), Radiat. Res., 38, 34.

FUCIARELLI, A.F., SHUM, F.Y. and RALEIGH, J.A., (1986), Biochem Biophys. Res. Comm., 134, 883.

FUJITA, S. and STEENKEN, S., (1981), J. Am. Chem. Soc., 103, 2540.

FULLER, W., WILKINS, M.H.F., WILSON, H.R. and HAMILTON, L.D., (1965), J. Mol. Biol., 12, 60.

FURLONG, E.A., JORGENSEN, T.J. and HENNER, W.D., (1986), Biochemistry, 25, 4344.

GARRARD, W.T., NOBIS, P. and HANCOCK,R., (1977), J. Biol. Chem., 252, 4962.

GARRISON, W.M., (1972), Radiat. Res. Rev., 3, 305.

GAUBATZ, J., HARDISON, R., MURPHY, J., EICHNER, M.E. and CHALKLEY, R., (1978), Cold Spring Harb. Symp. Quant. Biol., 42, 265.

GILLESPIE, C.J., GISLASON, G.S., DUGLE, D.L. and CHAPMAN, J.D., (1972), Radiat. Res., 51, 272.

GOLDSTEIN, S. and CZAPSKI, G., (1984), Int. J. Radiat. Biol., 46, 725.

GOODWIN, D.C. and BRAHMS, J., (1978), Nucl. Acids Res., 5,

835.

GORDY, W. and SHIELDS, H., (1958), Radiat. Res., 9, 611.

GRASLUND, A., EHRENBERG, A. and RUPPRECHT, A., (1977), Int. J. Radiat. Biol., 31, 145.

GRASLUND, A., EHRENBERG, A., RUPPRECHT, A. and STROM, G., (1971), Biochim. Biophys. Acta, 254, 172.

GRASLUND, A., EHRENBERG, A., RUPPRECHT, A., TJALLDIN, B. and STROM, G., (1975), Radiat. Res., 61, 488.

GREENSTOCK, C.L., (1981), Radiat. Res., 86, 196.

GREENSTOCK, C.L. and DUNLOP, I., (1975), in "Fast Processes in Radiation Chemistry and Biology", Adams, G.E., Fielden, E.M. and Michael, B.D. eds. (John Wiley and Sons, New York) p.247.

GREGOLI, S., OLAST, M. and BERTINCHAMPS, A., (1970a), Int. J. Radiat. Biol., 17, 39.

GREGOLI, S., OLAST, M. and BERTINCHAMPS, A., (1976), Radiat. Res., 65, 202.

GREGOLI, S., OLAST, M. and BERTINCHAMPS, A., (1977a), Radiat. Res., 70, 255.

GREGOLI, S., OLAST, M. and BERTINCHAMPS, A., (1977b), Radiat. Res., 72, 201.

GREGOLI, S., OLAST, M. and BERTINCHAMPS, A., (1979), Radiat. Res., 77, 417.

GREGOLI, S., OLAST, M. and BERTINCHAMPS, A., (1982), Radiat. Res., 89, 238.

GREGOLI, S., TAVERNA, C. and BERTINCHAMPS A., (1970b), Int. J. Radiat. Biol., 18, 577.

GROSCH, D.S. and HOPWOOD, L.E., (1979), "Biological Effects of Radiations", 2nd ed. (Academic Press, New York).

HABER, M. and STEWART, B.W. (1981), FEBS Lett., 133, 72.

HANAWALT, P.C., COPPER, P.K., GANESAN, A.K. and SMITH, C.A., (1979), Ann. Rev. Biochem., 48, 783.

HASKILL, J.S., and HUNT, J.W., (1967), Radiat. Res., 32, 827.

HECHT, H.G., (1967), "Magnetic Resonance Spectroscopy" (Wiley, New York).

HELD, K.D., (1986), in "Free Radicals, Aging and Degenerative Diseases", (Alan R. Liss, Inc.), p.527.

HELD, K.D., HARROP, H.A. and MICHAEL, B.D., (1981), Int. J. Radiat. Biol., 40, 613; (1984), ibid., 45, 615, (1984), ibid., 45, 627.

HELD, K.D., HARROP, H.A. and MICHAEL, B.D., (1985), Radiat. Res., 103, 171.

HENNER, W.D., GRUNBERG, S.M. and HASELTINE, W.A., (1983a), J. Biol. Chem., 258, 15198.

HENNER, W.D., RODRIGUEZ, L.O., HECHT, S.M. and HASELTINE, W.A., (1983b), J. Biol. Chem., 258. 711.

HENRIKSEN, T., (1968), Scand. J. Clin. Lab. Invest. Suppl., 22, 7.

HERTZBERG, R.P. and DERVAN, P.B., (1982), J. Am. Chem. Soc., 104, 313.

HOARD, D.E., HAYES, F.N. and GOAD, W.B., (1974), Int. J. Radiat. Biol., 25, 603.

HOGAN, M.E. and JARDETZKY, O., (1980), Biochemistry, 19,

3460.

HOLBROOK, S.R. and KIM, S.-H., (1984), J. Mol., Biol., 173, 361.

HOLIAN, J. and GARRISON, W.M., (1969), Nature, 221, 57.

HOWARD, J.A., (1973), in "Free Radicals", Kochi, J.K., ed., Vol. II, (Wiley, New York) p.3.

HOWARD-FLANDERS, P., (1960), Nature, 186, 485.

HRUSKA, F.E., BERGER, M., CADET, J. and REMIN, M., (1985), Can. J. Chem., 63, 15.

HULSEWEDE, J.W., (1985), Dissertation Ruhr-Universitat Bochum.

HUTCHINSON, F., (1961), Radiat. Res., 14, 721.

HUTCHINSON, F., (1966), Cancer Res., 26, 2045.

HUTCHINSON, F., (1978), Workshop Summary in "DNA Repair Mechanisms", Hanawalt, P.C., Friedberg, E.C. and Fox, C.F. eds. (Academic Press, New York) p.457.

HUTTERMANN, J., KOHNLEIN, W. and TEOULE, R. eds.; BERTINCHAMPS, A.J., co-ordinating ed., (1978), Molecular Biology, Biochemistry and Biophysics 27, "Effects of Ionizing Radiation on DNA" (Springer-Verlag, Berlin-Heidelberg-New York).

HUTTERMANN, J. and VOIT, K., (1986), in "Proc. of CIC Conf. of 'Electronic Magnetic Resonance", Saskatoon (Canada), in press.

HUTTERMANN, J., VOIT, K., OLOFF, H., KOHNLEIN, W., GRASLUND, A. and RUPPRECHT, A., (1984), Faraday Discuss. Chem. Soc., 78, 135.

IGO-KEMENES, T. and ZACHAU, H.G., (1978), Cold Spring Harb. Symp. Quant. Biol., 42, 109.

INGRAM, D.J.E., (1958), "Free Radicals as Studied by Electron Spin Resonance" (Butterworths, London).

INOKUTI, M., (1983), Appl. Atomic Coll. Phys., 4, 179.

JORCANO, J.L. and RUIZ-CARRILLO, A., (1979), Biochemistry, 18, 768.

JUNG, H., HAGEN, U., ULLRICH, M. and PETERSEN, E.E., (1969), Z. Naturforsch. 24b, 1565.

KAPLAN, H.S. and MOSES, L.E., (1964), Science, 145, 21.

KAR, L. and BERNHARD, W.A., (1983), Radiat. Res., 93, 232.

KASAI, H., TANOOKA, H. and NISHIMURA, S., (1984), Gann, 75, 1037.

KEEBLE, D.J., (1986), Ph.D. Thesis, University of Keele.

KEENE, J.P., (1964), J. Sci. Instr., 41, 493.

KIRBY-SMITH, J.S., (1960), Radiat. Res. Suppl., 2, 668.

KLAYMAN, D.L., GRENAN, M.M. and JACOBUS, D.P., (1969), J. Med. Chem., 12, 510.

KLUG, A., JACK, A., VISWAMITRA, M.A., KENNARD, O., SHAKKED, Z. and STEITZ, T.A., (1979), J. Mol. Biol., 131, 669.

KLUG, A., RHODES, D., SMITH, J., FINCH, J.T. and THOMAS, J.O., (1980), Nature, 287, 509.

KNEUBUHL, F.K., (1960), J. Chem. Phys., 33, 1074.

KOHN, K.W. (1986), Basic Life Sciences, Vol. 38, "Mechanisms of DNA Damage and Repair", Simic, M.G., Grossman, L. and Upton, A.C., eds. (Plenum Press, New York-London) p.101.

KORNBERG, R.D., (1977), Annu. Rev. Biochem., 46, 931.

KUWABARA, M., HAYASMI, M. and YOSHII, G., (1973), J. Radiat. Res., 14, 198.

KUWABARA, M., HAYASHI, M. and YOSHII, G., (1977), J. Radiat. Res., 17, 342.

KUWABARA, M. and YOSHII, G., (1976), Biochim. Biophys. Acta, 432, 292.

LEMARIE, D.G.E., BOTHE, E. and SCHULTE-FROHLINDE, D., (1984), Int. J. Radiat. Biol., 45, 351.

LENHERR, A.D. and ORMEROD, M.G., (1968), Biochim. Biophys. Acta, 166, 298.

LENNARTZ, M., COQUERELLE, T., BOPP, A. and HAGEN, U., (1975), Int. J. Radiat. Biol., 27, 577.

LESKO, S.A., LORENTZEN, R.J. and TS'O, P.O.P., (1980), Biochemistry, 19, 3023.

LEVITT, M., (1978), Proc. Natl. Acad. Sci., USA., 75, 640.

LILLEY, D.M.J. and PARDON, J.F., (1979), Annu. Rev. Genet., 13, 197.

LILLICRAP, S.C. and FIELDEN, E.M., (1972), Int. J. Radiat. Biol., 21, 137.

LUCKE-HUHLE, C., BRAUN, A. and HAGEN, U., (1970), Z. Naturforsch., 25b, 1264.

LUNING, K.G., FROLEN, H. and NELSON, A., (1961), Radiat. Res., 14, 813.

LUTTER, L.C., (1978), J. Mol. Biol., 124, 391.

MacDERMOTT, A.J., (1985), Phil. Trans. R. Soc. Lond., A 313, 453.

MAHENDRASINGAM, A., (1983), Ph.D. Thesis, University of

Keele.

MANDL, A.M., (1959), Int. J. Radiat. Biol., 1, 131.

MANNING, G.S., (1979), Acc. Chem. Res., 12, 443.

MARVIN, D.A., SPENCER, M., WILKINS., M.H.F. and HAMILTON, L.D., (1961), J. Mol. Biol., 3, 547.

MATHUR DE VRE, R., (1979), Prog. Biophys. Mol. Biol., 35, 103.

MATHUR DE VRE, R. and BERTINCHAMPS, A.J., (1977), Radiat. Res., 72, 181.

MATHUR DE VRE, R., BERTINCHAMPS, A.J. and BERENDSEN, H.J.C., (1976), Radiat. Res., 68, 197.

MAURA, A., GRILLO-RUGGIERI, F. and LAVANNA, M., (1981), Soc. Ital. Biol., 57, 1282.

MEE, L.K. and ADELSTEIN, S.J., (1979), Int. J. Radiat. Biol., 36, 359.

MEE, L.K. and ADELSTEIN, S.J., (1981), Proc. Natl. Acad. Sci. USA., 78, 2194.

MEE, L.K., ADELSTEIN, S.J. and STEIN, G., (1978), Int. J. Radiat. Biol., 33, 443.

MICHAEL, B.D., HELD, K.D. and HARROP, H.A., (1983), in "Radioprotectors and Anticarcinogens", Nygaard, O.F. and Simic, M.G. eds. (Academic Press, New York) p.325.

MICHAELS, H.B. and HUNT, J.W., (1978), Radiat. Res., 74, 23.

MILVY, P., (1971), Radiat. Res., 48, 206.

MONTENAY-GARESTIER, T., CHARLIER, M. and HELENE, C., (1976), in "Photochemistry and Photobiology of Nucleic Acids", Wang, S.Y. ed., Vol.1, (Academic Press, New York)

p.381.

MORRIS, N.R., (1976), Cell, 8, 357; (1976), ibib, 9, 627.

MOZUMDER, A. and MAGEE, J.L., (1966), Radiat. Res. 28, 203.

NEIDLE, S. and BERMAN, H.M., (1983), Prog. Biophys. Mol. Biol., 41, 43.

NELSON, D.L., PETERSEN, R.L. and SYMONS, M.C.R., (1977), J. Chem. Soc. Perkin Trans. 2, 2005.

NOLL, M., (1976), Cell, 8, 349.

NUCIFORA, G., SMALLER, B., REMKO, R., and AVERY, E.C., (1972). Radiat. Res., 49, 96.

OKADA, S. (1970), Radiation Biochemistry, Vol. 1, (Academic Press, New York).

OLINS, A.L., (1978), Cold Spring Harb. Symp. Quant. Biol., 42, 325.

O'NEILL, P., (1983), Radiat. Res., 96, 198.

ORMEROD, M.G., (1965), Int. J. Radiat. Biol., 9, 291.

ORMEROD, M.G. and ALEXANDER, P., (1963), Radiat. Res., 18, 495.

ORMEROD, M.G. and RIESZ, P., (1967), Biochim. Biophys. Acta, 149, 451.

OUDET, P., GERMOND. J.E., SURES, M., GALLWITZ, D., BELLARD, M. and CHAMBON, P., (1978), Cold Spring Harb. Symp. Quant. Biol., 42, 287.

PANYIM, S., BILEK, D. and CHAKLEY, R., (1971), J. Biol. Chem., 246, 4206.

PARDON, J.F., WORCESTER, D.L., WOOLEY, J.C., COTTER, R.I., LILLEY, D.M.J. and RICHARDS, B.M., (1977), Nucl. Acids

Res., 4, 3199.

PATT, H.M., TYREE, E.B., STRAUBE, R.L. and SMITH, D.E., (1949), Science, 110, 213.

PAULSON, J.R. and LAEMMLI, U.K., (1977), Cell, 12, 817.

POHLIT, W. and DRENKARD, S., (1985), Radiat. Prot. Dosim., 13, 195.

QUINTILIANI, M., BADIELLO, R., TAMBA, M., ESFANDI, A. and GORIN, G., (1977), Int. J. Radiat. Biol., 32, 195.

RADFORD, I.R., (1985), Int. J. Radiat. Biol., 48, 45.

RADFORD, I.R., (1986), Int. J. Radiat. Biol., 49, 611.

RAO, D.N.R. and SYMONS, M.C.R., (1982), Chem. Phys. Lett., 93, 495.

RAO, D.N.R., SYMONS, M.C.R. and WREN, B.W., (1984), J. Chem. Soc. Perkin Trans. 2, 1681.

RAY, D.K. and HUTCHINSON, F., (1967), Biochim. Biophys. Acta., 147, 357.

RENZ, M., NEHLS, P. and HOZIER, J., (1977), Proc. Natl. Acad. Sci. USA., 74, 1879.

REVELL, S.H., (1974), Adv. Radiat. Biol., 4, 367.

REVESZ, L. and MALAISE, E.P., (1983), in "Functions of Glutathione: Biochemical, Physiological, Toxicological, and Clinical Aspects", Larsson, A. *et al*. eds. (Raven Press, New York) p.163.

RICHARDS, B., PARDON, J., LILLEY, D., COTTER, R. and WOOLEY, J., (1977), Cell Biol. Int. Rep., 1, 107.

RIEDERER, H., HUTTERMANN, J., BOON, P.J. and SYMONS, M.C.R., (1983), J. Magn. Reson., 54, 54.

RIEDERER, H., HUTTERMANN, J. and SYMONS, M.C.R., (1981), J. Phys. Chem., 85, 2789.

RIESZ, P. and WHITE, F.H., (1970), Radiat Res, 44, 24.

RIESZ, P., WHITE, F.H. and KON, H., (1966), J. Am. Chem. Soc., 88, 872.

ROBERTS, J.M., (1972), Radiat. Res., 49, 311.

ROBINSON, M.G., WEISS, J.J. and WHEELER, C.M., (1966), Biochim. Biophys. Acta, 124, 181.

ROMITO, S., (1969), Fracastoro, 62, 571.

ROOTS, R. and OKADA, S., (1972), Int. J. Radiat. Biol., 21, 329.

SANNER, T. and PIHL, A., (1969), Radiat. Res., 37, 216.

SCHAFER, K., BONIFACIC, M., BAHNEMANN, D. and ASMUS, K.-D., (1978), J. Phys. Chem., 82, 2777.

SCHOLES, G., (1983), Br. J. Radiol., 56, 221.

SCHOLES, G., WARD, J.F. and WEISS, J., (1960), J. Mol. Biol., 2, 379.

SCHOLES, G. and WEISS, J., (1959), Radiat. Res. Suppl., 1, 177.

SCHOLES, G., WILLSON, R.L. and EBERT, M., (1969), Chem. Commn., 17.

SCHUCHMANN, M.N. and VON SONNTAG, C., (1977), J. Chem. Soc. Perkin Trans. 2, 1958.

SCHUESSLER, H. and HARTMANN, H., (1985), Int. J. Radiat. Biol., 47, 509.

SCHULTE-FROHLINDE, D., (1986), Basic Life Sciences Vol. 38, "Mechanisms of DNA Damage and Repair", Simic, M.G.,

Grossman, L. and Upton, A.C. eds. (Plenum Press, New York-London) p.19.

SCHULTE-FROHLINDE, D., BOTHE, E. and BEHRENS, G., (1985a), Radiat. Phys. Chem., 26, 481.

SCHULTE-FROHLINDE, D., OPITZ, J., GORNER, H. and BOTHE, E., (1985b), Int. J. Radiat. Biol., 48, 397.

SCHULZ, G.E. and SCHIRMER, R.-H., (1979), "Principles of Protein Structure", (Springer-Verlag, Heidelberg).

SCHWARZ, H.A., (1981), J. Chem. Educ., 58, 101.

SEDAT, J. and MANUELIDIS, L., (1978), Cold Spring Harb. Symp. Quant. Biol., 42, 331.

SEQUARIS, J.M. and VALENTA, P., (1980), Analytical Chem. Symp. Ser., 99.

SEVILLA, M.D., (1977), in "Excited States in Organic Chemistry and Biochemistry", Pullman, B. and Goldblum, N. eds. (Reidel, Dordrecht, Holland) p.15.

SEVILLA, M.D., D'ARCY, J.B. and MOREHOUSE, K.M., (1979a), J. Phys. Chem., 83, 2887.

SEVILLA, M.D., D'ARCY, J.B., MOREHOUSE, K.M. and ENGELHARDT, M.L., (1979b), Photochem. Photobiol., 29, 37.

SIMIC, M.G., GROSSMAN, L. and UPTON, A.C. eds., (1986), Basic Life Sciences, Vol. 38, "Mechanisms of DNA Damage and Repair" (Plenum Press, New York-London).

SIMPSON, R.T., (1978), Biochemistry, 17, 5524.

SIMPSON, R.T. and SHINDO, H., (1979), Nucl. Acids Res., 7, 481.

SINGH, B.B., (1968), Adv. Biol. Med. Phys., 12, 245.

SMOLIAR, V., (1962), C.R. Soc. Biol., 156, 1202.

SOBELL, H.M., TSAI, C.-C., GILBERT, S.G., JAIN, S.C. and SAKORE, T.D., (1976), Proc. Natl. Acad. Sci. USA., 73, 3068.

SPERLING, L. and KLUG, A., (1977), J. Mol. Biol., 112, 253.

SPINKS, J.W.T. and WOODS, R.J., (1976), "An Introduction to Radiation Chemistry, 2nd ed." (John Wiley and Sons, New York).

STANGER, H.K., FIELDER, E. and GRILLMAIER, R.E., (1982), Proc. 8th Symp. Julich, Federal Republic of Germany, Commission of the European Communities, Radiation Protection, Microdosimetry, p.517.

STARKIE, C.M., (1961), Int. J. Radiat. Biol., 3, 609.

STEENKEN, S., BEHRENS, G. and SCHULTE-FROHLINDE, D., (1974), Int. J. Radiat. Biol., 25, 205.

STELTER, L., VON SONNTAG, C. and SCHULTE-FROHLINDE, D., (1975a), Z. Naturforsch., 30b, 609.

STELTER, L., VON SONNTAG, C. and SCHULTE-FROHLINDE, D., (1975b), Z. Naturforsch., 30b, 656.

STEVENS, C.O., SAUBERLICH, H.E. and BERGSTROM, G.R., (1967), J. Biol. Chem., 242, 1821.

STRATLING, W.H., MULLER, U. and ZENTGRAF, H., (1978), Exp. Cell Res., 117, 301.

SUSSMAN, J.L. and TRIFONOV, E.N., (1978), Proc. Natl. Acad. Sci. USA., 75, 103.

SWEENEY, M.C., (1986), Ph.D. Thesis, University of Leicester.

SYMONS, M.C.R., (1974), J. Chem. Soc., Perkin Trans. 2, 1618.

SYMONS, M.C.R., (1978), "Chemical and Biochemical Aspects of Electron Spin Resonance Spectroscopy", (Van Nostrand Reinhond, Wokingham, Berks).

TAIT, M.J. and FRANKS, F., (1971), Nature, 230, 91.

TEXTER, J., (1978), Prog. Biophys. Mol. Biol., 33, 83.

THOMA, F., KOLLER, Th. and KLUG, A., (1979), J. Cell Biol., 83, 403.

THOMAS, J.O., (1983), in "Eukaryotic Genes: Their Structure, Function and Regulation", Maclean, N., Gregory, S.P. and Flavell, R.A., eds. (Academic Press, London) p.9.

THOMAS, J.O. and KORNBERG, R.D., (1975), Proc. Natl. Acad. Sci. USA, 72, 2626.

ULLRICH, M. and HAGEN, U., (1971), Int. J. Radiat. Biol., 19, 507.

VAN DE VORST. A. and LION, Y., (1971), Biochim. Biophys. Acta, 238, 417.

VAN DE VORST. A., RICHIR, M. and KRSMANOVIC-SIMIC, D., (1965), C.R. Hebd. Seanc. Acad. Sc. Paris, 261, 5682.

VAN HEMMEN, J.J. and BLEICHRODT, J.F., (1971), Radiat. Res., 46, 444.

VAN LITH, D., DE HASS, M.-P., WARMAN, J.M. and HUMMEL, A., (1983), Biopolymers, 22, 807.

VAN TOUW, J.H., VERBERNE, J.B., RETEL, J. and LOMAN, H., (1985), Int. J. Radiat. Biol., 48, 567.

VERBERNE, J.B., LOMAN, H., WARMAN, J.M., DE HASS, M.-P.,

HUMMEL, A. and PRINSEN, L., (1978), Nature, 272, 343.

VON SONNTAG, C., (1980), Adv. Carbohydr. Chem. Biochem., 37, 7.

VON SONNTAG, C. and DIZDAROGLU, M., (1977), Carbohydr. Res., 58, 21.

VON SONNTAG, C., HAGEN, U., SCHON-BOPP, A. and SCHULTE-FROHLINDE, D., (1981), Adv. Radiat. Biol., 9, 109.

VON SONNTAG, C. and SCHULTE-FROHLINDE, D., (1978), in "Effects of Ionising Radiation on DNA", Hüttermann, J., Kohnlein, W., Teoule, R. and Bertinchamps, A. J., eds. (Springer-Verlag, Berlin-Heidelberg-New York) p.204.

WANG, A.H.-J., QUIGLEY, G.J., KOLPAK, F.J., CRAWFORD, J.L., VAN BOOM, J.H., VAN DER MAREL, G. and RICH, A., (1979), Nature, 282, 680.

WARD, J.F., (1971), Int. J. Radiat. Phys. Chem., 3, 239.

WARD, J.F., (1975), Adv. Radiat. Biol., 5, 181.

WARD, J.F., (1981), Radiat. Res., 86, 185.

WARD, J.F., (1983), in "Radioprotectors and Anticarcinogens," Nygaard, O.F. and Simic, M.G. eds. (Academic Press, New York) p.73.

WARD, J.F. and KUO, I., (1976), Radiat. Res., 66, 485.

WARMAN, J.M., DE HASS, M.-P. and VERBERNE, J.B., (1980), J. Phys. Chem., 84, 1240.

WASHINO, K. and SCHNABEL, W., (1982), Int. J. Radiat. Biol., 41, 271.

WATSON, J.D. and CRICK, F.H.C., (1953), Nature, 171, 737.

WERTZ, J.E. and BOLTON, J.R., (1986), "Electron Spin

Resonance" (Chapman and Hall, New York-London).

WILLSON, R.L., (1983), in "Radioprotectors and Anticarcinogens", Nygaard, O.F. and Simic. M.G. eds. (Academic Press, New York) p.1.

WILLSON, R.L., WARDMAN, P. and ASMUS, K.-D., (1974), Nature, 252, 323.

WRAY, W., MACE, M., DASKAL, Y. and STUBBLEFIELD, E., (1978), Cold Spring Harb. Symp. Quant, Biol., 42, 361.

WREN, B.W., (1985), Ph.D. Thesis, University of Leicester.

WU, Z., AHMED, R. and ARMSTRONG, D.A., (1984), Radiat. Phys. Chem., 23, 251.

ZIRKLE, R.E., (1957), Adv. Biol. Med. Phys., 5, 103.

PUBLICATIONS

Paul M. Cullis, Martyn C. R. Symons, Marion C. Sweeney, George D. D. Jones and John D. McClymont 'The effects of ionising radiation on deoxyribonucleic acid. Part 4. The role of hydrogen peroxide' in *J. Chem. Soc., Perkin Trans. 2*, 1986, 1671-1676, DOI: 10.1039/P29860001671.